HEINRICH HEINE
UNIVERSITÄT
DÜSSELDORF

Analysis of the HlyA toxin secretion system of *Escherichia coli*

Inaugural-Dissertation

zur Erlangung des Doktorgrades
der Mathematisch-Naturwissenschaftlichen Fakultät
der Heinrich-Heine Universität Düsseldorf

vorgelegt von

Thorsten Jumpertz
aus Mannheim

Düsseldorf, Juni 2010

Aus dem Institut für Biochemie
der Heinrich-Heine-Universität Düsseldorf

Gedruckt mit der Genehmigung der Mathematisch-Naturwissenschaftlichen
Fakultät der Heinrich-Heine-Universität Düsseldorf.

Referent: Prof. Dr. Lutz Schmitt
Koreferent: PD Dr. Ulrich Schulte

Tag der mündlichen Prüfung: 28. Juni 2010

1. Introduction

The present work contains scientific publications that I prepared (as first or co-author) during my PhD thesis at the Institute of Biochemistry at the Heinrich Heine University Duesseldorf.

The thesis deals with the Type I secretion system of an enterohaemorragic strain of *E. coli*. During infection with this strain a toxin (Haemolysin A, (HlyA)) is secreted via a Type I system which was identified due to its ability to lyse red blood cells. Untreated, this infection can lead to a systemic disease and to the death of persons suffering from this infection. Apart from lysing red blood cells it has been shown that HlyA is able to induce calcium spikes and therefore might somehow interact with subsequent signal transduction pathways (Uhlen *et al.*, 2000). However, the underlying molecular mechanism of transport and the mode of action of the toxin are still not understood.

1.1 Architecture of the Type I secretion complex

The Type I secretion system which is responsible for transporting the toxin HlyA consists of various proteins – since an *E. coli* cell possesses an inner and outer membrane substrates have to cross both lipid bilayers to reach the extracellular space. The 107 kDa toxin HlyA has never been detected in the periplasmic space and therefore a continuous channel/tunnel was proposed to exist that spans the periplasmic space (Holland *et al.*, 2005). This rather complex molecular machine designated for secretion of HlyA consists of an inner membrane complex which includes the ABC transporter Haemolysin B (HlyB) and the so-called membrane fusion protein Haemolysin D (MFP, HlyD). Together with the porin-like protein TolC, which is located in the outer membrane, a ternary complex for secretion of the toxin is assembled (Figure 01) (Zaitseva *et al.*, 2005b). The periplasmic parts of HlyD and TolC most likely interact extensively with each other to form a tunnel-like structure guiding HlyA through the periplasm.

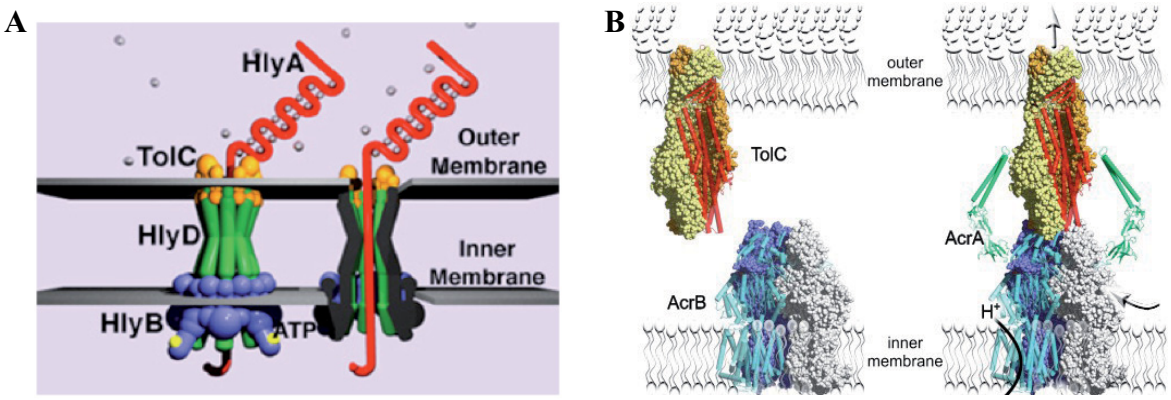

Figure 01: Panel A, schematic representation of a Type I secretion system of *E. coli*. HlyB (in blue) resides in the inner membrane. The nucleotide-binding domain (NBD) of HlyB is shown with ATP (yellow) bound. The second inner membrane component HlyD shown in green. HlyD has a huge periplasmic part and interacts with the ABC transporter HlyB and the outer membrane porin-like protein TolC (orange) to form a continuous channel/tunnel across the periplasm. The toxin HlyA which is the substrate of the Type I secretion system is shown in red during the transport process. The grey spheres in the extracellular space represent Ca^{2+} ions that bind to calcium-binding motifs in HlyA. The right part of panel A shows a cross section of the secretion complex to highlight the continuity of the channel and illustrates the idea that the 107 kDa substrate HlyA is probably transported in an unfolded state. The picture was taken from Zaitseva *et al.*, 2005b.
Panel B shows a modelling approach to visualize a similar intact tripartite complex derived from a different transport system that involves TolC. The AcrAB-TolC comple is a multidrug-resistance pump (MDR) that was identified due to its ability to transport a wide range of substrates, preferentially some beta-lactams. Subsequent experiments showed that AcrB is a drug/proton antiporter (Nikaido & Takatsuka, 2009). In contrast to HlyB, AcrB has a larger periplasmic domain and AcrA lacks the membrane spanning part which anchors HlyD in the inner membrane. The right part of panel B illustrates how all three components interact tightly and how AcrA wraps around the AcrB/TolC interface. A similar role is proposed for the membrane fusion protein HlyD. Panel B was taken from http://www.csb.bit.uni-bonn.de/ with courtesy of Dr. Christian Kandt.

The crystal structure of TolC in its closed conformation was solved in the year 2000 (Koronakis *et al.*, 2000) and clearly shows that a gating mechanism exists. This mechanism was proven two years later by disrupting the hydrogen bonds and salt bridges responsible for arresting TolC in the closed conformation (Andersen *et al.*, 2002). Since TolC is a ubiquitous outer membrane protein and interacts with different components of the inner membrane it is not yet clear if this gating mechanism is directly responsible for the secretion of HlyA. Probably, the interaction of TolC with HlyB/HlyD triggers TolC to open and guarantees access to the extracellular space.

Not much is known about the membrane fusion protein HlyD. It is thought to connect HlyB and TolC and therefore seal the channel/tunnel protruding through the periplasm (Figure 01) (Zaitseva et al., 2005b). With its quite huge periplasmic domain it is perfectly suited to fulfill this task. Certain mutations in HlyD cause a lysis-deficient HlyA but after unfolding and refolding of the toxin it gains its usual activity (Pimenta *et al.*, 2005). These mutations might interfere with recognition or transport processes. Maybe the substrate is inserted differently into the secretion complex or the mutations in HlyD disturb the assembly of the complex

itself in a rather subtle manner. But what exactly happens during this process is not clear at all.

Interestingly, there is evidence that HlyD is more than a mere protein-glue that holds the ternary complex together – it can compensate a symmetry break in the secretion complex. The crystal structure of TolC unveiled that this outer membrane protein acts as a trimer. Unpublished results from our laboratory propose a dimer for a functional HlyB which is in agreement with the available crystal structures of other ABC transporters (Kos & Ford, 2009, Jumpertz & al., 2009). In this context HlyD appears probably as a hexamer so that a TolC monomer interacts with two HlyD molecules. On the other hand every HlyB monomer binds to three HlyD molecules. Modelling studies are in favor of such a model where the periplasmic protein functions as the least common multiple between inner membrane transporter HlyB and the outer membrane porin TolC (Symmons *et al.*, 2009).

The ABC transporter HlyB is the molecular motor that drives the export of the toxin HlyA. It is generally believed that this protein is involved in substrate recognition and fueling of the transport process. The hydrolysis of ATP provides chemical energy to induce structural changes that facilitate transport of the substrate. The size of HlyA (1023 amino acids) implies that several cycles of ATP hydrolysis are necessary to secrete the toxin. In addition, the proton motive force across the cellular membrane may also contribute to the secretion process (Koronakis *et al.*, 1991). In contrast to several other ABC transporters that recognize a wide variety of e.g. hydrophobic substances, HlyB specifically identifies the toxin HlyA via a unique secretion signal and initiates transport of the toxin. A remarkable characteristic of the HlyA secretion machinery is the ability to recognize and transport substrates that are fused to the 50-60 C-terminal amino acids of HlyA (Li *et al.*, 2000, Fernandez *et al.*, 2000). These amino acids obviously form the secretion signal and are required and sufficient for effective secretion of proteins other than HlyA. Therefore, the Type I secretion system can also be exploited for interesting biotechnological applications.

In addition to the transmembrane part and the nucleotide-binding domain, HlyB has a third domain of approximately 140 amino acids at its N-terminal. This domain is homologous to C39 peptidases that have been found associated with ABC transporters involved in secretion of bacteriocins or quorum sensing peptides where they cleave a leader peptide of the substrate after a canonical double glycine motif (Havarstein *et al.*, 1995, Wu & Tai, 2004, Kotake *et al.*, 2008). The C39-like domain in HlyB is degenerated and therefore inactive due to the lack of the catalytic cystein. The simultaneous presence of multiple calcium binding sites in HlyA

that also contain double glycine motifs and an active C39 peptidase would obviously lead to degradation of HlyA. Deletion of the C39 domain abolishes secretion of HlyA (unpublished results, this laboratory).

The toxin Haemolysin A (HlyA) is the substrate of the Type I secretion complex assembled by HlyB-HlyD-TolC. As has been discussed before, certain distinct binding sites for nutrients or toxic compounds were identified in ABC transporters. These substances are small molecules that easily fit entirely into a cavity within the transmembrane part. A protein that consists of more than 1000 amino acids and has almost the same size as its designated transporter needs a different transport mechanism than simply binding to a site of high affinity in the transporter and being presented either to the intra- or extracellular space by a structural rearrangement of the transporter. The C39-like domain of HlyB mentioned before may play a crucial role in the transport mechanism of HlyA since it is essential for secretion of the toxin. In a possible scenario the C39-like domain serves as an interaction platform for HlyA during secretion. The size of the toxin requires several rounds of ATP hydrolysis and the degenerated peptidase domain might assist in this process by binding the toxin and keeping it in a secretion competent state at the transporter. This makes sense since HlyA is thought to be transported as an unfolded polypeptide chain across the inner and outer membrane of *E. coli* as the cavity provided by HlyB/TolC would not harbor a folded protein of 107 kDa. Other studies from this laboratory (unpublished data) support this model in showing that fast folding proteins fused to the secretion signal of HlyA are not secreted.

Prior to secretion HlyA is modified with acyl chains at two positions by an acyl-transferase called Haemolysin C (Worsham *et al.*, 2001, Langston *et al.*, 2004). Without this modification and binding of calcium to calcium binding sites HlyA binds to but does not insert into lipid membranes what is necessary to induce cell lysis (Bakas *et al.*, 1996).

The N- and C-terminal part of HlyA harbors a hydrophobic domain which likely interacts with the host cell membrane and is responsible for lysis and the secretion signal including 50-60 amino acids, respectively.

How HlyA is secreted, folds into its native form, interacts with/attacks host cells, induces cell lysis, and causes electrophysiological effects in host cells that lead to disturbed signalling events is - even more than 30 years after its discovery - not clear at all.

The structural and functional aspects of the Type I secretion complex and its substrate are still an enigma although quite a lot is already known about this fascinating molecular machinery.

1.2 ABC transporters – the import/export business of cells

ABC transporters have been identified to play a crucial role in the homeostasis of the cellular physiology and have a high impact on health and disease. Numerous examples were identified and discussed over the last decades, including cystic fibrosis, hepatobiliary diseases and multidrug resistance in cancer.

ABC transporters can be divided into importers and exporters whereas importers can only be found in prokaryotes. All ABC transporters identified so far share a common architecture – they are made up of 2 transmembrane domains and 2 soluble nucleotide-binding domains. In contrast to the transmembrane part the nucleotide-binding domains are highly conserved. There are various possibilities how TMDs and NBDs can be assembled or rather fused: every subunit (TMD or NBD) can be encoded as a single polypeptide chain, both TMDs or NBDs can be fused, one TMD and one NBD can fused (half-size transporter), or all four subunits can be found as a single polypeptide chain (full-size transporter). Further details concerning the structural organization can be found in Paper I.

ABC transporters play crucial roles in different aspects of life:

(a) import of nutrients and trace elements,

(b) homeostasis of the asymmetry of the lipid bilayer,

(c) export of e.g. bacterial toxins,

(d) conferring resistance against toxic drugs.

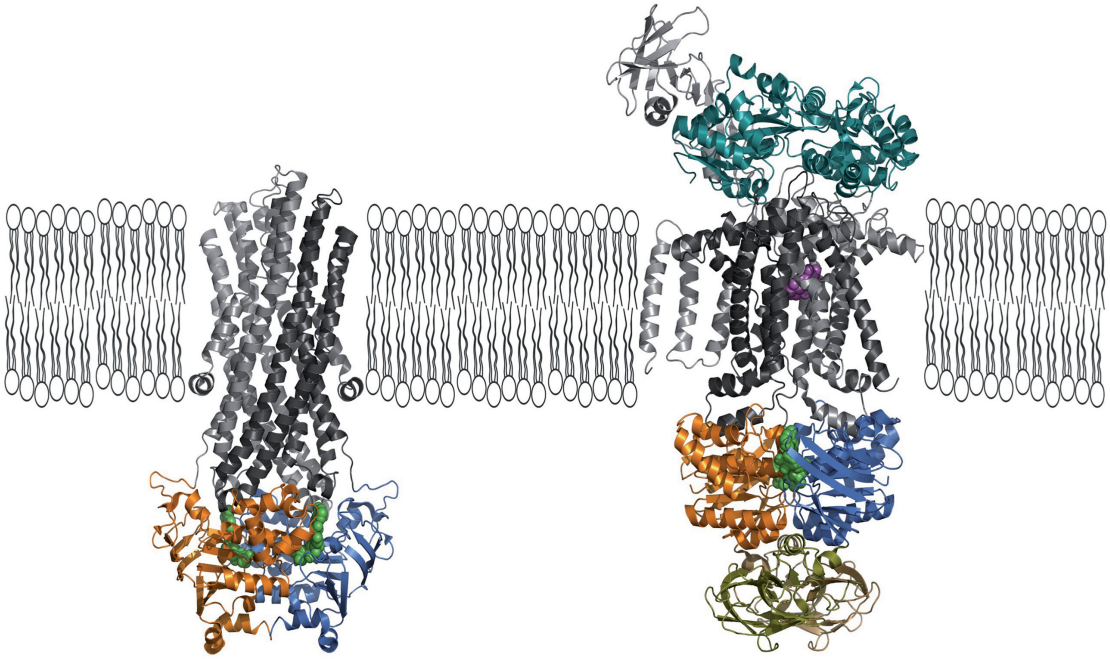

Figure 02: The picture on the left shows an example for an ABC exporter (Sav1866, PDB entry: 2HYD). The picture on the right shows the MalEFGK complex (PDB entry: 2R6G) as an example for an ABC importer. The transmembrane domains (TMDs) are depicted in light and dark grey. The nucleotide binding domains (NBDs) are shown in orange and blue, respectively. A striking difference between the exporter (left) and the importer (right) is the arrangement of the TMDs which are inter-twinned in case of the exporter but have a side-by-side orientation for all importers known so far. The substrate of the exporter interacts with the protein from the cytoplasmic side of the lipid bilayer. In contrast, the substrate for ABC importers is delivered by a substrate binding protein (SBP) from the extracellular space or the periplasm. For MalEFGK the SBP is shown on top of the complex in cyan and the substrate maltose (magenta) resides in its binding site within the transmembrane domains. The crystal structures of both ABC transporters have nucleotide bound to the NBDs (shown in green). The MalEFGK complex has an additional regulatory domain depicted in yellow. For a summary of the proposed transport mechanisms see Paper I and Paper II. The picture was taken from Jumpertz *et al.*, 2009.

Although, Pgp has been identified more than 30 years ago (Juliano & Ling, 1976, Riordan & Ling, 1979) as it confers resistance against drugs administered during chemotherapy, a basal expression of this multidrug resistance protein can be detected in healthy cells. Pgp and certain other ABC transporters have therefore been assigned a role in protecting cells against environmental or endogenous toxins.

Recently, stem cells have attracted a lot attention as it became clear that by a very simple mechanism differentiated cells can again turned into (induced) stem cells. Further investigation revealed ABC transporters being already present in stem cells and as a consequence the *cancer stem cell theory* evolved (Dean, 2009). This hypothesis has a huge impact on the understanding of cancer and its manifestation and progression since a cancer stem cell protected by multidrug resistance proteins withdraws itself from any clinical treatment.

In the last 10 years several crystal structures of ABC transporters have been solved (Jumpertz & al., 2009, Kos & Ford, 2009). These structures elucidated the three-dimensional arrangement and served as models to interpret biochemical data to understand the transport process. A major drawback of the available structures is that some of them represent proteins of open reading frames that have no assigned function or are importers for nutrients and trace elements. Concluding a transport mechanism for HlyB, which secretes a huge toxin, from these examples will definitely not offer a satisfying model.

From the two most important and interesting ABC transporters, namely Pgp and CFTR, only the crystal structure of Pgp is available so far (Aller *et al.*, 2009). Pgp has been identified to refer resistance against chemotherapeutics in cancer cells but what is even more stunning is the ability to transport a wide variety of substrates that are quite different in size and in their physical and chemical properties. This lack of stringency poses serious problems in the development of inhibitors and modulators directed against ABC transporters.

2. ABC transporters/Haemolysin B

2.1 ABC transporters – a smart example of molecular machineries

Paper I was published as a book chapter and describes in detail the structural and functional aspects of ABC transporters. First attempts on elucidating the structure of ABC transporters concentrated on the soluble nucleotide binding domains. These domains could be isolated and were not only a valuable target for structural biologists but bound and hydrolyzed nucleotides, preferably ATP, even without the transmembrane part. As a result, extensive studies on certain ABC proteins led to very good characterized model systems for this large membrane protein family. In addition, ABC importers have another soluble domain, the substrate binding protein (SBP), which delivers the substrate to the ABC transporter. These SBPs were also subject to early characterization. This laboratory made essential contributions on the structural and biochemical aspects of the nucleotide-binding domain of HlyB and different SBPs (Schmitt *et al.*, 2003, Zaitseva et al., 2005b, Hanekop *et al.*, 2007, Horn *et al.*, 2006, Oswald *et al.*, 2008).

Several crystal structures of complete ABC transporters are now available and data obtained from isolated NBDs as well as functional studies of full-length transporters shed light on the molecular mechanism of import and export of various substances.

The publication describes how all the available data on (prokaryotic) ABC transporters that covers structural and functional aspects fits into a general model that can describe the molecular events that take place during the transport cycle in exporters and importers.

Understanding the concept of ABC transporters enables us to get a deeper understanding of the cellular (patho)physiology and helps to find new approaches to target burning questions in biochemistry, biotechnology, and medicine.

2.2 Structure and function of the nucleotide binding domain of Haemolysin B

Paper II summarizes recent advances in understanding the molecular basis of ATP hydrolysis. The exact chemical reaction mechanism describing the elimination of the γ-phosphate moiety

of ATP and the interplay of nucleotide, co-factor, buffer conditions, and functional amino acid side-chains is explained.

The HlyB-NBD acts as a dimer – in the crystal structure two monomers are arranged in a head-to-tail orientation. Every monomer is able to bind one ATP molecule but is not able to hydrolyze the nucleotide. Only after dimerization has occurred a distinct microenvironment within the ATP binding site is established which enables hydrolysis. The changes in the binding site that can be observed during dimerization are mainly changes of pK_a-values of amino acids neccessary for eliminating the γ-phosphate and of the nucleotide itself (Hanekop *et al.*, 2006).

Two amino acids were shown to be essentially important for the efficient hydrolysis of ATP. A glutamate residue (Glu631) serves as a platform to stabilize a histidine residue in close vicinity (H662). Mutation of the glutamate leads to a protein with about 10% residual activity, whereas mutation of the histidine completely abolishes ATPase activity (Zaitseva *et al.*, 2005c). Analysis of molecular interactions (H-bridges, van-der-Waals interactions) revealed that the histidine residue holds all components of the catalytic site together which lead to the term “linchpin“. To further analyse the exact mechanism of hydrolysis two additional key experiments were neccessary:

(a) if a chemical reaction is the rate-limiting step of ATP hydrolysis, increasing the viscosity of the reaction buffer and therefore the hampering diffusion of the NBD monomers and the nucleotide should have no impact on the activity/reaction velocity. The experiment identifies a chemical reaction being the rate-limiting step and its exact nature was addressed in a second experimental set-up. **(b)** it has been proposed that a glutamate which is present in NTPases acts as a general base in hydrolysis. In the crystal structure of the HlyB-NBD dimer a water molecule is in close proximity of the catalytic histidine residue. The hydrolysis reaction was therefore performed in D_2O instead of H_2O. During general base catalysis a proton is abstracted – the difference in activation energy for abstracting a ^2H should slow down the reaction velocity. This was not observed and it could be concluded that a mechanism called *substrate assisted catalysis* is responsible for hydrolysis of ATP in the HlyB-NBD (Zaitseva *et al.*, 2005a).

A striking structural change upon dimerization of the HlyB-NBD occurs in the so-called D-loop of the nucleotide binding domain. It interacts with the histidine essential for ATP hydrolysis as mentioned above and with a serine residue of the second monomer. This interface is thought to act as a *molecular communication pathway* and transmits the functional

state (ATP-bound, ADP-bound, nucleotide-free) of one monomer to the other (Zaitseva et al., 2005b, Zaitseva et al., 2005a).

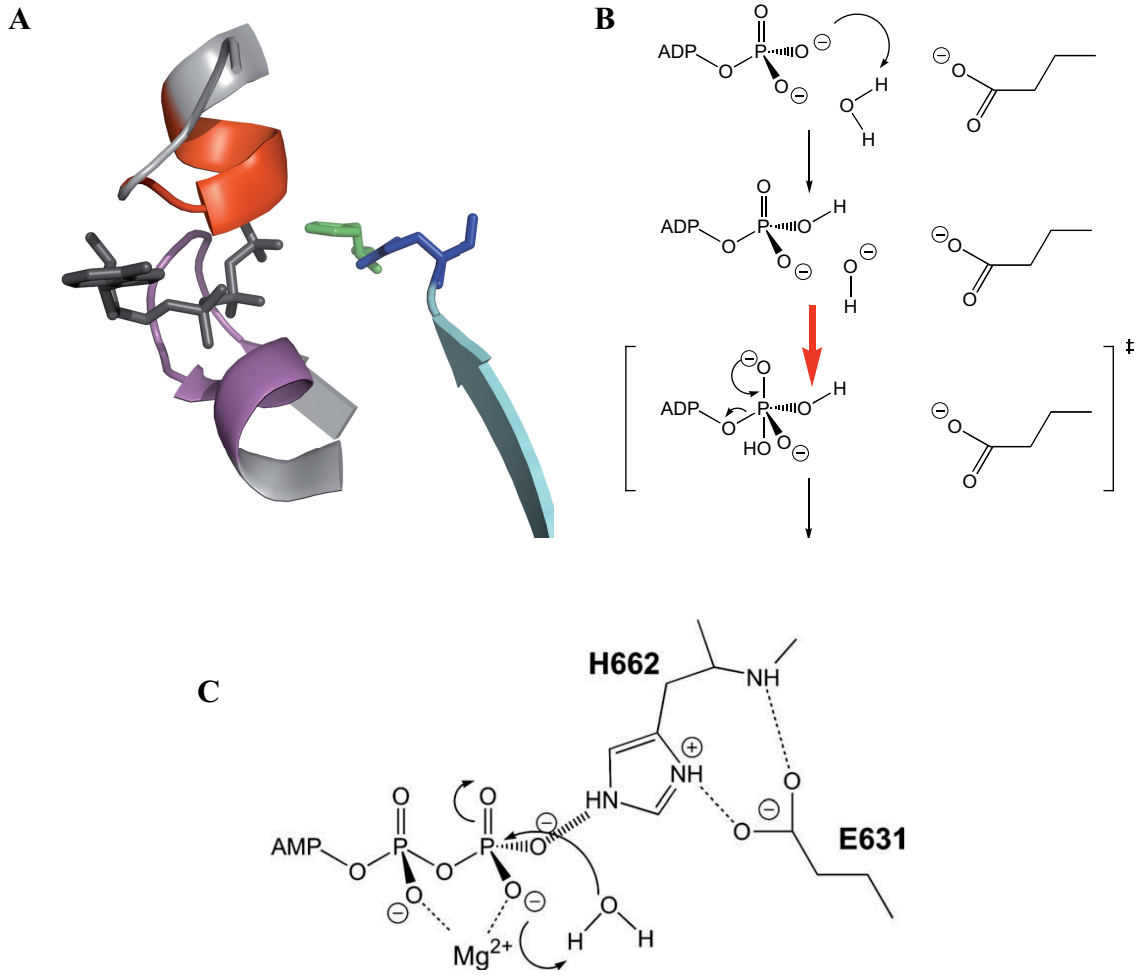

Figure 03: Panel A shows the orientation of the histidine residue H662 (green), glutamate E631 (blue), and ATP (dark gray) in the substrate binding site of the HlyB-NBD dimer (PDB entry: 1XEF). Panel B shows the underlying chemical reaction of ATP hydrolysis in the HlyB-NBD as can be concluded from the experiments explained in the text. Panel B is taken from Zaitseva *et. al*, 2005a. Panel C is a schematic drawing that summarizes the results of the ATP hydrolysis mechanism from structural and functional analysis of the HlyB-NBD depicted in Panels A and B. Panel C is taken from Zaitseva *et al.*, 2005c.

2.3 The catalytic cycle and the molecular basis of allostery in the HlyB-NBD

Paper III explains in detail how the nucleotide-binding domain of the ABC transporter HlyB functions on a molecular level. For the first time the complete catalytic cycle of a NBD has been shown in structural and functional aspects. Due to this characterization it is now possible to use this system as a platform to extensively test molecules acting as inhibitors, enhancers, or modulators of NBD activity. The nucleotide-binding domain is highly conserved among

ABC transporters from all three kingdoms of life and is therefore an ideal target to study energy conversion necessary for transport in a model system without making compromises in terms of transferring obtained data from a model system to higher organisms. The precise description of kinetics during the catalytic cycle of the NBD offers a great opportunity to study the impact of all kind of substances onto the protein. Apart from distinguishing between different forms of inhibition (competitive, non-competitive), elevation of activity or the influence on other kinetic parameters can be observed. The additional structural data makes it possible to address the question where substances bind and eventually tell us how they act on the protein. Lead substances can therefore be refined taking biochemical and structural data into account which altogether lead to highly specific drugs. An attempt to screen for drugs in cooperation with a pharmaceutical company unfortunately failed since the lead substances were unstable in pharmacokinetic analyses. Nonetheless, it proves that this system has the potency of being applied in the development of target molecules directed against the NBD of ABC transporters.

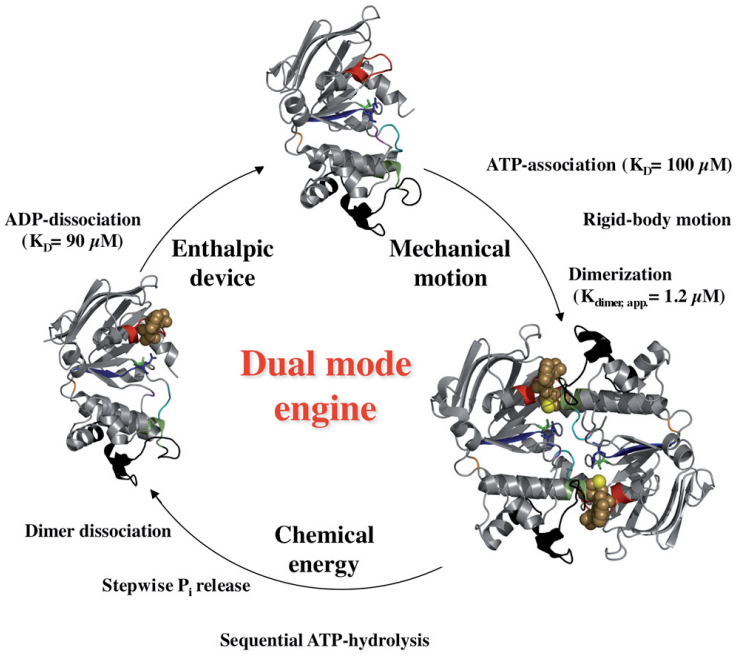

Figure 05: Upon binding of ATP the HlyB-NBD dimerizes to enable hydrolysis of the nucleotide. After hydrolysis of ATP the dimer dissociates and the NBD is again in its resting state, ready for another cycle of ATP hydrolysis (PDB entries: 1MT0, 1XEF, 2FF7). Important conserved motifs are highlighted in color: Walker A (red), Walker B (blue), H-loop (light green), D-loop (cyan), Q-loop (magenta), Pro-loop (orange), structural diverse region (SDR, black), C-loop (dark green), ATP (light brown), Mg^{2+} (yellow). A detailed description of the mechanism can be found in the text. An in-depth expanation of the conserved motifs as well as the figure can be found in Jumpertz *et al.*, 2009.

A thorough analysis of the structural and functional data of the HlyB-NBD led to the model shown in Figure 05. Binding of ATP induces dimerization of the NBD. After hydrolysis of the nucleotide the dimer dissociates and ADP is released. This catalytic cycle can be explained by an elegant underlying mechanism of structural changes that enable the protein to pass through certain states. Although the structures represent only snap-shots it became clear that helix 6 serves as a kind of spring since it is distorted upon binding of ATP. By this mechanism it stores energy that is released when the dimer dissociates and helps to release bound ADP and therefore resets the system to its initial state.

Furthermore the publication explains the cooperativity of the enzyme by identifying two amino acid residues, arginine (R611) and aspartate (D551), that act as gate keepers. They are close enough for a salt-bridge to occur which prevents the phosphate moiety to leave the substrate binding site through an exit tunnel that leads all the way to the protein surface. Mutation of R611 or D551 abolishes the cooperative behaviour of the enzyme (Figure 06).
For the first time, such a detailed and conclusive analysis of molecular mechanisms responsible for the function of a nucleotide binding domain of an ABC transporter have been achieved.

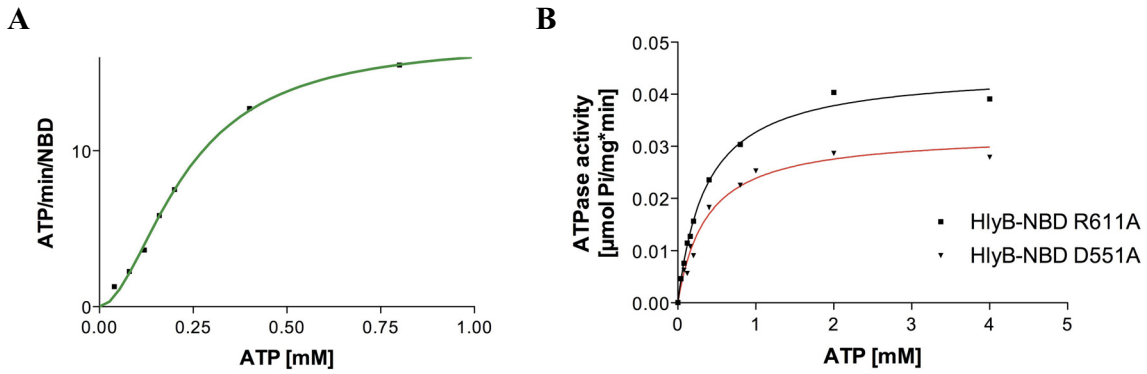

Figure 06: Panel A shows the ATPase activity of the wild-type HlyB-NBD. The data points have an apparent sigmoidal shape and can be fitted with a Hill plot. The resulting Hill coefficient specifies the degree of allostery/cooperativity of an enzyme. The Hill coefficient of the wild-type HlyB-NBD is 1.8 ± 0.09. In panel B the amino acids responsible for triggering phosphate release and therefore mediating cooperativity are mutated. The data points have no sigmoidal shape and can not be fitted into a Hill plot.

3. Haemolysin A – cell lysis and beyond

3.1 A secretion signal influences folding of a protein

The substrate of the ABC transporter HlyA is a 107 kDa toxin that belongs to the family of RTX proteins (repeats in toxin). Aside from its bare size the toxin displays several other interesting properties. Starting at the N-terminal an extended hydrophobic domain can be found which is thought to interact with the membrane of the host cell. It is not clear at all if the toxin forms a pore in the host cell membrane or only inserts into the outer leaflet applying strong lateral pessure and therefore rendering the membrane leaky (Sanchez-Magraner *et al.*, 2007, Ostolaza *et al.*, 1997, Bakas et al., 1996, Valeva *et al.*, 2008, Schmidt *et al.*, 1996, Soloaga *et al.*, 1999).

HlyA also shows two sites of modification where acyl chains are covalently bound to lysine residues. Without that modification HlyA still interacts with the membrane but is not able to lyse cells (Stanley *et al.*, 1994, Lim *et al.*, 2000). Beyond the lysine residues several Ca^{2+} binding sites can be found. The extracellular concentration of free calcium ions is much higher than inside the cell and provides enough calcium for HlyA to fold properly in the extracellular space. This mechanism has a great advantage – it keeps the protein from folding into its native form inside the bacterial cell and therefore ensures the efficient secretion of the toxin. Once it reaches the cell surface it can fold into its native form. There is much space for discussion if HlyA already has its native toxic form when it reaches the extracellular space or if certain structural rearrangements have to occur upon insertion into the host cell membrane.

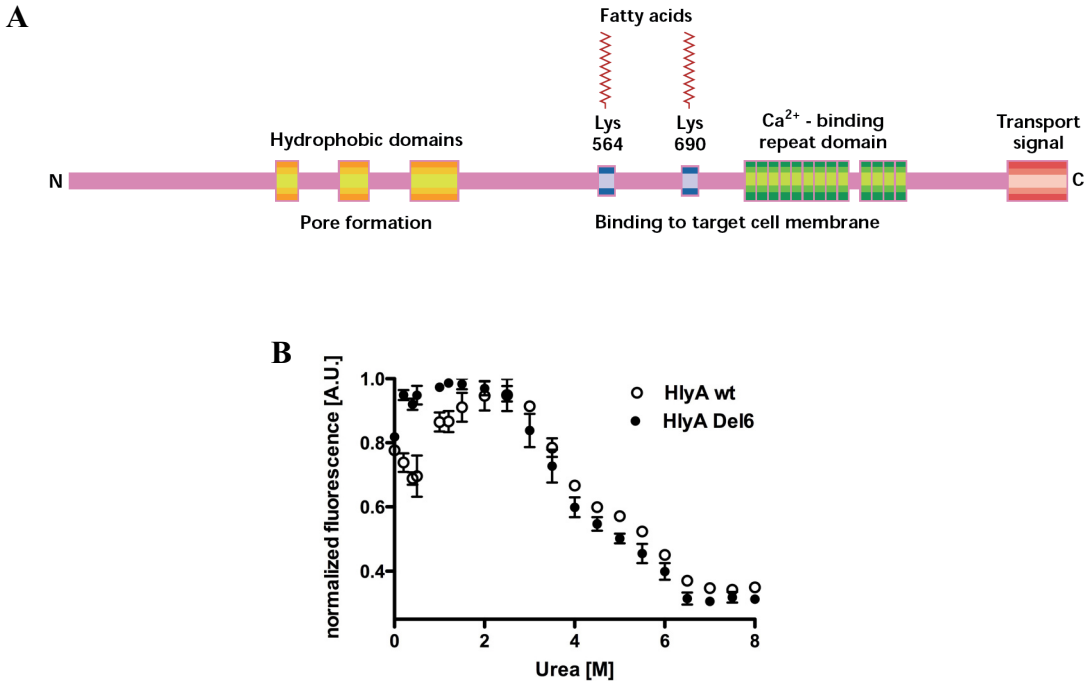

Figure 04: Panel A shows a schematic drawing of the toxin Haemolysin A. At the N-terminus several hydrophobic domains were identified. This part of the toxin is thought to interact with the host cell membrane (Soloaga et al., 1999). The lysine residues 564 and 690 are covalently modified via acylation (Lim et al., 2000). This modification as well as binding of Ca^{2+} ions render the toxin active in terms of its lytic activity. The secretion signal is located at the very C-terminal of HlyA and includes 50-60 amino acids. The figure in panel A is taken from (Ludwig & Goebel, 2000). Panel B shows a folding experiment of wild-type HlyA (open circles) and HlyA Del6 which is devoid of the last 6 amino acids (closed circles). Differences in fluorescence can be detected in the range between 0 and 2 M urea. Panel B is taken from (Jumpertz *et al.*, 2010).

Some results are in favor of a receptor binding region in HlyA that mediates binding of the toxin to the cell surface and subsequent insertion into the membrane (Cortajarena *et al.*, 2001, Cortajarena *et al.*, 2003) whereas other results do not see any effect of cell surface receptors on the efficiency of the toxin (Valeva *et al.*, 2005).

The secretion signal constitutes the C-terminal part of the toxin and includes the last 50-60 residues. Fusing the secretion signal of HlyA to different proteins turns them into substrates for the Type I secretion machinery (Fernandez *et al.*, 2000, Fernandez & de Lorenzo, 2001, Fraile *et al.*, 2004, Sugamata & Shiba, 2005). What catches the eye is the rather lengthy secretion signal which was investigated further in Paper IV presented in this work. Substitutions of four amino acids in the very C-terminus of HlyA led to a toxin that displayed drastically reduced haemolytic activity. Comparing the efficiency of secretion between wild-type and mutant HlyA showed no differences. The observed decrease in lytic activity is therefore not dependent on a difference in the amount of secreted protein but is rather a consequence of the altered amino acids. More detailed experiments lead to the conclusion that the amino acids at the very C-terminus influence folding of the toxin. The results identified a secretion signal with a dual function – the signal sequence of HlyA does not only direct the

toxin towards the Type I complex but is also involved in the process of correct folding of HlyA into its native and active state after secretion.

4. Biophysical Methods

4.1 A method to determine the CMC of biologically important detergents

The last work is focused on a method to determine the value of the critical micellar concentration of biologically relevant detergents.

All components of the Type I secretion system of *E. coli* are membrane proteins – this even includes the toxin HlyA which inserts into the host cell membrane. To study membrane proteins *in vitro* detergents are used to dissolve proteins from the lipid bilayer surrounding and substitute for a gross of the lipid molecules. The general idea behind this practice is to keep the proteins soluble in an aqueous environment while the detergent molecules bind to the hydrophobic transmembrane part of the proteins. A first obstacle is to find a detergent that effectively (and specifically) solubilizes the desired protein while preserving its activity. The number of detergents/detergent classes available increases every year. A commercial detergent screen to test for initial solubilization conditions is available from anatrace.com and contains 100 different detergents. This rather extensive screen offers the possibility to, at least, identify a class of detergents suitable for further experiments. The problem with this huge number of new detergents, that increases constantly, is an insufficient characterization of their physical properties. Using detergents in biological applications requires knowledge of the critical micellar concentration under various buffer/assay conditions. Since the CMC changes upon variation in salt content, pH, temperature, and so on it is essential to know how these parameters influence the CMC. Therefore, an easy-to-use assay for mid- to high-throughput analysis of the CMC value for biologically relevant detergents was established and is described in detail in Paper V.

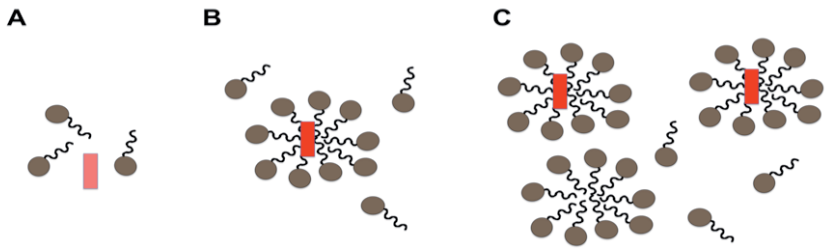

Figure 07: (A) The detergent concentration is below the critical micelle concentration (CMC). The fluorescent dye Hoechst33342 is located in an aqeous, hydrophilic environment and does not show fluorescence emission after exitation (pale red square). (B) At the CMC detergent micelles begin to form and Hoechst33342 is incorporated into the hydrophobic environment of the micelles. The fluorescence of Hoechst33342 starts to increase (bright red square). (C) Increasing concentrations of detergent lead to the formation of more micelles.

Since the concentration of Hoechst33342 is constant the fluorescence signal does not increase because newly formed micelles do not contain the fluorescent dye. The picture was taken from paper V.

The method is based on the incorporation of the fluorescent dye Hoechst33342 into detergent micelles (HDCE, Hoechst33342 dependent CMC evaluation). Hoechst33342 is non-fluorescent in a hydrophilic, aqueous environment but shows fluorescence upon entering a hydrophobic ambiance (Shapiro *et al.*, 1997). This property of Hoechst33342 is therefore ideally suited to follow formation of detergent micelles. The screening assay was adapted for use in 96-well micro-titer plates allowing for rapid and convenient read-out in a microplate-reader (BMG labtech, Halle, Germany) that was equipped with suitable bandpass filters for excitation and emission. The data obtained for detergents with known CMC values was in very good agreement with scientific publications and technical data sheets of manufacturers. For perfluorooctanoic acid (PFO) information about its CMC was hard to find in the literature (Shepherd & Holzenburg, 1995) and shown to be different from the values obtained by the HDCE method. This indicates that the HDCE method has the potential to be more sensitive and accurate than other methods that address the issue of CMC determination.

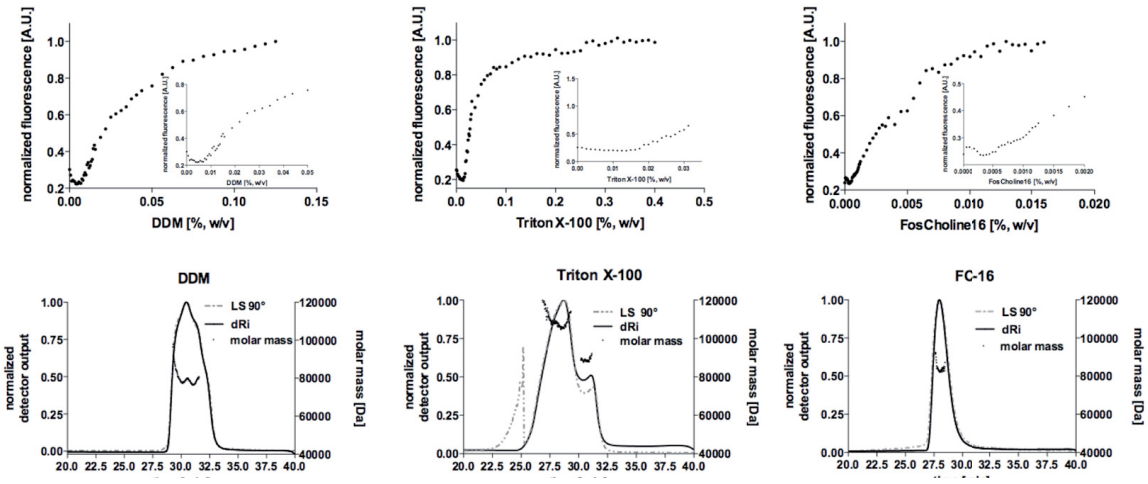

Figure 08: In the upper row the CMC values for DDM, Triton X-100, and FosCholine 16 determined in 96-well plates by the HDCE method are shown. The lower parts show the results of size exclusion chromatography coupled with a multi-angle light scattering device to determinde the molecular mass of the detergent micelles.

Furthermore, the dependency of the CMC on buffer substances and salt concentrations was determined. Interestingly, the formation of mixed micelles which has been described in the literature could not be detected with this method (Sehgal *et al.*, 2005, Aniansson & Wall, 1974). Formation of micelles only occurred when the CMC of one of the detergents was exceeded.

This method is therefore a valuable tool to investigate the properties of detergents in various buffer conditions to elucidate the environmental properties of a membrane protein during a purification procedure, in activity assays, or crystallization set-ups.

The HDCE method is currently used as an analytical tool by a company specialized in the synthesis of detergents to check the quality of every newly synthesized batch.

PAPER I

ABC Transporters in Microorganisms

Research, Innovation and Value
as Targets against Drug Resistance

A skilful selection of topics and a panel of acknowledged experts as authors ensure that this concise volume will be of exceptional importance to everyone involved in DNA research related to protein superfamilies, as well as scientists interested in microbial physiology and, in particular, multidrug resistance. This concise volume describes the latest theory, methodology and applications of ABC transporters in microorganisms. The topics include the structure, physiology and evolution of ABC transporters, as well as their special characteristics in specific microorganisms including bacteria, yeast, trypanosomes and malaria parasites. In particular, the book describes the most recent research and innovations relative to the role of ABC transporters in the design of strategies to circumvent drug resistance in microorganisms. Each chapter comprises an exhaustive review of the particular topic and provides insights into the future of the field from both the scientific and the clinical perspective. Essential reading for anyone involved in this field and a recommended volume for all microbiology laboratories.

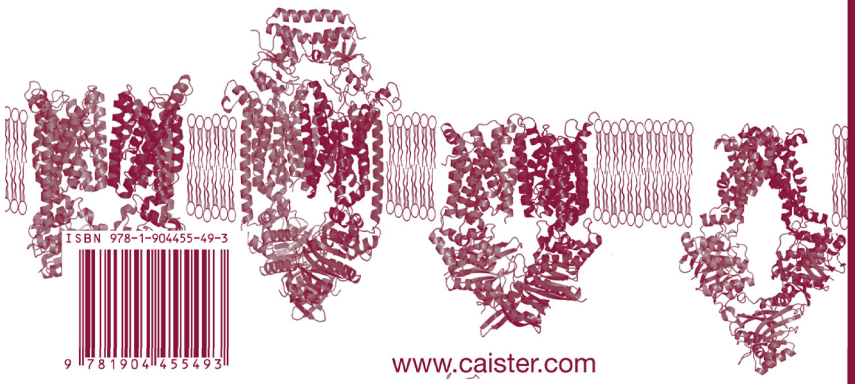

ISBN 978-1-904455-49-3
9 781904 455493

www.caister.com

ABC Transporters in Microorganisms

Ponte-Sucre

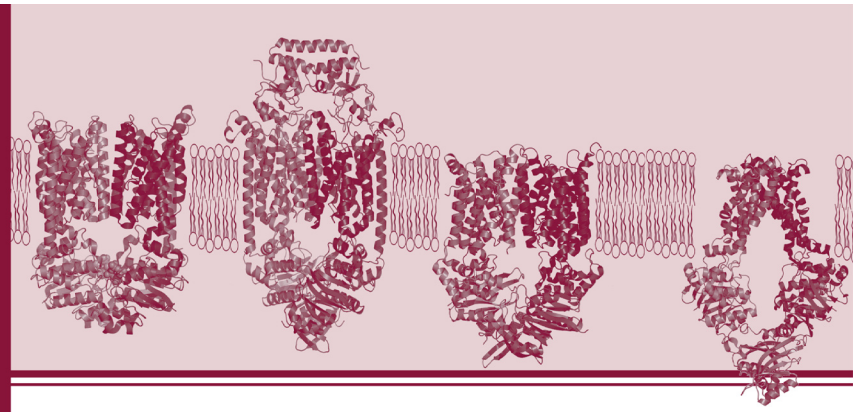

ABC Transporters in Microorganisms

Research, Innovation and Value
as Targets against Drug Resistance

Edited by Alicia Ponte-Sucre

Caister Academic Press

ABC Transporters – a Smart Example of Molecular Machineries

1

Thorsten Jumpertz, I. Barry Holland and Lutz Schmitt

Abstract

ABC transporters are fascinating molecular machines that use the energy of ATP to catalyse the transport of a tremendous variety of substrates across biological membranes in a vectorial fashion. Here, we will summarize our current knowledge of the domain organization and topology of this class of primary transporters. All ABC transporters analysed so far are composed of two nucleotide-binding domains (NBD) and two transmembrane domains (TMD) that can be arranged in any possible combination. However, additional transmembrane segments or extended NBDs, raise the possibility that these extensions act as platforms to interact with additional proteins with functional or regulatory consequences. In the light of the recent crystal structures of isolated NBDs in different functional states and the structures of intact ABC transporters, we will also focus on the three-dimensional architecture, domain–domain interactions and putative signaling pathways in these membrane proteins that guarantee efficient substrate recognition and translocation in an ATP-dependent manner.

Introduction

A short tale of ABC transporters

ABC transporters are one of the largest membrane protein families discovered so far. In *E. coli* ABC transport systems constitute 5% of the coding capacity of the organism (Linton and Higgins, 1998). The number of ABC transporters for different *E. coli* strains varies between 52 and 83 (Moussatova *et al.*, 2008) while in humans 48 genes for ABC proteins have been identified (Dean *et al.*, 2001), which are now assigned to seven subfamilies. Initially, proteins with an ATP binding cassette (ABC-) motif were identified and subsequently were shown to be part of a transport system composed of an integral membrane component and the ABC domain. This was the beginning of the discovery of a new superfamily of transport proteins. The first ABC transporters identified were the histidine permease and the maltose importer (Ames and Lever, 1970; Hazelbauer, 1975) driven by the ATPase motors, HisP and MalK respectively. Subsequently, ABC proteins were identified, however, with no associated transmembrane components and no transport function but that instead participate in DNA repair mechanisms (Husain *et al.*, 1986), antibiotic resistance (Jacquet *et al.*, 2008), or regulation of gene expression (Vazquez de Aldana *et al.*, 1995). ABC proteins are now divided into three major classes corresponding to their overall quaternary structure organization. Class 1 contains ABC transporters whose transmembrane components and ABC domains are fused in a single polypeptide chain. Class 2 is comprised of ABC proteins lacking an integral membrane component or transport function. Class 3 identifies ABC transport systems where the ABC and membrane components are encoded on separate polypeptide chains and where an additional component essential for import processes can be present. As may be expected it is hypothesized that all ABC proteins have evolved from a last universal common anchestor (LUCA) but this will not be

discussed further here (Saurin *et al.*, 1999; Dassa and Bouige, 2001; Davidson *et al.*, 2008).

Most ABC proteins are essentially membrane proteins and function as transporters. The cellular membrane bilayer is impermeable towards charged molecules and substances that exceed a certain size. Proteins in the membrane are essential to mediate exchanges across this barrier allowing cells to import nutrients or expel toxic compounds. ABC transporters are essential players in these tasks, being involved in the transport of a huge variety of different molecules. The functions range from import of small ions to the extrusion of macromolecules that can be much larger than the transporter itself as in the case of the RTX polypeptide toxins such as HlyA (Holland *et al.*, 2005). An interesting class of transport substrates comprises mostly hydrophobic drugs (e.g. Hoechst, rhodamine, verapamil, and many more; see (Sharom, 2008). For this reason, ABC transporters have been ascribed an important role in the development of multi drug resistance. To avoid possible confusion between hydrolysed substrates for an ABC protein like ATP as opposed to a *transport* substrate, we shall use the term 'allocrite' for the latter substrate.

In this chapter, knowledge available until the end of 2008, in terms of structure and function of ABC transporters will be summarized and recent models directed towards a more detailed molecular understanding are discussed. Several structures of complete ABC transporters have now been solved and many more isolated ABC motor domains and substrate binding proteins have been structurally described. Among the structures of complete transporters are importers as well as exporters captured in inward or outward facing conformations. These structures illustrate conversion of energy generation into mechanical movement involving communication between the motor domains and the transmembrane component.

Without doubt the most prominent examples of the ABC transporter family are P-glycoprotein (Pgp, MDR1, Multidrug resistance protein 1, ABCB1) and CFTR (Cystic fibrosis transmembrane conductance regulator, ACBC7). P-glycoprotein was first identified in cells showing resistance to drugs usually administered during cancer therapy (Kartner *et al.*, 1983) and is now recognized as a major problem in humans undergoing chemotherapy, conferring multidrug resistance, as expression levels are increased. P-glycoprotein is endogenously expressed in epithelial cells lining the colon or kidney proximal tubules and protects cells from toxic compounds (Leslie *et al.*, 2005). A knock-out of the gene Pgp disrupts the blood-brain barrier in mice and leads to neurotoxic effects (Doran *et al.*, 2005). After the first sequence of the Pgp clone appeared, Victor Ling and colleagues immediately discovered that the closest similarity was to the HlyB gene; this similarity allowed them to propose that Pgp was no doubt a drug pump. Interestingly, in addition to strong conservation in the NBDs (nucleotide binding domains) the two proteins had small shared motifs in the distal region of the TMDs (transmembrane domains) which, while still remaining a puzzle, may indicate some conservation of an energy coupling mechanism to transport in exporters.

Mutations in the CFTR gene cause cystic fibrosis with the most common mutation F508Δ leading to misfolding of the protein. This results in subsequent degradation of the transporter through the quality control system of the cell, while the wild type protein is transported to the cell surface. The F508Δ mutation is the most widespread cause of cystic fibrosis, the genetically most inherited disease among Caucasians (i.e. people from Europe, western Asia, North Africa and parts of the Indian subcontinent). The severe course of the disease, which is characterized by viscous mucus literally gluing together the bronchia of the lungs and the pancreas, often leads to death of the patients when they reach their mid-thirties, most frequently caused by bacterial infection of the lungs (Cystic Fibrosis Foundation, 2006; http://www.cff.org/).

At this point it should have become clear that a detailed knowledge of ABC transporters is essential since they function in important physiological and patho-physiological processes. To study these molecular systems different research groups have concentrated on ABC transporters found in prokaryotes. This preference stems from the fact that genes in bacteria are usually easier to manipulate and the protein products easier to purify. Proteins can be overproduced using commercially available and well characterized

systems. The yield of protein in bacteria is often much higher compared to mouse or human cell lines. One can search for the best suitable bacterial homologue in terms of sequence identity compared to the eukaryotic protein or even stability of the transporter in various *in vitro* assays. Moreover, bacterial cell culture is much cheaper, which is quite important when proteins have to be produced in milligram quantities for structural studies. The strategy to use bacterial systems as models is not only appealing in terms of simplification, but is fundamentally supported by studies demonstrating that the evolutionary divergence of ABC proteins occurred prior to the separation of archea, bacteria, and eukarya. Additionally, these proteins have remained highly conserved in the nucleotide binding domain (NBD) (Saier *et al.*, 1998; Fuellen *et al.*, 2005). This justifies bacterial homologues of human ABC proteins as excellent model systems to evaluate and describe the underlying mechanisms common to all members of the ABC transporter family.

In recent years, some crystal structures of intact bacterial ABC transporters have been solved and many more isolated motor domains that fuel the import or export of substances have been described in great detail. Recently, a bioinformatics approach has allowed us to list all the functional ABC transporters identified in *E. coli* and summarize the crystal structures of every ABC component (full transporter, isolated motor domain (NBD), substrate binding protein (SBP), or complexes of transporter and SBP) that have been deposited in the Brookhaven Protein Data Bank (http://www.rcsb.org) (Moussatova *et al.*, 2008). Over 90 structures of ABC transporter components have been obtained and represent the basis for structural and functional interpretation of the mechanisms of allocrite transport.

ABC transporters in molecular detail

In order to gain insight into how ABC transporters work it is important to understand the basic architecture of these proteins. In general, ABC transporters consist of a membrane spanning component (transmembrane domain, TMD) and a nucleotide binding or motor domain exposed to the cytoplasm. A fully assembled and functional transporter commonly consists of two TMDs and two NBDs, either as a homo- or heterodimer depending on the TMD and NDB subunits being identical e.g. $BtuC_2D_2$ (Locher *et al.*, 2002) or different e.g. $MalFGK_2$ (Oldham *et al.*, 2007). For exporters, usually a total of twelve transmembrane domains are detected, whereas the number for importers differs between ten and twenty TMDs per fully assembled transporter (Hollenstein *et al.*, 2007a). The motor domains bind ATP, which provides chemical energy upon hydrolysis, producing mechanical energy for transport. In some cases the NBDs have a regulatory domain at the C-terminal (Chen *et al.*, 2003a; Verdon *et al.*, 2003; Scheffel *et al.*, 2005; Gerber *et al.*, 2008; Kadaba *et al.*, 2008) whose proposed role is explained in more detail later. While ABC transporters involved in export normally require only the NBDs and TMDs for function, importers need a further component – the so-called substrate binding protein (SBP). The SBP binds the extracellular allocrite and delivers it to the transport domain.

ABC transporters involved in import are only present in prokaryotes and every component (TMD, TMD, NBD, NBD) is often encoded by separate genes with the protein then assembling into a functional transporter. Additionally, either both TMDs or both NBDs can be fused in a single polypeptide chain (Buckel *et al.*, 1986; Bohm *et al.*, 1996; Biemans-Oldehinkel *et al.*, 2006). The substrate binding protein can either be found diffusing freely in the periplasm for Gram-negative bacteria or attached to the membrane via lipid or protein anchors or covalently linked to the TMD for Gram-positive species (van der Heide and Poolman, 2002; Davidson and Chen, 2004; Borths *et al.*, 2005;). In the case of ABC importers each individual subunit (TMD, NBD, SBP) may be encoded as a seperate polypeptide chain and the transport complex assembles from up to five modules.

For some ABC exporters both transmembrane domains and both nucleotide-binding domains are fused into a single polypeptide chain, designated as a full-size transporter. On the other hand, one TMD and one NDB can be found as separate polypeptide chains and these exporters are consequently called half-size transporters, with two copies of the NBD and TMD assembling as a homo- or heterodimer to form a func-

tional transporter. Heterodimers can arise either with respect to the transmembrane components (MalFG; (Froshauer and Beckwith, 1984; Dassa and Hofnung, 1985;) or the nucleotide-binding domains (LmrCD; (Lubelski *et al.*, 2006).

For structural analysis of ABC transporters initial attempts concentrated on the small, approximately 30 kDa NBDs since these relatively water soluble components of the transporter were easier to over-express and purify in reasonable amounts. Several structures of NDBs have now been obtained, both as monomers with and without nucleotide bound and also as dimers that reflect the relevant physiological state necessary for ATP hydrolysis. The first structure of the HisP ABC-ATPase was published in 1998 (Hung *et al.*, 1998) and revealed the now familiar, largely β-stranded lobe, constituting the catalytic domain, with the helical domain containing the signature motif which was presumed to have a regulatory role.

Despite the fact that ABC transporters as a family have a broad range of transport substrate specificity, vectorial transport and even a variety of different architectures (number of TMDs, degenerate NBDs, additional regulatory domains), certain highly conserved amino acid motifs can be found in the NBDs. However, the transmembrane part is not highly conserved although recent crystal structures have revealed some structural similarities. The overall diversity of the amino acid sequence has led to the assumption that the TMDs of the transporter mediate allocrite selectivity. However, one strictly conserved motif in the TMDs of ABC importers in bacteria is the EAA motif located in a cytoplasmic loop implicated in an interaction with the NBDs. As will be discussed below, this region interacting with the NBD seems to be involved in the communication between the transporting and energy generating domains. Contacts between the EAA loop and the NBDs in MalK were first shown in mutational studies and then in cross-linking experiments that demonstrated the close proximity of the helical domain of the NBD and the intracellular loops of MalF and MalG, each containing the EAA-motif (Hunke *et al.*, 2000; Mourez *et al.*, 1997).

In contrast to importers, ABC exporters lack the conserved EAA motif, although recently a sequence possibly undertaking the task of ensuring proper communication between TMDs and motor domains was identified (Dawson and Locher, 2006). Thus, in the Sav1866 crystal structure the region of TMD–NBD interaction is characterized by the TEVGERG sequence (designated as the x-loop) with a similar sequence in other ABC exporters, as well as by sequence alignments. This sequence is not located in the intracellular loops of the transmembrane part but lies within the structurally diverse region (SDR) of the NBD helical domain (see Fig. 1.8B). The SDR was first identified by an analysis of the crystal structure of the nucleotide-free state of the HlyB-NBD. A structural comparison with the crystal structures available at that time revealed that roughly 30 amino acids of the helical domain located just upstream of the C loop showed the highest structural variation within the analysed NBDs. Importantly, the SDR can be found in ABC exporters as well as importers and it was proposed that this variable structural motif was vital for the specificity of different ABC proteins, allowing the otherwise conserved NBD to interact uniquely with the cognate TMD.

Unlike the diversity shown by the TMDs, the NBDs display an extensive conservation of sequences. This is to be expected since the hydrolysis of ATP that fuels transport is a mechanism found in all ABC transporters throughout all kingdoms of life and irrespective of the allocrite specificity or transport direction. The conserved sequences are the Walker A and Walker B motifs, characteristic for the large family of P-loop NTPases (nucleotide triphosphatases) (Vetter and Wittinghofer, 1999), the C-loop/signature motif, D-loop, Pro-loop, H-loop and the structurally diverse region (SDR) containing the x-loop, a motif restricted to exporters. The C-loop is localized to the helical domain of the NBD (Ames and Lecar, 1992), while the Walker A motif is located to the catalytic domain. The Walker A is involved in ATP binding and this has the consensus amino acid sequence GXXGXGKS/T where X stands for any amino acid (Walker *et al.*, 1982). The Walker B motif is composed of an amino acid stretch that resembles ΦΦΦΦD where Φ is any hydrophobic residue. The Walker B element is the typical nucleotide binding fold of P-loop ATPases and forms part of the binding site for nucleotides (Vetter and Wittinghofer, 1999). Together, the

Walker A and B motifs resemble part of the RecA-like (Story and Steitz, 1992) or F_1-like (Abrahams *et al.*, 1994) subdomain of the NBD which contains mostly β-sheet structures. Additionally, the D-loop (SALD) and H-loop, approximately 25 residues downstream of the Walker B motif, are localized in this catalytic subdomain.

The hallmark of ABC transporters is the signature motif or C-loop (Schmitt and Tampé, 2002). Its consensus sequence is highly conserved and can be found in any NBD with only minor variations (e.g. Q → E in BtuD). A degenerate C-loop sequence results in a loss of ATP-hydrolysis. Further motifs found close to the helical domain are the Q-loop, and the Pro-loop; in fact, these essentially connect the catalytic and helical domains.

This plethora of conserved and important motifs may be confusing at first sight, but the sequence along the polypeptide chain and the resulting three-dimensional arrangement are not too complex (Fig. 1.1 and 1.2A). Starting from the N-terminus of the NBD along the motor domain, the Walker A motif in the catalytic domain is encountered first. The next motif is the Q-loop serving as a hinge between the catalytic and helical domains. The helical domain contains the structurally diverse region (SDR) immediately followed by the signature motif or C-loop. About 15 amino acids beyond the C-loop, the Pro-loop, the second hinge for the movement of the helical domain appears and delineates simultaneously the way back to the catalytic domain. The remaining motifs are the Walker B sequence adjacent to the D-loop and the H-loop the closest of all the consensus motifs to the C-terminus (see Chapter 3 for further details).

All stretches of conserved amino acids indicated above have specific tasks to ensure proper functioning of the motor domain and hence the transport process. We shall focus on all these structural motifs and explain how the characteristic amino acid side chains and the orientation of the residues and the nucleotide catalyse chemical reactions in a concerted manner. Since malfunctioning of several ABC transporters in humans is associated with severe diseases, a thorough understanding of such molecular details of the action of the ABC domain is a prerequisite for successful design of effective drugs in the future. Thus, our focus will be on residues interacting with the nucleotide, those that interact with the transmembrane part, and those that mediate NBD-NBD contacts in the functional dimer. A comprehensive schematic drawing of a nucleotide-binding domain is shown in Fig. 1.2 and the respective motifs are colour-coded.

Fig. 1.2A shows the overall structure of the nucleotide binding domain for HisP from the ABC histidine importer of *S.* Typhimurium. The structure of the monomeric NBD displays a more or less L-shaped form and can be divided into two subdomains that have certain unique functions. First the domain consisting of α-helices, therefore the 'helical domain', while the second subdomain (catalytic domain, RecA-like domain, F_1-like domain) contains a central antiparallel β-sheet which is flanked by α-helices. This arrangement was first described by Ames and coworkers in the crystal structure of the ABC motor domain from the histidine permease of *S.* Typhimurium ten years ago (Hung *et al.*, 1998). Important structural elements in the helical domain are the C-loop (pale green), the designated signature motif for ABC transporters and the SDR (black) (Schmitt *et al.*, 2003) which contains the x-loop (Dawson and Locher, 2006).

Under physiological conditions the NBDs of an ABC transporter have to dimerize to bring all residues necessary for hydrolysis of the substrate into close proximity. Thus, each monomer contributes to the binding pocket of ATP in a head-to-tail arrangement with the Walker A motif of one monomer and the signature motif of the other monomer sandwiching the ATP (Chen *et al.*, 2003a; Smith *et al.*, 2002; Zaitseva *et al.*, 2005a).

The structurally diverse region interacts with cytoplasmic loops extending from the transmembrane components of the ABC transporter and is therefore involved in conveying information about the actual status of the two major components of the ABC transporter, the NBD and TMD (Schmitt *et al.*, 2003). Thus, it is reasonable to suppose that binding of nucleotide, hydrolysis of ATP or binding of the allocrite (transport substrate) must induce intramolecular structural changes that in turn promote appropriate changes in the TMDs, finally leading to import or export of the allocrite via a membrane pathway.

```
MsbA_S.typhimurium       1     EKDEGKRVIDRATGDLEFRNVTFTYPGREVPALRNINLKIPAGKTVALVGRSGSGKSTIASLITRFY..DIDEGHILMDGHD.........LREYT
MsbA_E.coli              1     EKDEGKRVIERATGDVEFRNVTFTYPGRDVPALRNINLKIPAGKTVALVGRSGSGKSTIASLITRFY..DIDEGEILMDGHD.........LREYT
Sav1866_S.aureus         1 DYDIKNGVGAQPIEIKQGRIDIDHVSFQYNDNEAPILKDINLSIEKGETVAFVGMSGGGKSTLINLIPRFY..DVTSGQILIDGHN.........IKDFL
LmrA_L.lactis            1                   MLSARHVDFAYDDSEQ.ILRDISFEAQPNSIIAFAGPSGGGKSTIFSLLERFY..QPTAGEITIDGQP.........IDNIS
HlyB_E.coli              1                   DITFRNIRFRYKPDSPVILDNINLSIKQGEVIGIVGRSGSGKSTLTKLIQRFY..IPENGQVLIDGHD.........LALAD
MetN_E.coli              1                 MIKLSNITKVFHQGTRTIQALNNVSLHVPAGQIYGVIGASGAGKSTLIRCVNLLE..RPTEGSVLVDGQ..........ELTTL
HisP_S.typhimurium       1                MMSENKLHVIDLHKRYGGHEVLKGVSLQARAGDVISIIGSSGSGKSTFLRCINFLE..KPSEGAIIVNGQNINLVRDKDGQLKVA
MalK_P.horikoshii        1          GNNIEVIKMVEVKLENLTKRFG.NFTAVNKLNLTIKDGEFLVLLGPSGCGKTTTLRMIAGLE..EPTEGRIYFGDRD.........VTYLP
1VCI_P.horikoshii        1         MGNNIEVIKMVEVKLENLTKRFG.NFTAVNKLNLTIKDGEFLVLLGPSGCGKTTTLRMIAGLE..EPTEGRIYFGDRD.........VTYLP
MalK_E.coli              1                   MASVQLQNVTKAWG.EVVVSKDINLDIHEGEFVVFVGPSGCGKSTLLRMIAGLE..TITSGDLFIGEKR.........MNDTP
ModC_A.fulgidus          1                     MFLKVRAEKRLG.NFRLN...VDFEMGRDYCVLLGPTGAGKSVFLELIAGIV..KPDRGEVRLNGAD.........ITPLP
ModC_M.acetivorans       1                     MIEIESLSRKWK.NFSLDNLSLKVESG.EYFVILGPTGAGKTLFLELIAGFH..VPDSGRILLDGKD.........VTDLS
CysA_A.acidocaldarius    1      MRGHHHHHHHGSMTIEFVGVEKIYPGGARSVRGVSFQIREGEMVGLLGPSGSGKTTILRLIAGLE..RPTKGDVWIGGKR.........VTDLP
MJ1267_E.coli            1                 MIKLKNVTKTYKMGEEIIYALKNVNLNIKEGEFVSIMGPSGSGKSTMLNIIGCLD..KPTEGEVYIDNIK.........TNDLD
MJ0796_M.janaschii       1                 MIKLKNVTKTYKMGEEIIYALKNVNLNIKEGEFVSIMGPSGSGKSTMLNIIGCLD..KPTEGEVYIDNIK.........TNDLD
GlcV_S.solfataricus      1               MVRIIVKNVSKVFKKGK..VVALDNVNINIENGERFGILGPSGAGKTTFMRIIAGLD..VPSTGELYFDDRL.........VASNG
SufC_E.coli              1                     MLSIKDLHVSVEDKAILRGLSLDVHPGEVHAIMGPNGSGKSTLSATLAGREDYEVTGGTVEFKGKD.........LLALS
SufC_T.thermophilus      1                     MSQLEIRDLWASIDGETILKGVNLVVPKGEVHALMGPNGAGKSTLGKILAGDPEYTVERGEILLDGEN.........ILELS
TM0544_T.maritima        1      MGSDKIHHHHHHMGAVVVKDLRKRIGKKEILKGISFEIEEGEIFGLIGPNGAGKTTTLRIISTLIK..PSSGIVTVFGKN.........VVEEP
MJ1267_M.janaschii       1               MRDTMEILRTENIVKYFGEFKALDGVSISVNKGDVTLIIGPNGSGKSTLINVITGFL..KADEGRVYFENKD.........ITNKE
BtuD_E.coli              1                       MSIVMQLQDVAESTRLGPLSGEVRAGEILHLVGPNGAGKSTLLARMAGMT...SGKGSIQFAGQP.............
HI1470_H.inluenzae       1                 MNKALSVENLGFYYQAENFLFQQLNFDLNKGDILAVLGQNGCGKSTLLDLLLGIH..RPIQGKIEVYQSIG.............
                                                                              Walker A

MsbA_S.typhimurium      86 LAS....LRNQVALVSQNVHLFN...DTVANNIAYARTEEYSREQIEEAARMAYAMDFINKMDNGLDT.IIGENGVL.LSGGQRQRIAIARALLRDS...
MsbA_E.coli             86 LAS....LRNQVALVSQNVHLFN...DTVANNIAYARTEQYSREQIEEAARMAYAMDFINKMDNGLDT.VIGENGVL.LSGGQRQRIAIARALLRDS...
Sav1866_S.aureus        90 TGS....LRNQIGLVQQDNILFS...DTVKENILLGR.PTATDEEVVEAAKMANAHDFIMNLPQGYDT.EVGERGVK.LSGGQKQRLSIARIFLNNP...
LmrA_L.lactis           71 LEN....WRSQIGFVSQDSAIMA...GTIRENLTYGLEGDYTDEDLWQVLDLAFARSFVENMPDQLNT.EVGERGVK.ISGGQRQRLAIARAFLRNP...
HlyB_E.coli             72 PNW....LRRQVGVVLQDNVLLN...RSIIDNISLAN.PGMSVEKVIYAAKLAGAHDFISELREGYNT.IVGEQGAG.LSGGQRQRIAIARALVNNP...
MetN_E.coli             73 SESELTKARRQIGMIFQHFNLLS...SRTVFG.NVALPLELDN...TPKDEVKRRVTELLSLVGLGDK.HD.SYPSN.LSGGQKQRVAIARALASNP...
HisP_S.typhimurium      84 DKNQLRLLRTRLTMVFQHFNLWS...HMTVLENVMEAPIQVLG...LSKHDARERALKYLAKVGIDER.AQGKYPVH.LSGGQQQRVSIARALAMEP...
MalK_P.horikoshii       80 P......KDRNISMVFQSYAVWP...HMTVYE.NIAFPLKIKK...FPKDEIDKRVRWAAELLQIEE..LLNRYPAQ.LSGGQRQRVAVARAIVVEP...
1VCI_P.horikoshii       81 P......KDRNISMVFQSYAVWP...HMTVYE.NIAFPLKIKK...FPKDEIDKRVRWAAELLQIEE..LLNRYPAQ.LSGGQRQRVAVARAIVVEP...
MalK_E.coli             72 P......AERGVGMVFQSYALYP...HLSVAE.NMSFGLKLAG...AKKEVINQRVNQVAEVLQLAH..LLDRKPKA.LSGGQRQRVAIGRTLVAEP...
ModC_A.fulgidus         67 P......ERRGIGFVPQDYALFP...HLSVYR.NIAYGLRNVE...RVER..DRRVREMAEKLGIAH..LLDRKPAR.LSGGERQRVALARALVIQP...
ModC_M.acetivorans      69 P......EKHDIAFVYQNYSLFP...HMNVKK.NLEFGMR.MK...KIKD..PKRVLDTARDLKIEH..LLDRNPLT.LSGGEQQRVALARALVTNP...
CysA_A.acidocaldarius   84 P......QKRNVGLVFQNYALFQ...HMTVYD.NVSFGLREKR...VPKDEMDARVRELLRFMRLES..YANRFPHE.LSGGQQQRVALARALAPRP...
MJ1267_E.coli           74 DDELTKIRRDKIGFVFQQFNLIP...LLTALE.NVELPLIFKYRGAMSGEERRKRALECLKMAELEER.FANHKPNQ.LSGGQQQRVAIARALANNP...
MJ0796_M.janaschii      74 DDELTKIRRDKIGFVFQQFNLIP...LLTALE.NVELPLIFKYRGAMSGEERRKRALECLKMAELEER.FANHKPNQ.LSGGQQQRVAIARALANNP...
GlcV_S.solfataricus     74 KLIVPPEDR.KIGMVFQTWALYP...NLTAFE.NIAFPLTNMK...MSKEEIRKRVEEVAKILDIHH..VLNHFPRE.LSGGQQQRVALARALVKDP...
SufC_E.coli             72 PED...RAGEGIFMAFQYPVEIPGVSNQFFLQTALNAVRSYRGQETLDRFDFQDLMEEKIALLKMPED.LLTRSVNVGFSGGEKKRNDILQMAVLEP...
SufC_T.thermophilus     74 PDE...RARKGLFLAFQYPVEVPGVTIANFLRLALQAKLGR....EVGVAEFWTKVKKALELLDWDES.YLSRYLNEGFSGGEKKRNEILQLLVLEP...
TM0544_T.maritima       84 HEV.....RKLISYLPEEAGAYR.......NMQGIEYLRFVAGFYASSSSEIEEMVERATEIAGLGEK.IKDRVSTY..SKGMVRKLLIARALMVNP...
MJ1267_M.janaschii      76 PAELYHYGIVRTFQTPQPLKEMTVLENLLIGEINPGESPLNSLFYKKWIPKEEEMVEKAFKILEFLKLSHLYDRKAGELSGGQMKLVEIGRALMTNP...
BtuD_E.coli             63 ......LEAWSATKLALHRAYLS.....QQQTPPFATPVWHYLTLHQHDKTRTELLNDVAGALALDDK..LGRSTNQ.LSGGEWQRVRLAAVVLQITPQA
HI1470_H.inluenzae      70 ..........FVPQFFSSPFAYS......VLDIVLMGRSTHIN...TFAKPKSHDYQVAMQALDYLNLTHLAKREFTSLSGGQRQLILIARAIASEC...
                                  Q-loop                                           Stuctural diverse region  C-loop        Pro-loop
```

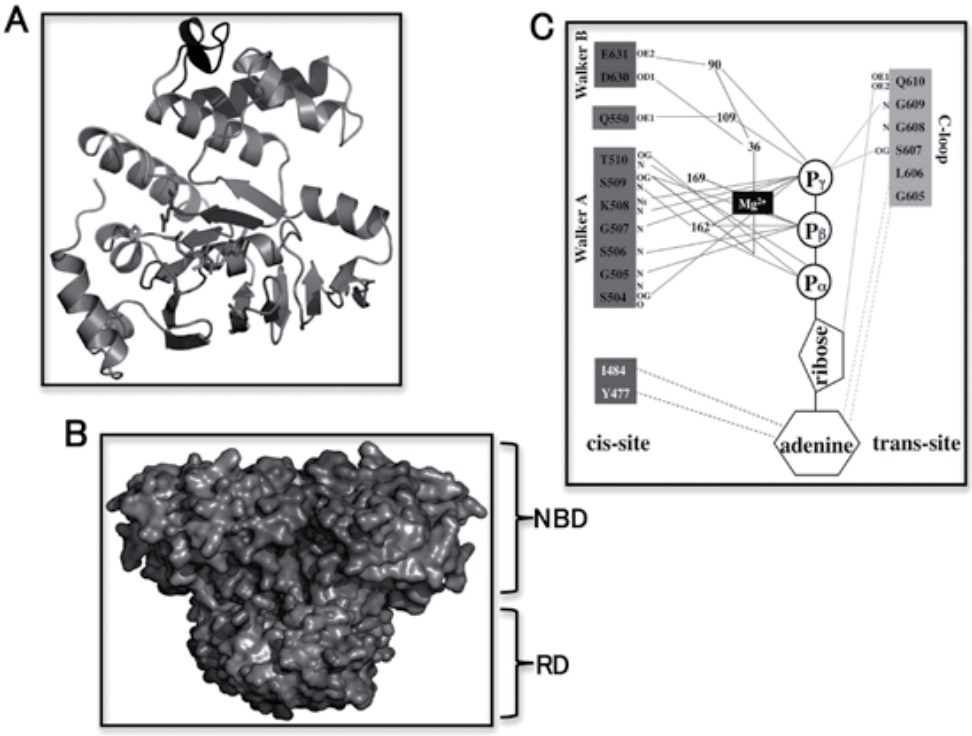

Figure 1.2 A Crystal structure of HisP, the nucleotide binding domain of the histidine permease from *S.* Typhimurium with bound ATP (pdb entry 1B0U). The helical domain contains the C-loop (pale green) and the structural diverse region (SDR; black) and is linked via the Q-loop (magenta) and the Pro-loop (orange) to the catalytic domain. The catalytic domain contains the Walker A (red) and Walker B (blue) motifs and the D-loop (cyan) as well as the H-loop (green). The glutamate at the end of Walker B and the histidine of the H-loop are depicted in stick-representation as they are crucial in ATP hydrolysis. **B** Structural superposition of the nucleotide free (grey) and ATP-bound (magenta) structure of the nucleotide binding domain MalK (pdb entries: 1Q1E, 1Q12). The NBDs come into close contact upon ATP binding whereas only minor changes can be detected in the regulatory domains (RD). **C** Detailed network of ATP coordination in the binding pocket of the HlyB-NBD. Solid lines indicate hydrogen bonds and dashed lines show van-der-Waals interactions. Colour-coding is equivalent to Fig. 1.2A. The black numbers indicate water molecules that are part of the extensive network of interactions. Letters next to the amino acid labels indicate involvement via main-chain or side-chain interactions. A colour version of this figure is located in the plate section at the back of the book.

We shall discuss the binding of the nucleotide in more detail since this molecule constitutes the energy source for transport and therefore a closer look is of great importance to understand how this molecular motor functions (Fig. 1.2C). In all P-loop NTPases (Vetter and Wittinghofer, 1999) the Walker A motif wraps around the phosphate moiety of the nucleotide. Acidic residues located at the end of the Walker B motif further coordinate the γ-phosphate moiety. Exceptionally important is the glutamate residue, which stabilizes and positions the γ-phosphate group, together with the H-loop histidine, in a position where the P-O-bond can be attacked. These two residues, glutamate and histidine, likely constitute a catalytic dyad essential for the final hydrolysis of

Figure 1.1 (opposite) Amino acid sequence alignment of the nucleotide binding domains of prokaryotic ABC transporters whose structures have been solved. The conserved motifs are colour-coded: Walker A (red), Q-loop (magenta), structural diverse region (SDR; black), C-loop (pale green), Pro-loop (orange), Walker B (blue), D-loop (cyan), and H-loop (green). The function of the distinct residues is explained in detail in the text. A colour version of this figure is located in the plate section at the back of the book.

ATP in all ABC-NBDs (Zaitseva *et al.*, 2005a). In addition, a glutamine residue from the Q-loop is also implicated in the hydrolysis of ATP. This, together with the glutamate of the Walker B, forms hydrogen bonds to a water molecule that could fulfill the role of the attacking water to break the P-O-bond between the γ- and β-phosphate of ATP. However, in addition to contacts between the phosphate residues of the nucleotide and the protein, the adenine moiety of ATP interacts with a tyrosine residue in the catalytic domain via π-π-stacking.

Interestingly, due to this rather nonspecific interaction, the ABC motor domains generally can bind different nucleotides (at least *in vitro*) even though with less affinity and therefore with reduced activity. The Pro-loop (orange) and Q-loop (magenta) shown in Fig. 1.1, as indicated above, serves as hinges between the helical and the RecA-like domain. If the structures of nucleotide free and ATP-bound NBDs are compared, a relative movement of the helical domain towards the catalytic domain is clearly visible. This conformational change is referred to as a 'rigid body movement' or 'nucleotide-mediated induced fit' (Fig. 1.2B) (Karpowich *et al.*, 2001).

NBD dimers and the catalytic cycle

To further investigate how the mechanism of ATP hydrolysis is accomplished it was essential to obtain structures of NBD dimers to investigate protein – protein interactions at the dimer interface and consequent structural changes upon formation of the complex. Several groups succeeded in crystallizing NBD dimers but not every assembly of the desired complex met the criteria expected for a physiological arrangement of the NBDs. From the information obtained from monomeric structures and biochemical studies it was clear that particular motifs should be in close contact in the dimers. Their absence in certain dimeric crystal structures could therefore be judged as non-physiological artifacts. For example, ortho-vanadate added to MalK (the NBD of the maltose importer) during the hydrolysis reaction becomes trapped in the position formerly engaged by the γ-phosphate of ATP and catalyses a photocleavage reaction. Analysis of the cleavage sites revealed that both the Walker A and the signature (LSGGQ) motif contribute residues to the ATP binding site (Fetsch and Davidson, 2002). Another hint indicating the importance of the C-loop in MalK came from mutagenesis studies showing that C-loop mutants had considerably reduced ATPase-activity (Schmees *et al.*, 1999). Surprisingly the monomeric structure of HisP showed that the Walker A motif and the C-loop were too far apart to interact with each other and a different dimer geometry was proposed (Hung *et al.*, 1998). Finally, the structures of the ABC proteins MJ0796 from *Methanococus jannaschii* (Smith *et al.*, 2002), MalK from *E. coli* (Chen *et al.*, 2003a), and the HlyB-NBD from *E. coli* (Zaitseva *et al.*, 2005a) were recognized to fulfill all the criteria necessary to represent a native conformation of the motor domain dimer of ABC transporters.

In order to represent an informative dimer ATP should be present in the structure but this is difficult to achieve with a protein specifically designed to hydrolyse this nucleotide. Thus, minor modifications to the protein were necessary to obtain suitable crystals. This problem was circumvented by mutating amino acids essential for hydrolysis of ATP. For MJ0796 the glutamate residue at the end of the Walker B motif was changed to a glutamine, while for the HlyB-NBD the histidine of the H-loop was mutated to an alanine. In the case of the MalK structure, Mg^{2+} was omitted from the crystallization protocol. For MJ0796 and HlyB, these mutations resulted in proteins where the ATPase activity was completely abolished (Davidson and Sharma, 1997; Nikaido and Ames, 1999; Moody *et al.*, 2002; Zaitseva *et al.*, 2005b). However, solving a crystal structure of a protein is just the beginning – the interpretation of the three dimensional arrangement of the amino acid residues and hypotheses with respect to molecular function then arise, and the accuracy of these hypotheses is dependent upon having good biochemical data on the properties of the enzyme. With this in hand an informative picture of how these molecular machines carry out their function, can be obtained.

Now we may consider what insights have been revealed from the structures of the dimeric complex of the ABC motor domains. First of all it is clearly visible that the Walker A motif from one monomer and the C-loop of the second mono-

mer complement each other to form the binding pocket for ATP (see Fig. 1.1B). This organization of the two subunits is called a 'head-to-tail' arrangement and interestingly this was anticipated earlier via a molecular modeling approach (Jones and George, 1999), before the first correct structure of an NBD dimer was published. The Walker A motif forms extensive backbone and side chain interactions with all three phosphate moieties of the ATP. A conserved lysine residue of the Walker A interacts with the β- and γ-phosphates consequently fixing them in a defined orientation. The Walker B motif interacts mainly with the γ-phosphate of the nucleotide, as does the C-loop of the opposing monomer. Thus, ATP is sandwiched between the two NBD monomers and acts as molecular glue. Since the three phosphate moieties of ATP carry a distinct negative charge, which might result in electrostatic repulsion, a Mg^{2+} ion is coordinated by the β- and γ-phosphates of the nucleotide.

This Mg^{2+} cofactor is essential for hydrolysis and hence forms an extensive network of interactions (a detailed analysis of the interactions of ATP and Mg^{2+} with the HlyB-NBD is depicted in Fig. 1.2C). A residue from the Walker A motif interacts with water molecules and the β- and γ-phosphate residues constitute the octahedral coordination sphere of the Mg^{2+} ion – in total six oxygen atoms from the surrounding residues have the ideal distances and angles to provide this octahedral coordination (Harding, 2000). Two further water molecules connect the γ-phosphate with the Walker B motif and the Q-loop. Possible analysis of the interaction between glutamine 550 from the Q-loop and aspartate 630 from the Walker B in the HlyB-NBD (Zaitseva *et al.*, 2005a) detects only van-der-Waals interactions in the nucleotide free form of the protein, while binding of ATP promotes hydrogen bond formation between those two residues, indicating a structural reorganization. Indeed, this change can be linked to an induced fit mechanism first described for MJ1267 that is assumed now to be a general feature of the motor domains of ABC transporters (Karpowich *et al.*, 2001). The Q- and Pro-loops function as linkers mediating an inward rotation of the helical domain of roughly 20° when ATP binds (Fig. 1.2B) (Lu *et al.*, 2005; Zaitseva *et al.*, 2005a). Thus, the effect of the presence of the γ-phosphate at the Walker B site is transferred to the Q-loop glutamine causing the rigid body movement of the helical domain. Through this mechanism the NBD 'senses' and responds to the binding of ATP. An additional structural change that also occurs during the conversion from the nucleotide free to the ATP-bound state has been observed in the NBD of the ABC transporter Haemolysin B. This is the conversion of the last three amino acids of the Walker A motif from a 3_{10} helix towards a regular α-helix upon binding of ATP. The 3_{10} helix/α-helix conversion is expected to be a mechanism to control the ATPase activity of this motor domain *in vivo*. Other examples for structures disturbed are, for example, SufC from *T. thermophilus* where a similar transition at the Walker B motif occurs (Watanabe *et al.*, 2005) and the regulatory inserts and extensions in the NBD of CFTR (Lewis *et al.*, 2004).

The most prominent inter-protein interaction in the ABC domain is obviously the completion of the nucleotide binding site when ATP is sandwiched between the Walker A and the C-loop. A second motif highly characteristic for ABC proteins in addition to the C-loop is the D-loop, which is almost exclusively involved in interactions between the two monomers. Close proximity between the D-loop and the highly conserved histidine residue involved in ATP hydrolysis lead to the assumption that information about the functional state of one ATP binding site is transferred to the other monomer. The histidine may therefore not only act catalytically but also as a phosphate sensor transmitting information about progress in the chemical reaction.

In order to ensure that all the inter-protein interactions described above are relevant to a hydrolysis competent NBD dimer, an analysis of the surface accessible solvent area (ASA) was performed. The results demonstrated that the buried protein surface at the dimer interface is in the range for protein-protein complexes and therefore not an artifact of crystal contacts (Bahadur and Zacharias, 2008). Additionally, it has also been shown that a specific microenvironment at the nucleotide binding sites is established upon ATP binding and dimerization. Local pK_a values of amino acid site chains (mostly in the Walker A and Walker B region as well as in the D- and H-loop) and the intrinsic pK_a of the ATP

molecule are presumably essential to provide the basis for efficient catalysis (Hanekop *et al.*, 2006). A final remark concerning ATP binding should be made. Thus, for at least the NBDs, positive cooperativity of ATP hydrolysis has been demonstrated. This is consistent with dimerization being dependent on nucleotide binding to both NBDs although only one composite site competent for ATP hydrolysis is found in certain systems (Davidson *et al.*, 1996; Liu *et al.*, 1997; Steinfels *et al.*, 2004; Zaitseva *et al.*, 2005a). This aspect will be discussed later in this chapter.

Further studies have revealed the structures of monomeric and dimeric NBDs crystallized with and without nucleotide (ADP/ATP) or with non-hydrolysable substrates (AMP-PNP). But the description of how residues are arranged in a crystal structure are not sufficient to understand the mechanism of catalytic activity since they represent only a snap-shot of the catalytic cycle of the NBDs and must be complemented by relevant biochemical experiments. Thus, structural studies plus insights from biochemical studies have yielded a model of the catalytic cycle of the motor domains of ABC transporters. This model basically explains the molecular steps involved in generating and utilizing the energy provided by ATP binding/hydrolysis necessary to promote the essential structural changes required for transport (Fig. 1.3) (Lu *et al.*, 2005; Zaitseva *et al.*, 2006).

What might be the precise nature of the chemical mechanism of ATP hydrolysis? It has been shown that the NBDs are capable of cleaving the γ-phosphate of ATP and that the motor domains display positive cooperativity during this process (Davidson *et al.*, 1996; Nikaido *et al.*, 1997; Benabdelhak *et al.*, 2005; Zaitseva *et al.*, 2005b) and that a chemical reaction rather than diffusion controlled processes is the rate-limiting step in hydrolysis. In fact, two general mechanisms can be proposed to explain the hydrolysis of ATP: 1. general base catalysis (Fersht, 1997), and 2. substrate assisted catalysis or SAC (Dall'Acqua and Carter, 2000). The first candidate for the general base catalysis in this case is the glutamate at the end of the Walker B motif, which was proposed to be responsible for proton abstraction or polarization of a catalytic water mediating contact between the γ-phosphate and the Walker B glutamate (Orelle *et al.*, 2003). In this model, this process should be rate-limiting in terms of enzyme kinetics. In studies with the HlyB-NBD, designed to distinguish between a general base and SAC mechanism, hydrolysis rates in D_2O (rather than H_2O) and pH profiles of activity of the WT and an E→Q mutant, were determined. This led to the conclusion that substrate assisted catalysis is the predominant mechanism in hydrolysis of ATP (Zaitseva *et al.*, 2005a). Importantly in this case, the pK_a values of the microenvironment at the ATP binding site support the idea of SAC. The C-loop, which completes the composite ATP binding site, drastically influences the pK_a values of both amino acid residues and ATP (Hanekop *et al.*, 2006).

In the course of the above described and similar experiments from other groups (Shyamala *et al.*, 1991; Davidson and Sharma, 1997; Moody *et al.*, 2002; Verdon *et al.*, 2003) it became clear nevertheless that both the glutamate at the end of the Walker B and the H-loop histidine play crucial roles in catalysis and likely form a 'catalytic dyad'. The histidine residue forms hydrogen bonds with the glutamate side chain and the γ-phosphate. These interactions position and stabilize the key residues, including the glutamate, into the optimum orientation for cleaving the P-O bond of the γ-phosphate. However, whether the histidine fixes the glutamate in a position competent for hydrolysis, or *vice versa,* remains an open question. Certainly, it is clear that deletion of either one of these residues can greatly decrease or abolish ATPase activity due to the resulting higher intrinsic flexibility of either the glutamate or the histidine preventing a correct alignment for catalysis of ATP (Smith *et al.*, 2002; Zaitseva *et al.*, 2006).

Comparison of ABC-NBD dimer structures reveals that either ADP or ATP is bound in the respective substrate-binding site, as expected from the mechanism of nucleotide-induced dimerization observed in biochemical experiments. Unfortunately, despite detailed insights into the network of interactions between nucleotide and NBD described above, no conclusion can be drawn whether one or two ATP molecules are hydrolysed per catalytic cycle of the ABC protein. Biochemical analyses similarly provide no definite conclusion with respect to the stoichiometry of

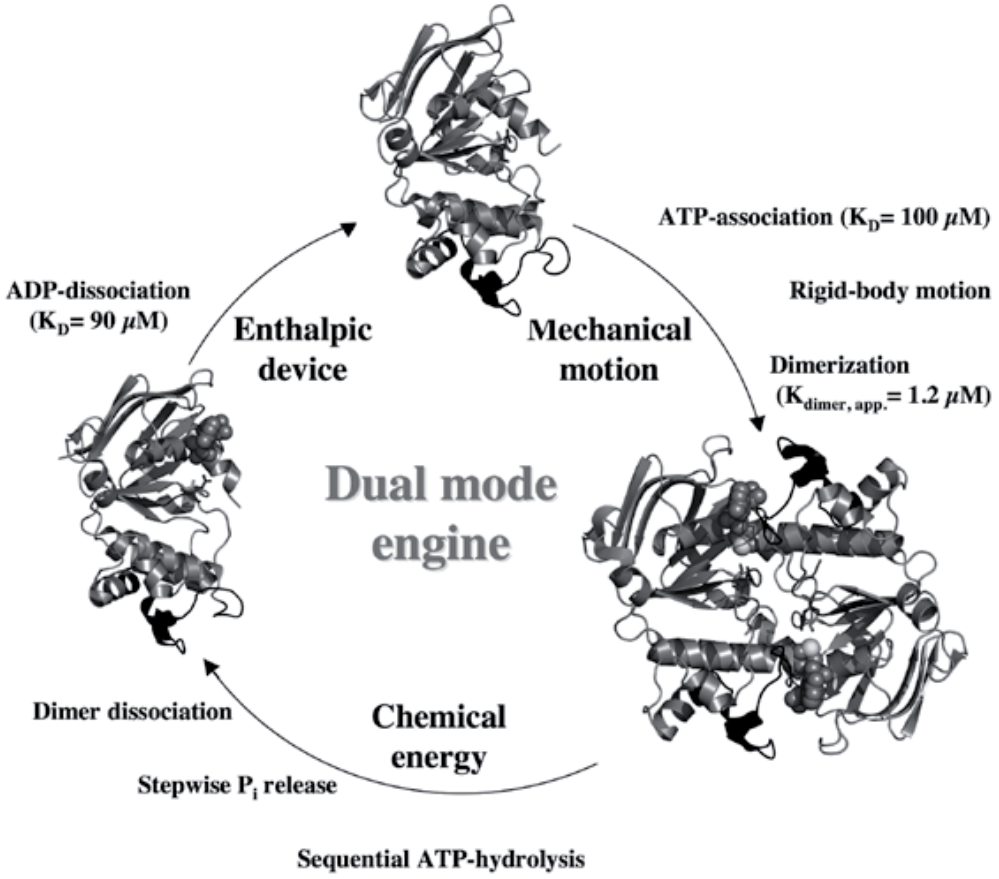

Figure 1.3 Schematic representation of the catalytic cycle of the HlyB-NBD. Colour-coding is identical to Fig. 1.2A. The cycle starts with the nucleotide free state of the monomer (pdb entry: 1MT0). Binding of ATP to both monomers induces dimer formation (ATP in brown and Mg^{2+} in yellow; pdb entry: 1XEF). After hydrolysis of ATP the dimer dissociates and ADP is subsequently released (pdb entry: 2FF7). A detailed description of each step can be found in the corresponding section of the text. A colour version of this figure is located in the plate section at the back of the book.

ATP consumption (Senior *et al.*, 1995; Sauna and Ambudkar, 2001; Patzlaff *et al.*, 2003;). This difficulty is even more evident when huge allocrites are to be transported across the membrane, like the 110 kDa toxin HlyA (Holland *et al.*, 2003), where additionally the proton motive force is apparently required during transport (Koronakis *et al.*, 1991).

Our journey through the catalytic cycle of an ABC-NBD starts with the apo (i.e. nucleotide free) form of the motor domain (Fig. 1.3). When ATP is present and binds in its cognate binding pocket, dimerization and an inward rotation of the helical domain occur. The Q-loop and Pro-loop regions are involved in this movement that affects both subdomains of the NBD. When ATP is hydrolysed and ADP remains in the binding pocket, the Walker B and D-loop region, together with helix 6, in addition to the Q- and Pro-loop, are involved in structural realignment and dimer dissociation. However, an ADP-bound dimer is predicted to be unstable due to steric clashes of the opposing D-loops. Alternatively, in the structure of the MJ0796 dimer it was proposed that a negative charge distribution, resulting from ATP hydrolysis, accumulates with an electrostatic

potential sufficiently high to lead to disruption of the NBD dimer (Smith *et al.*, 2002). This proposal, however, is not compatible with the electrostatics observed in the HlyB-NBD dimer structure (Zaitseva *et al.*, 2006).

Following dimer disruption and in order to reset the NBD to the nucleotide free state, the Walker B and D-loop region, as well as helix 6, appear to act as mechanical hinges to return to the initial state. As pointed out before, the Q- and Pro-loops connect the catalytic domain to the helical subdomain, which in turn interacts with the transmembrane domain. On the other hand the Walker B and D-loop regions are also involved in contacts between the two monomers. Together, all these key motifs provide possible communication pathways in cis and in trans during every step of the catalytic cycle. This applies to interactions both between the motor domains and between the NBDs and the transmembrane domains. An interesting feature of helix 6 in the HlyB-NBD is its structural displacement in the ADP-bound state that is not present in the nucleotide free or ATP-bound state. Since the affinity of ADP for the NBDs is similar to that of ATP, spontaneous dissociation of the dinucleotide is unlikely. For this reason we suggest that some chemical energy from ATP hydrolysis might be stored in helix 6 acting as a potential mechanical spring that ultimately promotes the release of ADP and restores the resting state ready for the next ATP-hydrolysis/transport cycle (Lu *et al.*, 2005; Zaitseva *et al.*, 2006).

Previous extensive analysis of the NBD dimer structures of MJ0769, MalK and HlyB (Smith *et al.*, 2002; Chen *et al.*, 2003a; Zaitseva *et al.*, 2006), interestingly, revealed cavities inside the NBD dimer that led to a surprising discovery. This was the presence of tunnel-like formations extending from the surface to the inside of the NBDs leading directly to the ATP binding pocket. Thus, the adenine moiety is completely solvent accessible in these structures whereas the ribose and the phosphate moieties are shielded from the solvent. Moreover, two amino acid residues (D551 and R611 for the HlyB-NBD) form a salt bridge about 6 Å above the γ-phosphate, creating a dead end for the tunnel preventing it reaching the terminal phosphate residue. This scenario is true also for the MJ0796, MalK, and HlyB-NBD dimers crystallized in the presence of ATP. However, the analysis is more interesting when we consider the additional effect of Mg^{2+}. So far, there is only one NBD dimer structure available with ATP/Mg^{2+} bound. Consequently, the following discussion is based on the analysis of the HlyB-NBD. Thus, in particular in this ATP/Mg^{2+} bound state the asymmetry of interactions between the monomers in terms of NBD-ATP and NBD-NBD contacts is significantly increased compared to the ATP-bound structure. This is also reflected in the cavity analysis in the presence of Mg^{2+} where the salt bridge between D551 and R611 is broken in one of the two monomers.

In the dimer crystal structure of the HlyB-NBD with ATP/Mg^{2+} present, all the prerequisites for ATP hydrolysis are in place – with one major exception, the histidine essential for catalysis in this structure is mutated to an alanine. The snap-shot captured in these circumstances may reflect the state just before elimination of the terminal phosphate of ATP and the tunnel in one monomer is continuous all the way to the phosphate group. This architecture therefore allows for diffusion of free phosphate out of the NBD leaving ADP in the binding pocket. Interestingly, mutation of these amino acids engaged in this potential gating mechanism in the HlyB-NBD (D551A and R611A) abolishes the positive cooperativity observed for this and other ABC-NDBs (Davidson *et al.*, 1996; Nikaido *et al.*, 1997; Zaitseva *et al.*, 2005b). Based on all these data we can propose a 'sequential mode' of ATP hydrolysis in accordance with earlier biochemical studies of other ABC transporters (Smith *et al.*, 2002; Chen *et al.*, 2003a; Janas *et al.*, 2003). A prerequisite of the model is that the dimer is stable with one ATP and one ADP bound. Dissociation in this case should occur at the latest after hydrolysis of the second ATP, consistent with the second tunnel being still occluded by a salt bridge. The principle of an asymmetric phosphate exit tunnel in the NBD dimer was demonstrated for the prokarytic ABC transporter HlyB from *E. coli* (Zaitseva *et al.*, 2006) and now more recently with the mammalian transporter associated with antigen processing (TAP) from *Rattus norvegicus* (Procko and Gaudet, 2008).

Conformational changes in the NBDs

As a complementary approach to the analysis of the mechanism of action of the ABC-NBDs, electron paramagnetic resonance (EPR) experiments have been performed to elucidate possible conformational changes occurring during the catalytic and transport cycles (Grote *et al.*, 2008). Complementary cross-linking studies with linkers of different length support the measured distance changes between the NBDs during the transport cycle determined by EPR. Similar experiments were conducted with the lipid flippase MsbA and the results indicated a significant closing motion of the NBDs upon hydrolysis of ATP (Borbat *et al.*, 2007). For the $MalFGK_2$ complex, cysteine replacements inside the Q-loop sequence were generated and EPR spectra recorded for the apo-, ATP-bound-, vanadate-trapped- and post-hydrolysis states of the complete maltose importer. The results showed that upon transition from the apo- to the ATP-bound/vanadate-trapped state a decrease in distance between the NBDs of roughly 1 nm was observed. Thus, both NBDs appear to come into closer contact upon nucleotide binding (Fig. 1.2B). In the crystal structures of apo- compared to ATP-bound MalK a closing motion of 4 Å between the Walker A and the C-loop of opposing monomers was observed (Chen *et al.*, 2003a; Lu *et al.*, 2005). In contrast, spin labels placed on the surface of MalK through cysteine mutants or the use of wild type cysteines in the regulatory domain of MalK (for a definition of regulatory domain see below), showed no movement when ATP was bound at the dimer interface in the absence of the transport domain. In the post-hydrolysis state when ADP is bound and the ABC transporter is reset, an increase in distance between the two NBDs was detected in the EPR spectra.

Strikingly, the motor domains of the maltose importer have an additional C-terminal domain of roughly 150 amino acids, the so called regulatory domain. Such C-terminal elongations can also be found in other ABC transporters. It has been shown that these extensions play a role in the activity of the transporter when they bind substances that reversibly inhibit the transporter (Gerber *et al.*, 2008) or interact with transcription factors and hence regulate the expression of the transport system at the genetic level (Joly *et al.*, 2004; Richet *et al.*, 2005). In summary, these results encourage the idea of a tweezer-like motion of the NBDs during the transport cycle as proposed earlier by Chen *et al.* (Chen *et al.*, 2003a). In this model, the NBDs are connected through a specific regulatory domain at the C-terminus of MalK in the cytoplasm, to a pivotal-point at the membrane interface. It is proposed that binding of ATP induces movements of the NBDs towards each other without affecting the regulatory domain in terms of a major structural reorientation. With the regulatory domain fixed and the NBDs moving the picture of a tweezer-like motion emerges.

Substrate binding proteins (SBP) / periplasmic binding proteins (PBP)

Surprisingly, ABC importers are only found in prokaryotes and archaea (Davidson and Chen, 2004; see also Chapters 2 and 3 for further details). Nevertheless, they are vitally important, delivering nutrients and trace elements to the cells. The auxiliary binding proteins transfer the allocrite to the cognate transporter and therefore ensure substrate specificity and transport directionality (Boos and Lucht, 1996). In the case of Gram-positive bacteria possessing only a single cell membrane, the substrate binding proteins (SBPs) are tethered to the membrane via a lipid anchor (Boos and Lucht, 1996; Gilson *et al.*, 1988; Kempf *et al.*, 1997) or covalently attached to the transmembrane domain of the ABC transporter in some cases (van der Heide and Poolman, 2000). In Gram-negative bacteria, ABC-allocrites must first cross the outer membrane and this is facilitated by specific porins, proteins present in the outer membrane. The binding proteins necessary for the next step are located in the periplasm and are therefore sometimes referred to as periplasmic binding proteins (PBPs). To ensure effective delivery of substrates to the transporter in the inner membrane the concentration of binding proteins is in great excess compared to the amount of ABC transporters. For the maltose import system there are approximately 30,000 SBPs per 1000 molecules of the ABC transporter (Treptow and Shuman, 1985).

The mode of action of binding proteins is rather 'simple'. First, the molecule can be divided into two subdomains that are linked via one, two, or three segments. In general, the subdomains contain a five-stranded antiparallel β-sheet that is surrounded by α-helices. The substrate/allocrite binding site is located between both subdomains (also referred to as lobes). Upon binding of the substrate molecule both lobes move towards each other in a fashion described as a 'Venus fly trap' mechanism (Sack *et al.*, 1989; Miles *et al.*, 2002). Without substrate the binding proteins exist largely in the open conformation with both subdomains spread apart (Fig. 1.4A and B) (Quiocho and Ledvina, 1996).

In the following part of the chapter, we shall describe in detail the well studied BtuF and MalE (MBP, maltose binding protein) as typical examples of SBPs. BtuF is the binding protein of the cognate ABC transporter BtuCD from *E. coli* and resides in the periplasm. Both subdomains of BtuF consist of a central five-stranded β-sheet surrounded by α-helices connected by a single α-helix and thus belongs to the so-called group III SBPs (Lawrence *et al.*, 1998; Lee *et al.*, 1999; Clarke *et al.*, 2000;). This class of SBPs apparently does not undergo major structural changes upon ligand binding due to restrictions of the helices spanning the back of the protein. In fact, in the case of BtuF no opening of the lobes was observed in the apo-form (Karpowich *et al.*, 2003) compared to the ligand-bound form of the SBP (Borths *et al.*, 2002). However, a significant change in the organization of BtuF occurs when it is co-crystallized with its cognate ABC transporter (BtuCD). In this complex, the lobes of

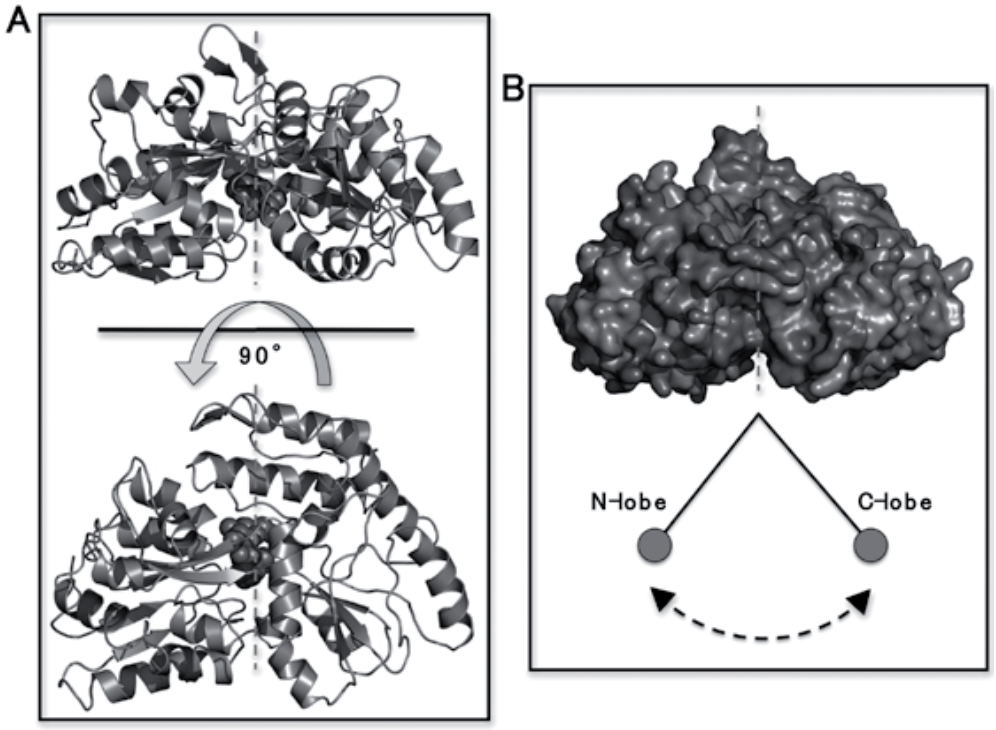

Figure 1.4 A In the upper part the side view of the periplasmic binding protein BtuF with bound vitamin B_{12} (magenta) is shown (pdb entry 1N2Z). The five-stranded antiparallel β-sheets are depicted in orange and blue, respectively. N- and C-lobe are connected by loop regions; here shown in green. In the lower part BtuF is rotated about 90° to look at the protein from above. **B** Structural superposition of the ligand-free (grey) and ligand-bound (blue) structure of the maltose binding protein. Upon binding of maltose a domain displacement leading to closure of the lobes of roughly 30° is observed. A colour version of this figure is located in the plate section at the back of the book.

BtuF are spread approximately 4 Å further apart compared to the crystal structure of BtuF alone (Hvorup *et al.*, 2007). The substrate binding site for vitamin B_{12} is located in a deep cleft between both lobes of BtuF (Borths *et al.*, 2002) and each subdomain contributes three aromatic residues that interact with vitamin B_{12} in the binding pocket. Despite the fact that even in the presence of BtuCD only a small structural change is induced in BtuF, this seems to be sufficient to displace the ligand. Periplasmic loops from the transmembrane domains of BtuCD that invade the substrate binding site also participate in transferring B_{12} to the transmembrane translocation pore. For the Zn^{2+} SBP TroA a similar minor rearrangement is sufficient to displace the ion into the tranlocation pore (Lee *et al.*, 1999; Lee *et al.*, 2002). Interestingly, positive cooperativity and enhanced rates of transport can be observed when two or even more copies of a SBP are fused to the TMD of an ABC transporter (Biemans-Oldehinkel and Poolman, 2003).

The crystal structures of MBP in an open and a closed state were dependent on the presence of maltose (Quiocho *et al.*, 1997; Sharff *et al.*, 1992). In fact, it has long been assumed that an equilibrium between those two states exists in solution even in the absence of a suitable ligand. However, it took 15 years before this hypothesis was supported with the help of nuclear magnetic resonance paramagnetic relaxation enhancement (NMR-PRE) experiments and finally the results were surprising (Tang *et al.*, 2007). Indeed, a minor species of MBP in a closed-like conformation without substrate could be detected due to the convergence of the two lobes. However, this species, which is in rapid equilibrium with the open (ligand-free) form, is different from the holo (ligand-bound) state. Notably, since the ligand binding site is made up of negatively charged residues and consequently the convergence of these residues towards each other is energetically unfavorable. Therefore, the orientation of both lobes is distorted with respect to each other, exposing the negatively charged residues of one lobe to the solvent. In fact, a crystal structure of MBP exists where the ligand is bound only to the C-terminal lobe of the apo conformation of the binding protein (Duan and Quiocho, 2002).

The binding of maltose by MBP is necessary to bridge both lobes and induce domain closure. Thus, the analysis of mutants demonstrated that the stability of MBP decreases upon closure when no ligand is present, due to unfavorable exposure of distinct amino acid side chains (Millet *et al.*, 2003). In contrast, a different mechanism was observed in the glucose/galactose binding protein where a water-network mediates protein–ligand interactions and therefore the data from MBP cannot easily be transferred to the glucose/galactose SBP (Flocco and Mowbray, 1994; Quiocho and Ledvina, 1996).

An important property of the binding proteins is thought to be their participation in triggering the translocation process upon interacting with the TMDs of the transporter. Consequently, the structural characterization of transporters in complex with their SBPs has been a major goal in understanding ABC import systems. For further information on the mechanism of action and properties of SBPs several reviews are available (Boos and Lucht, 1996; Felder *et al.*, 1999; Quiocho and Ledvina, 1996).

Structure and functional analysis of ABC transporters

ABC importers

Crystallization of proteins is always a challenge – taking a complex molecule out of its dedicated environment (in the case of membrane proteins with the help of large amounts of detergents), concentrating it to high concentrations and precipitation under conditions leading to crystals, followed by exposure to an ultra-high-energetic x-ray beam, can easily lead, at least occasionally, to the appearance of non-physiological states of the desired protein. Nonetheless, roughly 53,000 protein structures are now present in the Protein Data Bank to date (http://www.rcsb.org) although only 168 entries are for membrane proteins (http://blanco.biomol.uci.edu/Membrane_Proteins_xtal.html).

After at the last 15 years of accumulating biochemical knowledge of ABC transport systems, and more recently the elucidation of several crystal structures of NBDs, the atomic structure of an intact ABC transporter was eagerly awaited. Finally, the first such crystal structure

was published in 2001 at a resolution of 4.5 Å in the absence of nucleotide and allocrite (Chang and Roth, 2001). The ABC transporter MsbA transports lipid A to the outer leaflet of the *E. coli* envelope and cells die if lipid A accumulates in the inner leaflet of the membrane, as a result of mutations or complete loss of MsbA. Disappointingly, the crystal structure of MsbA did not agree with biochemical data or MD simulations (Campbell *et al.*, 2003; Haubertin *et al.*, 2006; Stenham *et al.*, 2003) and was retracted in 2006 due to problems in data analysis. The structure was re-published in 2007 at a resolution of 3.7 Å with AMP-PNP bound to the NBDs (Ward *et al.*, 2007). The next crystal structure of an ABC transporter was published one year later (Locher *et al.*, 2002). This was an importer for vitamin B_{12} from *E. coli*, BtuCD (Fig. 1.5A). The structure was solved at 3.2 Å resolution and was completely different from MsbA. The BtuCD structure consists of two copies of BtuC, the transmembrane domain and two copies of the motor domain, BtuD. The transmembrane subunit (BtuC) consists of ten transmembrane helices making up a total of 20 helices in the functional dimer.

What might be the function of accessory transmembrane helices, compared to the more usual number of 12? This structure of Btu was without bound nucleotide in the NBDs and also without allocrite but cyclovanadate, known to inhibit ABC-ATPases, is bound to the motor domains. The TMDs of this BtuCD structure are open towards the periplasm and closed towards the cytoplasm of the cell and this was interpreted to be an equivalent to the ATP-bound state. As discussed above, when ATP is bound to the NBDs, dimer formation is induced and consequently the interface of dimerization is buried from the solvent (Smith *et al.*, 2002; Chen *et al.*, 2003a; Zaitseva *et al.*, 2005a). In fact, the solvent

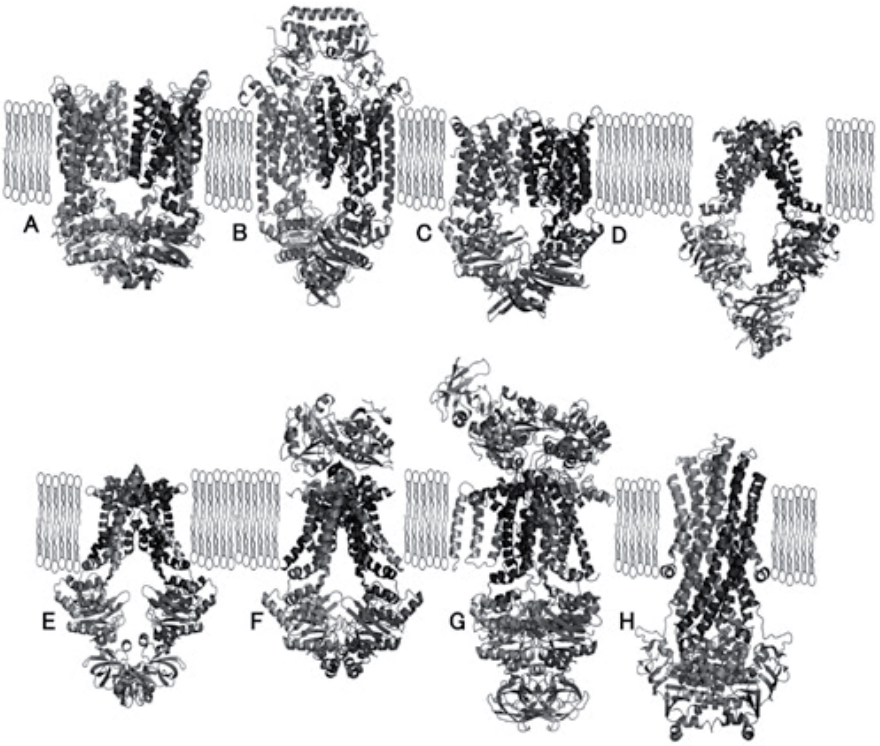

Figure 1.5 Crystal structures of ABC transporters. The importers **A** BtuCD, **B** BtuCD-F, **C** HI1470/1471, **D** MetNI, **E** ModBC, **F** ModBC-A, **G** MalFGK-E, and the exporter **H** Sav1866 are depicted. More information about a particular transporter can be found in the respective section of the chapter. A colour version of this figure is located in the plate section at the back of the book.

accessible surface area of the BtuD interface was about 740 Å^2 which pointed towards crystal induced contacts rather than a physiological protein–protein interface (Bahadur and Zacharias, 2008). Nonetheless, this apparently more authentic structure of an ABC transporter revealed some important and interesting aspects. Viewed from the periplasmic side, each TMD has three exposed and conserved arginines that can interact with two glutamates, one on the very left and one on the right hand side of the binding protein BtuF (Borths *et al.*, 2002; Locher *et al.*, 2002). The substrate translocation pathway appears to be formed by helices five and ten from opposing BtuC subunits, respectively (Fig. 1.6A). TM5 of one subunit packs against helix 10 of the second TMD. The resulting inward-facing cavity is large enough to incorporate the substrate vitamin B_{12} (Fig. 1.7A and B).

A closer look at the transmembrane part of BtuCD reveals an eye-catching structural element between TM helix 6 and TM helix 7. About 16 amino acids form an L-shaped helix-turn-helix motif (the 'L-loop' motif) which interacts extensively with the structurally diverse region (Schmitt *et al.*, 2003) in the helical domain of the NBDs (Fig. 1.8C). Examining the sequence of the L-loop reveals that this structural element contains the importer characteristic EAA-motif described earlier for bacterial importers (Mourez *et al.*, 1997). Thus, structural changes described for the helical domain of NBDs during the catalytic cycle may be transduced to the membrane embedded part of the transporter via interaction with the L-loop. Equally, a reverse rearrangement of distinct TMD segments upon allocrite binding or its subsequent release could be envisaged to be communicated to the motor domains.

It took five years before the next structure of an ABC importer was solved (Pinkett *et al.*, 2007). This was a putative metal-chelate-type ABC transporter HI1470(NBD)/1471(TMD) from *Haemophilus influenzae* (Fig. 1.5C) that displays high sequence identity with BtuCD, and both proteins are members of the same binding protein dependent transporter family. However, the ligand of HI1470/1471 has not been identified so far. The resolution of 2.4 Å for the HI1470/1471

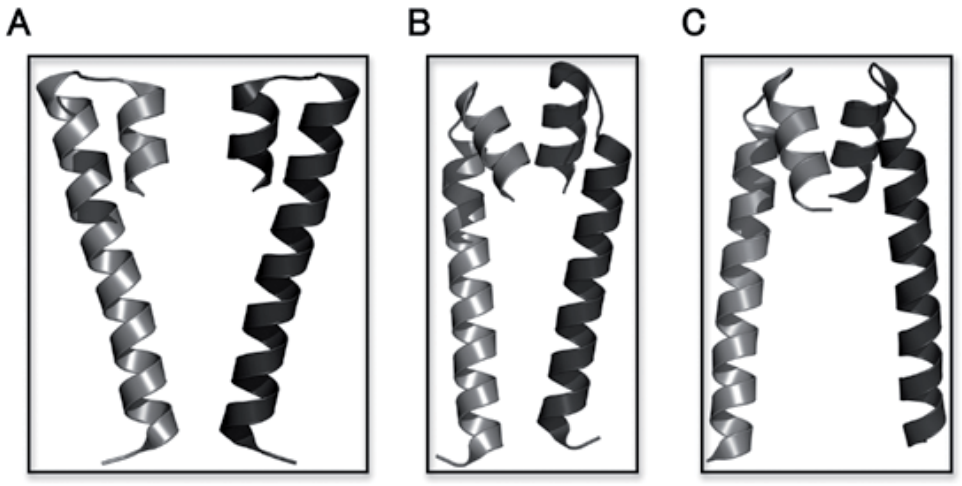

Figure 1.6 Helix 5/5a of the ABC importers has a pivotal role in forming the translocation pore **A** BtuCD, **B** BtuCD-F, and **C** HI1470/1471. The structure of BtuCD **A** was crystallized in an outward facing conformation with the translocation pore accessible from the periplasm. The structure of HI1470/1471 **C** reveals an inward facing conformation where the translocation pathway is only open to the cytoplasm. Figures **A** and **C,** where only helices 5 and 5a are depicted, show the involvement of this structural element in a postulated gating mechanism. In **B** the arrangement of the helices from the BtuCD-F structure is shown. Interaction of the substrate binding protein appears to provoke a conformation of the TMDs where the translocation pore is accessible neither from the periplasm nor the cytosol. The light and dark shaded helices belong to different transmembrane domains of the transporter.

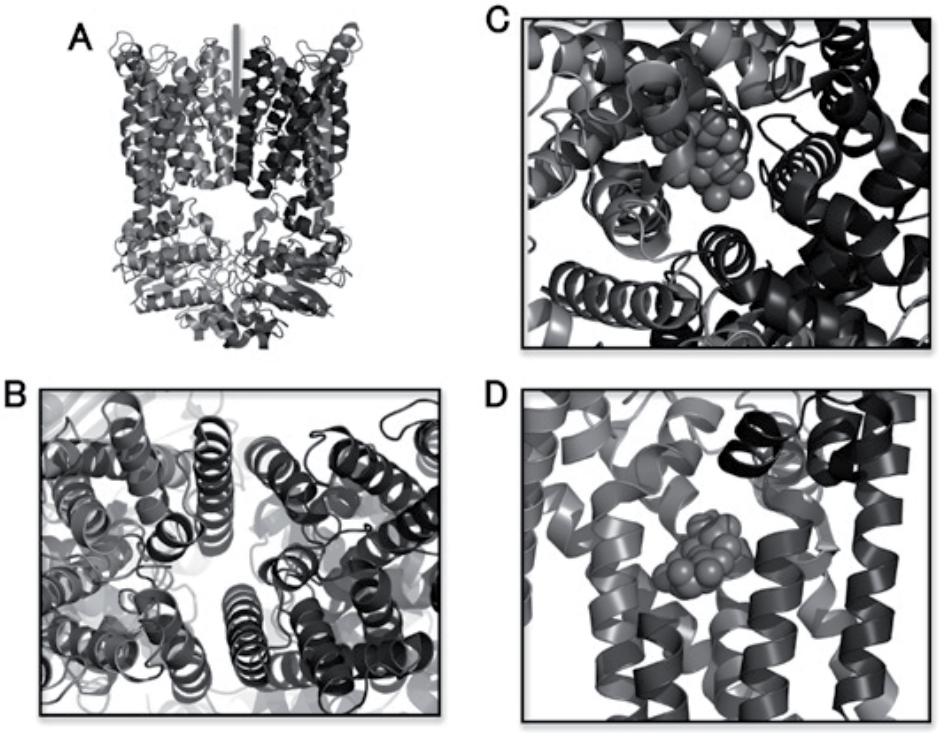

Figure 1.7 A Quaternary structure of the vitamin B_{12} importer BtuCD. **B** BtuCD is viewed from above through the postulated substrate translocation pore. Helices from each TMD subunit lining the translocation pore are coloured red and blue, respectively. **C** View from above into the translocation pore of the $MalEFGK_2$ transporter with bound maltose (magenta). **D** Side view of the maltose binding site in the transmembrane domains of the $MalEFGK_2$ importer complex. For clarity some helices have been omitted. A colour version of this figure is located in the plate section at the back of the book.

structure is a substantial improvement in comparison to BtuCD. Moreover, HI1470/1471 composed of two copies of HI1470 and HI1471, respectively, is crystallized in an inward facing conformation. Interestingly, cavity analysis of the outward facing conformation of BtuCD and the inward facing state of HI1470/1471, both resulted in a hypothetical allocrite translocation pore formed by the transmembrane domains of approximately 10 Å at the widest point. In contrast to BtuCD, the transmembrane domains of HI1470/1471 are composed of ten helices and TM5 and TM10 mediate bulk contact between both TMD subunits. In HI1470/1471, TM-helix 5 deviates about 20° from its position in the BtuCD structure (Fig. 1.6C). This change implies a reorganization of the whole transmembrane domain architecture resulting in the inward facing conformation of HI1470/1471. Further differences include the relative orientation of the NBDs which are further apart in HI1470/1471 compared to the BtuCD structure. This arrangement likely presents therefore the post hydrolysis state of the NBDs after cleaving off the γ-phosphate of ATP (Chen *et al.*, 2003a; Lu *et al.*, 2005; Pinkett *et al.*, 2007).

The interpretation of the crystallized states of these proteins inevitably has to be highly descriptive. This is particularly so in the case of HI1470/1471, which is presumed to be a metal-chelate transporter. This assumption is based only on sequence homology and unfortunately, there is no biochemical data and no allocrite identified so far. Our ability to identify specific structural elements participating in a transition from an inward to an outward facing conforma-

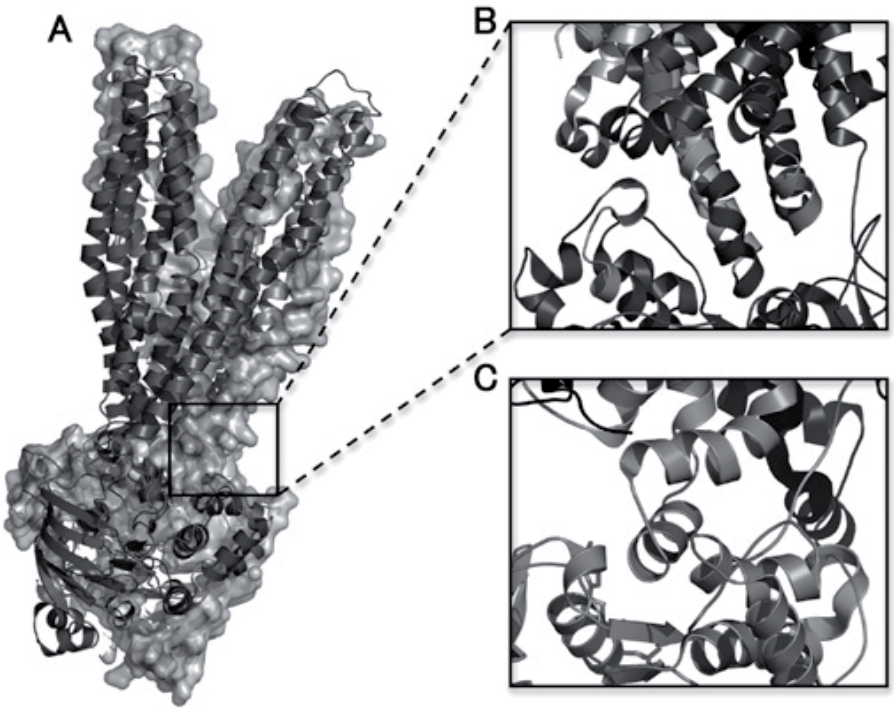

Figure 1.8 **A** Cartoon representation of the ABC exporter Sav1866. **B** The inset is a magnification of the postulated interaction site between TMDs and NBDs. In blue and slate intracellular loops from both membrane subunits are shown. Residues in red represent the TEVGERG sequence found to interact extensively with the intracellular loops. The C-loop is depicted in pale green. **C** Interaction site between TMD and NBD of the $MalEFGK_2$ complex. The transmembrane part is shown in grey and the NBD in brown. In the L-loop from the transmembrane domain the EAA motif characteristic for ABC importers (red) is highlighted. The C-loop is depicted in pale green and the D-loop in cyan. A colour version of this figure is located in the plate section at the back of the book.

tion is therefore limited in this case. Nevertheless, structural changes can be deduced and these mainly involve rigid body movements arising from the different arrangement of the NBDs in BtuCD and HI1470/1471. In fact, we cannot exclude some contribution to the deduced rigid body motions that result from lateral pressure of detergent, compensating for the absence of the native membranous environment. Alternatively, a contribution to apparent rigid body motions could even be caused by crystal lattice contacts.

To sum up: although the structures of two distinct, albeit closely similar ABC transporters, are available in two states probably resembling the extreme scenarios of the transport process with an inward and outward facing configuration, these findings are not sufficient to reveal the mechanistic basis of the transport process. In 2007, one year after the structure of HI1470/1471 was published, BtuCD in complex with its cognate binding protein BtuF was solved (Fig. 1.5B) (Hvorup *et al.*, 2007). Additionally as shown in Fig. 1.5E, another putative ABC transporter $ModB_2C_2$ from *Velociraptor fulgidus*, responsible for molybdate import, in complex with the binding protein ModA expanded the list of ABC transporter crystal structures (Hollenstein *et al.*, 2007b; Gerber *et al.*, 2008). Last but nor least, Fig. 1.5H shows the complex of MalFGK, together with the maltose binding protein in the presence of substrate and ATP/Mg^{2+} that has recently been solved (Oldham *et al.*, 2007).

BtuCDF was resolved to 2.6 Å and displays major differences when compared to the structure of the vitamin B_{12} importer without the complexed binding protein. The most intriguing observation is the difference in conformation between the two transmembrane subunits (BtuC) leading to closure of the translocation pathway both from the cytoplasm and the periplasmic space. Vitamin B_{12} is no longer present in the TMD region or in the binding pocket of the SBP BtuF. This has adopted a conformation with both lobes spread apart, indicating a post ATP hydrolysis state and consistent with release of Vitamin B_{12} into the cytoplasm. In summary, these findings are consistent with the new BtuCDF structure being a posttranslocation intermediate.

The two lobes of BtuF are not identical and therefore different loops of the BtuC subunits interact with the binding protein generating asymmetry in the interaction. Interestingly, the loop of TM helix 5, seen to participate intimately in TMD–TMD interaction, inserts into the binding pocket for vitamin B_{12} and may force displacement of the allocrite. TM helices 3 to 5a in BtuCDF interact differently with the C- and N-lobe of the binding protein. On one side, the orientation of the helices of one BtuC subunit is similar to the arrangement present in the BtuCD structure in the absence of binding protein, resembling an outward facing conformation. In the second BtuC subunit, the helix conformation resembles the one present in HI1470/1471 with its inward facing orientation. Consequently, this asymmetry could present a state that 'allows' the transporter to switch to the outward or inward-facing conformation. To support this rather unexpected finding of asymmetry, obviously induced by TM helix 5, spin labels were introduced in the region preceding and following this central structural element. Comparison of EPR spectra from BtuCD and BtuCDF revealed differences in mobile and immobile components that can be explained by rearrangements of structural elements observed in the crystal structure (Fig. 1.6B) (Hvorup *et al.*, 2007).

Also in 2007, the structure of the putative molybdate importer ModBC from *Archaeoglobus fulgidus*, in complex with the binding protein ModA, was solved at 3.1 Å resolution. The protein has 12 transmembrane helices (Fig. 1.5F) with helices 3 and 5 contributing to the gating region, which closes the translocation pathway towards the extracellular space (Hollenstein *et al.*, 2007b). Molybdate is bound to ModA in an oxyanion binding site providing an octahedral coordination sphere. ModA in turn interacts with extracellular loops of the TMD region of ModB. This interaction involves charged amino acid residues as demonstrated for BtuCD (Hvorup *et al.*, 2007). The NBDs are separated by a gap between the Walker A and C-loop which reflects the nucleotide free state. The focus of this structure is on the interaction of the ModBC units with the binding protein. In the absence of ATP, an inward facing conformation of the TMDs is visible. The binding protein displays a closed conformation, hence trapping the substrate inside. The cytosolic L-loops containing the EAA motif are also present in the ModBC structure and interact with the helical domain of the NBDs. In line with the generally accepted model, the structure is consistent with the binding of ATP inducing the motor domains to converge to dimerize. This would produce a rigid body motion of the helical domain relative to the catalytic domain. Through an interaction between the helical domain and the L-loops, the required structural rearrangement should flip the transmembrane part to an outward facing conformation. At the same time this latter movement will pull apart both lobes of the binding protein, inducing the open conformation of ModA and consequent displacement of molybdenum into the translocation cavity. Thus, despite obvious differences in the helix arrangement of ModBC compared to BtuCD and HI1470/1471, these structural studies have led to a plausible mechanism of allocrite import. As a note of caution, these ideas are still based on nucleotide free structures, SBPs analysed in different conformations with and without bound substrate, and *presumed* physiological inward and outward facing orientations.

Further experiments with a related molybdate/tungstate importer from *Methanosarcina acetivorans* recently revealed a striking example of how the structure of an ABC transporter can be modified through evolution to facilitate more efficient regulation of its activity. In contrast to the importer from *Archaeoglobus fulgidus*, the NBDs of this second molybdate transporter, as shown

in Fig. 1.5E, contain a C-terminal extension that functions to inhibit the transporter when a certain concentration of substrate inside the cell is exceeded (Gerber *et al.*, 2008). Like the binding protein, ModA from *Archaeoglobus fulgidus*, an oxyanion binding site is present in the regulatory cytoplasmic extension of the NBDs where tungstate binds. The inhibitory effect results from interaction of the regulatory domains forcing the NBDs apart, resulting in an inward facing conformation of the transmembrane entity as seen in the crystal structure. The importer is thus locked in a configuration where ATP hydrolysis is precluded because binding of nucleotide is unable to bring the motor domains into close contact. Cross-linking studies with cysteines introduced in TM helix 4 indicated an inward directed movement of the transmembrane domain when ATP was omitted. This was consistent with a conformational change leading towards an outward facing conformation as observed for the BtuCD or MalFGK crystal structures (Locher *et al.*, 2002; Oldham *et al.*, 2007).

A similar elegant story of regulation comes from the methionine importer MetNI from *E. coli*, solved recently at a resolution of 3.7 Å. This transporter has the smallest set of TM helices of all ABC transporters described structurally so far (Fig. 1.5D), with 5 helices in each TMD. In this case, the regulatory extension of the NBDs, stringently control methionine import via inhibition responding to the intracellular concentrations of methionine (Kadaba *et al.*, 2008; Kadner, 1975). Since inhibition is accomplished from the cytoplasmic side of the membrane, this phenomenon is called 'trans-inhibition'. Interestingly, the presence of an odd number of TM helices causes the C-terminus of the TMDs to reside in the cytoplasm whereas the N-terminus is in the extracellular space – an alignment not described for any other ABC transporter to this point. With methionine bound to the regulatory domain of the NBD, the NBDs are forced apart and as a result the rate of ATP hydrolysis and therefore substrate import is markedly decreased. An explanation for this fine-tuning of import function might reflect a need to conserve cellular energy. Since transport processes which work against concentration gradients need energy to fuel translocation of molecules, the effect of trans-inhibition immediately saves cellular energy by inactivating the transporter when the need for certain substances is satisfied.

In the structure of MetNI a large distance between the NBDs is observed. Such a configuration was first described for the lipid flippase MsbA whose crystal structures were subsequently withdrawn. Nonetheless, these structures suggest the possibility of substantial movement to separate the NBDs under some conditions. This has now actually been verified using EPR measurements to determine the distance between the motor domains in the nucleotide free and ATP bound states for MsbA in a reconstituted system (Borbat *et al.*, 2007). The relative motion of the NBDs was determined to be roughly 30 Å. In contrast to MetNI and ModBC from *Methanosarcina acetivorans*, where the substrate itself mediates inhibition of the transporter, a slightly different regulatory function can be assigned to the regulatory domains of MalK. A transcriptional activator (MalT) binds to MalK and thereby inactivates the ATPase activity (Joly *et al.*, 2004; Richet *et al.*, 2005).

An interesting approach to functional analysis that we have not discussed so far is overlaying of the structures of different transporters (Pinkett *et al.*, 2007). A good starting point is BtuCD with its outward facing conformation and HI1470/1471 which is open towards to cytoplasm, reflecting the inward facing arrangement of the TMDs. The result of overlaying these structures is that possible translational movements along certain symmetry axes can be envisaged, in this case, through a reversible interconversion of an outward facing into an inward facing orientation. This projected movement can be described as a screw-like rotation, which aligns the NBDs of both transporters and propagates a conformational change to the transmembrane domains. Thus, structural changes in the motor domains, resulting from nucleotide binding or hydrolysis, as well as rearrangements of the transmembrane helices upon binding of the allocrite can apparently be transmitted in either direction, via simple geometrical movements.

The maltose import system of *E. coli* ($MalFGK_2$) has been subjected to extensive structural, biophysical and biochemical analysis and is probably the best studied prokaryotic ABC

transporter (Davidson and Chen, 2004). MalF and MalG form a heterodimer in the membrane and MalK is the cytoplasmic motor domain. A striking feature of the heterodimeric maltose transporter is the obvious difference in the two transmembrane domains. MalF consists of eight transmembrane helices whereas MalG has only six. Additionally, MalF contains an extracytoplasmic domain P2 adopting the well-known Ig-like fold that interacts with the N-terminal domain of the maltose binding protein (MBP or MalE).

MalE delivers maltose (or maltodextrins) to the membrane-embedded transporter, following docking onto the MalFG complex before release of maltose into the transport channel. MalE exists in open and closed conformations that are in equilibrium in solution with or without bound substrate. In the open conformation, the affinity towards the substrate is substantially decreased. Thus, the open conformation is the one adopted while MalE is bound onto the cognate transporter. There are two possible explanations for this observation: (i) maltose binds to a low affinity site on the TMDs of the transporter or (ii) that maltose simply diffuses directly into the cytoplasm. When MalE binds to MalFG, this stimulates ATP hydrolysis and can result in vanadate trapping. Vanadate is an analogue of inorganic phosphate and mimics the transition state of the γ-phosphate moiety of ATP during hydrolysis. In a reconstituted MalE-MalFGK$_2$ system trapped with vanadate, no maltose can be detected. This is a clear indication that conformational changes occur in a concerted manner and maltose in such experiments is released only when the trapped transition state is formed (Chen *et al.*, 2001). This hypothesis is supported, as shown in Fig. 1.5G, through the crystallization of the transition state of the MalE-MalFGK$_2$ complex (Oldham *et al.*, 2007).

The resulting working model for the MBP-MalFGK$_2$ complex depends on certain assumptions and observations. The maltose binding protein has the ligand bound and exists in the closed ligated form. Binding of MalE to the MalFG transmembrane domains induces a conformational change in the binding protein producing the open form in which the affinity for maltose is substantially reduced. At the same time, an extracellular loop from MalG inserts into the cleft where the maltose is bound and aids in the displacement of the substrate. As a result, maltose is then able to occupy a binding site in MalF. MalG does not participate in the maltose-binding site and in the structure, only one substrate-binding site in the transmembrane region is visible. Since the ATP concentration inside a cell is much higher than the K_M value of the NBDs towards the nucleotide, it is presumed that ATP occupies the motor domains even in the absence of maltose in the periplasm. Therefore, it is proposed that to prevent hydrolysis the nucleotide binding domains are held far apart. In this model (Oldham *et al.*, 2007), the signal to hydrolyse ATP results from the binding of the MalE/maltose complex to MalFG, causing a conformational change in the transmembrane helices. Consequently the motor domains come into close contact to form a functional dimer able to catalyse the elimination of the γ-phosphate. It is also proposed that the hydrolysis of ATP is required to reset the transporter and complete the transport cycle.

It should be mentioned that the crystal structure of the MalEFGK$_2$ complex was successfully obtained by creating an NBD mutant, in which a glutamate at position 159 was replaced by a glutamine (E159Q). This mutation completely prevents hydrolysis of ATP and traps the ABC transporter in a conformation where both motor domains, although in close contact with ATP bound, remain as a stable dimer.

There are two other crystal structures of ABC importers described with bound SBP, BtuCDF and ModB$_2$C$_2$A. In contrast to MalEFGK$_2$, these structures are devoid of the allocrite, for which maltose is found within the transporter pathway. The absence of B_{12} is surprising since the affinity of vitamin B_{12} is reasonably high, in the range of 15 nM (Cadieux *et al.*, 2002). ATP was also omitted from the crystallization conditions for BtuCDF and ModABC since it interfered with crystal lattice formation. The maltose import system constitutes therefore the most complete view of an ABC transporter to date.

ABC exporters

ABC exporters are of a special interest because of their participation in some cases in the induction of multidrug resistance (MDR) in humans

undergoing chemotherapy (Kartner *et al.*, 1983). The most fascinating feature of these mammalian exporters (and their bacterial equivalents) is the wide variety of substrates that can be transported. The only apparent common characteristic of these compounds is their hydrophobicity – size or steric arrangements are of minimal relevance (Sharom, 2008; see also Chapters 4 and 9). There are of course examples of exporters with well characterized, apparently single allocrites, as in the case of the Haemolysin B transporter from *E. coli*. The allocrite in this case is a 110 kDa toxin secreted by enterohaemoragic *E. coli* strains via the Type I secretion system. Interestingly, however, by fusing the C-terminal secretion signal of this toxin to other proteins, many other proteins can be secreted (Blight and Holland, 1994; Fernandez *et al.*, 2000; Fraile *et al.*, 2004).

Much of our knowledge of the action of membrane proteins such as P-gp depend on *in vitro* experiments and although these are carried out under controlled conditions, the physiological significance *in vivo* of the many chemical compounds tested by the endogenous ABC exporters remains to be established. An interesting feature of ABC exporters such as Pgp (MDR-1) is that transport can also be affected by substances that bind to certain regulatory sites that then modulate transport of the true allocrite. However, the molecular details of allocrite and modulator binding sites are not yet clearly established (Sharom, 2008).

The only structure of an ABC exporter derived so far (see Fig. 1.5H) is the putative MDR (multidrug resistance) protein Sav1866 from *S. aureus* (Dawson and Locher, 2006). Sav1866 is homodimeric protein (a half size transporter) with 12 transmembrane helices and the structure was derived from crystals scattering up to 3 Å. A remarkable feature of Sav1866 is the fact that the transmembrane helices of the TMDs are twisted and embrace each other. This arrangement leads to extensive interactions between the TMD and NBD including, surprisingly, crossover interactions between the TMD of one monomer and the NBD of the opposing monomer. Crystals were formed in the presence of ATP but ADP is present in the structure and the NBDs remain in close contact with the Walker A motif and the C-loop interacting in a hydrolysis competent orientation. Another structure of Sav1866 with a non-hydrolyzable ATP analogue (Dawson and Locher, 2007) revealed the same outward facing orientation of the transmembrane domain as in the structure with ADP. The L-loop of the TMDs in importers discussed earlier that interacts with the NBDs apparently to transmit reciprocal structural changes between the cytoplasmic and the transmembrane domains, is not, however, present in the Sav1866 structure. Instead, two intracellular loops protruding from one TMD and connecting helices 2 and 3 and helices 4 and 5, both interact with the cis and trans NBDs (Fig. 1.8A and B). Notably, despite the absence of the L-loop, the site of interaction in the NBD, still coincides with the structurally diverse region preceding the C-loop sequence.

A closer look at the putative translocation pathway of Sav1866, reveals mostly hydrophilic amino acid residues lining a cavity in accordance with the expected properties of a low affinity-binding site, necessary for the extrusion of hydrophobic drugs from the cell. When the crystal structure of Sav1866 was published, no biochemical evidence for transport activity or any information about potential substrates was available. However, Sav1866 displayed increased ATPase activity in the presence of verapamil, tetraphenylphosphonium, Hoechst 33342 or vinblastine – all compounds previously used in functional assays with other multidrug transporters. Importantly, a recent study of Sav1866 provided direct evidence for a drug transport activity. Thus, transport of Hoechst 33342 by purified and reconstituted Sav1866 in proteoliposomes was demonstrated (Velamakanni *et al.*, 2008).

Estimations from the crystal structures of the importer BtuCD and the exporter Sav1866 indicated that considerable amounts of the transmembrane part of Sav1866, in contrast to BtuCD, protrude into the cytoplasm (Lomize *et al.*, 2006a; Lomize *et al.*, 2006b). This provides a hint that interaction with drug molecules for export is established via the TMDs of the transporter since a large interface of possible interactions is made available. Transport studies *in vitro* in fact show that drug molecules for MDR ABC transporters can be picked up from either the cytoplasm or the membrane (Bolhuis *et al.*, 1996; Sharom *et al.*, 2005). However, classical models of the action

of MDR transporters envisage direct access of drugs from the inner leaflet of the bilayer into the transporter.

With structural data at hand and a system that can be described by biochemical and biophysical approaches, the foundations for the characterization of at least one bacterial MDR ABC transporter have been laid. Future developments can be expected to provide a fundamental understanding of the Sav1866 molecular machine that will be usefully extrapolated to the mechanism of action of the mammalian ABC drug transporters.

How ABC transporters transport substrates

Although we have outlined above how ABC transporters like MalEFGK might function, some problems with the models still remain. How can one imagine all the requirements of the process of substrate transport via an ABC system? To address this question in relation to importers, the initial state of an ABC transporter remains to be established. In principle, two contrary scenarios are possible when no ATP is bound and the transporter is in its resting state: (i) the translocation pore is closed to the extracellular space and open to the cytoplasm (Oldham *et al.*, 2007) or (ii) the translocation pathway is open to the exterior and closed towards the inside of the cell (Locher *et al.*, 2002).

Two distinct mechanisms of ABC transporter function that depend on the action of the motor domain are presently in vogue. These are the *processive clamp model* (Smith *et al.*, 2002;Chen *et al.*, 2003a; Janas *et al.*, 2003; van der Does and Tampe, 2004; Zaitseva *et al.*, 2005a) and the *alternating site model* (Senior *et al.*, 1995; Urbatsch *et al.*, 1995; Sharma and Davidson, 2000; Tombline *et al.*, 2004a; Tombline *et al.*, 2004b). In the processive clamp model, two ATP molecules are present in the two composite binding sites, involving interactions at the NBD dimer interface following ATP induced dimerization. The nucleotides are hydrolysed sequentially before dissociation of the NBD dimer. This idea is in agreement with the crystal structures of NBD dimers where two ATP molecules are present at the dimer interface in their respective binding sites. Biochemical studies *in vitro* have revealed the presence of either two ATP (Smith *et al.*, 2002; Chen *et al.*, 2003a; Zaitseva *et al.*, 2005a) or two ADP molecules (Janas *et al.*, 2003; Dawson and Locher, 2006), or an ATP/ADP mixture bound to the NBD dimer (Chen *et al.*, 2001; Janas *et al.*, 2003). The existence of a state where two ATP molecules are bound is plausible if we assume that ATP bound monomers form dimers. The ATP/ADP state is in agreement with analyses revealing a phosphate exit tunnel for inorganic phosphate in the assembled dimer (Zaitseva *et al.*, 2006; Procko and Gaudet, 2008;). The presence of two ADP molecules in the NBD dimer has been detected but was only possible if a BeF_X trapped and hence stabilized system was generated (Janas *et al.*, 2003). Thus, a two-ADP state seems to be rather unstable under physiological conditions.

In the alternating site model, the starting point is also a dimer with two ATP molecules bound. Hydrolysis of one ATP opens up the dimer at the corresponding site and exchange of ADP for ATP is achieved. Following closing of the dimer the hitherto unaffected ATP is hydrolysed and the alternating cycle starts again following the second APD/ATP exchange. Support for the alternating site model comes from experiments where vanadate trapping was used to capture the hydrolysed ATP in the binding pocket since vanadate has the ability to mimic the transition state of the γ-phosphate on the point of elimination (Goodno, 1982; Shimizu, 1981; Smith and Rayment, 1996). The vanadate trapping experiments demonstrated that only one nucleotide molecule per NBD dimer could be detected, pointing towards an intermediate state where exchange of nucleotides is possible. This is good evidence that a mechanism for concerted hydrolysis dependent on alternating opening of the NBD at the two sites might exist (Vergani *et al.*, 2005). Of course, both models were established for different proteins and this leaves open the possibility that for different transporters different mechanisms may be required.

An intensely discussed question in the ABC field is also the number of allocrite binding sites in an ABC transporter and where these are located. For importers, it can clearly be stated that the binding site is inside the translocation pore formed by the transmembrane domains (Oldham *et al.*, 2007). For exporters that receive

their substrate from the membrane bilayer the site of interaction is also likely to be the transmembrane domain. However, it remains an open question for other exporters that transport compounds from the cytoplasm, whether the allocrite interacts directly with the transmembrane domain, with cytoplasmic loops of the TMDs or whether the first contact is made with the transporter via NBD interactions. And how, if the translocation pore is not entered directly, can one imagine the targeting of the allocrite to the exit tunnel? First, the number of binding sites needs to be addressed. Since it has been shown that importers do not necessarily have only one substrate binding protein but two or even four per transporter, this question becomes even more crucial (Biemans-Oldehinkel and Poolman, 2003; Schuurman-Wolters and Poolman, 2005). In the past, three major models have evolved that attempt to describe the concerted transport of substrate coupled to ATP hydrolysis. There was no consensus concerning whether there are one or two binding sites present in the TMDs, whether high and low-affinity sites can be interconverted and whether the energy provided by ATP is used to shuttle the allocrite from one binding site to the other or to induce structural rearrangements in the transmembrane helices.

The approach presented in the two-cylinder engine model, which incorporates alternating site hydrolysis of ATP (van Veen *et al.*, 2000), describes two allocrite binding sites that have either high or low affinity for a drug molecule in the bacterial multidrug ABC exporter LmrA. When ATP is bound at the NBD, a high affinity drug binding site becomes accessible which is subsequently transformed into a low affinity binding site by hydrolysis of ATP. At this stage in this model, one NBD with bound ADP and another with ATP will be present as well as one high and one low affinity binding site. Difficulties remain in identifying and characterizing the binding sites and the additional important specific sites where substances can bind that modulate allocrite transport. Another difficulty is the fact that multidrug resistance transporters are able to accept a wide variety of structurally diverse compounds as transport substrates. Therefore, a single binding site for all allocrites can almost be ruled out. For P-glycoprotein, for example, at least two substrate-binding sites (H- and R-site) were identified that are also accessible to inhibitors (Lugo and Sharom, 2005; Shapiro and Ling, 1998; Sharom, 2008).

An alternative model for MDR ABC mediated transport is the interconversion of a single binding site from a high to a low affinity site, also coupled to the alternating catalytic site model for ATP hydrolysis described above (Senior *et al.*, 1995; Urbatsch *et al.*, 2003). Yet another possibility to explain the experimental results is the presence of two distinct binding sites with high or low affinity, respectively, where the substrate is transferred physically from one to the other binding site with the energy provided by ATP hydrolysis. The second ATP will in this model be used to reset the transport cycle (Sauna and Ambudkar, 2000).

To clarify the developing confusion concerning which model best describes the molecular processes of binding, recognition, and consequent structural rearrangements, the 'ATP switch model for ABC transporters' (Higgins and Linton, 2004) have tried to summarize recent advances in ABC transporter function. This presumes that the NBDs of the transporter are initially in an open, nucleotide free-state and the high affinity substrate binding site is probably located close to the inner membrane. Binding of transport substrate induces binding of ATP to the NBDs which then results in NDB dimer formation. This dimerization of the motor domains induces a conformational change in the transmembrane domains of the ABC transporter leading to substrate release from a low affinity binding site. ATP hydrolysis and ADP + P_i release triggers NBD dimer decomposition and reconstitution of the initial state. This scheme should be applicable to both exporters and importers. However, predicted outcomes concerning sequential or alternate hydrolysis or altered affinity of ATP, or the exact nature of the binding sites, are not considered with respect to the general applicability of the model. To stress the point, we need to briefly reconsider the information available from the crystal structure of the $MalEFGK_2$ complex, with ATP and allocrite present. The SBP is able to bind to the translocator in the presence of ATP and maltose is found in the translocation pathway where a single allocrite binding site is visible. A possible scenario, in line

with the ATP switch model for the entire transportation process could be the following: the allocrite interacts with the ABC transporter in the presence of ATP this initiates dimerization of the motor domains which induces structural changes in the transmembrane domain. This then leads to the situation reflected in the crystal structure. The next step would probably be the hydrolysis of the nucleotide. The energy provided could be used to finalize transport of the allocrite while the binding site may undergo structural changes to assure efficient displacement of the drug or allocrite. Dimer dissociation and ADP release would then re-establish an 'initial state' competent for a new cycle of transport. This is by no means the final story but offers for the first time an insight into the transport mechanism at a molecular level and provides a perspective based on all theories developed so far.

Conservation versus degeneration in ABC transporters

Conservation of certain sequence motifs, particularly in the NBDs, has always been considered an important feature of ABC transporters. These motifs are used to identify ABC proteins and play a crucial role in predicting and modeling approaches to infer functions of putative ABC transporters. We need to emphasize, however, that the most highly conserved motifs can be found in only one composite catalytic ATP binding site, in a wide variety of eukaryotic ABC transporters, including families of the ABC C-subfamily (CFTR, MRP, SUR). In CFTR, the second site is degenerate and unable to hydrolyse the nucleotide (Gadsby *et al.*, 2006). Another prominent example is the transporter associated with antigen processing (TAP). The TAP1-NBD

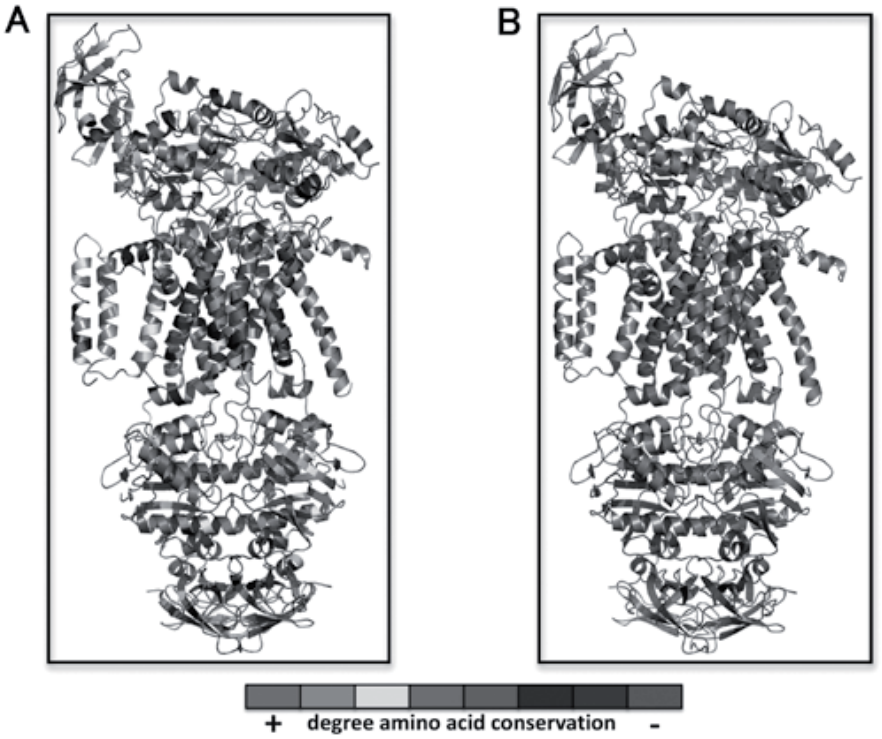

Figure 1.9 **A** Analysis of conserved amino acids in the MalEFGK$_2$ complex. The amino acid sequence of this importer was compared with 50 other ABC transporters and conserved amino acids are highlighted with the ConSurf Server (http://consurf.tau.ac.il/). **B** Only the highest conserved amino acids are shown in red. As explained in the text, the highest conservation is found in the nucleotide binding domains. A colour version of this figure is located in the plate section at the back of the book.

possesses the canonical signature sequence of the C-loop (LSGGQ), whereas the TAP2-NBD has a degenerate C-loop sequence LAAGQ (Chen *et al.*, 2004). The only prokaryotic ABC transporter displaying such asymmetry with respect to its NBD motifs, is LmrCD from *Lactococcus lactis* (Lubelski *et al.*, 2006).

Following the discussion above, reducing the number of sites for ATP hydrolysis has major implications for the nature of the catalytic cycle of the motor domains and in particular for the coupling of ATP binding and/or hydrolysis to transport. When only one active site is available, only one ATP molecule can be hydrolysed, the energy provided has to be sufficient to fuel translocation. With respect to CFTR, since this protein functions as a chloride channel, this might be considered a special case (Vergani *et al.*, 2005). Nevertheless, a single active hydrolytic site still raises the important question of the stoichiometry of the reaction: is one ATP sufficient to fulfill transport requirements?

Up to this point we have considered that the power stroke in the transport process is solely dependent on the energy provided by the hydrolysis of ATP. Taking a closer look at the catalytic cycle illustrated from structural studies of the isolated HlyB-NBD, the Gibbs free energy derived experimentally from dissociation constants is similar for ATP hydrolysis and NBD dimerization (Zaitseva *et al.*, 2006). Consequently, either of these steps might be sufficient to generate the power stroke. To phrase this differently, dimerization itself may be capable of complementing any deficiencies in nucleotide hydrolysis which might be crucial in an ABC transporter with only one canonical ATP binding site. Nevertheless, speculation about the importance of the stoichiometry of ATP consumption, begs the question why single active sites in ABC transporters have successfully evolved and whether the degenerate site retains some function. A detailed analysis of the degenerated motifs present in the transporter associated with antigen processing (TAP) led to a model that provides essential tasks in the transport process for the ATPase site lacking key catalytic residues (Ernst *et al.*, 2006; Procko *et al.*, 2006). As discussed above, starting from an open conformation, where both NBDs have separated, ADP-ATP exchange is stimulated by allocrite binding (Chen *et al.*, 2003b). Subsequent dimerization of the NBDs, hydrolysis of ATP, and consequent structural changes in the transmembrane domains drive export of the allocrite. In the case of TAP, the idea that dimerization is controlled by peptide binding offers a nice solution explaining the efficient use of ATP with prevention of consumption in the absence of the allocrite. For CFTR, for example, it was suggested that the degeneration in one of the two ATP composite sites results in an active, ATP hydrolyzing site, and one site that has a regulatory function. However, degenerate sites and their functional consequence in ABC transporters remain a matter of debate and we still await a clear experimental answer to this puzzle.

Conclusions and future trends

Finally, we must return to the starting point and clarify why we propose that ABC transporters constitute such a smart example. First, it is quite impressive that ABC proteins and their associates account for roughly 5% of the total coding capacity of the *E. coli* genome, clearly evidence of their important role in this and most microorganisms. It is equally significant that the highly conserved ABC motor is universally distributed throughout all kingdoms of life playing vitally important roles. Import of nutrients, export of toxic compounds or building the essential constituents of biological membranes are examples contributing to the fundamental requisites for life. Since the first definition of an ABC transporter system more than 25 years ago (Higgins *et al.*, 1982) many more of these amazing transport systems have been identified and the understanding of their function has advanced enormously. Many ABC transporters are involved in the immunity mechanism, detoxification, uptake of trace elements, mediation of drug resistance, osmoprotection, bile salt homeostasis and many more have been revealed. Moreover, studies of the proteins cover many disciplines, employing the whole range of techniques now available to modern science. The very diversity of ABC transporters in terms of sequence conservation or degeneration, allocrite import or export, modular assembly, and of course function from microorganisms to higher organisms simply adds to their fascination.

The main task for the future is to obtain a more detailed and thorough understanding of the

ABC proteins. This will no doubt be aided by the availability of many more structures. Importantly, these should include their dynamic properties indicated for example, from NMR studies combined with physical and biochemical studies *in vitro* and especially *in vivo.* In this way the true physiological roles of these fundamentally important proteins should be revealed. Certainly, many questions still remain to be answered: the precise sequence of different steps involving binding of nucleotide, allocrite, the dimerization of NBDs and finally the 'reversible' reorientation of the transmembrane helices completing the transport cycle are at the atomic level still not solved. Emerging techniques in the field of computational biology with the power to simulate processes together with previously intractable techniques such as single molecule flourescence spectroscopy or NMR are becoming more and more common and will provide many important new insights. These approaches will lead to answers to questions concerning protein dynamics and will enhance substantially our ideas gained from the static pictures of crystal structures.

ABC transporters are associated with severe diseases such as, for example, cystic fibrosis, multidrug resistance towards anti-tumour drugs, cholestasis (liver disease), adrenoleukodystrophy (damage of the nervous system), Dubin-Johnson-syndrome (liver disease), or the consequences of multi-drug resistance during cancer chemotherapy. Thus, in addition to our intense curiosity to see one of the largest families of membrane proteins characterized and understood fully at the structural and functional level, their medical importance is surely by itself sufficient to keep the interest in ABC transporters alive.

Acknowledgements

We apologize to all our colleagues, whose work could not be adequately referenced due to space limitations. We are indebted to all former and current members of our laboratories. Especially, we would like to acknowledge the financial support of the EU (FP-7, EDICT) and the DFG (Emmy Noether program, SFBs 575 and 628 and grants Schm1279 4–1, 5–3, 7–1) to L.S., and to CNRS and the University of Paris-Sud to I.B.H.

References

Abrahams, J.P., Leslie, A.G., Lutter, R., and Walker, J.E. (1994). Structure at 2.8 A resolution of F1-ATPase from bovine heart mitochondria. Nature *370*, 621–628.

Ames, G.F., and Lecar, H. (1992). ATP-dependent bacterial transporters and cystic fibrosis: analogy between channels and transporters. FASEB J *6*, 2660–2666.

Ames, G.F., and Lever, J. (1970). Components of histidine transport: histidine-binding proteins and hisP protein. Proc Natl Acad Sci U S A *66*, 1096–1103.

Bahadur, R.P., and Zacharias, M. (2008). The interface of protein-protein complexes: analysis of contacts and prediction of interactions. Cell Mol Life Sci *65*, 1059–1072.

Benabdelhak, H., Schmitt, L., Horn, C., Jumel, K., Blight, M.A., and Holland, I.B. (2005). Positive cooperative activity and dimerization of the isolated ABC-ATPase domain of HlyB from E.coli. Biochem J *368*, 1–7.

Biemans-Oldehinkel, E., Doeven, M.K., and Poolman, B. (2006). ABC transporter architecture and regulatory roles of accessory domains. FEBS Lett *580*, 1023–1035.

Biemans-Oldehinkel, E., and Poolman, B. (2003). On the role of the two extracytoplasmic substrate-binding domains in the ABC transporter OpuA. EMBO J *22*, 5983–5993.

Blight, M.A., and Holland, I.B. (1994). Heterologous protein secretion and the versatile *Eschericichia coli* haemolysin translocator. TIBTECH *12*, 450–455.

Bohm, B., Boschert, H., and Koster, W. (1996). Conserved amino acids in the N- and C-terminal domains of integral membrane transporter FhuB define sites important for intra- and intermolecular interactions. Mol Microbiol *20*, 223–232.

Bolhuis, H., van Veen, H.W., Molenaar, D., Poolman, B., Driessen, A.J., and Konings, W.N. (1996). Multidrug resistance in Lactococcus lactis: evidence for ATP-dependent drug extrusion from the inner leaflet of the cytoplasmic membrane. Embo J *15*, 4239–4245.

Boos, W., and Lucht, J.M. (1996). Periplasmic binding protein-dependent ABC transporters. In *Escherichia coli and Salmonella Cellular and Molecular Biology*, F.C. Neidhard, Curtiss R., III, Ingraham, J. L., Lin, E. C. C., Low, K. B., Magasanik, B., Reznikoff, W. S., Riley, M., Schaechter, M. & Umbarger, H. E., ed. (Washington, DC, American Society for Microbiology Press), pp. 1175–1209.

Borbat, P.P., Surendhran, K., Bortolus, M., Zou, P., Freed, J.H., and McHaourab, H.S. (2007). Conformational motion of the ABC transporter MsbA induced by ATP hydrolysis. PLoS Biol *5*, e271.

Borths, E.L., Locher, K.P., Lee, A.T., and Rees, D.C. (2002). The structure of Escherichia coli BtuF and binding to its cognate ATP binding cassette transporter. Proc Natl Acad Sci U S A *99*, 16642–16647.

Borths, E.L., Poolman, B., Hvorup, R.N., Locher, K.P., and Rees, D.C. (2005). In vitro functional characterization of BtuCD-F, the Escherichia coli ABC transporter for vitamin B12 uptake. Biochemistry *44*, 16301–16309.

Buckel, S.D., Bell, A.W., Rao, J.K., and Hermodson, M.A. (1986). An analysis of the structure of the product of

the rbsA gene of Escherichia coli K12. J Biol Chem *261*, 7659–7662.

Cadieux, N., Bradbeer, C., Reeger-Schneider, E., Koster, W., Mohanty, A.K., Wiener, M.C., and Kadner, R.J. (2002). Identification of the periplasmic cobalamin-binding protein BtuF of Escherichia coli. J Bacteriol *184*, 706–717.

Campbell, J.D., Biggin, P.C., Baaden, M., and Sansom, M.S. (2003). Extending the structure of an ABC transporter to atomic resolution: modeling and simulation studies of MsbA. Biochemistry *42*, 3666–3673.

Chang, G., and Roth, C.B. (2001). Structure of MsbA from E. coli: a homolog of the multidrug resistance ATP binding cassette (ABC) transporters. Science *293*, 1793–1800.

Chen, M., Abele, R., and Tampe, R. (2003b). Peptides induce ATP hydrolysis at both subunits of the transporter associated with antigen processing. J Biol Chem *278*, 29686–29692.

Chen, M., Abele, R., and Tampe, R. (2004). Functional non-equivalence of ATP-binding cassette signature motifs in the transporter associated with antigen processing (TAP). J Biol Chem *279*, 46073–46081.

Chen, J., Lu, G., Lin, J., Davidson, A.L., and Quiocho, F.A. (2003a). A tweezers-like motion of the ATP-binding cassette dimer in an ABC transport cycle. Mol Cell *12*, 651–661.

Chen, J., Sharma, S., Quiocho, F.A., and Davidson, A.L. (2001). Trapping the transition state of an ATP-binding cassette transporter: evidence for a concerted mechanism of maltose transport. Proc Natl Acad Sci U S A *98*, 1525–1530.

Clarke, T.E., Ku, S.Y., Dougan, D.R., Vogel, H.J., and Tari, L.W. (2000). The structure of the ferric siderophore binding protein FhuD complexed with gallichrome. Nat Struct Biol *7*, 287–291.

Dall'Acqua, W., and Carter, P. (2000). Substrate-assisted catalysis: molecular basis and biological significance. Protein Sci *9*, 1–9.

Dassa, E., and Bouige, P. (2001). The ABC of ABCS: a phylogenetic and functional classification of ABC systems in living organisms. Res Microbiol *152*, 211–229.

Dassa, E., and Hofnung, M. (1985). Sequence of gene malG in E. coli K12: homologies between integral membrane components from binding protein-dependent transport systems. Embo J *4*, 2287–2293.

Davidson, A.L., and Chen, J. (2004). ATP-binding cassette transporters in bacteria. Annu Rev Biochem *73*, 241–268.

Davidson, A.L., Dassa, E., Orelle, C., and Chen, J. (2008). Structure, function, and evolution of bacterial ATP-binding cassette systems. Microbiol Mol Biol Rev *72*, 317–364, table of contents.

Davidson, A.L., Laghaeian, S.S., and Mannering, D.E. (1996). The maltose transport system of Escherichia coli displays positive cooperativity in ATP hydrolysis. J Biol Chem *271*, 4858–4863.

Davidson, A.L., and Sharma, S. (1997). Mutation of a single MalK subunit severely impairs maltose transport activity in Escherichia coli. J Bacteriol *179*, 5458–5464.

Dawson, R.J., and Locher, K.P. (2006). Structure of a bacterial multidrug ABC transporter. Nature *443*, 180–185.

Dawson, R.J., and Locher, K.P. (2007). Structure of the multidrug ABC transporter Sav1866 from Staphylococcus aureus in complex with AMP-PNP. FEBS Lett *581*, 935–938.

Dean, M., Rzhetsky, A., and Allikmets, R. (2001). The human ATP-binding cassette (ABC) transporter superfamily. Genome Res *11*, 1156–1166.

Doran, A., Obach, R.S., Smith, B.J., Hosea, N.A., Becker, S., Callegari, E., Chen, C., Chen, X., Choo, E., Cianfrogna, J., *et al.* (2005). The impact of P-glycoprotein on the disposition of drugs targeted for indications of the central nervous system: evaluation using the MDR1A/1B knockout mouse model. Drug Metab Dispos *33*, 165–174.

Duan, X., and Quiocho, F.A. (2002). Structural evidence for a dominant role of nonpolar interactions in the binding of a transport/chemosensory receptor to its highly polar ligands. Biochemistry *41*, 706–712.

Ernst, R., Koch, J., Horn, C., Tampe, R., and Schmitt, L. (2006). Engineering ATPase activity in the isolated ABC cassette of human TAP1. J Biol Chem *281*, 27471–27480.

Felder, C.B., Graul, R.C., Lee, A.Y., Merkle, H.P., and Sadee, W. (1999). The Venus flytrap of periplasmic binding proteins: an ancient protein module present in multiple drug receptors. AAPS PharmSci *1*, E2.

Fernandez, L.A., Sola, I., Enjuanes, L., and de Lorenzo, V. (2000). Specific secretion of active single-chain Fv antibodies into the supernatants of Escherichia coli cultures by use of the hemolysin system. Appl Environ Microbiol *66*, 5024–5029.

Fersht, A. (1997). Enzyme Structure and Mechanism. W H Freeman and Company *second edition*.

Fetsch, E.E., and Davidson, A.L. (2002). Vanadate-catalyzed photocleavage of the signature motif of an ATP-binding cassette (ABC) transporter. Proc Natl Acad Sci U S A *99*, 9685–9690.

Flocco, M.M., and Mowbray, S.L. (1994). The 1.9 A x-ray structure of a closed unliganded form of the periplasmic glucose/galactose receptor from Salmonella typhimurium. J Biol Chem *269*, 8931–8936.

Fraile, S., Munoz, A., de Lorenzo, V., and Fernandez, L.A. (2004). Secretion of proteins with dimerization capacity by the haemolysin type I transport system of Escherichia coli. Mol Microbiol *53*, 1109–1121.

Froshauer, S., and Beckwith, J. (1984). The nucleotide sequence of the gene for malF protein, an inner membrane component of the maltose transport system of Escherichia coli. Repeated DNA sequences are found in the malE-malF intercistronic region. J Biol Chem *259*, 10896–10903.

Fuellen, G., Spitzer, M., Cullen, P., and Lorkowski, S. (2005). Correspondence of function and phylogeny of ABC proteins based on an automated analysis of 20 model protein data sets. Proteins *61*, 888–899.

Gadsby, D.C., Vergani, P., and Csanady, L. (2006). The ABC protein turned chloride channel whose failure causes cystic fibrosis. Nature *440*, 477–483.

Gerber, S., Comellas-Bigler, M., Goetz, B.A., and Locher, K.P. (2008). Structural basis of trans-inhibition in a

molybdate/tungstate ABC transporter. Science *321*, 246–250.

Gilson, E., Alloing, G., Schmidt, T., Claverys, J.P., Dudler, R., and Hofnung, M. (1988). Evidence for high affinity binding-protein dependent transport systems in gram-positive bacteria and in Mycoplasma. EMBO J *7*, 3971–3974.

Goodno, C.C. (1982). Myosin active-site trapping with vanadate ion. Methods Enzymol *85 Pt B*, 116–123.

Grote, M., Bordignon, E., Polyhach, Y., Jeschke, G., Steinhoff, H.J., and Schneider, E. (2008). A comparative EPR study of the nucleotide-binding domains' catalytic cycle in the assembled maltose ABC-importer. Biophys J. *95*, 2924- 2938

Hanekop, N., Zaitseva, J., Jenewein, S., Holland, I.B., and Schmitt, L. (2006). Molecular insights into the mechanism of ATP-hydrolysis by the NBD of the ABC-transporter HlyB. FEBS Lett *580*, 1036–1041.

Harding, M.M. (2000). The geometry of metal–ligand interactions relevant to proteins. II. Angles at the metal atom, additional weak metal–donor interactions. Acta Crystallogr D Biol Crystallogr *56 (Pt 7)*, 857–867.

Haubertin, D.Y., Madaoui, H., Sanson, A., Guerois, R., and Orlowski, S. (2006). Molecular dynamics simulations of E. coli MsbA transmembrane domain: formation of a semipore structure. Biophys J *91*, 2517–2531.

Hazelbauer, G.L. (1975). Maltose chemoreceptor of Escherichia coli. J Bacteriol *122*, 206–214.

Higgins, C.F., Haag, P.D., Nikaido, K., Ardeshir, F., Garcia, G., and Ames, G.F. (1982). Complete nucleotide sequence and identification of membrane components of the histidine transport operon of S. typhimurium. Nature *298*, 723–727.

Higgins, C.F., and Linton, K.J. (2004). The ATP switch model for ABC transporters. Nat Struct Mol Biol *11*, 918–926.

Holland, I.B., Benabdelhak, H., Young, J., De Lima Pimenta, A., Schmitt, L., and Blight, M.A. (2003). Bacterial ABC transporters involved in protein translocation. In ABC proteins: From bacteria to man, I.B. Holland, S.P. Cole, K. Kuchler, and C. Higgins, eds. (London, Academic Press), pp. 209–241.

Holland, I.B., Schmitt, L., and Young, J. (2005). Type 1 protein secretion in bacteria, the ABC-transporter dependent pathway (review). Mol Membr Biol *22*, 29–39.

Hollenstein, K., Dawson, R.J., and Locher, K.P. (2007a). Structure and mechanism of ABC transporter proteins. Curr Opin Struct Biol *17*, 412–418.

Hollenstein, K., Frei, D.C., and Locher, K.P. (2007b). Structure of an ABC transporter in complex with its binding protein. Nature *446*, 213–216.

Hung, L.-W., Wang, I.X., Nikaido, K., Liu, P.-Q., Ferro-Luzzi Ames, G., and Kim, S.-H. (1998). Crystal structure of the ATP-binding domain of an ABC transporter. Nature *396*, 703–707.

Hunke, S., Mourez, M., Jehanno, M., Dassa, E., and Schneider, E. (2000). ATP modulates subunit–subunit interactions in an ATP-binding cassette transporter (MalFGK2) determined by site-directed chemical cross- linking. J Biol Chem *275*, 15526–15534.

Husain, I., Van Houten, B., Thomas, D.C., and Sancar, A. (1986). Sequences of Escherichia coli uvrA gene and protein reveal two potential ATP binding sites. J Biol Chem *261*, 4895–4901.

Hvorup, R.N., Goetz, B.A., Niederer, M., Hollenstein, K., Perozo, E., and Locher, K.P. (2007). Asymmetry in the structure of the ABC transporter-binding protein complex BtuCD-BtuF. Science *317*, 1387–1390.

Jacquet, E., Girard, J.M., Ramaen, O., Pamlard, O., Levaique, H., Betton, J.M., Dassa, E., and Chesneau, O. (2008). ATP hydrolysis and pristinamycin IIA inhibition of the Staphylococcus aureus Vga(A), a dual ABC protein involved in streptogramin A resistance. J Biol Chem. *283*, 25332- 25338.

Janas, E., Hofacker, M., Chen, M., Gompf, S., van der Does, C., and Tampe, R. (2003). The ATP hydrolysis cycle of the nucleotide-binding domain of the mitochondrial ATP-binding cassette transporter Mdl1p. J Biol Chem *278*, 26862–26869.

Joly, N., Bohm, A., Boos, W., and Richet, E. (2004). MalK, the ATP-binding cassette component of the Escherichia coli maltodextrin transporter, inhibits the transcriptional activator malt by antagonizing inducer binding. J Biol Chem *279*, 33123–33130.

Jones, P.M., and George, A.M. (1999). Subunit interactions in ABC transporters: towards a functional architecture. FEMS Microbiol Lett *179*, 187–202.

Kadaba, N.S., Kaiser, J.T., Johnson, E., Lee, A., and Rees, D.C. (2008). The high-affinity E. coli methionine ABC transporter: structure and allosteric regulation. Science *321*, 250–253.

Kadner, R.J. (1975). Regulation of methionine transport activity in Escherichia coli. J Bacteriol *122*, 110–119.

Karpowich, N., Martsinkevich, O., Millen, L., Yuan, Y.R., Dai, P.L., MacVey, K., Thomas, P.J., and Hunt, J.F. (2001). Crystal structures of the MJ1267 ATP binding cassette reveal an induced-fit effect at the ATPase active site of an ABC transporter. Structure *9*, 571–586.

Karpowich, N.K., Huang, H.H., Smith, P.C., and Hunt, J.F. (2003). Crystal structures of the BtuF periplasmic-binding protein for vitamin B12 suggest a functionally important reduction in protein mobility upon ligand binding. J Biol Chem *278*, 8429–8434.

Kartner, N., Riordan, J.R., and Ling, V. (1983). Cell surface P-glycoprotein associated with multidrug resistance in mammalian cell lines. Science *221*, 1285–1288.

Kempf, B., Gade, J., and Bremer, E. (1997). Lipoprotein from the osmoregulated ABC transport system OpuA of Bacillus subtilis: purification of the glycine betaine binding protein and characterization of a functional lipidless mutant. J Bacteriol *179*, 6213–6220.

Koronakis, V., Hughes, C., and Koronakis, E. (1991). Energetically distinct early and late stages of HlyB/HlyD-dependent secretion across both Escherichia coli membranes. EMBO J *10*, 3263–3272.

Lawrence, M.C., Pilling, P.A., Epa, V.C., Berry, A.M., Ogunniyi, A.D., and Paton, J.C. (1998). The crystal structure of pneumococcal surface antigen PsaA reveals a metal-binding site and a novel structure for a putative ABC-type binding protein. Structure *6*, 1553–1561.

Lee, Y.H., Deka, R.K., Norgard, M.V., Radolf, J.D., and Hasemann, C.A. (1999). Treponema pallidum TroA

is a periplasmic zinc-binding protein with a helical backbone. Nat Struct Biol *6*, 628–633.

Lee, Y.H., Dorwart, M.R., Hazlett, K.R., Deka, R.K., Norgard, M.V., Radolf, J.D., and Hasemann, C.A. (2002). The crystal structure of Zn(II)-free Treponema pallidum TroA, a periplasmic metal-binding protein, reveals a closed conformation. J Bacteriol *184*, 2300–2304.

Leslie, E.M., Deeley, R.G., and Cole, S.P. (2005). Multidrug resistance proteins: role of P-glycoprotein, MRP1, MRP2, and BCRP (ABCG2) in tissue defense. Toxicol Appl Pharmacol *204*, 216–237.

Lewis, H.A., Buchanan, S.G., Burley, S.K., Conners, K., Dickey, M., Dorwart, M., Fowler, R., Gao, X., Guggino, W.B., Hendrickson, W.A., *et al.* (2004). Structure of nucleotide-binding domain 1 of the cystic fibrosis transmembrane conductance regulator. Embo J *23*, 282–293.

Linton, K.J., and Higgins, C.F. (1998). The Escherichia coli ATP-binding cassette (ABC) proteins. Mol Microbiol *28*, 5–13.

Liu, C.E., Liu, P.Q., and Ames, G.F.L. (1997). Characterization of the adenosine-triphosphatase activity of the periplasmic histidine permease, a traffic atpase (abc transporter). Journal of Biological Chemistry *272*, 21883–21891.

Locher, K.P., Lee, A.T., and Rees, D.C. (2002). The E. coli BtuCD structure: a framework for ABC transporter architecture and mechanism. Science *296*, 1091–1098.

Lomize, M.A., Lomize, A.L., Pogozheva, I.D., and Mosberg, H.I. (2006b). OPM: orientations of proteins in membranes database. Bioinformatics *22*, 623–625.

Lomize, A.L., Pogozheva, I.D., Lomize, M.A., and Mosberg, H.I. (2006a). Positioning of proteins in membranes: a computational approach. Protein Sci *15*, 1318–1333.

Lu, G., Westbrooks, J.M., Davidson, A.L., and Chen, J. (2005). ATP hydrolysis is required to reset the ATP-binding cassette dimer into the resting-state conformation. Proc Natl Acad Sci U S A *102*, 17969–17974.

Lubelski, J., van Merkerk, R., Konings, W.N., and Driessen, A.J. (2006). Nucleotide-binding sites of the heterodimeric LmrCD ABC-multidrug transporter of Lactococcus lactis are asymmetric. Biochemistry *45*, 648–656.

Lugo, M.R., and Sharom, F.J. (2005). Interaction of LDS-751 with P-glycoprotein and mapping of the location of the R drug binding site. Biochemistry *44*, 643–655.

Miles, G., Bayley, H., and Cheley, S. (2002). Properties of Bacillus cereus hemolysin II: a heptameric transmembrane pore. Protein Sci *11*, 1813–1824.

Millet, O., Hudson, R.P., and Kay, L.E. (2003). The energetic cost of domain reorientation in maltose-binding protein as studied by NMR and fluorescence spectroscopy. Proc Natl Acad Sci U S A *100*, 12700–12705.

Moody, J.E., Millen, L., Binns, D., Hunt, J.F., and Thomas, P.J. (2002). Cooperative, ATP-dependent association of the nucleotide binding cassettes during the catalytic cycle of ATP-binding cassette transporters. J Biol Chem *277*, 21111–21114.

Mourez, M., Hofnung, M., and Dassa, E. (1997). Subunit interactions in ABC transporters: a conserved sequence in hydrophobic membrane proteins of periplasmic permeases defines an important site of interaction with the ATPase subunits. Embo J *16*, 3066–3077.

Moussatova, A., Kandt, C., O'Mara, M.L., and Tieleman, D.P. (2008). ATP-binding cassette transporters in Escherichia coli. Biochim Biophys Acta. *1778*, 1757- 1771.

Nikaido, K., and Ames, G.F. (1999). One intact ATP-binding subunit is sufficient to support ATP hydrolysis and translocation in an ABC transporter, the histidine permease. J Biol Chem *274*, 26727–26735.

Nikaido, K., Liu, P.Q., and Ames, G.F. (1997). Purification and characterization of HisP, the ATP-binding subunit of a traffic ATPase (ABC transporter), the histidine permease of Salmonella typhimurium. Solubility, dimerization, and ATPase activity. J Biol Chem *272*, 27745–27752.

Oldham, M.L., Khare, D., Quiocho, F.A., Davidson, A.L., and Chen, J. (2007). Crystal structure of a catalytic intermediate of the maltose transporter. Nature *450*, 515–521.

Orelle, C., Dalmas, O., Gros, P., Di Pietro, A., and Jault, J.M. (2003). The conserved glutamate residue adjacent to the Walker-B motif is the catalytic base for ATP hydrolysis in the ATP-binding cassette transporter BmrA. J Biol Chem *278*, 47002–47008.

Patzlaff, J.S., van der Heide, T., and Poolman, B. (2003). The ATP/substrate stoichiometry of the ATP-binding cassette (ABC) transporter OpuA. J Biol Chem *278*, 29546–29551.

Pinkett, H.W., Lee, A.T., Lum, P., Locher, K.P., and Rees, D.C. (2007). An inward-facing conformation of a putative metal-chelate-type ABC transporter. Science *315*, 373–377.

Procko, E., Ferrin-O'Connell, I., Ng, S.L., and Gaudet, R. (2006). Distinct structural and functional properties of the ATPase sites in an asymmetric ABC transporter. Mol Cell *24*, 51–62.

Procko, E., and Gaudet, R. (2008). Functionally important interactions between the nucleotide-binding domains of an antigenic peptide transporter. Biochemistry *47*, 5699–5708.

Quiocho, F.A., and Ledvina, P.S. (1996). Atomic structure and specificity of bacterial periplasmic receptors for active transport and chemotaxis: variation of common themes. Mol Microbiol *20*, 17–25.

Quiocho, F.A., Spurlino, J.C., and Rodseth, L.E. (1997). Extensive features of tight oligosaccharide binding revealed in high-resolution structures of the maltodextrin transport/chemosensory receptor. Structure *5*, 997–1015.

Richet, E., Joly, N., and Danot, O. (2005). Two domains of MalT, the activator of the Escherichia coli maltose regulon, bear determinants essential for anti-activation by MalK. J Mol Biol *347*, 1–10.

Sack, J.S., Saper, M.A., and Quiocho, F.A. (1989). Periplasmic binding protein structure and function. J Mol Biol *206*, 171–191.

Saier, M.H., Jr., Paulsen, I.T., Sliwinski, M.K., Pao, S.S., Skurray, R.A., and Nikaido, H. (1998). Evolutionary origins of multidrug and drug-specific efflux pumps in bacteria. FASEB J *12*, 265–274.

Sauna, Z.E., and Ambudkar, S.V. (2000). Evidence for a requirement for ATP hydrolysis at two distinct steps during a single turnover of the catalytic cycle of human P-glycoprotein. Proc Natl Acad Sci USA *97*, 2515–2520.

Sauna, Z.E., and Ambudkar, S.V. (2001). Characterization of the catalytic cycle of ATP hydrolysis by human P-glycoprotein. The two ATP hydrolysis events in a single catalytic cycle are kinetically similar but affect different functional outcomes. J Biol Chem *276*, 11653–11661.

Saurin, W., Hofnung, M., and Dassa, E. (1999). Getting in or out: early segregation between importers and exporters in the evolution of ATP-binding cassette (ABC) transporters. J Mol Evol *48*, 22–41.

Scheffel, F., Demmer, U., Warkentin, E., Hulsmann, A., Schneider, E., and Ermler, U. (2005). Structure of the ATPase subunit CysA of the putative sulfate ATP-binding cassette (ABC) transporter from Alicyclobacillus acidocaldarius. FEBS Lett *579*, 2953–2958.

Schmees, G., Stein, A., Hunke, S., Landmesser, H., and Schneider, E. (1999). Functional consequences of mutations in the conserved 'signature sequence' of the ATP-binding-cassette protein MalK. Eur J Biochem *266*, 420–430.

Schmitt, L., Benabdelhak, H., Blight, M.A., Holland, I.B., and Stubbs, M.T. (2003). Crystal structure of the nucleotide binding domain of the ABC-transporter haemolysin B: Identification of a variable region within ABC helical domains. J Mol Biol *330*, 333–342.

Schmitt, L., and Tampé, R. (2002). Structure and mechanism of ABC-transporters. Cur Opin Struc Biol *12*, 754–760.

Schuurman-Wolters, G.K., and Poolman, B. (2005). Substrate specificity and ionic regulation of GlnPQ from Lactococcus lactis. An ATP-binding cassette transporter with four extracytoplasmic substrate-binding domains. J Biol Chem *280*, 23785–23790.

Senior, A.E., al-Shawi, M.K., and Urbatsch, I.L. (1995). The catalytic cycle of P-glycoprotein. FEBS Lett *377*, 285–289.

Shapiro, A.B., and Ling, V. (1998). The mechanism of ATP-dependent multidrug transport by P-glycoprotein. Acta Physiol Scand Suppl *643*, 227–234.

Sharff, A.J., Rodseth, L.E., Spurlino, J.C., and Quiocho, F.A. (1992). Crystallographic evidence of a large ligand-induced hinge-twist motion between the two domains of the maltodextrin binding protein involved in active transport and chemotaxis. Biochemistry *31*, 10657–10663.

Sharma, S., and Davidson, A.L. (2000). Vanadate-induced trapping of nucleotides by purified maltose transport complex requires ATP hydrolysis. J Bacteriol *182*, 6570–6576.

Sharom, F.J. (2008). ABC multidrug transporters: structure, function and role in chemoresistance. Pharmacogenomics *9*, 105–127.

Sharom, F.J., Lugo, M.R., and Eckford, P.D. (2005). New insights into the drug binding, transport and lipid flippase activities of the p-glycoprotein multidrug transporter. J Bioenerg Biomembr *37*, 481–487.

Shimizu, T. (1981). Steady-state kinetic study of vanadate-induced inhibition of ciliary dynein adenosinetriphosphatase activity from Tetrahymena. Biochemistry *20*, 4347–4354.

Shyamala, V., Baichwal, V., Beall, E., and Ames, G.F. (1991). Structure–function analysis of the histidine permease and comparison with cystic fibrosis mutations. J Biol Chem *266*, 18714–18719.

Smith, C.A., and Rayment, I. (1996). X-ray structure of the magnesium(II).ADP.vanadate complex of the Dictyostelium discoideum myosin motor domain to 1.9 A resolution. Biochemistry *35*, 5404–5417.

Smith, P.C., Karpowich, N., Millen, L., Moody, J.E., Rosen, J., Thomas, P.J., and Hunt, J.F. (2002). ATP binding to the motor domain from an ABC transporter drives formation of a nucleotide sandwich dimer. Mol Cell *10*, 139–149.

Steinfels, E., Orelle, C., Fantino, J.R., Dalmas, O., Rigaud, J.L., Denizot, F., Di Pietro, A., and Jault, J.M. (2004). Characterization of YvcC (BmrA), a multidrug ABC transporter constitutively expressed in Bacillus subtilis. Biochemistry *43*, 7491–7502.

Stenham, D.R., Campbell, J.D., Sansom, M.S., Higgins, C.F., Kerr, I.D., and Linton, K.J. (2003). An atomic detail model for the human ATP binding cassette transporter P-glycoprotein derived from disulfide cross-linking and homology modeling. FASEB J *17*, 2287–2289.

Story, R.M., and Steitz, T.A. (1992). Structure of the recA protein-ADP complex. Nature *355*, 374–376.

Tang, C., Schwieters, C.D., and Clore, G.M. (2007). Open-to-closed transition in apo maltose-binding protein observed by paramagnetic NMR. Nature *449*, 1078–1082.

Tombline, G., Bartholomew, L., Gimi, K., Tyndall, G.A., and Senior, A.E. (2004a). Synergy between conserved ABC signature Ser residues in P-glycoprotein catalysis. J Biol Chem *279*, 5363–5373.

Tombline, G., Bartholomew, L.A., Urbatsch, I.L., and Senior, A.E. (2004b). Combined mutation of catalytic glutamate residues in the two nucleotide binding domains of P-glycoprotein generates a conformation that binds ATP and ADP tightly. J Biol Chem *279*, 31212–31220.

Treptow, N.A., and Shuman, H.A. (1985). Genetic evidence for substrate and periplasmic-binding-protein recognition by the MalF and MalG proteins, cytoplasmic membrane components of the Escherichia coli maltose transport system. J Bacteriol *163*, 654–660.

Urbatsch, I.L., Sankaran, B., Weber, J., and Senior, A.E. (1995). P-glycoprotein is stably inhibited by vanadate-induced trapping of nucleotide at a single catalytic site. J Biol Chem *270*, 19383–19390.

Urbatsch, I.L., Tyndall, G.A., Tombline, G., and Senior, A.E. (2003). P-glycoprotein catalytic mechanism: studies of the ADP-vanadate inhibited state. J Biol Chem *278*, 23171–23179.

van der Does, C., and Tampe, R. (2004). How do ABC transporters drive transport? Biol Chem *385*, 927–933.

van der Heide, T., and Poolman, B. (2000). Osmoregulated ABC-transport system of Lactococcus lactis senses water stress via changes in the physical

state of the membrane. Proc Natl Acad Sci U S A *97*, 7102–7106.

van der Heide, T., and Poolman, B. (2002). ABC transporters: one, two or four extracytoplasmic substrate-binding sites? EMBO Rep *3*, 938–943.

van Veen, H.W., Margolles, A., Muller, M., Higgins, C.F., and Konings, W.N. (2000). The homodimeric ATP-binding cassette transporter LmrA mediates multidrug transport by an alternating two-site (two-cylinder engine) mechanism. EMBO J *19*, 2503–2514.

Vazquez de Aldana, C.R., Marton, M.J., and Hinnebusch, A.G. (1995). GCN20, a novel ATP binding cassette protein, and GCN1 reside in a complex that mediates activation of the eIF-2 alpha kinase GCN2 in amino acid-starved cells. EMBO J *14*, 3184–3199.

Velamakanni, S., Yao, Y., Gutmann, D.A., and van Veen, H.W. (2008). Multidrug Transport by the ABC Transporter Sav1866 from Staphylococcus aureus. Biochemistry *47,* 9300- 9308.

Verdon, G., Albers, S.V., van Oosterwijk, N., Dijkstra, B.W., Driessen, A.J., and Thunnissen, A.M. (2003). Formation of the productive ATP-Mg2+-bound dimer of GlcV, an ABC-ATPase from Sulfolobus solfataricus. J Mol Biol *334*, 255–267.

Vergani, P., Lockless, S.W., Nairn, A.C., and Gadsby, D.C. (2005). CFTR channel opening by ATP-driven tight dimerization of its nucleotide-binding domains. Nature *433*, 876–880.

Vetter, I.R., and Wittinghofer, A. (1999). Nucleoside triphosphate-binding proteins: different scaffolds to achieve phosphoryl transfer. Q Rev Biophys *32*, 1–56.

Walker, J.E., Saraste, M., Runswick, M.J., and Gay, N.J. (1982). Distantly related sequences in the alpha- and beta-subunits of ATP synthase, myosin, kinases and other ATP-requiring enzymes and a common nucleotide binding fold. Embo J *1*, 945–951.

Ward, A., Reyes, C.L., Yu, J., Roth, C.B., and Chang, G. (2007). Flexibility in the ABC transporter MsbA: Alternating access with a twist. Proc Natl Acad Sci U S A *104*, 19005–19010.

Watanabe, S., Kita, A., and Miki, K. (2005). Crystal structure of atypical cytoplasmic ABC-ATPase SufC from Thermus thermophilus HB8. J Mol Biol *353*, 1043–1054.

Zaitseva, J., Jenewein, S., Jumpertz, T., Holland, I.B., and Schmitt, L. (2005a). H662 is the linchpin of ATP hydrolysis in the nucleotide-binding domain of the ABC transporter HlyB. Embo J.

Zaitseva, J., Jenewein, S., Wiedenmann, A., Benabdelhak, H., Holland, I.B., and Schmitt, L. (2005b). Functional characterization and ATP-induced dimerization of the isolated ABC-domain of the haemolysin B transporter. Biochemistry *44*, 9680–9690.

Zaitseva, J., Oswald, C., Jumpertz, T., Jenewein, S., Wiedenmann, A., Holland, I.B., and Schmitt, L. (2006). A structural analysis of asymmetry required for catalytic activity of an ABC-ATPase domain dimer. EMBO J *25*, 3432–3443.

MsbA_S.typhimurium 1 EKDEGKRVIDRATGDLEFRNVTFTYPGREVPALRNINLKIPAGKTVALVGRSGSGKSTIASLITRFY..DIDEGHIMDGHD.....LREVT
MsbA_E.coli 1 EKDEGKRVIERATGDVEFRNVTFTYPGRDVPALRNINLKIPAGKTVALVGRSGSGKSTIASLITRFY..DIDEGEIMDGHD.....LREVT
Sav1866_S.aureus 1 DYDIKNGVGAQPIEIKQGRIDIDHVSFQYNDNEAPILKDINLSIEKGETVAFVGMSGGGKSTLINLIPRFY..DVTSGQILIDGHN.....IKDFL
LmrA_L.lactis 1 MLSARHVDFAYDDSEQ..ILRDISFEAQPNSIIAFAGPSGGGKSTIFSLLERFY..QPTAGEITIDGQP.....IDNIS
HlyB_E.coli 1 DITFRNIRFRYKPDSPVILDNINLSIKQGEVIGIVGRSGSGKSTLTKLIQRFY..IPENGQVLIDGHD.....LALAD
MetN_E.coli 1 MIKLSNITKVFHQGTRTIQALNNVSLHVPAGQIYGVIGASGAGKSTLIRCVNLLE..RPTEGSVLVDGQ.....ELTTL
HisP_S.typhimurium 1 MMSENKLHVIDLHKRYGGHEVLKGVSLQARAGDVISIIGSSGSGKSTFLRCINFLE..KPSEGAIIVNGQNINLVRDKDGQLKVA
MalK_P.horikoshii 1 GNNIEVIKMVEVKLENLTKRFG.NFTAVNKLNLTIKDGEFLVLLGPSGCGKTTTLRMIAGLE..EPTEGRIYFGDRD.....VTYLP
1VCI_P.horikoshii 1 MGNNIEVIKMVEVKLENLTKRFG.NFTAVNKLNLTIKDGEFLVLLGPSGCGKTTTLRMIAGLE..EPTEGRIYFGDRD.....VTYLP
MalK_E.coli 1 MASVQLQNVTKAWG.EVVVSKDINLDIHEGEFVVFVGPSGCGKSTLLRMIAGLE..TITSGDLFIGEKR.....MNDTP
ModC_A.fulgidus 1 MFLKVRAEKRLG.NFRLN...VDFEMGRDYCVLLGPTGAGKSVFLELIAGIV..KPDRGEVRLNGAD.....ITPLP
ModC_M.acetivorans 1 MIEIESLSRKWK.NFSLDNLSLKVESG.EYFVILGPTGAGKTLFLELIAGFH..VPDSGRILLDGKD.....VTDLS
CysA_A.acidocaldarius 1 MRGHHHHHHHGSMTIEFVGVEKIYPGGARSVRGVSFQIREGEMVGLLGPSGSGKTTILRLIAGLE..RPTKGDVWIGGKR.....VTDLP
MJ1267_E.coli 1 MIKLKNVTKTYKMGEEIIYALKNVNLNIKEGEFVSIMGPSGSGKSTMLNIIGCLD..KPTEGEVYIDNIK.....TNDLD
MJ0796_M.janaschii 1 MIKLKNVTKTYKMGEEIIYALKNVNLNIKEGEFVSIMGPSGSGKSTMLNIIGCLD..KPTEGEVYIDNIK.....TNDLD
GlcV_S.solfataricus 1 MVRIIVKNVSKVFKKGK..VVALDNVNINIENGERFGILGPSGAGKTTFMRIIAGLD..VPSTGELYFDDRL.....VASNG
SufC_E.coli 1 MLSIKDLHVSVEDKAILRGLSLDVHPGEVHAIMGPNGSGKSTLSATLAGREDYEVTGGTVEFKGKD.....LLALS
SufC_T.thermophilus 1 MSQLEIRDLWASIDGETILKGVNLVVPKGEVHALMGPNGAGKSTLGKIIAGDPEYTVERGEILLDGEN.....ILELS
TM0544_T.maritima 1 MGSDKLHHHHHHMGAVVKDLRKRIGKKEILKGISFEIEEGEIFGLIGPNGAGKTTTLRIISTLIK..PSSGIVTVFGKN.....VVEEP
MJ1267_M.janaschii 1 MRDTMEILRTENIVKYFGEFKALDGVSISVNKGDVTLIIGPNGSGKSTLINVITGFL..KADEGRVYFENKD.....ITNKE
BtuD_E.coli 1 MSIVMQLQDVAESTRLGPLSGEVRAGEILHLVGPNGAGKSTLLARMAGMT...SGKGSIQFAGQP.....
HI1470_H.inluenzae 1 MNKALSVENLGFYYQAENFLFQQLNFDLNKGDIIAVLGQNGCGKSTLLDLLLGIH..RPIQGKIEVYQSIG.....
Walker A
MsbA_S.typhimurium 86 LAS....LRNQVALVSQNVHLFN...DTVANNIAYARTEEYSREQIEEAARMAYAMDFINKMDNGLDT.IIGENGVL.LSGGQRQRIAIARALLRDS...
MsbA_E.coli 86 LAS....LRNQVALVSQNVHLFN...DTVANNIAYARTEQYSREQIEEAARMAYAMDFINKMDNGLDT.VIGENGVL.LSGGQRQRIAIARALLRDS...
Sav1866_S.aureus 90 TGS....LRNQIGLVQQDNILFS...DTVKENILLGR.PTATDEEVVEAAKMANAHDFIMNLPQGYDT.EVGERGVK.LSGGQKQRLSIARTFLNNP...
LmrA_L.lactis 71 LEN....WRSQIGFVSQDSAIMA...GTIRENLTYGLEGDYTDEDLWQVLDLAFARSFVENMPDQLNT.EVGERGVK.ISGGQRQRIAIARAFLRNP...
HlyB_E.coli 72 PNW....LRRQVGVVLQDNVLLN...RSIIDNISLAN.PGMSVEKVIYAAKLAGAHDFISELREGYNT.IVGEQGAG.LSGGQRQRIAIARALVNNP...
MetN_E.coli 73 SESELTKARRQIGMIFQHFNLLS...SRTVFG.NVALPLELDN....TPKDEVKRRVTELLSLVGLGDK.HD.SYPSN.LSGGQKQRVAIARALASNP...
HisP_S.typhimurium 84 DKNQLRLLRTRLTMVFQHFNLWS...HMTVLENVMEAPIQVLG....LSKHDARERALKYLAKVGIDER.AQGKYPVH.LSGGQQQRVSIARALAMEP...
MalK_P.horikoshii 80 P.......KDRNISMVFQSYAVWP...HMTVYE.NIAFPLKIKK....FPKDEIDKRVRWAAELLQIEE..LLNRYPAQ.LSGGQRQRVAVARAIVVEP...
1VCI_P.horikoshii 81 P.......KDRNISMVFQSYAVWP...HMTVYE.NIAFPLKIKK....FPKDEIDKRVRWAAELLQIEE..LLNRYPAQ.LSGGQRQRVAVARAIVVEP...
MalK_E.coli 72 P.......AERGVGMVFQSYALYP...HLSVAE.NMSFGLKLAG....AKKEVINQRVNQVAEVLQLAH..LLDRKPKA.LSGGQRQRVAIGRTLVAEP...
ModC_A.fulgidus 67 P.......ERRGIGFVPQDYALFP...HLSVYR.NIAYGLRNVE....RVER..DRRVREMAEKLGIAH..LLDRKPAR.LSGGERQRVALARALVIQP...
ModC_M.acetivorans 69 P.......EKHDIAFVYQNYSLFP...HMNVKK.NLEFGMR.MK....KIKD..PKRVLDTARDLKIEH..LLDRNPLT.LSGGEQQRVALARALVTNP...
CysA_A.acidocaldarius 84 P.......QKRNVGLVFQNYALFQ...HMTVYD.NVSFGLREKR....VPKDEMDARVRELLRFMRLES..YANRFPHE.LSGGQQQRVALARALAPRP...
MJ1267_E.coli 74 DDELTKIRRDKIGFVFQQFNLIP....LLTALE.NVELPLIFKYRGAMSGEERRKRALECLKWAELEER.FANHKPNQ.LSGGQQQRVAIARALANNP...
MJ0796_M.janaschii 74 DDELTKIRRDKIGFVFQQFNLIP....LLTALE.NVELPLIFKYRGAMSGEERRKRALECLKWAELEER.FANHKPNQ.LSGGQQQRVAIARALANNP...
GlcV_S.solfataricus 74 KLIVPPEDR.KIGMVFQTWALYP....NLTAFE.NIAFPLTNMK....MSKEEIRKRVEEVAKILDIHH...VLNHFPRE.LSGGQQQRVALARALVKDP...
SufC_E.coli 72 PED....RAGEGIFMAFQYPVEIPGVSNQFFLQTALNAVRSYRGQETLDRFDFQDLMEEKIALLKMPED.LLTRSVNVGFSGGEKKRNDILQMAVLEP...
SufC_T.thermophilus 74 PDE....RARKGLFLAFQYPVEVPGVTIANFLRLALQAKLGR.....EVGVAEFWTKVKKALELLDWDES.YLSRYLNEGFSGGEKKRNEILQLLVLEP...
TM0544_T.maritima 84 HEV.....RKLISYLPEEAGAYR.........NMQGIEYLRFVAGFYASSSEIEEMVERATEIAGLGEK.IKDRVSTY..SKGMVRKLLIARALMVNP...
MJ1267_M.janaschii 76 PAELYHYGIVRTFQTPQPLKEMTVLENLLIGEINPGESPLNSLFYKKWIPKEEEMVEKAFKILEFLKLSHLYDRKAGELSGGQMKLVEIGRALMTNP...
BtuD_E.coli 63 .....LEAWSATKLALHRAYLS.....QQQTPPFATPVWHYLTLHQHDKTRTELLNDVAGALALDDK..LGRSTNQ.LSGGEWQRVRLAAVVLQITPQA
HI1470_H.inluenzae 70 .....FVPQFFSSPFAYS.....VLDIVLMGRSTHIN....TFAKPKSHDYQVAMQALDYLNLTHLAKREFTSLSGGQRQLLILARAIASEC...
Q-loop
Stuctural diverse region
C-loop
Pro-loop

Plate 1.1 (overleaf) Amino acid sequence alignment of the nucleotide binding domains of prokaryotic ABC transporters whose structures have been solved. The conserved motifs are colour-coded: Walker A (red), Q-loop (magenta), structural diverse region (SDR; black), C-loop (pale green), Pro-loop (orange), Walker B (blue), D-loop (cyan), and H-loop (green). The function of the distinct residues is explained in detail in the text.

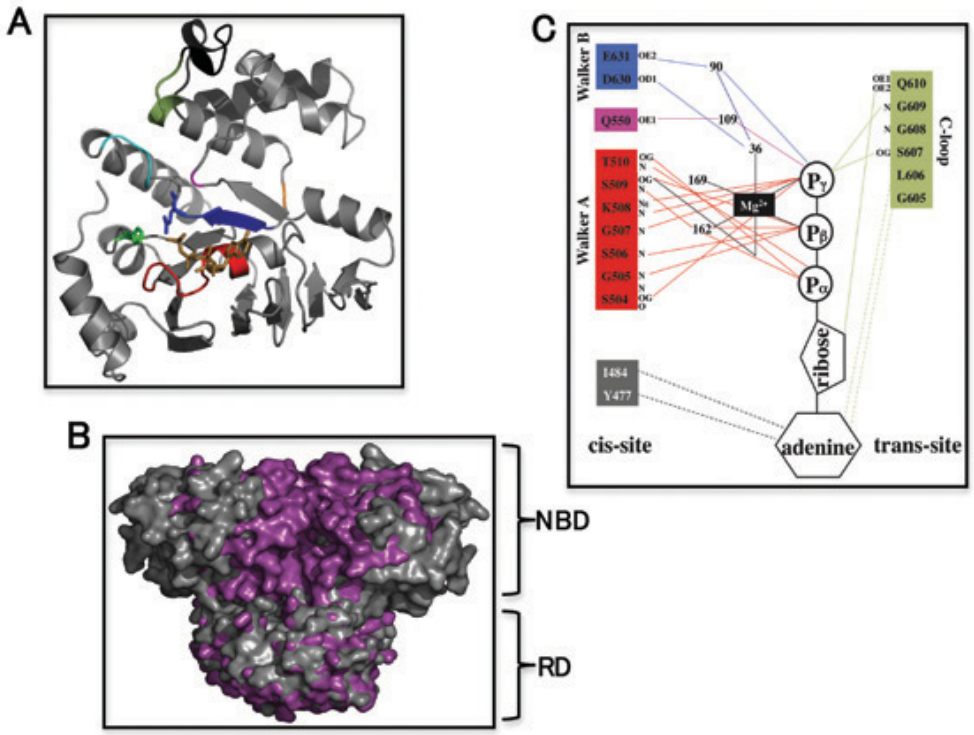

Plate 1.2 A Crystal structure of HisP, the nucleotide binding domain of the histidine permease from *S.* Typhimurium with bound ATP (pdb entry 1B0U). The helical domain contains the C-loop (pale green) and the structural diverse region (SDR; black) and is linked via the Q-loop (magenta) and the Pro-loop (orange) to the catalytic domain. The catalytic domain contains the Walker A (red) and Walker B (blue) motifs and the D-loop (cyan) as well as the H-loop (green). The glutamate at the end of Walker B and the histidine of the H-loop are depicted in stick-representation as they are crucial in ATP hydrolysis. **B** Structural superposition of the nucleotide free (gray) and ATP-bound (magenta) structure of the nucleotide binding domain MalK (pdb entries: 1Q1E, 1Q12). The NBDs come into close contact upon ATP binding whereas only minor changes can be detected in the regulatory domains (RD). **C** Detailed network of ATP coordination in the binding pocket of the HlyB-NBD. Solid lines indicate hydrogen bonds and dashed lines show van-der-Waals interactions. Colour-coding is equivalent to Plate 1.2A. The black numbers indicate water molecules that are part of the extensive network of interactions. Letters next to the amino acid labels indicate involvement via main-chain or side-chain interactions.

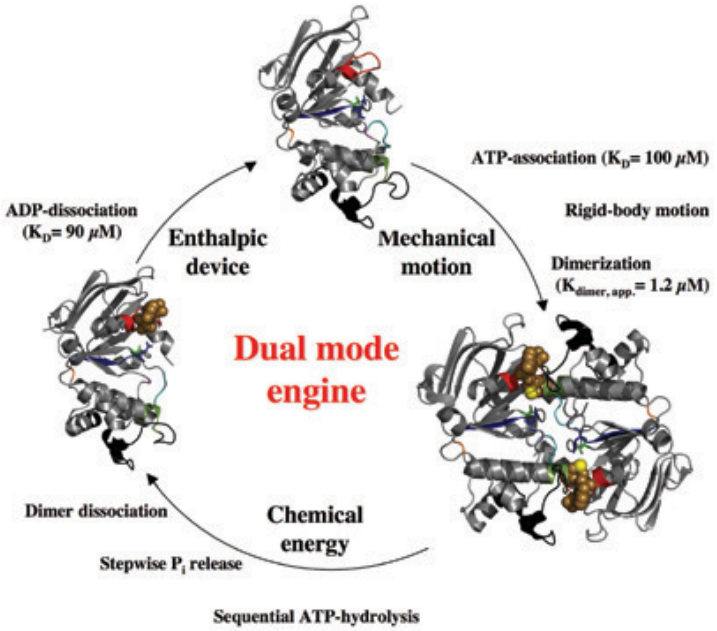

Plate 1.3 Schematic representation of the catalytic cycle of the HlyB-NBD. Colour-coding is identical to Plate 1.2A. The cycle starts with the nucleotide free state of the monomer (pdb entry: 1MT0). Binding of ATP to both monomers induces dimer formation (ATP in brown and Mg^{2+} in yellow; pdb entry: 1XEF). After hydrolysis of ATP the dimer dissociates and ADP is subsequently released (pdb entry: 2FF7). A detailed description of each step can be found in the corresponding section of the text.

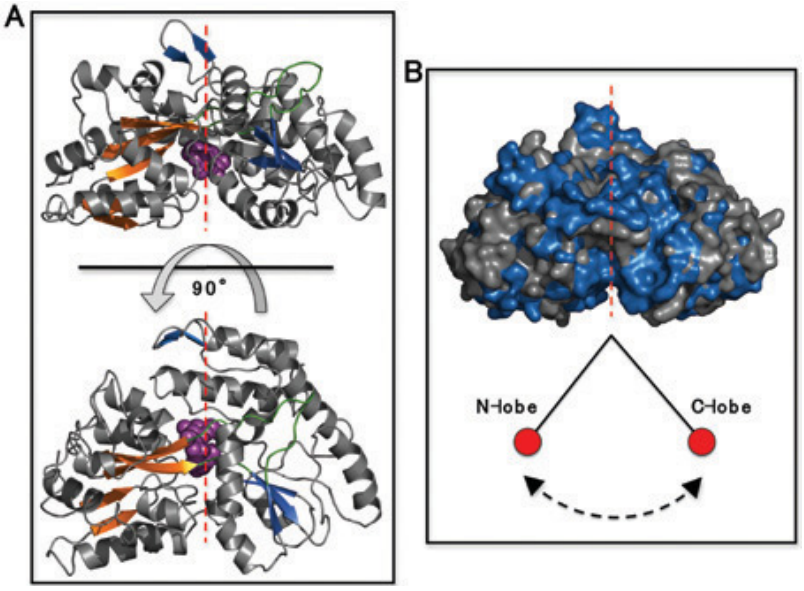

Plate 1.4 **A** In the upper part the side view of the periplasmic binding protein BtuF with bound vitamin B_{12} (magenta) is shown (pdb entry 1N2Z). The five-stranded antiparallel β-sheets are depicted in orange and blue, respectively. N- and C-lobe are connected by loop regions; here shown in green. In the lower part BtuF is rotated about 90° to look at the protein from above. **B** Structural superposition of the ligand-free (grey) and ligand-bound (blue) structure of the maltose binding protein. Upon binding of maltose a domain displacement leading to closure of the lobes of roughly 30° is observed.

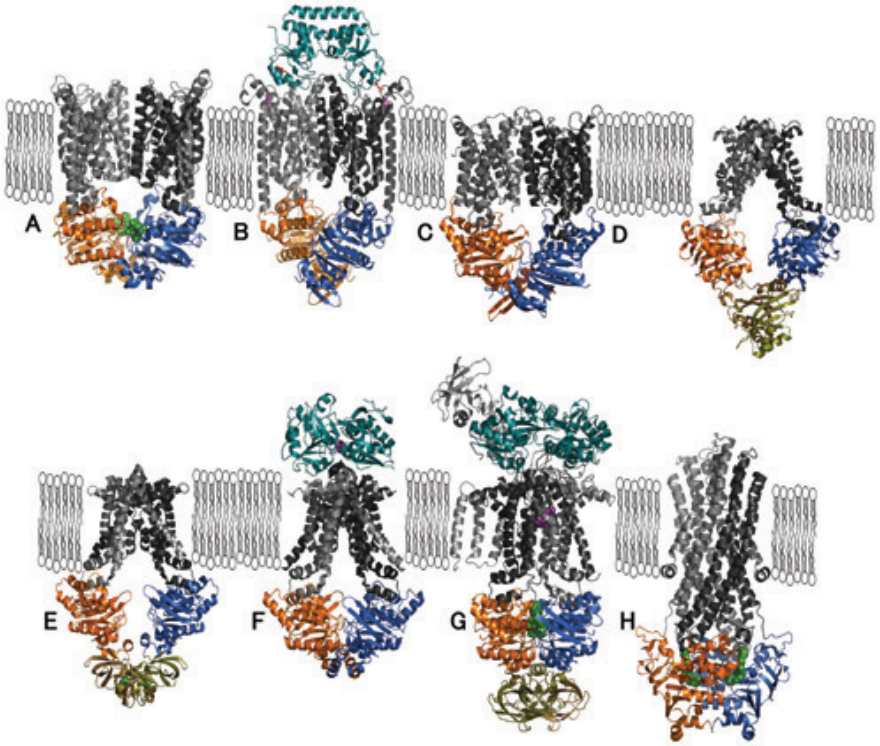

Plate 1.5 Crystal structures of ABC transporters. The importers **A** BtuCD, **B** BtuCD-F, **C** HI1470/1471, **D** MetNI, **E** ModBC, **F** ModBC-A, **G** MalFGK-E, and the exporter **H** Sav1866 are depicted. More information about a particular transporter can be found in the respective section of the chapter.

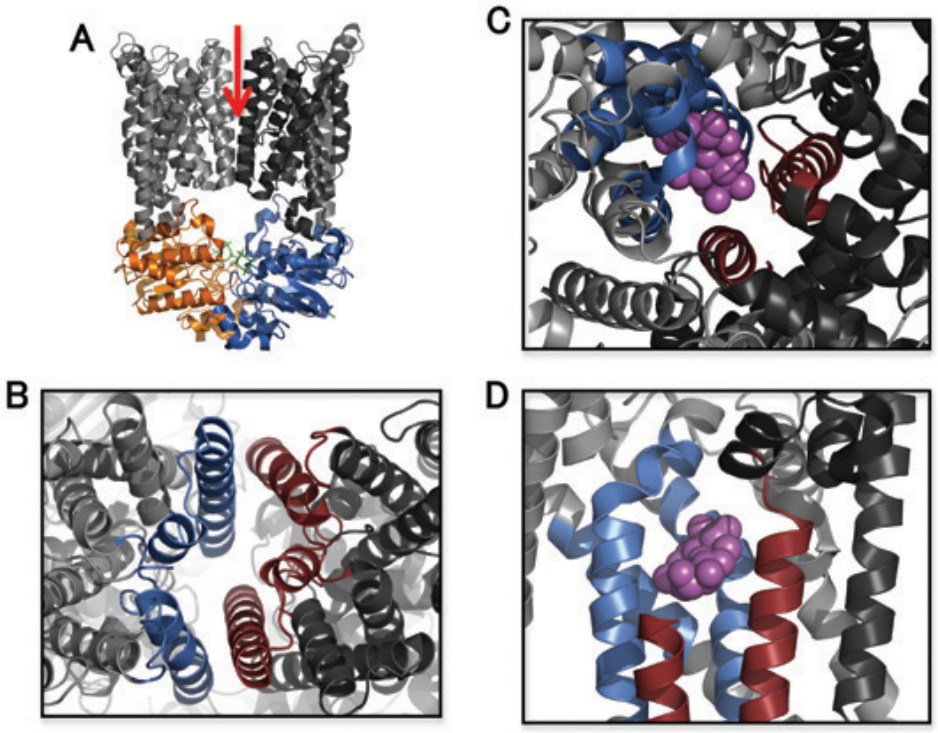

Plate 1.7 **A** Quaternary structure of the vitamin B_{12} importer BtuCD. **B** BtuCD is viewed from above through the postulated substrate translocation pore. Helices from each TMD subunit lining the translocation pore are coloured red and blue, respectively. **C** View from above into the translocation pore of the $MalEFGK_2$ transporter with bound maltose (magenta). **D** Side view of the maltose binding site in the transmembrane domains of the $MalEFGK_2$ importer complex. For clarity some helices have been omitted.

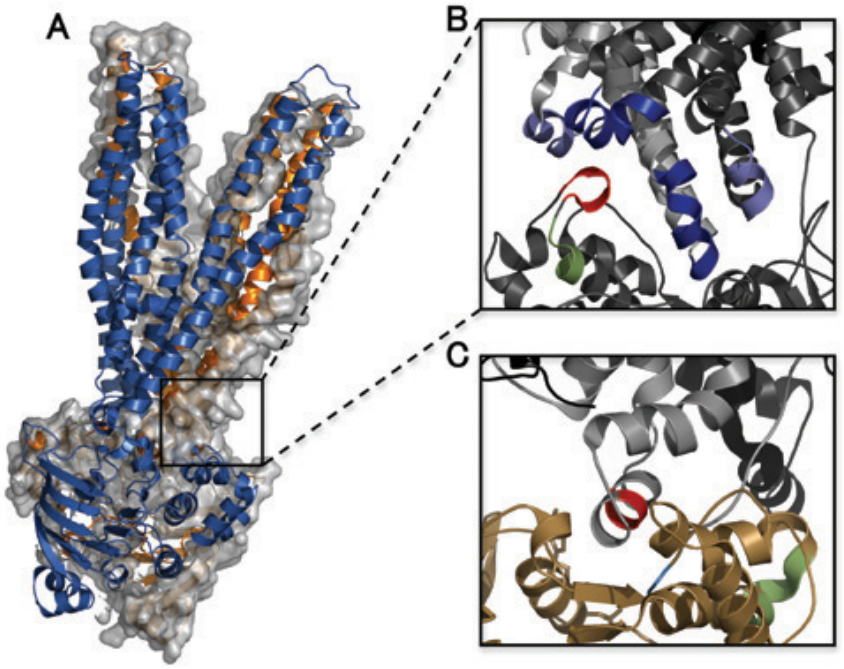

Plate 1.8 A Cartoon representation of the ABC exporter Sav1866. **B** The inset is a magnification of the postulated interaction site between TMDs and NBDs. In blue and slate intracellular loops from both membrane subunits are shown. Residues in red represent the TEVGERG sequence found to interact extensively with the intracellular loops. The C-loop is depicted in pale green. **C** Interaction site between TMD and NBD of the $MalEFGK_2$ complex. The transmembrane part is shown in grey and the NBD in brown. In the L-loop from the transmembrane domain the EAA motif characteristic for ABC importers (red) is highlighted. The C-loop is depicted in pale green and the D-loop in cyan.

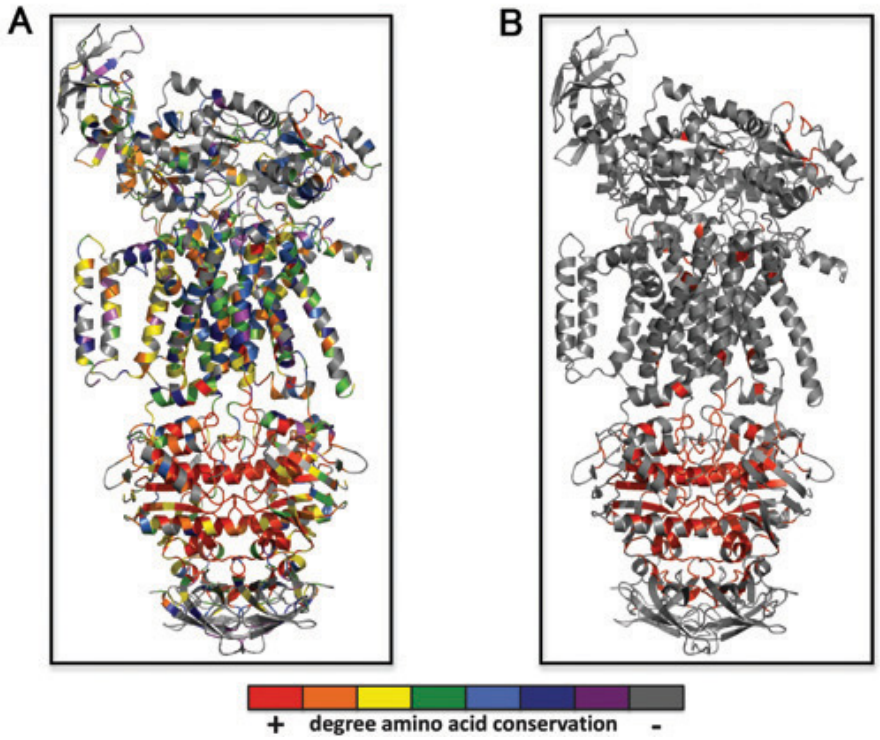

Plate 1.9 **A** Analysis of conserved amino acids in the MalEFGK$_2$ complex. The amino acid sequence of this importer was compared with 50 other ABC transporters and conserved amino acids are highlighted with the ConSurf Server (http://consurf.tau.ac.il/). **B** Only the highest conserved amino acids are shown in red. As explained in the text, the highest conservation is found in the nucleotide binding domains.

Proportionate work on this publication: 70 %

Published in: ABC transporters in Microorganisms, Caister Academic Press

Impact factor: n.a.

"This book represents an interdisciplinary review of the role of ABC transporters in microorganisms, combining data from structural biology, biochemistry, clinical research and pharmacology ... a comprehensive review with a general outline given in each chapter that is essential and useful not only for readers interested in the fascinating ABC transporter family." *from* Britta Kunert, Webcritics (2009)

"offers insights into the future of the field from both scientific and clinical perspectives" *from* SciTech Book News

PAPER II

990 Biochemical Society Transactions (2005) Volume 33, part 5

A molecular understanding of the catalytic cycle of the nucleotide-binding domain of the ABC transporter HlyB

J. Zaitseva*[1], S. Jenewein*[1], C. Oswald*[1], T. Jumpertz*[1], I.B. Holland† and L. Schmitt*[1,2]

*Institute of Biochemistry, Biocenter, Johann-Wolfgang Goethe University Frankfurt, Marie Curie Strasse 9, 60439 Frankfurt, Germany, and †Institut de Génétique et Microbiologie, Bâtiment 409, Université de Paris XI, 91405 Orsay, France

Abstract

The ABC transporter (ATP-binding-cassette transporter) HlyB (haemolysin B) is the central element of a type I secretion machinery, dedicated to the secretion of the toxin HlyA in *Escherichia coli*. In addition to the ABC transporter, two other indispensable elements are necessary for the secretion of the toxin across two membranes in a single step: the transenvelope protein HlyD and the outer membrane protein TolC. Despite the fact that the hydrolysis of ATP by HlyB fuels secretion of HlyA, the essential features of the underlying transport mechanism remain an enigma. Similar to all other ABC transporters, ranging from bacteria to man, HlyB is composed of two NBDs (nucleotide-binding domains) and two transmembrane domains. Here we summarize our detailed biochemical, biophysical and structural studies aimed at an understanding of the molecular principles of how ATP-hydrolysis is coupled to energy transduction, including the conformational changes occurring during the catalytic cycle, leading to substrate transport. We have obtained individual crystal structures for each single ground state of the catalytic cycle. From these and other biochemical and mutational studies, we shall provide a detailed molecular picture of the steps governing intramolecular communication and the utilization of chemical energy, due to ATP hydrolysis, in relation to resulting structural changes within the NBD. These data will be summarized in a general model to explain how these molecular machines achieve translocation of molecules across biological membranes.

Many Gram-negative bacteria use ABC (ATP-binding cassette)-dependent type I secretion machineries for the translocation of toxins, lipases, proteases, surface layer proteins and cytolysins across both membranes in a single step [1,2]. The paradigm of these Sec-independent systems is the HlyA (haemolysin A) translocase of *Escherichia coli*, the genes for which were originally isolated from a human uropathogenic strain [3]. The only common feature of the great majority of the transport substrates, or allocrites [4] of the type I pathway, is the presence of Gly-rich repeats. Thus HlyA, a 1023-amino-acid protein, belongs to the family of RTX (repeat in toxins) toxins [5], containing repetitive amino acid sequences with the consensus sequence GGXGXDL/IFX, where X represents any amino acid. The repeats bind Ca^{2+} with high affinity and are thought to trigger refolding after successful secretion on to the cell surface prior to release to the extracellular medium [6]. In addition to the Gly-rich repeats, many studies have demonstrated that all information necessary and sufficient for the secretion of HlyA and other type I proteins is encoded in the C-terminal region of the allocrite [7,8]. Although the importance of the C-terminal secretion sequence has been clearly established, the nature of the precise recognition features remains unclear [9,10]. There are no clear indications of highly conserved residues or motifs, nor secondary structure elements that could be detected in aqueous solution [11,12]. This is in clear contrast with the Sec-machinery [13], where the signal sequence is located at the N-terminus, contains readily recognizable features and is cleaved by a signal peptidase after translocation.

The HlyA transport machinery is composed of three indispensable components [14–18]: HlyB, an ABC transporter, HlyD, the so-called MFP (membrane fusion protein), both of which reside in the inner membrane, and the outer membrane protein TolC (see Figure 1). Genetic studies have shown that removal of any one of the three components results in abrogation of allocrite secretion. TolC, whose trimeric structure was solved in 2000 by Koronakis et al. [19], forms a 'channel-tunnel'. The β-barrel resides within the outer membrane and elongates into 12 antiparallel α-helices protruding into the periplasmic space. It is thought that TolC and HlyD form a continuous tunnel capable of accommodating an unfolded protein during passage across both membranes of *E. coli*. HlyD contains a small cytoplasmic domain (residues 1–60), a single transmembrane spanning helix, and a large periplasmic, helical domain (residues 81–478), which is thought to interact at some stage of allocrite transport with

Key words: ATP-binding cassette transporter (ABC transporter), ATP-hydrolysis, haemolysin B (HlyB), nucleotide-binding domain, substrate-assisted catalysis, X-ray structure.

Abbreviations used: ABC transporter, ATP-binding-cassette transporter; Hly, haemolysin; MFP, membrane fusion protein; NBD, nucleotide-binding domain; SDR, structurally diverse region; TMD, transmembrane-binding domain.

[1]**Present address:** Institute of Biochemistry, Heinrich Heine University Düsseldorf, Universitätsstrasse 1, 40225 Düsseldorf, Germany.

[2]**To whom correspondence should be addressed, at Institute of Biochemistry, Biocenter, Johann-Wolfgang Goethe University Frankfurt (email lschmitt@em.uni-frankfurt.de).**

Figure 1 | **Cartoon of the HlyA transport machinery**

The allocrite HlyA is shown in red, the ABC transporter HlyB in blue, the MFP HlyD in green and the outer-membrane protein TolC in orange. The white spheres in the extracellular media represent Ca^{2+}, which catalyse toxin refolding.

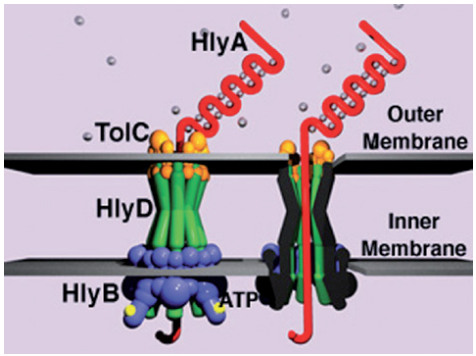

the helices of TolC [1,18,20,21]. The third and last component is HlyB, a member of the ABC transporter family [22], which will be described in detail below.

Based on more than a decade of research, a molecular picture of the complex interplay and communication between the single components of the HlyA secretion machinery is now emerging. In the absence of allocrite, HlyB and HlyD form a rather stable complex within the inner membrane of *E. coli* [23]. As shown by Koronakis and co-workers [23], the secretion sequence of HlyA interacts with the small cytoplasmic domain of HlyD resulting in the recruitment of TolC. In addition, we showed that the NBD (nucleotide-binding domain) of HlyB specifically interacts with the secretion sequence of HlyA [24]. These two events, involving simultaneous or sequential interactions with HlyB and HlyD, probably represent the first steps of recognition, assembly of the machinery, and, as described below, the insertion of HlyA into the allocrite channel. After this HlyA–HlyB–HlyD complex has been assembled at the inner membrane [25], a continuous channel is formed across the periplasmic space [26]. Such a channel explains two most important observations: the absence of any periplasmic HlyA intermediate during transport and the indispensability of the three components, HlyB, HlyD and TolC.

In the Sec-system, both co- and post-translational translocation are known to occur. In the case of HlyA, it is commonly assumed that the allocrite is transported in the unfolded state. Since the secretion signal is encoded in the C-terminal part of the 107 kDa protein, co-translation secretion can be certainly ruled out [27]. Nevertheless, it remains unknown how HlyA is retained in an unfolded state before and during post-translational transport and whether certain chaperones are involved in this process. So far, only a single report has described the involvement of the SecB chaperone in the secretion of one type I allocrite HasA [28]. However, the small HasA protein might be exceptional in using SecB.

It is expected that such a translocation mechanism has to be energy dependent and studies have shown that ATP-hydrolysis by the ABC transporter HlyB is required for allocrite secretion [29]. However, it is currently unknown which step of the secretion cycle has to be energized, how many ATPs are consumed for the secretion of a single HlyA molecule, or how the chemical energy of ATP is coupled to allocrite translocation at the molecular level.

HlyB is a member of the largest membrane protein families, the ABC transporters [22]. These ATP-dependent channels and pumps are found in all three kingdoms of life [30]. The definition relies solely on the presence of a TMD (transmembrane-binding domain) associated with an NBD carrying a number of highly conserved, distinct motifs: the Walker A (consensus sequence: GXX(G)XGKST, where X can be any amino acid) and B (ΦΦΦΦD, where Φ can be any hydrophobic amino acid) motifs, the C-loop or signature motif (consensus sequence LSGGQQ/R), which is considered the hallmark of ABC transporters, although the D-loop sequence (consensus sequence SALD) is equally diagnostic. Despite the highly conserved NBD, the TMD is poorly conserved, explaining the myriad of allocrites that are transported by ABC transporters. These range from small inorganic ions such as chloride, nutrients such as amino acids, sugars or peptides, a variety of hydrophobic substances and even extremely large proteins. Despite the enormous diversity of the allocrite, all ABC transporters have the same basic blue print of their core components: two NBDs and two TMDs.

In 1998, the first crystal structure of an NBD, HisP – the motor domain of the histidine permease, was reported [31]. Subsequently, an increasing number of NBD crystal structures appeared [32–39]. In addition, three crystal structures of intact ABC transporters have now been determined [40–42]. These NBDs originate from archeal, bacterial and eukaryotic organisms and cover ABC transporters with import or export functions. All share the same overall fold, which, as shown in Figure 2, is an L-shaped molecule with two domains. The catalytic domain harbours the nucleotide-binding site and can be further subdivided into the ABC-β subdomain and the F_1-core [43]. The second, the helical domain, interacts with the TMDs as shown by mutational and cross-linking analysis, and is connected to the catalytic domain via the Q- and Pro-loop [39].

The ABC–NBDs are an excellent example of structure–function conservation in biology. However, this raises the question, how, especially in archea and prokarya, where the different domains are normally encoded on separate genes, the isolated NBDs are targeted to their corresponding TMD. Notably, there have been few if any reports of the successful substitution of one NBD in another ABC transporter. On the contrary, already in the early 1990s, the properties of a MalK-HisP chimaera [44] indicated that the helical domain contains recognition sites 'specific' for its cognate TMD. Moreover, based on the published crystal structures, we were able to identify an SDR (structurally diverse region)

Figure 2 | **Crystal structure of the HlyB-NBD comprising residues 467–707 of HlyB**
Conserved motifs are coloured and labelled. The helical domain has also been described as the ABC-α domain.

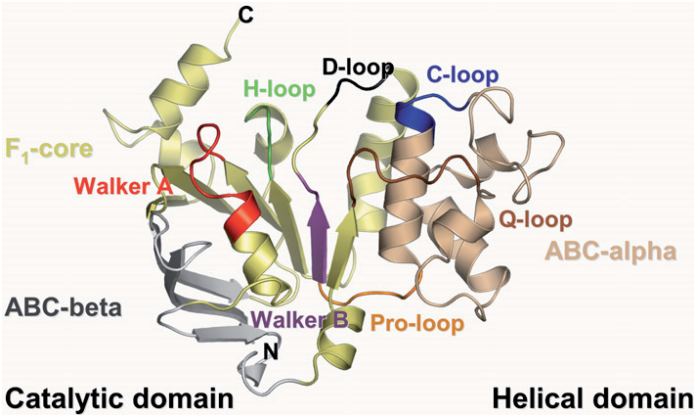

within the helical domain of different NBDs that appeared to adopt an NBD-specific conformation [39]. In our proposal, this SDR is responsible for proper interaction of the subunits and signal transmission between the NBDs and TMDs, indicating that each NBD is essentially unique. This has important implications for future drug design in relation to modulating the action of human ABC transporters.

The isolated NBD of HlyB was studied in detail by various biochemical, biophysical and structural approaches [24,32,39,45–48]. Most important was our observation of an ATP-induced dimerization of the NBD. For ABC transporters, it has been proposed that NBDs undergo changes in their oligomeric state during the catalytic cycle. It is now assumed that a monomeric state predominantly exists in the nucleotide-free or ADP-bound state, while NBDs dimerize upon ATP-binding. Since the isolated NBD of HlyB also displayed ATP-dependent dimerization, not only in solution, but also in the crystal structure of a mutant incapable of ATP hydrolysis (see below), we conclude that the isolated NBD can serve as an appropriate model system for full-length HlyB, at least under certain conditions. In addition to the fact that the isolated NBD displayed ATP-induced dimerization, equally important was the observation that ATP-hydrolysis displayed nonlinear kinetics, dependent on ATP and NBD concentration [45]. The sigmoidal velocity versus concentration plots (either ATP or protein) revealed a Hill coefficient of close to two. From the protein concentration dependence, an apparent dimerization constant for the NBDs of 1.2 ± 0.2 μM was also calculated. This clearly demonstrated that an oligomeric form of the NBD rather than the monomer is the active species during ATP hydrolysis.

Mutational studies have revealed the importance of certain key residues in ATP-hydrolysis by the HlyB-NBD [48]. Most important for our understanding of the catalytic cycle were mutations of Glu^{631} and His^{662}. Based on studies initially performed with the NBDs of MJ1276 and MJ0796 from *M. janashii* [49], the equivalent glutamate located C-terminal to the Walker B motif, was previously proposed to act as a 'general base' required for catalysis [50]. In line with this model, Glu/Gln mutants locked in ATPase-activity, of various systems were reported. This was consistent with the notion that the glutamate residue orients and polarizes the nucleophilic water molecule within the active site [50–52]. However, in other studies, including our own, a Glu/Gln mutation resulted in NBDs retaining substantial amounts of ATPase activity [32,53–56], thus casting doubt on the precise role of the glutamate. On the other hand, another interesting residue is the highly conserved His^{662} in the so-called H-loop of HlyB (Figure 1). Mutation of this histidine in the maltose and histidine permease systems resulted in transporters without detectable ATPase activity and an inability to translocate the allocrite *in vivo* [57,58]. Thus, while the E631Q ($Glu^{631} \rightarrow$ Gln) mutation in HlyB retained around 10% ATPase activity [32], the H662A mutant was completely ATPase-deficient (up to a protein concentration of more than 20 mg/ml) [46]. Using the H662A mutation, we subsequently performed experiments pioneered for HisP [59], in which equal molar ratios of wild-type and H662A NBD were mixed and the ATPase activity of the corresponding mixtures was determined. ATPase activity proved to be linear, dependent on the molar amount of wild-type enzyme, and constant over time, indicating that in the HlyB-NBD dimer composed of one wild-type and one H662A subunit single-site hydrolysis was possible [45]. Such a sequential mechanism was already described for HisP, the NBD of the histidine permease [59], and the NBD of Mdl1p, an ABC transporter from yeast [51].

Figure 3 | **The linchpin model of ATP-hydrolysis of the HlyB-NBD**
Asterisks indicate conserved motifs of the *trans* monomer.

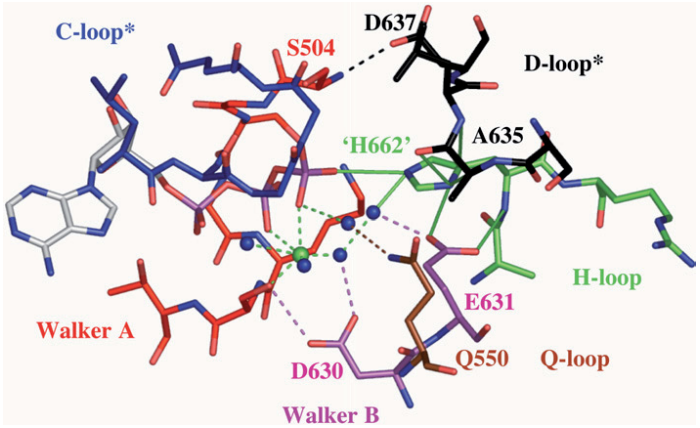

Based on detailed biochemical and functional knowledge of the HlyB-NBD, we succeeded in crystallizing each single state of the catalytic cycle of the NBD [32,39,46]. In the nucleotide-free state [39], an interesting conformation of the last three residues of the Walker A motif (coloured red in Figure 2) was observed. These residues form the N-terminus of helix 1 and adopt a 3_{10}-helical conformation rather than the usual α-helix, which is present in all NBD structures solved in the presence of nucleotide. The 3_{10} helix is further stabilized by a salt bridge between Lys^{508} and Glu^{631}, which caps the helix. Such a 3_{10} helix prevents nucleotide binding because Ser^{509} and the α-phosphate moiety of any nucleotide would result in a steric clash. This alternative rearrangement might present a molecular switch used to regulate ATPase activity *in vivo*.

Using the H662A or the E631Q mutant, crystal structures in the ATP- and ATP/Mg^{2+}-bound states were obtained at 2.6 and 2.5 Å (1 Å = 10^{-10} m) respectively [32,46]. In these structures a dimeric architecture was observed, in which ATP glues together two monomers through interaction of the Walker A motif of one monomer and the C-loop of the opposing monomer. Such a sandwich dimer was also described for MJ0796 [35] and MalK from *E. coli* [60] and suggests that such a composite dimer is a universal feature of all ABC transporters. The dimer interface of the HlyB-NBD is stabilized by interaction of the extended C-terminal region of HlyB. More important, however, is the fact that the D-loops (residues 634–637) are involved in monomer–monomer communication (Figure 3) [32]. Thus the structure of the HlyB-NBD, in the presence of ATP and ATP/Mg^{2+}, revealed for the first time a molecular communication pathway by which the functional state of the nucleotide-binding site of monomer, e.g. ATP- or ADP-bound or nucleotide-free, could be transmitted to the other monomer. Notably, Ala^{635} (SALD) of the *trans* monomer interacts across the dimer interface with His^{662}, which performs the vital function of a linchpin in catalysis (see below). In addition, Asp^{637} (SALD) of the *trans* monomer forms a hydrogen bond with Ser^{504} of the Walker A motif of the *cis* monomer.

What are the precise molecular functions of Glu^{631} and His^{662}? Re-introducing the histidine *in silico* in the HlyB-NBD H662A mutant, resulted in a complex network of interactions (Figure 3) [32]. In the modelled structure, Glu^{631} forms a bidentate interaction with the backbone and the side chain of His^{662}, thereby positioning His^{662} in a proper orientation to stabilize the transition state of the HlyB-NBD/ATP-Mg^{2+} complex. His^{662}, on the other hand, acts as a linchpin. It interacts with ATP and the D-loop of the *trans* monomer, and co-ordinates a water molecule, which is in the proper position to act as the catalytic water. We propose that in this structure Glu^{631} acts as a platform. Without this glutamate, the conformational restriction imposed on His^{662} is relaxed and the probability of obtaining the correct orientation is drastically reduced. However, the intrinsic flexibility of individual NBDs might explain the varying levels of residual ATPase activity found after mutation of the glutamate. In contrast, substitution of the histidine removes the linchpin, ATP is not fixed in space anymore and the catalytic water is not co-ordinated. Thus, ATPase activity is abolished. This model is supported by a variety of biochemical evidence [32]. First, ATPase activity in solutions of increasing viscosity revealed that the reaction velocity did not change. This is a clear indication that a 'chemical' reaction is the rate-limiting step of the catalytic cycle rather than nucleotide association, dissociation or NBD-dimerization, since the latter depend on the diffusion rate, which is slowed in solutions of higher viscosity. Secondly, reaction velocities of the ATPase activity are insensitive to the presence of ^2H_2O. This experiment

allowed us to eliminate general base catalysis as the 'rate-limiting reaction', since by definition such a process requires a proton abstraction or polarization step [61]. When a reaction is performed in ^2H_2O, the zero-point energy changes and the activation barrier for any proton-abstraction process is raised, with a consequent reduction in the reaction velocity [61]. The absence of a deuterium isotope effect [62] clearly demonstrates that protons are not involved. This implies that ATP-hydrolysis might be the 'rate-limiting step' of the catalytic cycle, i.e. that the step of bond cleavage has the highest activation barrier. This model is further supported by the fact that ATPase activity is modulated by the nature of the divalent ion present, going hand in hand with the pK_a value of the corresponding ion rather than with the ionic radius. This suggests that the bound cofactor influences the pK_a value of the γ-phosphate moiety, resulting in modulation of the reaction velocity. As a consequence, the substrate, ATP, acts as a base and ATP-hydrolysis by the HlyB-NBD should then follow 'substrate-assisted catalysis' [63], a mechanism already described for another branch of P-loop enzymes, the GTPase ras^{p21} [64] or EcoRI and V [65].

The biochemical and structural investigations performed on isolated NBDs have provided a molecular picture that allows us to start to understand the 'mode of action' of NBDs at the molecular level. Slowly, the pieces of a molecular puzzle are coming together and a scenario starts to emerge which explains how chemical energy is converted, via ATP-hydrolysis, into vectorial transport of the allocrite across biological membranes. Thus, it may be envisioned that rotational movement of the helical subdomain of the NBD upon ATP binding and a dissociation of the NBD-dimer following hydrolysis may provide the physical driving force linking the different steps of the catalytic cycle to allocrite movement.

We apologize to all colleagues whose work was not cited in this brief review. We thank Sander Smits, Rupert Abele, Robert Ernst, Carsten Horn and Nils Hanekop for many discussions and support. We are indebted to G. Bourenkov for his excellent assistance during data collection and structure refinement. L.S. thanks Robert Tampé for constant support and encouragement. Work in our laboratories was supported by grants from CNRS and University of Paris-Sud (to I.B.H.) and the Deutsche Forschungsgemeinschaft (Emmy Noether programme and SFB 628 to L.S.).

References

1 Holland, I.B., Benabdelhak, H., Young, J., De Lima Pimenta, A., Schmitt, L. and Blight, M.A. (2003) in ABC Proteins: From Bacteria to Man (Holland, I.B., Cole, S.P., Kuchler, K. and Higgins, C., eds.), pp. 209–241, Academic Press, London
2 Delepelaire, P. (2004) Biochim. Biophys. Acta **1694**, 149–161
3 Welch, R.A. and Pellet, S. (1985) J. Bacteriol. **170**, 1622–1630
4 Blight, M.A. and Holland, I.B. (1994) TIBTECH **12**, 450–455
5 Welch, R.A. (1991) Mol. Microbiol. **5**, 521–528
6 Baumann, U., Wu, S., Flaherty, K.M. and McKay, D.B. (1993) EMBO J. **12**, 3357–3364
7 Gray, L., Baker, K., Kenny, B., Mackman, N., Haigh, R. and Holland, I.B. (1989) J. Cell Sci. Suppl. **11**, 45–57
8 Gray, L., Mackman, N., Nicaud, J.M. and Holland, I.B. (1986) Mol. Gen. Genet. **205**, 127–133
9 Kenny, B., Chervaux, C. and Holland, I.B. (1994) Mol. Microbiol. **11**, 99–109
10 Jarchau, T., Chakraborty, T., Garcia, F. and Goebel, W. (1994) Mol. Gen. Genet. **245**, 53–60
11 Wolff, N., Delepelaire, P., Ghigo, J.M. and Delepierre, M. (1997) Eur. J. Biochem. **243**, 400–407
12 Yin, Y., Zhang, F., Ling, V. and Arrowsmith, C.H. (1995) FEBS Lett. **366**, 1–5
13 Driessen, A.J., Fekkes, P. and van der Wolk, J.P. (1998) Curr. Opin. Microbiol. **1**, 216–222
14 Letoffe, S., Delepelaire, P. and Wandersman, C. (1996) EMBO J. **15**, 5804–5811
15 Binet, R. and Wandersman, C. (1995) EMBO J. **14**, 2298–2306
16 Mackman, N., Nicaud, J.M., Gray, L. and Holland, I.B. (1985) Mol. Gen. Genet. **201**, 529–536
17 Mackman, N., Nicaud, J.M., Gray, L. and Holland, I.B. (1985) Mol. Gen. Genet. **201**, 282–288
18 Holland, I.B., Schmitt, L. and Young, J. (2005) Mol. Membr. Biol. **22**, 29–39
19 Koronakis, V., Sharff, A., Koronakis, E., Luisi, B. and Hughes, C. (2000) Nature (London) **405**, 914–919
20 Koronakis, V., Eswaran, J. and Hughes, C. (2004) Annu. Rev. Biochem. **73**, 467–489
21 Johnson, J.M. and Church, G.M. (1999) J. Mol. Biol. **287**, 695–715
22 Schmitt, L. and Tampé, R. (2002) Curr. Opin. Struct. Biol. **12**, 754–760
23 Thanabalu, T., Koronakis, E., Hughes, C. and Koronakis, V. (1998) EMBO J. **17**, 6487–6496
24 Benabdelhak, H., Kiontke, S., Horn, C., Ernst, R., Blight, M.A., Holland, I.B. and Schmitt, L. (2003) J. Mol. Biol. **327**, 1169–1179
25 Koronakis, V., Hughes, C. and Koronakis, E. (1991) EMBO J. **10**, 3263–3272
26 Balakrishnan, L., Hughes, C. and Koronakis, V. (2001) J. Mol. Biol. **313**, 501–510
27 Blight, M.A., Menichi, B. and Holland, I.B. (1995) Mol. Gen. Genet. **247**, 73–85
28 Delepelaire, P. and Wandersman, C. (1998) EMBO J. **17**, 936–944
29 Koronakis, E., Hughes, C., Milisav, I. and Koronakis, V. (1995) Mol. Microbiol. **16**, 87–96
30 Higgins, C.F. (1992) Annu. Rev. Cell Biol. **8**, 67–113
31 Hung, L.-W., Wang, I.X., Nikaido, K., Liu, P.-Q., Ferro-Luzzi Ames, G. and Kim, S.-H. (1998) Nature (London) **396**, 703–707
32 Zaitseva, J., Jenewein, S., Jumpertz, T., Holland, I.B. and Schmitt, L. (2005) EMBO J. **24**, 1901–1910
33 Yuan, Y.R., Blecker, S., Martsinkevich, O., Millen, L., Thomas, P.J. and Hunt, J.F. (2001) J. Biol. Chem. **276**, 32313–32321
34 Verdon, G., Albers, S.V., Dijkstra, B.W., Driessen, A.J. and Thunnissen, A.M. (2003) J. Mol. Biol. **330**, 343–358
35 Smith, P.C., Karpowich, N., Millen, L., Moody, J.E., Rosen, J., Thomas, P.J. and Hunt, J.F. (2002) Mol. Cell **10**, 139–149
36 Karpowich, N., Martsinkevich, O., Millen, L., Yuan, Y.R., Dai, P.L., MacVey, K., Thomas, P.J. and Hunt, J.F. (2001) Structure **9**, 571–586
37 Diederichs, K., Diez, J., Greller, G., Muller, C., Breed, J., Schnell, C., Vonrhein, C., Boos, W. and Welte, W. (2000) EMBO J. **19**, 5951–5961
38 Gaudet, R. and Wiley, D.C. (2001) EMBO J. **20**, 4964–4972
39 Schmitt, L., Benabdelhak, H., Blight, M.A., Holland, I.B. and Stubbs, M.T. (2003) J. Mol. Biol. **330**, 333–342
40 Chang, G. and Roth, C.B. (2001) Science **293**, 1793–1800
41 Locher, K.P., Lee, A.T. and Rees, D.C. (2002) Science **296**, 1091–1098
42 Chang, G. (2003) J. Mol. Biol. **330**, 419–430
43 Abrahams, J.P., Leslie, A.G., Lutter, R. and Walker, J.E. (1994) Nature (London) **370**, 621–628
44 Walter, C., Wilken, S. and Schneider, E. (1992) FEBS Lett. **303**, 41–44
45 Zaitseva, J., Jenewein, S., Wiedenmann, A., Holland, I.B. and Schmitt, L. (2005) Biochemistry **44**, 9680–9690
46 Zaitseva, J., Holland, I.B. and Schmitt, L. (2004) Acta Crystallogr. D **60**, 1076–1084
47 Koronakis, V., Hughes, C. and Koronakis, E. (1993) Mol. Microbiol. **8**, 1163–1175
48 Benabdelhak, H., Schmitt, L., Horn, C., Jumel, K., Blight, M.A. and Holland, I.B. (2005) Biochem. J. **368**, 1–7
49 Moody, J.E., Millen, L., Binns, D., Hunt, J.F. and Thomas, P.J. (2002) J. Biol. Chem. **277**, 21111–21114
50 Orelle, C., Dalmas, O., Gros, P., Di Pietro, A. and Jault, J.M. (2003) J. Biol. Chem. **278**, 47002–47008

51 Janas, E., Hofacker, M., Chen, M., Gompf, S., van der Does, C. and Tampe, R. (2003) J. Biol. Chem. **278**, 26862–26869
52 Payen, L.F., Gao, M., Westlake, C.J., Cole, S.P. and Deeley, R.G. (2003) J. Biol. Chem. **278**, 38537–38547
53 Verdon, G., Albers, S.V., van Oosterwijk, N., Dijkstra, B.W., Driessen, A.J. and Thunnissen, A.M. (2003) J. Mol. Biol. **334**, 255–267
54 Tombline, G., Bartholomew, L.A., Tyndall, G.A., Gimi, K., Urbatsch, I.L. and Senior, A.E. (2004) J. Biol. Chem. **279**, 46518–46526
55 Sauna, Z.E., Muller, M., Peng, X.H. and Ambudkar, S.V. (2002) Biochemistry **41**, 13989–14000
56 Urbatsch, I.L., Julien, M., Carrier, I., Rousseau, M.E., Cayrol, R. and Gros, P. (2000) Biochemistry **39**, 14138–14149
57 Shyamala, V., Baichwal, V., Beall, E. and Ames, G.F. (1991) J. Biol. Chem. **266**, 18714–18719
58 Davidson, A.L. and Sharma, S. (1997) J. Bacteriol. **179**, 5458–5464
59 Nikaido, K. and Ames, G.F. (1999) J. Biol. Chem. **274**, 26727–26735
60 Chen, J., Lu, G., Lin, J., Davidson, A.L. and Quiocho, F.A. (2003) Mol. Cell **12**, 651–661
61 Fersht, A. (1997) Enzyme, Structure and Mechanism, Freemann, New York
62 Schowen, K.B. and Schowen, R.L. (1982) Methods Enzymol. **87**, 551–606
63 Dall'Acqua, W. and Carter, P. (2000) Protein Sci. **9**, 1–9
64 Schweins, T., Geyer, M., Scheffzek, K., Warshel, A., Kalbitzer, H.R. and Wittinghofer, A. (1995) Nat. Struct. Biol. **2**, 36–44
65 Jeltsch, A., Alves, J., Wolfes, H., Maass, G. and Pingoud, A. (1993) Proc. Natl. Acad. Sci. U.S.A. **90**, 8499–8503

Received 9 June 2005

Proportionate work on this publication: 20 %

Published in: Biochemical Society Transactions

Impact factor: 2.979

Paper III

The EMBO Journal (2006), 1–12 | © 2006 European Molecular Biology Organization | All Rights Reserved 0261-4189/06
www.embojournal.org

THE
EMBO
JOURNAL

A structural analysis of asymmetry required for catalytic activity of an ABC-ATPase domain dimer

Jelena Zaitseva[1], Christine Oswald[1], Thorsten Jumpertz[1], Stefan Jenewein[1], Alexander Wiedenmann[1,3], I Barry Holland[2] and Lutz Schmitt[1,*]

[1]Institute of Biochemistry, Heinrich Heine University Duesseldorf, Duesseldorf, Germany and [2]Institut de Génétique et Microbiologie, Université de Paris XI, Orsay, France

The ATP-binding cassette (ABC)-transporter haemolysin (Hly)B, a central element of a Type I secretion machinery, acts in concert with two additional proteins in *Escherichia coli* to translocate the toxin HlyA directly from the cytoplasm to the exterior. The basic set of crystal structures necessary to describe the catalytic cycle of the isolated HlyB-NBD (nucleotide-binding domain) has now been completed. This allowed a detailed analysis with respect to hinge regions, functionally important key residues and potential energy storage devices that revealed many novel features. These include a structural asymmetry within the ATP dimer that was significantly enhanced in the presence of Mg^{2+}, indicating a possible functional asymmetry in the form of one open and one closed phosphate exit tunnel. Guided by the structural analysis, we identified two amino acids, closing one tunnel by an apparent salt bridge. Mutation of these residues abolished ATP-dependent cooperativity of the NBDs. The implications of these new findings for the coupling of ATP binding and hydrolysis to functional activity are discussed.

The EMBO Journal advance online publication, 6 July 2006; doi:10.1038/sj.emboj.7601208
Subject Categories: structural biology
Keywords: ABC-transporter; ATPase; catalytic cycle; X-ray crystallography

Introduction

Many Gram-negative bacteria use Type I secretion systems to translocate toxins, hydrolytic enzymes or surface-bound proteins across the cell envelope (Holland *et al*, 2005). The paradigm of such a transport complex is the haemolysin (Hly)A apparatus, discovered in the early 1980s in uropathogenic *Escherichia coli* strains (Welch *et al*, 1981), which like all Type I systems rely on the presence of a C-terminal secretion signal in the transported substrate. The HlyA secretion machinery is composed of three indispensable elements: the ABC-(ATP-binding cassette) transporter HlyB, the membrane fusion protein HlyD, both residing in the inner membrane of *E. coli*, and the outer membrane protein TolC (Holland *et al*, 2005).

ABC-transporters, such as HlyB, are ubiquitous ATP-dependent transmembrane proteins (Higgins, 1992; Schmitt and Tampé, 2002) that transport an astonishing variety of transport substrates across membranes, coupled to the consumption of ATP. Despite this transport substrate diversity, all ABC-transporters share the same architecture, comprised of two transmembrane domains or subunits (TMDs) and two nucleotide-binding domains (NBDs) (Schmitt and Tampé, 2002; Davidson and Chen, 2004; Jones and George, 2004). Whereas the α-helical TMDs are divergent in primary structure, the NBDs are rather conserved with respect to sequence and three-dimensional structure. Nevertheless, we could identify a structurally diverse region (SDR) within several different ABC-NBDs (Schmitt *et al*, 2003) that might be involved in signal transmission to the TMDs. The conservation of the NBDs is also reflected by the fact that all conserved motifs of ABC-transporters, the Walker A and B motif, the C-loop or ABC-signature motif, the Q- and Pro-loop, and the D- and H-loops are located within the NBD.

Over the last decade, we have seen tremendous advances in ABC-transporter research including crystal structures of isolated NBDs (for recent reviews see Ye *et al*, 2004; Oswald *et al*, 2006) and full-length transporters (Chang and Roth, 2001; Locher *et al*, 2002; Chang, 2003; Reyes and Chang, 2005). Based on these structural and biochemical data obtained for isolated NBDs (Chen *et al*, 2001; Janas *et al*, 2003), it is now believed that they form a composite dimer in the ATP-bound state. Here, ATP acts as a molecular glue, which is sandwiched between the Walker A motif of one monomer (the *cis* monomer) and the ABC-signature motif of the other monomer (the *trans* monomer) (Smith *et al*, 2002). However, despite rapidly increasing knowledge of the biochemistry and the three-dimensional structure of ABC-transporters, we are still far away from a detailed, molecular understanding of the catalytic cycle of the NBD. Moreover, a comprehensive analysis of the mechanical switches involved in domain movements associated with substrate binding or dissociation is still missing. Importantly, one finds that these features are generally less conserved than the active site geometry. Consequently, a reliable analysis of domain movements, conformational changes and changing patterns of protein–ligand or protein–protein interactions can only be carried out using structures derived from the same protein. So far, this has only been achieved for MalK by solving the structures of the apo-, ATP- and ADP-bound forms (Chen *et al*, 2003; Lu *et al*, 2005). In contrast to the HlyB-NBD, MalK fuels transport substrate import and, more importantly, deviates from a canonical NBD by the presence of a large C-terminal domain, required for regulation of the *mal* operon.

*Corresponding author. Institute of Biochemistry, Heinrich Heine University Duesseldorf, Universitaetsstrasse 1, 40225 Duesseldorf, Germany. Tel.: +49 211 81 10773; Fax: +49 211 81 15310;
E-mail: lutz.schmitt@uni-duesseldorf.de
[3]Present address: Institute of Microbiology, ETH Zürich, ETH-Hönggerberg, Wolfgang-Pauli-Strasse 10, 8093 Zurich, Switzerland

Received: 11 January 2006; accepted: 30 May 2006

We have now obtained the crystal structures of two mutated forms of the HlyB-NBD, H662A and E631Q, in complex with ATP (dimers) or ADP (monomers), and the crystal structure of the wild-type monomer protein with bound ADP. In combination with the recently published crystal structures of the H662A/ATP-Mg^{2+} (Zaitseva *et al*, 2005a) dimer and the structure of the HlyB-NBD in the absence of bound nucleotide (Schmitt *et al*, 2003), a basic ABC-catalytic cycle can now be described in structural detail. This has revealed important mechanistic insights and several novel features including a structural asymmetry within the dimer in the presence of ATP/Mg^{2+}. We propose that this represents one open and one closed phosphate exit tunnel. Further analysis of this asymmetry enabled us to identify two amino acids of crucial importance for ATP-dependent cooperativity. In combination with a mechanism to store the energy of ATP within the NBD, we now describe the molecular mechanisms that operate to coordinate NBD dimerization, ATP hydrolysis and associated conformational changes in order to fuel transport substrate translocation.

Results and discussion

The NBD of HlyB, comprising residues 467–707, was purified and crystallized in the ATP- and ADP-bound forms (see Materials and methods). For crystallization of the ATP-loaded composite dimer, the H662A and E631Q mutants had to be employed because no suitable crystals could be grown for the wild-type enzyme. ADP-bound forms were obtained for the wild type, the H662A and the E631Q mutant. Data statistics are summarized in Table I.

The catalytic cycle of the HlyB-NBD

The catalytic cycle, represented by the nucleotide-free and the ATP- and ADP-bound forms of the HlyB-NBD, together with the relevant dissociation constants, is depicted in Figure 1. Crystals of other intermediates of the catalytic cycle such as a vanadate trapped state or an ATP/ADP mixed dimer as proposed to exist for the Mdl1p-NBD (Janas *et al*, 2003) could not be obtained despite numerous efforts. However, the structures reported here are sufficient to describe important functional states of the basic catalytic cycle of the HlyB-NBD. Whereas the nucleotide-free and ADP states crystallized as monomeric proteins, the ATP and ATP/Mg^{2+} states formed dimers. As already reported for MJ0796 (Smith *et al*, 2002) and MalK (Chen *et al*, 2003), ATP (highlighted in ball-and-stick representation; Figure 1) is sandwiched between the Walker A motif of the *cis* monomer and the ABC-signature motif of the *trans* monomer (colored blue and red, respectively, in Figure 1). This composite architecture of the dimer in the ATP- (Smith *et al*, 2002; Chen *et al*, 2003) and ATP/Mg^{2+}-bound states (Zaitseva *et al*, 2005a) shown here is now commonly believed to be the functional, productive catalytic state. It is important to note that in the crystal structures of MalK (Chen *et al*, 2003; Lu *et al*, 2005), BtuCD (Locher *et al*, 2002) and MsbA (Chang, 2003; Reyes and Chang, 2005) lacking ATP, the NBDs are also in an apparent 'sandwich-like' arrangement in the nucleotide-free state.

Table I Data quality and refinement statistics of the crystal structures determined

Protein	Wild type	H662A	E631Q	H662A	E631Q
Ligand	ADP	ADP	ADP	ATP	ATP
Crystal parameters					
Space group	C2	C2	C2	$P2_1$	$P2_1$
Cell constants at 100 K					
a, *b*, *c* (Å)	180.37, 34.84, 37.82	180.16, 34.77, 38.1	178.57, 34.75, 37.52	46.56, 195.17, 63.23	47.14, 189.26, 63.48
β (deg)	98.41	98.58	97.97	110.85	111.87
Data collection and processing					
Wavelength (Å)	1.05	1.05	1.05	1.05	1.05
Resolution (Å)	20–1.6	20–1.7	20–1.9	20–2.6	20–2.7
Mean redundancy	10.9	12.2	6.9	10.2	6.8
Completeness (%)	90.5 (69.5)	99.2 (88.5)	94.1 (88.1)	96.4 (93.2)	98.9 (98.3)
I/σ	14.7 (2.1)	26 (3.2)	10.8 (2.3)	12.1 (3.2)	22.5 (5.2)
R_{sym} (%)	8.8 (25.4)	6.2 (16.3)	4.9 (27.7)	5.7 (19.3)	9.4 (25.7)
Refinement					
R_F (%)	19.2 (26.8)	20.5 (24.0)	20.2 (29.7)	21.1 (27.3)	22.6 (29.3)
R_{free} (%)	23.1 (36.6)	24.0 (32.0)	25.0 (30.1)	27.9 (37.1)	28.0 (36.9)
R.m.s.d.					
Bond length (Å)	0.013	0.015	0.013	0.007	0.012
Bond angle (deg)	1.434	1.498	1.414	1.085	1.214
Average *B*-factor (Å^2)	30.2	25.1	37.0	51.0	51.5
Ramachandran plot					
Most favored (%)	93.5	93.0	92.0	90.0	88.7
Allowed (%)	5.6	6.0	7.1	8.7	10.2
Generously allowed (%)	0.9	0.9	0.9	0.9	0.8
Disallowed (%)	—	—	—	0.4	0.2
Model content					
Protein residues	242	243	243	964	964
Ligands	ADP	ADP	ADP	4 ATP	4 ATP
Water molecules	176	246	128	197	152

Values in parentheses correspond to the highest resolution shell (1.65–1.6 Å for the wild-type ADP, 1.76–1.7 Å for the ADP H662A, 1.95–1.9 Å for the E631Q-ADP, 2.65–2.6 Å for the ATP H662A and 2.75–2.7 Å for the ATP E631Q structure).

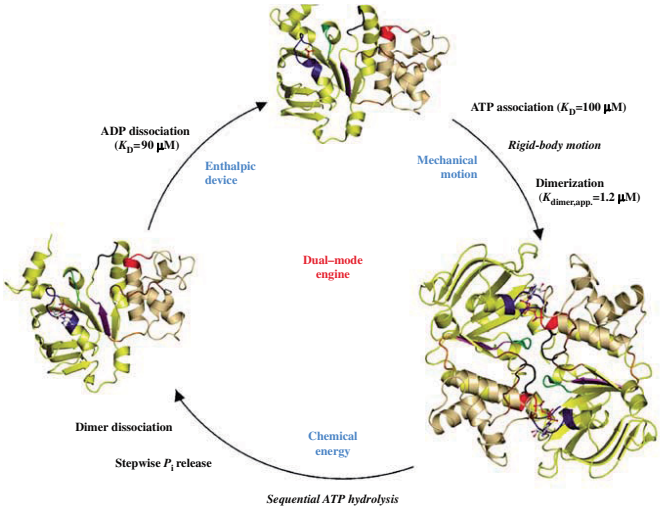

Figure 1 The catalytic cycle of the HlyB-NBD. Crystal structures of the monomeric nucleotide-free (Schmitt *et al*, 2003), dimeric ATP-bound (H662A and E631Q) and monomeric ADP-bound (wild type, E631Q and H662A) forms (this study) are shown. For simplicity, the structure of the ATP/Mg^{2+}-bound form (Zaitseva *et al*, 2005a) is not shown. The catalytic domain is colored in light yellow and the helical domain in light tan. Conserved motifs are highlighted and color-coded as follows: Walker A (residues 502–510, blue), Q-loop (residues 549–556, brown), ABC-signature motif (residues 606–610, red), Pro-loop (residues 623–625, orange), Walker B (residues 626–630, magenta), D-loop (residues 634–637, black) and H-loop (residues 661–663, green). Bound ligands are shown in ball-and-stick representation. K_D values were taken from Zaitseva *et al* (2005b).

However, the buried surface area of the NBD:NBD interface in these crystal structures is rather small, 480 $Å^2$ in the case of BtuD (Locher *et al*, 2002) compared to 1890 $Å^2$ in the case of the ATP/Mg^{2+}-bound state of the HlyB-NBD (Zaitseva *et al*, 2005a). It is reasonable to suppose that the lateral constraint imposed by the additional C-terminal domain of MalK (Chen *et al*, 2003; Lu *et al*, 2005), or the TMDs of BtuCD or MsbA, keeps the NBDs close together in a 'dimer-like' or open configuration even in the absence of ATP. Importantly, such structures are still readily accessible to nucleotides and we conclude that these ATP-free forms of MsbA and BtuD should be regarded as monomers from a structural point of view. In solution, all other isolated NBDs are also apparently monomers and only in the presence of ATP or in a vanadate-trapped state, can true dimers be identified (Janas *et al*, 2003; Verdon *et al*, 2003b; Zaitseva *et al*, 2005b).

As shown in Figure 1, the catalytic cycle represents a 'dual mode' mechanism, combining mechanical movement with the generation of chemical energy in order to ensure function. The catalytic cycle starts with the transition of the NBD from the nucleotide-free to the ATP-bound state, accompanied by a rigid-body motion of the helical domain (shown in light tan in Figure 1) towards the catalytic domain (shown in light yellow), as discussed in more detail below. An additional major change accompanying nucleotide binding in HlyB involves the N-terminus of helix 1, which harbors the last three residues of the Walker A motif (shown in blue). Whereas these three residues adopt a 3_{10}-helical conformation in the nucleotide-free state (Schmitt *et al*, 2003), a regular α-helical structure is observed in all other structures with bound nucleotide. Similarly, a non-canonical conformation of the Walker A motif was observed in the nucleotide-free state of GlcV (Verdon *et al*, 2003a). This implies that such localized alternative conformations might be important *in vivo* in controlling ATP binding to particular NBDs. We have also shown that ATP binding promotes dimerization of the HlyB-NBD, not only in the crystal structure but also in solution (Zaitseva *et al*, 2005b). This is expected as ATP plays an important role in the initiation of the catalytic cycle, engaging both NBDs and driving the formation of the composite dimer.

Comparison of the dimeric ATP- and ATP/Mg^{2+}-bound crystal structures of either the H662A or the E631Q mutant forms revealed a root mean square deviation (r.m.s.d.) of 0.6 Å for 482 Cα-atoms. However, we noted a striking difference, dependent upon Mg^{2+}, in the nature and composition of the water network within the nucleotide-binding site (also see below). Comparison of the three crystal structures of the HlyB-NBD (wild type, E631Q and H662A) in the ADP-bound state revealed an even smaller r.m.s.d., around 0.2 Å over 241 Cα-atoms (wild type/E631Q, 0.209 Å and wild type/H662A, 0.187 Å). This is further supported by an analysis of the *B*-factors of these ADP-bound structures that are qualitatively identical for all three structures (data not shown). Therefore, we shall only describe in detail the structure of the wild-type HlyB-NBD with bound ADP.

Architecture of the nucleotide-binding site

As shown in Figure 2A, ATP is bound at the dimer interface of the HlyB-NBD via interactions with the Walker A, B and the Q-loop from the *cis* monomer and interactions with the

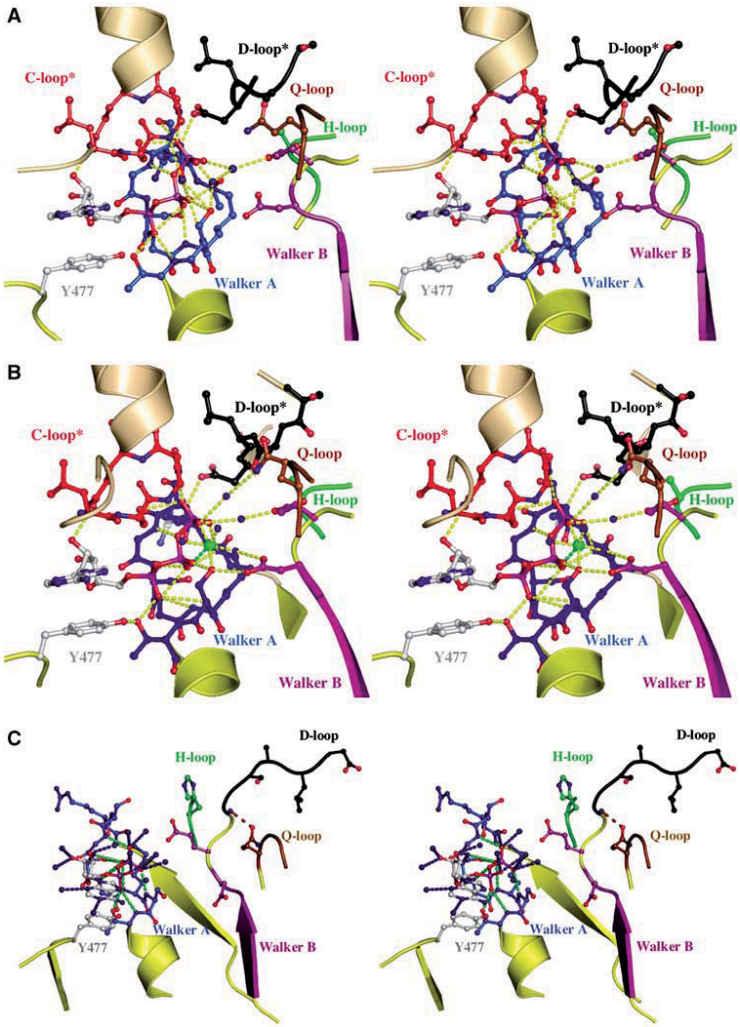

Figure 2 Nucleotide-binding sites. Stereoview of the ATP-binding (**A**) and ATP/Mg^{2+}-binding(**B**) sites. Color-coding is identical to Figure 1. Direct and water-mediated protein–ATP interactions are highlighted in yellow. Water molecules are shown as blue spheres and Mg^{2+} as a green sphere. The interaction between D637 of the D-loop of the *trans* monomer and S504 of the Walker A motif of the *cis* monomer is indicated. ATP and amino acids involved in ligand interactions are shown in ball-and-stick representation. * indicates conserved motifs of the *trans* monomer participating in ATP coordination. (**C**) Stereoview of the ADP-binding site. ADP and residues involved in ligand interactions are shown in ball-and-stick representation, water molecules are blue spheres, protein–ADP interactions are highlighted in green and ADP–water interactions in blue. Color-coding is identical to Figure 1. The interaction between the side chain of Q550 and the amide backbone of T633 is highlighted by a dashed, brown line.

ABC-signature motif of the *trans* monomer. Furthermore, the D-loop of the *trans* monomer interacts with the backbone of S504 (Walker A) of the *cis* monomer, opening up the possibility to transmit the nature of the functional state of one ATP-binding site to the other site. This canonical arrangement was also observed for MJ0796 (Smith *et al*, 2002), MalK (Chen *et al*, 2003) and the HlyB-NBD with bound ATP/Mg^{2+} (Zaitseva *et al*, 2005a). Importantly, we note that in contrast to the ATP/Mg^{2+} structure (Figure 2B), the absence of Mg^{2+} results in a different arrangement of the water molecules within the ATP-binding site (Figure 2A). As a consequence of this difference, D630 (Walker B) is not in direct contact with the bound nucleotide and the ATP-bound structure has twice as many water-mediated contacts in the

active site as the ATP/Mg^{2+}-bound structure, resulting in a larger ligand–protein buried surface.

A closer look into the ADP-binding site is presented in Figure 2C. The adenine ring of ADP interacts with an aromatic amino acid, Y477 in HlyB, via π–π stacking of the two aromatic ring systems. Furthermore, the phosphate moiety of ADP is bound via both side- and main-chain interactions with residues of the Walker A motif. This pattern has been observed in all other crystal structures of NBDs in the ADP-bound state (Gaudet and Wiley, 2001; Karpowich *et al*, 2001; Yuan *et al*, 2001; Verdon *et al*, 2003a) with the exception of the CFTR-NBD1 (Lewis *et al*, 2004). In contrast to other NBD structures with ADP (Gaudet and Wiley, 2001; Karpowich *et al*, 2001; Verdon *et al*, 2003a; Lu *et al*, 2005), we were not able to obtain a structure for the ADP/Mg^{2+}-bound state, despite the fact that we obtained crystals starting from ATP/Mg^{2+}. This fits with our thermodynamic data (Zaitseva *et al*, 2005b) and implies that the cofactor Mg^{2+} is not tightly bound in the ADP state. However, more interesting is the direct interaction of Q550 (Q-loop) with the main chain of T633 (extended D-loop region) when ADP is bound. Thus, after ATP hydrolysis, but only after dissociation of inorganic phosphate (Karpowich *et al*, 2001), the helical domain rotates outward as a rigid body and is pinned in this position via the Q550–T633 interaction. Strikingly, a hinge axis (see below) covering the Walker B/D-loop region was identified for this particular step in the catalytic cycle. Consequently, it appears that the Walker B/D-loop region is not only involved in NBD–NBD communication and cofactor binding but also serves as an important control point, locking the helical domain into a non-productive position in the absence of ATP.

Structural plasticity of E631

We have recently proposed a 'linchpin' model for ATP hydrolysis (Zaitseva *et al*, 2005a, b). A key feature of the model is the catalytic dyad formed by E631 and H662 of HlyB. As a further test of this model, we determined the crystal structure of the E631Q NBD in the presence of ATP, with Mg^{2+} omitted in view of the residual ATPase activity of the E631Q mutant (Zaitseva *et al*, 2005a). Data statistics are summarized in Table I. As shown in Figure 3, the substituting

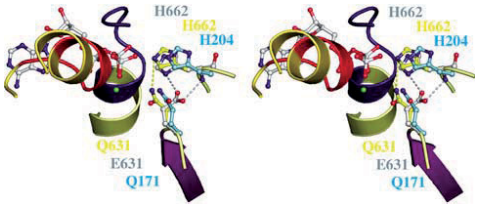

Figure 3 Structural flexibility of the H662–E631 interaction. Stereoview of the ATP-binding site of the HlyB-NBD E631Q mutant, the E171Q mutant of MJ 0796 (PDB entry 1L2T) and the hypothetical model of the wild-type HlyB-NBD in complex with ATP. Side chains of the E631Q mutant of HlyB-NBD (Q631 and H662) are shown in yellow, side chains of the E171Q mutant of MJ0796 (Q171 and H204) in cyan and side chains of the model of wild-type HlyB-NBD (E631 and H662) in gray. The single interaction of Q631 with the side chain of H662 is highlighted in yellow; the bidentate interaction of H662 and E631 proposed in the linchpin model is highlighted in gray. Color-coding is identical to Figure 1.

Q631 interacts with the side chain of H662 (distance of 3.3 Å; highlighted in yellow in Figure 3) through a single H-bond. This is in contrast to its positioning in the linchpin model where E631 contacts H662 via one main-chain and one side-chain interaction (highlighted in gray in Figure 3). Thus, in the E631Q mutant, H662 is less restricted, resulting in a higher degree of flexibility. Moreover, the geometry of the single hydrogen bond in the E631Q mutant of HlyB-NBD is unfavorable, indicating that the stabilization of the side-chain conformation of the histidine will be minimal. On the other hand, in the ATP-bound dimer of MJ0796 (Smith *et al*, 2002), the corresponding Q171 forms no interaction at all with the corresponding histidine (H204) (highlighted in cyan in Figure 3). This fits with the strongly reduced ATPase activity of the mutant. Thus, this structure is informative in explaining why the HlyB-NBD E631Q mutant (Zaitseva *et al*, 2005a), but not the MJ0796 E171Q mutant (Moody *et al*, 2002), displays residual ATPase activity.

Hinge regions within the individual structures of the catalytic cycle

The two-domain architecture of ABC-NBDs was first described for HisP (Hung *et al*, 1998). In the case of HlyB, the catalytic domain corresponds to residues 467–549 and 626–707. This contains the motifs Walker A (residues 502–510) and B (residues 626–630), the D-loop (residues 634–637) and the H-loop (residues 661–663). The helical domain, presumed to act as a communicator between the catalytic domain and the TMDs, corresponds to residues 557–622 of HlyB and contains the ABC-signature motif (residues 606–610) and the SDR (residues 578–605), unique to each type of ABC-transporter (Schmitt *et al*, 2003). The helical domain is connected to the catalytic domain via the Q-loop (residues 550–556) and the Pro-loop (residues 623–625) (Schmitt *et al*, 2003). Despite the accumulating structural information however, potential hinges or bending residues within an NBD necessary to facilitate intramolecular movement were not previously identified. An analysis of potential hinges in the HlyB-NBD revealed that in the first step of the catalytic cycle, that is, nucleotide-free to ATP-bound, residues 549–553 (Q-loop) and 617–619 (C-terminus of helix 5) act as mechanical hinges (highlighted in magenta in Figure 4A) allowing inward rigid-body rotation of the helical domain. Thus, the location of the bending residues coincides with the domain definition of the NBD.

In the crystal structure of BtuCD (Locher *et al*, 2002), the Q-loop of BtuD is in contact with the cytoplasmic L-loop of the membrane subunit BtuC. Locher (2004) proposed that this interaction is of importance for TMD–NBD communication. As the Q-loop also serves as a hinge, one can envision that any movement here is transmitted to the TMD in the form of a conformational rearrangement and ultimately the creation of a functional translocation pathway. In such an analysis, however, it is important to be aware of the possible effect of crystal packing on certain conformations under different conditions. In fact, in the apo structure, the Q-loop is partially involved in crystal contacts. Nevertheless, an analysis of the *B*-factors (Eyal *et al*, 2005) indicated no stabilization of the observed conformation due to these contacts.

Surprisingly, we find that apparently the requirement for bending residues is more complex in the reverse, outward

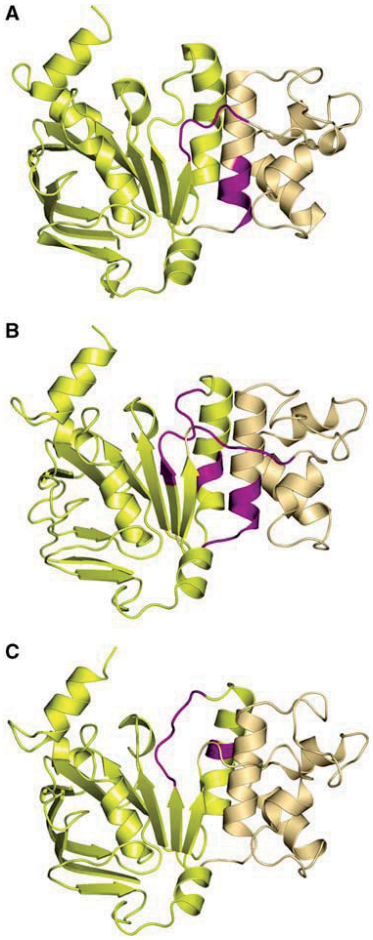

Figure 4 Hinges and bends during functional transitions. Hinges involved in (**A**) the transition from the nucleotide-free to the ATP-bound state, (**B**) the transition from the ATP/Mg^{2+}- to the ADP-bound state and (**C**) the transition from the ADP-bound to the nucleotide-free state. Hinge regions are highlighted in magenta. The catalytic domain is shown in light yellow and the helical domain in light tan. Structures shown correspond to the starting point of the functional transitions.

rotation of the helical domain in the transition ATP/Mg^{2+}-bound to the ADP-bound state (Figure 4B). Thus, in addition to the Q- and the Pro-loop, residues of the Walker B/D-loop region (629–635) and helix 6 (residues 647–648) also act as effective hinges (highlighted in magenta in Figure 4B). In contrast to the apo form, none of these hinges are involved in crystal packing contacts. Finally, in the conversion from the ADP-bound to the nucleotide-free state (Figure 4C), only residues 630–635 (Walker B/D-loop region) and helix 6 (residues 644–645) appear to act as mechanical hinges (highlighted in magenta). This further emphasizes the important role of the extended D-loop region of HlyB, which is located within the dimer interface in a position to play a pivotal role in the architecture of the ATP/Mg^{2+} dimer and in NBD–NBD communication (Locher *et al*, 2002; Smith *et al*, 2002; Chen *et al*, 2003). In the ADP-bound structure, the C-terminus of helix 6 is involved in crystal packing contacts, but again a *B*-factor analysis did not suggest that these contacts affect the conclusion that helix 6 acts as a mechanical hinge. Overall, our structural analysis of the HlyB-NBD in various functional states has demonstrated that all steps of the catalytic cycle involve significant conformational changes. In addition, we propose that distinct combinations of mechanical hinges within the protein are used to coordinate the corresponding conformational transitions corresponding to the individual steps of the catalytic cycle. Finally and in summary, whereas the inward rotation of the helical domain upon ATP binding uses the Q- and extended Pro-loops as hinges, the outward rotation in addition uses the Walker B/D-loop region and helix 6. Our analysis also provides a molecular picture of how functional changes during the catalytic cycle might be coupled to the action of mechanical hinges in a way that ultimately ensures efficient NBD–TMD (Q-loop/Pro-loop regions) and NBD–NBD (Walker B/D-loop region) communication.

Detection of asymmetry of the NBD dimer

Starting from the model proposed by Senior *et al* (1995) for the catalytic cycle of ABC-ATPases, several groups (see for example Senior *et al*, 1995; Sauna and Ambudkar, 2000; van Veen *et al*, 2000; van der Does and Tampe, 2004) have suggested that ATP hydrolysis within the NBD dimer is a sequential process leading to models of 'two cylinder' transporter machines. As most ABC-transporters function as homodimers, this implies some form of asymmetry within the NBD dimer. However, from a structural point of view, this has so far received little attention. To understand better the proposed functional asymmetry, we first analyzed the character of intersubunit protein–protein interactions in both the ATP- and ATP/Mg^{2+}-bound states of the HlyB-NBD (Figure 5). Whereas direct ATP–protein interactions are rather symmetric in both dimer structures (data not shown), symmetric and asymmetric protein–protein interactions do occur, in both the ATP- and the ATP/Mg^{2+}-bound states. As evident from the schematic summary (Figure 5), the pattern of interactions in both states is qualitatively different, with a more prominent asymmetry in the presence of Mg^{2+}. This emphasizes the crucial importance of the cofactor in generating asymmetry and explains why significant asymmetry was not detected in other previously studied ABC dimers, as Mg^{2+} was absent. The D-loop is heavily involved in asymmetric inter-monomer interactions in the ATP/Mg^{2+}-bound state (Figure 5B) and is therefore well suited to sense changes occurring in the Walker A and ABC-signature motif of the opposing monomers. Nevertheless, owing to the static picture of crystal structures, we cannot yet determine the initial signals and interactions that promote such profound asymmetry.

An asymmetric exit tunnel for inorganic phosphate in the presence of Mg^{2+}

The asymmetric pattern of interactions, in both the ATP- and ATP/Mg^{2+}-bound structures, prompted us to perform a detailed cavity analysis of the dimer structures in the hope

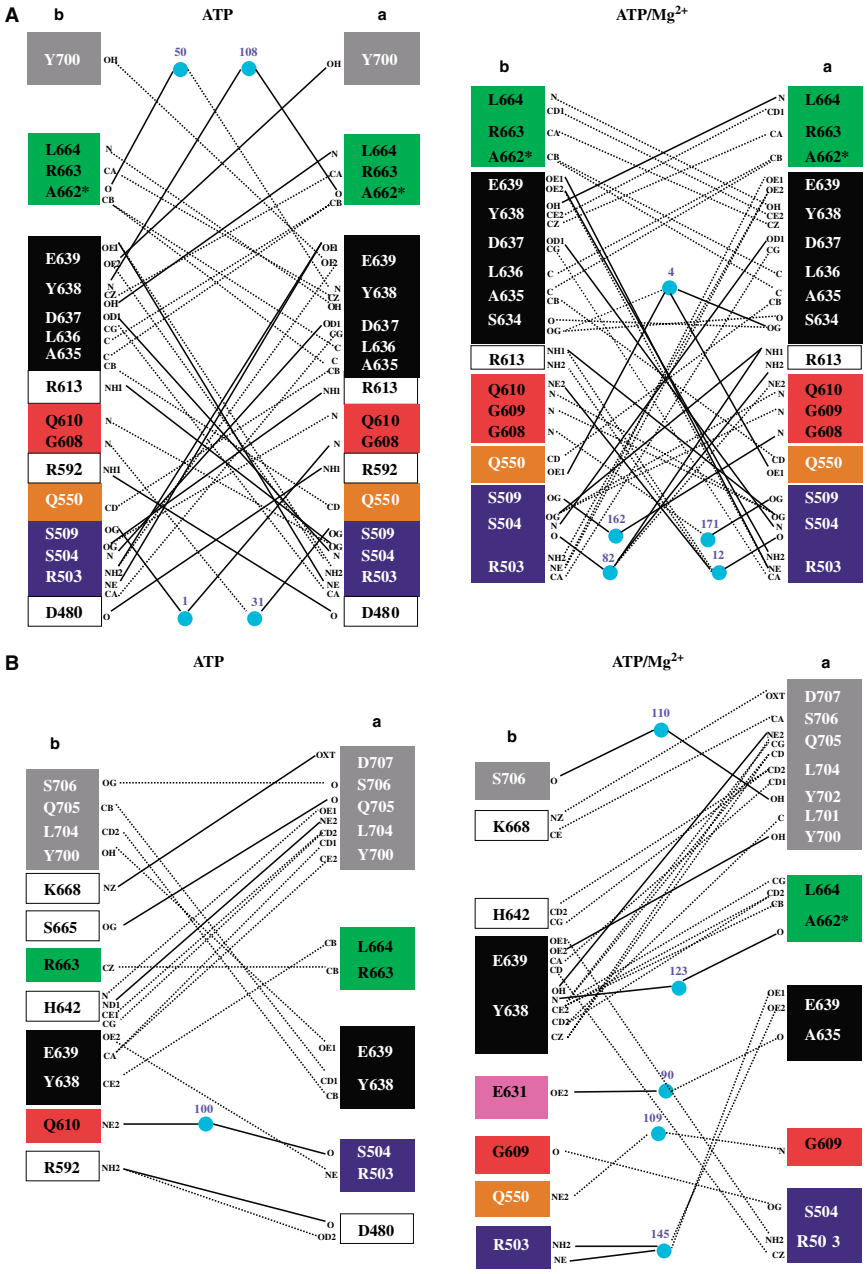

Figure 5 Importance of the cofactor Mg^{2+} in monomer–monomer interactions in the H662A dimer of HlyB. (**A**) Symmetric and (**B**) asymmetric interactions between the monomers of the ATP- (left panel) and ATP/Mg^{2+}- (right panel) bound complexes of the HlyB-NBD H662A. Color-coding is identical to Figure 1. Solid lines represent hydrogen bonds (distance cutoff of 3.2 Å) and dashed line van der Waals interactions (distance cutoff of 4.0 Å). Light blue spheres represent water molecules. Letters indicate the atoms involved in the interactions.

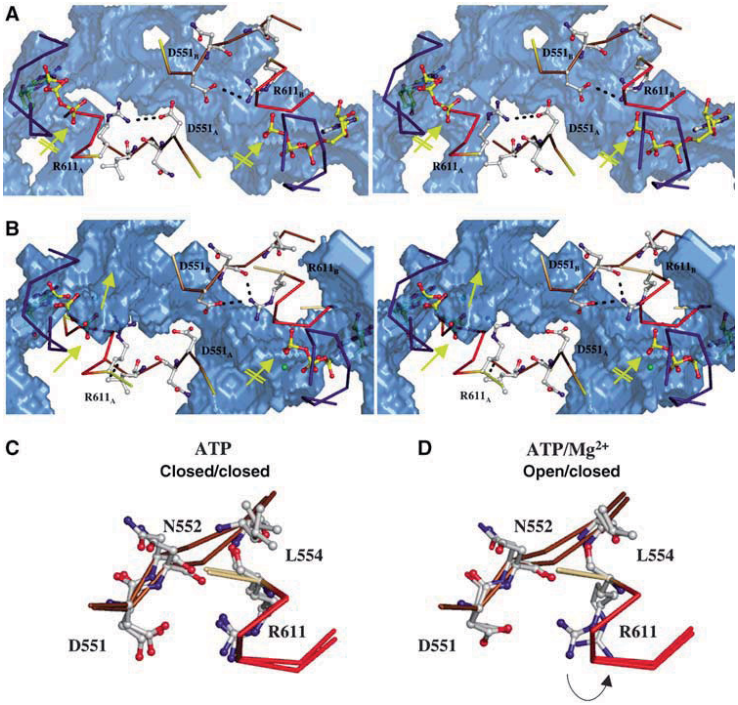

Figure 6 An exit tunnel for inorganic phosphate. Stereoview of the 'phosphate tunnel' within the two ATP-binding sites of the ATP-bound (**A**) and the ATP/Mg^{2+}-bound (**B**) composite dimer of HlyB-NBD H662A. Color-coding is identical to Figure 1. For simplicity only the Walker A, Q-loop and ABC-signature motif are shown in ribbon. Mg^{2+} is shown as a green sphere and amino acids involved in interactions in ball-and-stick representation. The subscripts indicate the monomer to which the amino acids belong. The accessible solvent area (ASA) of the HlyB-NBD dimer is presented as a transparent, blue solid. The interaction between D551 and R611, which acts as a gate for tunnel opening (no interaction between D551 and R611, closest distance of 4.7 Å) and closing (interaction distance of 3.3 Å), is highlighted. The arrows in panels A and B indicate the open (standard arrow) and closed (crossed arrow) phosphate tunnel. Structural superimposition of the individual monomers of the ATP (**C**) and ATP/Mg^{2+} (**D**) dimer of the HlyB-NBD H662A mutant. The flip of R611 in the ATP/Mg^{2+} complex, which acts as a tunnel gate, is indicated by an arrow.

that this might highlight any functional significance of asymmetry. In Figure 6, the calculated cavities and tunnels in the H662A composite dimer are shown as blue solids. First, in the case of the ATP-bound state with no Mg^{2+} (Figure 6A), symmetrical tunnels reaching down towards the nucleotide-binding site are detectable. However, these tunnels do not reach the nucleotide and are closed by a salt bridge between D551 and R611, roughly 6 Å above the γ-phosphate group in both ATP-binding sites (indicated by the crossed arrows). The situation is different for the adenine moiety, which is completely solvent accessible in both sites. However, the ribose, α-, and β-phosphate moieties of ATP are also excluded from solvent. Identical results were obtained when we analyzed the ATP-bound dimeric structures of MJ0796 (Smith *et al*, 2002) and MalK (Chen *et al*, 2003) (data not shown). Thus, based on a cavity analysis of three structures of dimeric ATP-bound NBDs, inorganic phosphate should not be able to diffuse freely out of the binding site. Rather, a conformational change would have to occur within the protein in order to open an exit path for the cleaved inorganic phosphate.

We next performed a cavity analysis of the composite ATP dimer with bound Mg^{2+}, calculating the positions of the adenine ring and the α- and β-phosphate moieties of ATP/Mg^{2+} with respect to their exposure to solvent. The results showed that these were equivalent to those observed in the ATP-bound dimer without Mg^{2+}. However, quite dramatically, the presence of Mg^{2+} (absolutely required for hydrolysis) in the composite dimer results in a clear asymmetry with respect to the γ-phosphate region (compare the positions of the standard and crossed arrows in Figure 6B). One site is still closed roughly 6 Å above the γ-phosphate, whereas, in the other site, a 'phosphate exit tunnel' extends to the γ-phosphate group of the bound ATP. This open tunnel has a smallest diameter of roughly 4.4 Å, which should be sufficient to allow rather unrestricted passage of inorganic phosphate. Superimposition of the individual monomers of the dimeric ATP- and ATP/Mg^{2+}-bound states emphasizes the importance of the salt bridge between D551 and R611 (Figures 6C and D). In the closed state, the salt bridge (distance 3.3 Å) locks the tunnel entrance, whereas in the open state the salt bridge open up owing to a flip of the R611

side chain (Figure 6D). Interestingly, statistical analysis of the conservation of these residues, using more than 10 000 ABC-transporter sequences (derived from www.sanger.ac.uk/cgi-bin/Pfam/getacc?PF0005), revealed conservation of residue 611 (allowing conservative substitutions with respect to the ability to form salt bridges or the alternative to form hydrogen bonds, that is, R (35%), K (31%) and Q (21%)). Position 551 displayed a lower but still significant degree of conservation (E (19%), D (22%), N (11%)). The pairwise distribution of amino acids at positions 551 and 611 further supports the idea of an interacting amino-acid pair. For example, residues capable of forming a salt bridge or a hydrogen bond appear in 66% of the sequences, with a K at position 611 (position 551: D (24%), E (24%), N (10%) and Q (8%)). The same applies if an R is present at position 611 (position 551: D (28%), E (19%), N (10%) and Q (9%)). Thus, we would like to propose that the interaction between R611 and D551 acts as a gate to close or open the phosphate exit tunnel in the HlyB-NBD structure. In the open state, this would allow the free diffusion of the product of ATP hydrolysis, inorganic phosphate. Strong support for the function of R611 and D551 as 'door-keepers' comes from mutational analysis (Supplementary Figure S1). Mutating R611 or D551 to alanine resulted in proteins that retained ATPase activity although substantially reduced. More importantly, however, substitution of these residues abolished detectable cooperativity with respect to ATP hydrolysis. In contrast, the conservative mutation of R611 to lysine resulted in an enzyme with comparable activity and more importantly that retained positive cooperativity (Supplementary Figure S1). The loss of cooperativity is not simply a nonspecific effect due to the low level of residual activity, as the E631Q mutant of HlyB-NBD still displayed cooperative ATP hydrolysis, despite a reduced ATPase activity comparable to that in the R611A and D551A mutants (Zaitseva *et al*, 2005a). Thus, these two conserved amino acids may not only be important for asymmetric phosphate release from the HlyB-NBD, but may also be involved in molecular communication between the two ATP-binding sites, which normally results in the so far poorly understood positive cooperativity (Zaitseva *et al*, 2005b). It is equally important to note here that the presence of the phosphate tunnels could explain biochemical data derived from other isolated NBDs and full-length ABC-transporters, which strongly suggested sequential ATP hydrolysis (see for example (Urbatsch *et al*, 1995; Janas *et al*, 2003; Tombline *et al*, 2005). Janas *et al* (2003) showed that an NBD dimer could be still detected after single site ATP hydrolysis, but not after the second hydrolysis event. Extrapolated to our structural analysis, this result implies that the release of the first phosphate through the exit tunnel may occur in a fully assembled dimer without significant conformational change, whereas the second release would require a conformational change within the protein. Nevertheless, further investigations are necessary to determine whether this mechanism and its gating through the action of a salt bridge of the precise type discussed above are universal for ABC-ATPase, specific for ABC exporters or unique to HlyB.

The role of helix 6 as an enthalpic device

The F_1 motor of the ATP synthase achieves a nearly 100% efficiency by converting chemical energy stored within ATP into elastic strain. Thus, no heat dissipates and all energy can be stored within the protein owing to 'deformations' of certain structural motifs or secondary structure elements (Wang and Oster, 1998; Sun *et al*, 2003). A similar situation could arise in ABC-transporters, which ultimately use the energy of ATP to drive transport substrate translocation. We present below one such possibility in relation to the ADP-bound state of the HlyB-NBD and the associated deformation of helix 6. A superimposition of the individual structures of the catalytic cycle indicated that whereas ATP binding results in a rigid-body *inward* rotation of the helical domain, ATP hydrolysis and NBD dimer disassembly generate the *outward* rotation of the helical domain together with bending and displacement of helix 6 (residues 637–652), which is located immediately C-terminal to the D-loop. A 15° tilting of helix 6 in the ADP-bound state occurs owing to the breaking of one and the formation of four new hydrogen bonds, when compared with helix 6 in either the ATP-bound or the nucleotide-free state (Figure 7). This tilt is present in all three structures determined for the ADP state (wild type, E631Q and H662A) but not the two ATP dimers (H662A and E631Q). This suggests that helix 6 has an intrinsic conformational flexibility and we would like to suggest that tilting of this helix is used to store energy in the form of elastic strain during the catalytic cycle (Figure 7). It is important to note here that based on the principle of microscopic reversibility (Fersht, 1997), the ADP-bound state is structurally identical whether reached as a result of ATP hydrolysis or conversely from *de novo* binding of ADP. Thus, based on the observed helix tilting, it is feasible that helix 6 serves as a molecular device to store part of the energy released upon ATP hydrolysis in the form of elastic strain. This strain could be used for functional purposes such as ADP release. This presumably must require an active process of some kind, as the affinity of ADP for the NBD appears to be too high to allow spontaneous dissociation (see below). The utilization of stored energy in this way would provide a route for a programmed release of ADP from monomers, after an outward rotation of the helical domain following ATP hydrolysis and dimer disassembly, with concomitant transmission of conformational changes to the membrane domains.

Mechano-chemistry associated with the action of ABC-NBDs

In contrast to channels, membrane transport proteins require a source of energy input to translocate the substrate across a membrane and against a concentration gradient. In the case of membrane transporters of the ABC-transporter family, this energy is directly provided by the NBDs. However, as elaborated above, ABC domains not only hydrolyze ATP, but also undergo an ATP-induced dimerization. Consequently, an NBD can use two fundamentally different mechanisms to fuel transport substrate translocation. First, mechanical energy from the rigid-body motion associated with ATP-induced dimerization and second chemical energy obtained from the hydrolysis of ATP.

For a detailed structural and functional analysis of the catalytic cycle, it is important to consider the nature and possible use of all energy generating steps. From the affinity constants for nucleotides and the ATP-induced dimerization constant of the NBD (Zaitseva *et al*, 2005b), the inherent energies of the individual steps can be calculated based on the Gibbs free energy relation. The ΔG values for ATP binding

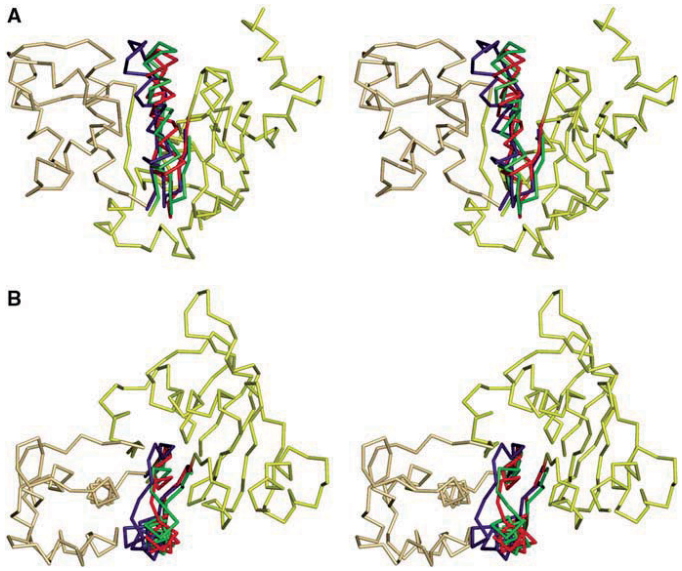

Figure 7 An enthalpic storage device for the chemical energy of ATP. (**A**) Structural superimposition of the nucleotide-free and ATP- and ADP-bound forms. For simplicity, only the structure of the ATP-bound form is shown as ribbons. Helix 6 of the nucleotide-free state is shown in green, for the ATP-bound state in red and for the ADP-bound state in blue. (**B**) 90° rotation in the plane with respect to panel A.

($K_D = 87.8 \pm 11.2\,\mu M$), ADP binding ($K_D = 77.1 \pm 13.2\,\mu M$) and NBD dimerization ($K_D = 1.2 \pm 0.2\,\mu M$) were calculated to be −17.3, −17.6 and −33.4 kJ/mol, respectively. From an energetic point of view, as ATP hydrolysis (around −30 to −35 kJ/mol) and NBD dimerization (−33.4 kJ/mol) are very similar, either step could represent the potential 'power stroke' of the catalytic cycle. However, one has to keep in mind that the above ΔG values are derived from isolated NBDs and the presence of the TMDs of HlyB might change significantly the value of certain steps of the catalytic cycle, shifting the actual energetic distribution. Nevertheless, we emphasize that ABC-ATPases are capable of acting as dual mode engines as a source of both mechanical and chemical energy (Figure 1).

This analysis leads us to propose the following description of the catalytic cycle of the NBD and its functional implications. First, ATP induces dimerization, accompanied by a rigid-body movement of the helical domain, employing the Q- and Pro-loop as hinges. These conformational changes are transmitted to the TMDs and result in a rearrangement of the membrane helices and in initiation of transport. Secondly and equally important is ATP hydrolysis: this is the rate-limiting step of the catalytic cycle and therefore the point of control (Zaitseva *et al*, 2005a). We now propose that the sequential hydrolysis of two ATPs, reflected by the apparent sequential release of the two inorganic phosphates (see Figure 5), is due to the inherent asymmetry of the dimer. This raises the possibility to couple the hydrolysis steps, accompanied by sequential release of the phosphates for separate purposes. Therefore, overall, one catalytic cycle of the ABC domain would consume two ATPs. This closely resembles, for example, the ATP/transport substrate stoichiometry determined for OpuA from *Lactobacillus lactis* (Patzlaff *et al*, 2003). In HlyB, many cycles might be necessary to translocate the large HlyA molecule, although the proton motif force is possibly also involved in HlyA secretion (Koronakis *et al*, 1991).

An alternative explanation for the molecular events resulting in dimer dissociation has been proposed by Hunt and co-workers (Smith *et al*, 2002); here, the increased negative charge distribution within the nucleotide-binding site resulting from ATP hydrolysis is suggested to be sufficient for spontaneous dissociation of the dimer. We investigated this idea with respect to HlyB and have calculated the electrostatic surface potential of a monomer of the ATP-bound dimer of H662A. To our surprise and in contrast to the results obtained for MJ0796 (Smith *et al*, 2002) (Supplementary Figure S2), no significant increase in negative charges accompanying ATP hydrolysis was detected within the ATP-binding site of HlyB. Therefore, it appears unlikely that such a mechanism is sufficient to induce dimer disassembly in HlyB. In fact, superimposition of the hypothetical ADP-bound HlyB-NBD 'dimer' on the structure of the NBD of BtuCD identical to the ADP-bound form (Locher *et al*, 2002) strongly suggests that the D-loops are involved in dimer dissociation (Supplementary Figure S3). Here, the resulting steric clashes occurring between opposing D-loops in the modeled HlyB-NBD/ADP dimer clearly indicate that such a 'dimer' is not stable. As the region of the Walker B/D-loop region acts as one of the four hinges in the ATP–ADP transition (Figure 4), HlyB dimer disassembly could easily be coupled to conformational changes of the ABC domain upon catalysis.

In summary, we propose that the catalytic cycle of the isolated ABC-NBDs is divided into distinct steps that involve different conserved sequence motifs as key players, acting to

coordinate intramolecular movements. The energy to drive rearrangement of the TMDs and substrate translocation is provided by two different molecular steps: *mechanical energy* derived by the rigid-body motion of the helical domain, which is induced by ATP binding 'to create' the translocation pathway, while sequential ATP hydrolysis provides the *chemical energy* to complete the movement of the transport substrate across the membrane and to enable ADP dissociation. In this model, one can assign distinct functions to the conserved motifs of NBDs: the Walker A and B motifs, as well as the ABC signature and H-loops are required for ATP binding and hydrolysis, whereas the Pro-, Q- and D-loops act as hinges and are likely central to NBD–NBD and NBD–TMD communication. Finally, we have identified a novel salt bridge in a position capable of controlling sequential release of inorganic phosphate, and essential for cooperative activity.

Materials and methods

Protein purification, ATPase assays, crystallization and data collection

Purification and crystallization of HlyB-NBD and the mutants used were as described previously (Zaitseva *et al*, 2004). To obtain the E631Q, D551A, R611K and R611A mutants of HlyB-NBD, plasmid pPSG122 was used as a template. The mutation was introduced using the ligase chain reaction according to the protocol of the manufacturer (Epicentre). ATPase activity measurements were performed as described (Zaitseva *et al*, 2005b). For crystallization of the ADP-bound states, 25 mg/ml of the NBD in 70 mM CAPS pH 10.4, 30% glycerol and 10 mM ADP or ATP/Mg^{2+} was mixed with an equal volume of 100 mM Tris pH 8.0, 10% PEG 6000 and 5% MPD at 277 K. Crystals of the ATP-bound state of the HlyB-NBD H662A were obtained by mixing equal ratios of 10 mg/ml protein in 1 mM CAPS pH 10.4, 30% glycerol, 2 mM ATP, 1 mM EDTA with 100 mM sodium malonate pH 5.6, 10% PEG 5500-MME and 0.25 mM sodium acetate. Crystals of the ATP-bound state of the HlyB-NBD E631Q were obtained by mixing equal ratios of 10 mg/ml protein in 1 mM CAPS pH 10.4, 30% glycerol, 10 mM ATP, 1 mM EDTA with 100 mM Tris pH 8.5, 10% PEG 6000 and 5% MPD. Crystals were flash-frozen in a nitrogen stream. Data from single crystals were collected at beamline BW-6, DESY, Hamburg. Data were processed using DENZO and SCALEPACK (Otwinowski and Minor, 1997).

Structure determination and refinement

The structures were solved by molecular replacement using AMoRe (Navaza, 1994). The initial solutions were refined using REFMAC5 (Murshudov *et al*, 1997) employing TLS-grouped refinement, followed by repetitive rounds of manual rebuilding into $1F_o-F_c$ and $2F_o-F_c$ maps using O (Jones *et al*, 1991). In the initial state of refinement of the ATP-bound structure, strict non-crystallographic symmetry (NCS) was applied, which was released in the last four cycles of rebuilding and refinement. In the case of the E631Q mutant structure with bound ATP, NCS of the catalytic domains (residues 467–549 and 625–707) A/C and B/D was kept during all stages of refinement. ARP/wARP (Lamzin and Wilson, 1993) was used to determine water molecules at a conservative threshold of 3σ.

Structural alignments, determination of hinge bending residues and cavity analysis

Structural alignments were performed with LSQMAN (Kleywegt, 1996) using a 'reduced' catalytic domain (residues 467–540 and 626–707) or the whole NBD (alignments of the different mutants in the same functional state). Bending residues/regions of the HlyB-NBD during the catalytic cycle were determined using the DynDom software (www.cmp.uea.ac.uk/dyndom/main.jsp). Analysis of potential cavities and tunnels in the ATP- and ATP/Mg^{2+}-bound structures of HlyB-NBD H662A was performed using VOIDOO (Kleywegt and Jones, 1994) and MAMA (Kleywegt and Jones, 1999).

Figure preparation

All figures were prepared using Pymol (www.pymol.org).

Protein Data Bank accession code

Coordinates have been deposited under accession numbers 2FF7 (wild-type ADP), 2FFB (ADP E631Q), 2FFA (ADP H662A), 2FGJ (ATP H662A) and 2FGK (ATP E631Q).

Supplementary data

Supplementary data are available at *The EMBO Journal* Online.

Acknowledgements

We thank Sander Smits, Eckhard Hoffmann, Robert Ernst and Nils Hanekop for many discussions and support during data collection. We are indebted to Gleb Bourenkov for his excellent assistance. The University of Paris-Sud (IBH) and the DFG (grant Schm1279/2-3 and SFB 628 to LS) supported this work.

References

Chang G (2003) Structure of MsbA from *Vibrio cholera*: a multidrug resistance ABC transporter homolog in a closed conformation. *J Mol Biol* **330:** 419–430

Chang G, Roth CB (2001) Structure of MsbA from *E. coli*: a homolog of the multidrug resistance ATP binding cassette (ABC) transporters. *Science* **293:** 1793–1800

Chen J, Lu G, Lin J, Davidson AL, Quiocho FA (2003) A tweezers-like motion of the ATP-binding cassette dimer in an ABC transport cycle. *Mol Cell* **12:** 651–661

Chen J, Sharma S, Quiocho FA, Davidson AL (2001) Trapping the transition state of an ATP-binding cassette transporter: evidence for a concerted mechanism of maltose transport. *Proc Natl Acad Sci USA* **98:** 1525–1530

Davidson AL, Chen J (2004) ATP-binding cassette transporters in bacteria. *Annu Rev Biochem* **73:** 241–268

Eyal E, Gerzon S, Potapov V, Edelman M, Sobolev V (2005) The limit of accuracy of protein modeling: influence of crystal packing on protein structure. *J Mol Biol* **351:** 431–442

Fersht A (1997) *Enzyme Structure and Mechanism*. New York: WH Freeman and Company

Gaudet R, Wiley DC (2001) Structure of the ABC ATPase domain of human TAP1, the transporter associated with antigen processing. *EMBO J* **20:** 4964–4972

Higgins CF (1992) ABC transporters: from microorganisms to man. *Annu Rev Cell Biol* **8:** 67–113

Holland IB, Schmitt L, Young J (2005) Type 1 protein secretion in bacteria, the ABC-transporter dependent pathway. *Mol Memb Biol* **22:** 29–39

Hung LW, Wang IXY, Nikaido K, Liu PQ, Ames GFL, Kim SH (1998) Crystal structure of the ATP-binding subunit of an ABC transporter. *Nature* **396:** 703–707

Janas E, Hofacker M, Chen M, Gompf S, van der Does C, Tampe R (2003) The ATP hydrolysis cycle of the nucleotide-binding domain of the mitochondrial ATP-binding cassette transporter Mdl1p. *J Biol Chem* **278:** 26862–26869

Jones PM, George AM (2004) The ABC transporter structure and mechanism: perspectives on recent research. *Cell Mol Life Sci* **61:** 682–699

Jones TA, Zou JY, Cowan SW, Kjeldgaard M (1991) Improved methods for binding protein models in electron density maps and the location of errors in these models. *Acta Crystallogr A* **47:** 110–119

Karpowich N, Martsinkevich O, Millen L, Yuan YR, Dai PL, MacVey K, Thomas PJ, Hunt JF (2001) Crystal structures of the MJ1267 ATP binding cassette reveal an induced-fit effect at the ATPase active site of an ABC transporter. *Structure* **9:** 571–586

Kleywegt GJ (1996) Use of non-crystallographic symmetry in protein structure refinement. *Acta Crystallogr D* **52:** 842–857

Kleywegt GJ, Jones TA (1994) Detection, delineation, measurement and display of cavities in macromolecular structures. *Acta Crystallogr D* **50:** 178–185

Kleywegt GJ, Jones TA (1999) Software for handling macromolecular envelopes. *Acta Crystallogr D* **55:** 941–944

Koronakis V, Hughes C, Koronakis E (1991) Energetically distinct early and late stages of HlyB/HlyD-dependent secretion across both *Escherichia coli* membranes. *EMBO J* **10:** 3263–3272

Lamzin VS, Wilson KS (1993) Automated refinement of protein models. *Acta Crystallogr D* **49:** 129–147

Lewis HA, Buchanan SG, Burley SK, Conners K, Dickey M, Dorwart M, Fowler R, Gao X, Guggino WB, Hendrickson WA, Hunt JF, Kearins MC, Lorimer D, Maloney PC, Post KW, Rajashankar KR, Rutter ME, Sauder JM, Shriver S, Thibodeau PH, Thomas PJ, Zhang M, Zhao X, Emtage S (2004) Structure of nucleotide-binding domain 1 of the cystic fibrosis transmembrane conductance regulator. *EMBO J* **23:** 282–293

Locher KP (2004) Structure and mechanism of ABC transporters. *Curr Opin Struct Biol* **14:** 426–431

Locher KP, Lee AT, Rees DC (2002) The *E. coli* BtuCD structure: a framework for ABC transporter architecture and mechanism. *Science* **296:** 1091–1098

Lu G, Westbrooks JM, Davidson AL, Chen J (2005) ATP hydrolysis is required to reset the ATP-binding cassette dimer into its resting state conformation. *Proc Natl Acad Sci USA* **102:** 17969–17974

Moody JE, Millen L, Binns D, Hunt JF, Thomas PJ (2002) Cooperative, ATP-dependent association of the nucleotide binding cassettes during the catalytic cycle of ATP-binding cassette transporters. *J Biol Chem* **277:** 21111–21114

Murshudov G, Vagin AA, Dodson EJ (1997) Refinement of macromolecular structures by the maximum-likelihood method. *Acta Crystallogr D* **53:** 240–255

Navaza J (1994) AMoRe: an automated package for molecular replacement. *Acta Crystallogr D* **50:** 157–163

Oswald C, Holland IB, Schmitt L (2006) The motor domains of ABC-transporters/what can structures tell us? *Naunyn Schmiedebergs Arch Pharmacol* **372:** 385–399

Otwinowski Z, Minor W (1997) Processing of X-ray diffraction data collected in oscillation mode. In *Methods in Enzymology*, Carter CW, Sweet RM (eds) London: Academic Press

Patzlaff JS, van der Heide T, Poolman B (2003) The ATP/substrate stoichiometry of the ATP-binding cassette (ABC) transporter OpuA. *J Biol Chem* **278:** 29546–29551

Reyes CL, Chang G (2005) Structure of the ABC transporter MsbA in complex with ADP.vanadate and lipopolysaccharide. *Science* **308:** 1028–1031

Sauna ZE, Ambudkar SV (2000) Evidence for a requirement for ATP hydrolysis at two distinct steps during a single turnover of the catalytic cycle of human P-glycoprotein. *Proc Natl Acad Sci USA* **97:** 2515–2520

Schmitt L, Benabdelhak H, Blight MA, Holland IB, Stubbs MT (2003) Crystal structure of the nucleotide binding domain of the ABC-transporter haemolysin B: identification of a variable region within ABC helical domains. *J Mol Biol* **330:** 333–342

Schmitt L, Tampé R (2002) Structure and mechanism of ABC-transporters. *Curr Opin Struct Biol* **12:** 754–760

Senior AE, al-Shawi MK, Urbatsch IL (1995) The catalytic cycle of P-glycoprotein. *FEBS Lett* **377:** 285–289

Smith PC, Karpowich N, Millen L, Moody JE, Rosen J, Thomas PJ, Hunt JF (2002) ATP binding to the motor domain from an ABC transporter drives formation of a nucleotide sandwich dimer. *Mol Cell* **10:** 139–149

Sun S, Chandler D, Dinner AR, Oster G (2003) Elastic energy storage in beta-sheets with application to F1-ATPase. *Eur Biophys J* **32:** 676–683

Tombline G, Muharemagic A, White LB, Senior AE (2005) Involvement of the 'occluded nucleotide conformation' of p-glycoprotein in the catalytic pathway. *Biochemistry* **44:** 12879–12886

Urbatsch IL, Sankaran B, Weber J, Senior AE (1995) P-glycoprotein is stably inhibited by vanadate-induced trapping of nucleotide at a single catalytic site. *J Biol Chem* **270:** 19383–19390

van der Does C, Tampe R (2004) How do ABC transporters drive transport? *Biol Chem* **385:** 927–933

van Veen HW, Margolles A, Muller M, Higgins CF, Konings WN (2000) The homodimeric ATP-binding cassette transporter LmrA mediates multidrug transport by an alternating two-site (two-cylinder engine) mechanism. *EMBO J* **19:** 2503–2514

Verdon G, Albers SV, Dijkstra BW, Driessen AJ, Thunnissen AM (2003a) Crystal structures of the ATPase subunit of the glucose ABC transporter from *Sulfolobus solfataricus*: nucleotide-free and nucleotide-bound conformations. *J Mol Biol* **330:** 343–358

Verdon G, Albers SV, van Oosterwijk N, Dijkstra BW, Driessen AJ, Thunnissen AM (2003b) Formation of the productive ATP-Mg^{2+}-bound dimer of GlcV, an ABC-ATPase from *Sulfolobus solfataricus*. *J Mol Biol* **334:** 255–267

Wang H, Oster G (1998) Energy transduction in the F1 motor of ATP synthase. *Nature* **396:** 279–282

Welch RA, Dellinger EP, Minshew B, Falkow S (1981) Haemolysin contributes to virulence of extra-intestinal *E. coli* infections. *Nature* **294:** 665–667

Ye J, Osborne AR, Groll M, Rapoport TA (2004) RecA-like motor ATPases—lessons from structures. *Biochim Biophys Acta* **1659:** 1–18

Yuan YR, Blecker S, Martsinkevich O, Millen L, Thomas PJ, Hunt JF (2001) The crystal structure of the MJ0796 ATP-binding cassette. Implications for the structural consequences of ATP hydrolysis in the active site of an ABC transporter. *J Biol Chem* **276:** 32313–32321

Zaitseva J, Holland IB, Schmitt L (2004) The role of CAPS in expanding the crystallisation space of the nucleotide binding domain of the ABC-transporter from *E. coli*. *Acta Crystallogr D* **60:** 1076–1084

Zaitseva J, Jenewein S, Jumpertz T, Holland IB, Schmitt L (2005a) H662 is the linchpin of ATP hydrolysis in the nucleotide-binding domain of the ABC transporter HlyB. *EMBO J* **24:** 1901–1910

Zaitseva J, Jenewein S, Wiedenmann A, Benabdelhak H, Holland IB, Schmitt L (2005b) Functional characterization and ATP-induced dimerization of the isolated ABC-domain of the haemolysin B transporter. *Biochemistry* **44:** 9680–9690

Supplementary material

Figure S1:

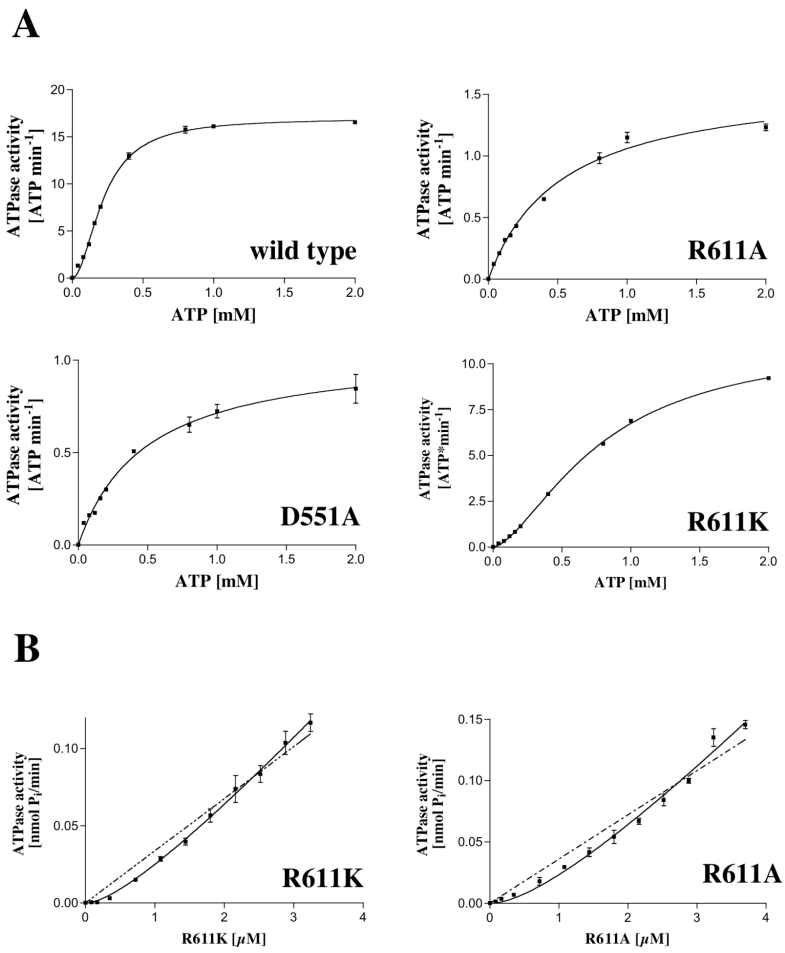

ATPase activity of wild type HlyB-NBD and the R611A, D551A and R611K mutants.
(A) Steady state ATPase activity was determined at 22 ± 1°C as described in detail in Zaitseva et al. (Zaitseva, J., *et al*. (2005) Functional characterization and ATP-induced dimerization of the isolated ABC-domain of the haemolysin B transporter *Biochemistry* **44** 9680- 9690). Final protein concentration used in the assay was 0.06 mg/ml (2.2 μM, wild type, upper left panel), 0.05 mg/ml (2 μM, R611A, upper right panel), 0.04 mg/ml (1.6 μM, D551A, lower left panel)

and 0.05 mg/ml (2 μM, R611K, lower right panel). The ATPase activity was analyzed according to the Hill equation. Kinetic parameters were determined as: wild type enzyme ($K_{0.5}$= 0. 23 ± 0.06 mM, k_{cat}= 17.3 ± 0.3 ATP min^{-1}, Hill coefficient= 1.8 ± 0.1), R611A (K_M= 0.39 ± 0.07 mM, k_{cat}= 1.4 ± 0.1 ATP min^{-1}), D551A (K_M= 0.49 ± 0.01 mM, k_{cat}= 1.1 ± 0.1 ATP min^{-1}), and R611K ($K_{0.5}$= 0.58 ± 0.03 mM, k_{cat}= 11.3 ± 0.3 ATP min^{-1}, Hill coefficient= 1.6 ± 0.1). Thus, these residues are crucial to the observed positive cooperativity of ATPase activity. (B) Protein concentration dependent ATPase activity of the R611K (left panel) and R611A mutants (right panel). Data points were analyzed according to Nikaido et al. (Nikaido, H., Liu, P.-Q. & Ferro-Luzzi Ames, G. (1997) Purification and Characterization of the of HisP, the ATP-binding subunit of the traffic ATPase (ABC transporter), the histidine permease of *Salmonella typhimurium J. Biol. Chem.* **272** 27745- 27752). The dashed line corresponds to a simulated protein concentration dependent ATPase activity in the absence of any dimer formation of the NBD, which assumes that ATPase activity arises only from the monomeric NBD. This analysis demonstrates that the mutants (R611K, R611A and D551A (data not shown) still dimerize although cooperativity is strongly dependent on the nature of the mutations.

2

Figure S2:

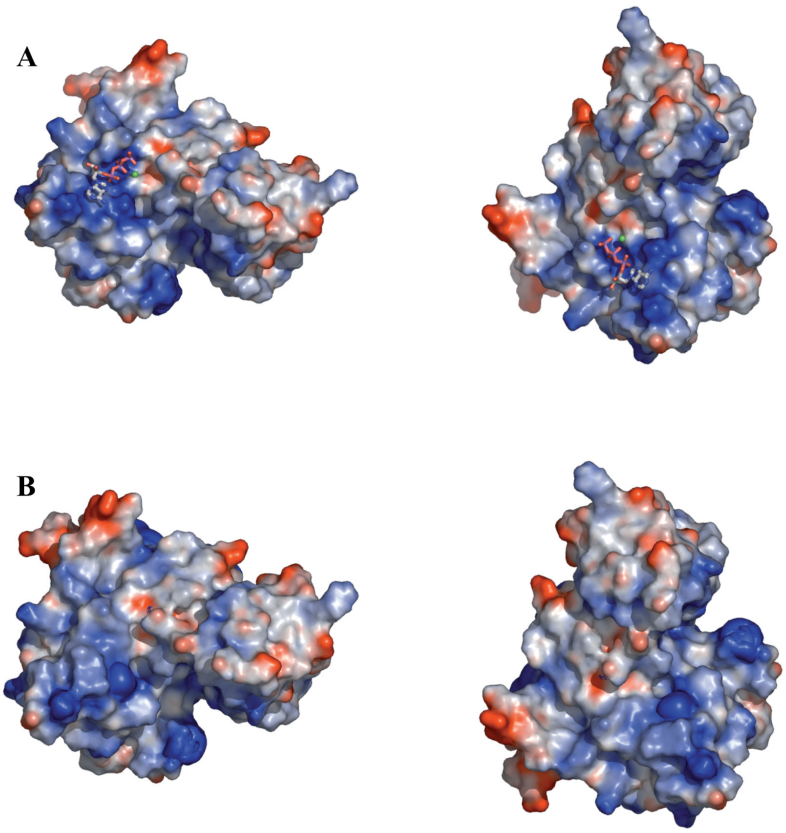

Electrostatic surface potential of a monomer of the ATP/Mg^{2+}-loaded dimer of the HlyB-NBD H662A.

The color-coding was set according to electrostatic potentials assuming an ionic strength of 100 mM. Red and blue are used to represent negative and positive potentials, with blue indicating a magnitude of the potential of > 4 kT and red indicating a magnitude of the potential of < - 4 kT. Here, k is the Boltzman constant and T the absolute temperature. Calculations were performed with PyMol using the APBS tool. The orientation of the NBD is identical to Figure 4. Right panels are rotated 90° perpendicular to the plane of the paper. (A) ATP/Mg^{2+} was not included in the calculations and is shown in sticks (ATP) and as a green sphere (Mg^{2+}). (B) The ATP/Mg^{2+} complex was included in the calculations.

Figure S3:

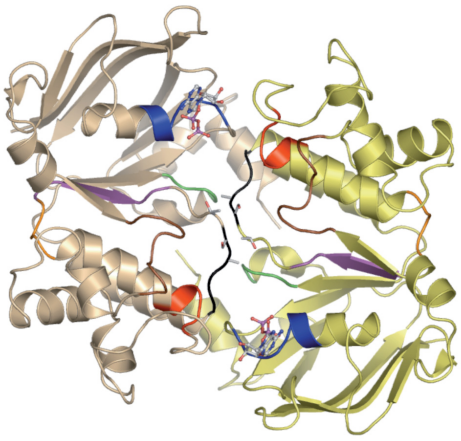

Figure S3: The hypothetical dimer of the HlyB-NBD in the ADP bound state.
The dimeric state was obtained by superimposition of two post catalysis, ADP-bound monomers of the HlyB-NBD and the crystal structure of BtuD (pdb entry 1L7V), which is structurally identical to the ADP-bound form (Locher, K.P. (2004) Structure and mechanism of ABC transporters. Curr Opin Struct Biol, 14, 426-431). For simplicity, the BtuD dimer is not shown. The rmsd of the individual ADP monomers of HlyB-NBD and BtuD was 1.98 Å over 231 Cα-atoms. Color-coding of the conserved motifs is identical to Figure 1, with one monomer shown in light yellow and the other in light tan. ADP is shown in ball-and-sticks representation. Immediately evident is the steric clash of the D-loops of the opposing HlyB monomers (shortest distance of 2.9 Å between the Cα atoms of S634 and A635).

Proportionate work on this publication: 30 %

Published in: EMBO Journal

Impact factor: 8.295

PAPER IV

Microbiology Papers in Press. Published April 29, 2010 as doi:10.1099/mic.0.038562-0

Mutations affecting the extreme C-terminus of *E. coli* haemolysin A reduce haemolytic activity by altering the folding of the toxin.

(Running title: A dual role for the HlyA secretion signal)

Thorsten Jumpertz[1] Christian Chervaux[3], Kathleen Racher[4], Maria Zouhair[2], Mark A. Blight[2], I. Barry Holland[2] & Lutz Schmitt[1*]

[1]Institute of Biochemistry, Heinrich Heine University, Universitaetsstrasse 1, 40225 Duesseldorf, Germany

[2]Institut de Génetique et Microbiologie, URA 1354, Université Paris Sud, Bâtiment 409, 91405 Orsay Cedex, France

Tel: 49-211 81 10 77 3; fax: 49-211 81 15 31 0; email: lutz.schmitt@uni-duesseldorf.de

Tel: 33-1-69 15 77 06; fax: 33-1-69 15 78 08; e-mail: barry.holland@igmors.u-psud.fr

(Key words: Haemolysin, Secretion, *E. coli*, Signal sequence mutations, protein folding)

[3] Danone Research Center, Daniel Carasso, Paliseau, Cedex 91767, France

[4] Water Resources, Indian and Northern Affairs (INAC-AINC), Canada

*corresponding author: tel: 49-211 81 10 77 3; fax: 49-211 81 15 31 0

Summary

E. coli Haemolysin A, an RTX toxin, is secreted probably as an unfolded intermediate, by the Type I (ABC transporter dependent) pathway, utilising a C-terminal secretion signal. However, the mechanism of translocation and post translocation folding is not understood. We identified a mutation (*hlyA99*) at the extreme C-terminus, which is dominant in competition experiments, blocking secretion of the wild type toxin co-expressed in the same cell. This suggests that unlike recessive mutations which affect recognition of the translocation machinery, the *hlyA99* mutation interferes with some later step in secretion. Indeed, the mutation reduced haemolytic activity of the toxin and the activity of β-lactamase when the latter was fused to a C-terminal 23 kDa fragment of HlyA carrying the *hlyA99* mutation. A second mutant (*hlyAdel6*), lacking the 6 C-terminal residues of HlyA also showed reduced haemolytic activity and neither mutant protein regained normal haemolytic activity in *in vitro* unfolding/refolding experiments. Tryptophan fluorescence spectroscopy indicated differences in structure between the secreted forms of wild type HlyA and the HlyA Del6 mutant. These results suggested that the mutations affected the correct folding of both HlyA and the β-lactamase fusion. Thus, we propose a dual function for the HlyA C-terminus involving an important role in post translocation folding as well as targeting HlyA for secretion.

Introduction

Bacteria have developed a wide range of defence strategies to survive in hostile and competitive environments. Some of these strategies rely on the secretion of toxins that have various effects, including disruption of host membranes. The secretion of proteins by Gram-negative bacteria involves an extraordinarily wide variety of distinct mechanisms. The 107 kDa toxin Haemolysin A (a member of the RTX protein family; repeat in toxin) produced by invasive *E. coli* strains, in particular, in uropathogenic *E. coli,* is secreted via the Type I (ABC) system (Holland *et al.*, 2005) (Figure S1).

HlyA secretion (for recent reviews see (Delepelaire, 2004; Holland *et al.*, 2005) is accomplished via a trans-envelope conduit or tunnel assembled in response to the presence of nascent HlyA (Balakrishnan *et al.*, 2001). This tunnel connects the cytoplasm of *E. coli* directly to the external surface and is composed of three proteins, HlyB (an ABC transporter), TolC an outer membrane protein with an extensive helical domain extending into the periplasm (Koronakis *et al.*, 2000), and HlyD, a so-called MFP (membrane fusion protein), which likely bridges HlyB and TolC to complete the tunnel. Secretion is initiated by the docking of the C-terminal secretion signal of HlyA to the HlyBD complex, which appears to involve direct interaction between the secretion signal and HlyB in competition with ATP (Benabdelhak *et al.*, 2003). HlyA is then transported directly to the cell surface through the HlyB:HlyD:TolC transenvelope tunnel, where the restricted diameter of TolC (Andersen *et al.*, 2002) indicates that HlyA must be translocated as an unfolded polypeptide chain. Previous evidence suggests that HlyA molecules can then proceed to the external medium by two distinct mechanisms: directly to the medium as the free protein or following accumulation in a trypsin accessible form on the cell surface (Pimenta *et al.*, 2005) with a final release step in association with outer membrane vesicles (Balsalobre *et al.*, 2006).

In Type I secretion systems, the unprocessed targeting sequence, which is necessary and sufficient for secretion, is located at the C-terminus of the protein. For HlyA this has been subjected to extensive mutational and deletion studies and shown to consist of a stretch of 50 – 60, amino acids at the extreme C-terminus of the protein (Holland *et al.*, 2005). However, the targeting signal sequence is not apparently strongly conserved in either HlyA or other Type I proteins. Nevertheless, while many individual residues can be substituted with little effect, some residues and some putative structural motifs, distributed throughout the targeting

sequence are required for full secretion activity. In particular, at least seven residues dispersed between positions -15 to -46 reduced secretion levels by 50% or more when substituted. Moreover, the effect of these mutations were additive. Although overall the signal sequences for Type 1 substrates are highly variable, some conservation at the extreme terminus is apparent when subfamilies of RTX proteins are compared. Thus, the last five C-terminal residues appear to constitute a relatively well-conserved motif in the haemolysin and leukotoxin subfamily which clearly differs, for example, from the C-terminus of the RTX proteases (Holland *et al.*, 2003). This suggests that the extreme terminal may confer specificity on the secretion process at some level.

Calcium ions, bound to each RTX repeat, are required for the haemolytic activity of RTX proteins such as HlyA (Holland *et al.*, 2005), with calcium ions seemingly triggering refolding of the RTX proteins, either while they are still bound to the cell envelope or after release to the extracellular space. It is also assumed that intracellular refolding of RTX proteins is prevented due to the low cytosolic Ca^{2+} concentration (300 nM), despite extracellular Ca^{2+} concentrations up to 10 mM (Jones *et al.*, 2002). Sanchez-Magraner *et al.* (Sanchez-Magraner *et al.*, 2007) demonstrated that in the presence of Ca^{2+}, the β-roll structure of the RTX domain of HlyA is compacted and stabilized and Chenal *et al.* (Chenal *et al.*, 2009) recently described similar effects of Ca^{2+} on the otherwise disordered RTX domain of the adenylate cyclase toxin. These results and further studies (Herlax & Bakas, 2007) appear to point towards HlyA being a conformationally flexible molecule, whose properties are commensurate with secretion in a relatively unfolded state on the one hand and the requirement for radical conformational changes for insertion into membranes on the other. For HlyA or for other bacterial proteins secreted (in a presumably unfolded form) directly to the exterior, the mechanism of final folding on the cell surface remains an intriguing puzzle, with *extracellular* calcium playing an important role.

In a previous study we identified a fusion protein, CIZ-HlyA (containing most of the LacZ protein), which blocked the Hly-translocator. This enabled us to develop a secretion competition system involving co-expression of wild type HlyA and the fusion protein to analyse the role of some important residues between positions -46 to -15 that affected secretion. Such mutations, when incorporated into the C-terminal of the fusion were shown to be recessive, suggesting that the affected amino acids are involved in an early step of translocation, probably the recognition of the translocator (Holland *et al.*, 2003). Importantly,

this system, in contrast to competition for secretion between wild type and mutant HlyA, easily distinguishes the two forms of HlyA and gives an essentially null end point unless secretion inhibition by the fusion is alleviated by a particular mutation. Here, we describe a mutant, *hlyA99* carrying four substitutions in the last 6 residues of HlyA (Figure S2). This mutation displayed a dominant phenotype, since, when present in the CIZ-HlyA fusion, secretion of the wild type HlyA is inhibited, indicating a defect in a later step in the translocation pathway. In fact, further studies described in this report indicate that the *hlyA99* mutation and another mutation, which removes the 6 C-terminal residues of HlyA (*HlyA Del6*), appear primarily to affect the folding and therefore the activity of the toxin, suggesting a novel role for the extreme C-terminal residues of HlyA.

5

Results

Isolation of the HlyA99 mutant and its initial characterization

An analysis of HlyA secretion using random hydroxylamine mutagenesis revealed a C-terminal mutation (*hlyA99*) corresponding to four substitutions (all GC to AT transitions as expected for hydroxylamine mutagenesis) in the last six residues of the protein. This resulted in a sequence change from –TLTASA to –ILIVSV (Figure 1A). This part of the normal signal sequence is particularly rich in hydroxylated amino acids and has been shown previously to be important but not essential for secretion (Holland *et al.*, 2003). Thus, deletion of the seven C-terminal residues was reported to allow secretion of HlyA protein to the medium of at least 30 % of wild type levels (Koronakis *et al.*, 1989). However, no effect of such mutations on the *activity* of HlyA was examined. The *hlyA99* mutant in fact has a phenotype of low haemolytic activity on blood agar plates at 37°C, giving colonies with small haloes (data not shown). Moreover, in liquid LB medium at 37°C, levels of haemolytic activity were detected in the culture supernatant at approximately 10 % of that of the wild type as shown in Figure 1B (see also Table 1).

The *hlyA99* mutant protein is secreted relatively efficiently but haemolytic activity is reduced

In order to measure any secretion defect associated with the *hlyA99* mutation, the amount of HlyA protein in the supernatant of both mutant and wild type cultures grown at 37°C in LB medium, was analysed by Western blotting with anti-HlyA antibodies (Figure 1C) and by SDS-PAGE with Coomassie-Blue staining (Figure 1D). Surprisingly, densitometric analysis (see Methods) indicated that the amount of protein secreted to the medium by the mutant was as high as 40-50% of that obtained with wild type haemolysin. Figure 1D also indicates that the antibody detects some lower molecular weight bands in the culture supernatant however, these are unlikely to be HlyA degradation products as they are also detected in the supernatant from cells not expressing HlyBD. The same relatively high level of secretion was obtained (data not shown) when the C-terminal 217 amino acids of HlyA (23kDa) carrying the *hlyA99* mutation, were expressed from the *lac* promoter of the M13mp18 phage (see Methods). The combination of all these results indicated that the mutant toxin was primarily defective in haemolytic activity.

To completely eliminate the possibility of other upstream mutations in *hlyA* being responsible for these properties, a 3' fragment of the mutant *hlyA99* gene, corresponding to the C-terminal 27 amino acids, was exchanged *in vitro* for the 3' end of an otherwise wild type *hlyA* (see Methods) The reconstituted gene was then co-expressed in cells with *hlyBD* and again the secreted protein was found to have reduced activity. Thus, the level of secretion of the mutant protein was approximately 40% of wild type levels but the haemolytic activity corresponded to approximately 12% of the wild type level in the culture supernatant, giving an apparent reduction in specific activity of at least 2.5 fold (see Table 1, Panel A).

The *hlyA99* mutant is dominant in competition experiments with wild type haemolysin A

We showed previously that co-expression of wild type HlyA and a large fusion protein composed of virtually the whole β-galactosidase protein fused upstream of the C-terminal 81kDa of HlyA (CIZ-HlyA) in cells also expressing *hlyCBD* (Kenny *et al.*, 1994), leads to inhibition of wild type HlyA secretion. The CIZ-HlyA fusion protein itself (encoded by pLG811) is secreted to the medium but only at very low levels while large amounts of the fusion accumulate in the cell envelope in a *hlyBD* dependent manner, presumably blocking the translocator. Importantly, we also showed that mutations located between residues -15 and -46 with respect to the HlyA C-terminus, introduced into the CIZ-HlyA signal sequence, alleviated the inhibition of secretion of the co-expressed HlyA. These mutations could therefore be considered recessive.

In order to test the dominance or recessitivity of *hlyA99 (*substitution ILVSV at the C-terminus*)* in such a competition experiment, the HlyA99 mutation was introduced into the CIZ-HlyA secretion signal by *in vitro* recombination (see Methods). The CIZ-HlyA fusion itself has no haemolytic activity (data not shown), presumably because it lacks most of the N-terminal hydrophobic region of HlyA. In competition experiments therefore, only the haemolytic activity of the co-expressed wild type HlyA is detected in the culture medium. In cells expressing the CIZ-HlyA fusion, together with *hlyCBD* and wild type *hlyA*, the colony halo size on blood agar was small or undetectable but increased as expected when mutations reducing secretion of HlyA were introduced into the fusion (data not shown).However, when the *hlyA99* mutant secretion signal was introduced into the CIZ-HlyA molecule no increase in halo size was observed. This result is in clear contrast to the recessive secretion signal mutations analysed previously, indicating that the HlyA mutation is dominant.

The competitive effect of CIZ-HlyA99 was then analysed in liquid culture by measuring the levels of haemolytic activity of co-expressed HlyA toxin released into the culture supernatant. Samples of supernatant and total cell proteins were taken at intervals from an exponentially growing culture and analysed for activity and by SDS-PAGE. Figure 2(A) shows that on the basis of activity measurements, CIZ-HlyA99 inhibited the secretion of co-expressed HlyA as efficiently as a fusion carrying the wild type signal. As expected, the presence of a nonsense mutation (Δ55), leading to the deletion of the 55 C-terminal amino acids of the CIZ-HlyA fusion, in contrast to *hlyA99* also alleviated this inhibition by CIZ-HlyA. Moreover, another control, a point substitution at position -35 (Phe to Pro) which reduces secretion of HlyA when present in the CIZ-HlyA fusion (Chervaux & Holland, 1996), also alleviated the inhibition of HlyA secretion, as measured by haemolytic activity.

Data shown in Figure 2(B) confirmed that CIZ-HlyA99 inhibited secretion of the co-expressed HlyA when immunoblotting was used to reveal the amount of each protein present in the culture supernatants. Thus, expression of CIZ-HlyA reduced the amount of HlyA protein found in the supernatant (Figure 2(B) lanes 1 and 5). In contrast, as expected when mutation F989P (position -35) or the nonsense mutation (Δ55) are present in CIZ-HlyA, the competitive effect was alleviated and significantly more HlyA protein was found in the supernatant (Figure 2(B), lanes 2 and 4). However, with *hlyA99* present in the CIZ-HlyA secretion signal, the amount of HlyA protein secreted and detected in the supernatant remained very low, while the amount of CIZ-HlyA itself present in the supernatants was reduced as expected according to the particular secretion signal mutation introduced.

The data in Figure 2 clearly show that the *hlyA99* mutation when present in the CIZ-HlyA fusion is dominant, since it specifically inhibited secretion of co-expressed wild type HlyA. Consequently, whilst the previously analysed mutations appeared to affect an early step in translocation, probably the initial recognition step, this *hlyA* mutation (Figure S2), must affect a later step in the transport pathway, resulting in secreted protein with reduced activity.

Localisation of cell associated wild type HlyA and HlyA99 probed by trypsin accessibility

Previous studies have indicated that production of *hlyA* mRNA is blocked when HlyA is not secreted, for example, in strains not expressing *hlyBD* (MB and IBH, unpublished data). On the other hand significant amounts of secreted HlyA remain associated with the cell

envelope, accessible to extracellular trypsin, in strains expressing *hlyBD* (Pimenta *et al.*, 2005). When wild type HlyA and HlyA99 were compared in the presence of HlyBD, high levels of the wild type protein were found to be cell associated, with apparently even higher levels detected in the case of the mutant HlyA99 protein (Figure 3). Treatment of the cells with trypsin, the HlyA99 protein, like wild type HlyA, as also shown in Figure 3 was completely degraded by addition of trypsin to cells, under conditions where the protease does not penetrate the cell envelope ((Halegoua & Inouye, 1979) and Methods). In both wild type and mutant, therefore, all cell associated HlyA molecules have been secreted to the surface, accessible to trypsin and apparently neither WT nor mutant HlyA accumulates in the cytosplasm. The control experiments shown in Figure S3 demonstrate that trypsin treatment has no detectable effect on total protein profiles from treated cells nor the low levels of cytoplasmic HlyA present in cells lacking HlyBD, indicating that trypsin does not penetrate into cells under these conditions. The results shown in Figure 3 also suggest that the true secretion levels of HlyA99 were underestimated, with relatively more protein accumulating at the cell surface. Thus, these results indicated that the secretion of the HlyA99 mutant was relatively unimpaired. However, no conclusions about the kinetics of translocation can be drawn from these experiments.

Kinetics of translocation of wild type HlyA and HlyA99

In order to compare the kinetics of translocation of wild type HlyA and HlyA99 to the medium, cells expressing *hlyBD* and either mutant or wild type *hlyA*, were grown in M63 minimal medium at 37°C, pulse labelled with [^{35}S]-methionine and chased with cold methionine (see Methods). As shown in Figure 4, HlyA99 was secreted to the medium at levels about 40% of that of the wild type toxin but the time course of secretion was similar to that of the wild type HlyA. In summary, these results indicated that the translocation of HlyA99 was not defective *per se* although its ability to fold and leave the cell surface may be perturbed.

The *hlyA99* mutation also affects the specific activity of β-lactamase in the chimeric βlac-23kDaHlyA protein

The HlyA99 mutation markedly affected the haemolytic activity of HlyA (Table 1). This is particularly evident in the case of HlyA Del6, where the mutation has relatively little

effect on the levels of HlyA toxin secreted to the medium (see below). However, it has been generally assumed that the haemolytic domain of HlyA is delimited by the presence of the glycine-rich repeats located between residues 730-840. Consequently, it was surprising that mutations at the extreme C-terminus of HlyA, within the approximately 50 residues thought to constitute the secretion signal, appeared to influence the activity of haemolysin molecules. We therefore considered the possibility that the secretion signal region has an additional function and that the effect of the mutations might indicate that the C-terminal region also plays an important role in the correct folding of HlyA molecules.

In an attempt to test the idea that the C-terminus may be involved in folding of the protein we analysed the effect of the *hlyA99* mutation on *secretion* and *activity* of a chimeric protein composed of *E.coli* TEM β-lactamase and a C-terminal part (23kDa) of HlyA, which lacks the majority of the RTX-repeats and the large N-terminal toxin domain. This fusion protein is only secreted in the presence of the translocator proteins HlyBD. Moreover, the secreted form of this fusion appeared to have the same specific activity as normal β-lactamase (Holland *et al.*, 2003). We introduced the cluster of 4 substitutions constituting the *hlyA99* mutation into the signal sequence of the β-lactamase-HlyA23kDa fusion (βlac-23kDaHlyA) (see Methods). Secretion of the chimeric proteins, carrying either the wild type or the mutant secretion signal, was followed both by measurement of β-lactamase activity in the medium and by quantification of the amount of the corresponding protein in culture supernatants. Typical results are shown in Figure 5 where panels (a) and (b) show Coomassie-Blue stained and Western blot analyses of supernatant proteins, respectively. In these experiments, cultures were grown to late exponential phase for maximal levels of secretion. The amount of βlac-23kDaHlyA99 detected was usually between 30 to 50% compared with the hybrid protein carrying a wild type secretion signal. Both staining and immunodetection gave similar results. This level of secretion is close to the level of secretion of the HlyA toxin itself carrying the same mutation (see Figure 1, panels (C) and (D)).

However, when the β-lactamase activity in culture supernatants was measured, an eight fold reduction in activity levels of the chimeric protein carrying the *hlyA99* mutation, relative to the wild type, was obtained, equivalent to a reduction in specific activity of 2.5 fold (40%). When the stability of the βlac-23kDaHlyA99 molecules, following secretion to the medium, was measured by its penicillinase activity, over two hours this remained essentially identical to that of the fusion with a wild type secretion signal (data not shown). These results

therefore demonstrated that the *hlyA99* mutation has a similar debilitating effect on the specific activity of the attached β-lactamase as found for the HlyA toxin itself. This result also clearly indicated that the *hlyA99* mutation does not simply affect the haemolytic activity *per se*, i.e. because the C-terminal is directly required for toxin activity. Rather this suggested that the mutation affects in some way the correct folding of molecules, for example, with the C-terminal of HlyA normally acting as a folding nucleation centre as the polypeptide emerges from the HlyBD-TolC translocator.

Deletion of the C-terminal 6-residues mimics the effect of the *hlyA99* mutation

To examine further the role of the amino acids at the extreme C-terminus of HlyA we simply deleted the C-terminal 6-residues, to generate HlyA Del6. The properties of this mutant were very similar to the effect of the *hlyA99* mutation. As shown in Table 1 removal of the 6 C-terminal residues had a modest effect on the level of secretion of the HlyA protein to the medium - approximately 70% of the wild type level. However, as found with *hlyA99*, a major effect of the deletion of the terminal 6-residues was on the haemolytic activity in the culture medium, with a reduction in the apparent specific activity of close to 3-fold. Therefore, with both mutants, *hlyA99* and *hlyAdel6,* the results indicated that the extreme C-terminus was in some way essential for activity.

The HlyA99 and HlyA Del6 mutations inhibit re-naturation of HlyA to the haemolytic form following denaturation *in vitro*

Haemolysin inactivated *in vitro* by de-naturation with urea or guanidine chloride (GnCl) can be re-natured and therefore reactivated to the haemolytic form by rapid dilution. Moreover, we have shown that HlyA molecules with reduced activity due to mutations in HlyD can be restored to full activity following de-naturation and then re-naturation (Pimenta *et al.*, 2005). Wild type haemolysin, HlyA99 and HlyA Del6 in culture supernatants were therefore concentrated by precipitation by ammonium sulphate, denatured by resuspending in 6 M GnCl and renatured by dilution into assay buffer (see Methods) to measure haemolytic activity.

As shown in Table 1 (Panel B), wild type haemolysin regained slightly greater than 100% activity after renaturation, a result not unexpected due to the tendency of even wild type HlyA to aggregate and lose activity in the growth medium (Goni & Ostolaza, 1998). Both mutant proteins, HlyA99 and HlyA Del6, showed a slight increase in activity after

renaturation; however, their calculated specific activities remained at only 40% relative to the wild type protein. Therefore, *in vitro* these mutant proteins appear to display essentially the same reduced ability to re-fold to the active form as observed when they are initially secreted to the medium. This result rules out the possibility that initial misfolding is simply a consequence of perturbations *occurring during* translocation onto the surface or prior to final release into the medium.

Protein folding of wild type pro-HlyA and pro-HlyA Del6 monitored by fluorescence spectroscopy

To validate further our data that the extreme C-terminus of HlyA plays a specific role in protein folding, we chose fluorescence spectroscopy to detect structural changes within the protein. For technical reasons we used the pro-form of HlyA (see Methods), which without acylation is not able to lyse red blood cells (Holland *et al.*, 2003). Nevertheless, the non-acylated pro-HlyA was shown previously to bind and insert into liposome membranes as efficiently as the acylated form (Hyland *et al.*, 2001). Together these results indicated that pro-HlyA and acylated HlyA molecules fold similarly. Thus, in light of the technical problems encountered during the purification of HlyA, we chose pre-HyA as a suitable model protein to follow-up our initial hypothesis that the C-terminus of HlyA may provide a folding as well as a targeting function.

When we compared the normalized tryptophan fluorescence of both the wild type pro-HlyA and pro-HlyA Del6 proteins at high concentrations of urea (2 - 8 M), the results obtained were very similar (Fig.6). In both cases the observed constant decrease in fluorescence paralleling the increase in urea can be assigned to the unfolding of the HlyA protein. In support of this conclusion, lysis of red blood cells by HlyA treated with > 3 M urea resulted in the complete loss of lytic activity (data not shown). In contrast to the above results, at low concentrations of urea (in the range of 0.5 - 1 M) the wild type protein and the HlyA mutant lacking the 6 C-terminal amino acid residues, differed with respect to the effect on tryptophan fluorescence and therefore the structure of the pro-HlyA molecule. Thus, under these conditions the mutant protein appeared relatively more compact, more resistant to the significant conformational changes undergone by the wild type protein. We therefore conclude that the fluorescence spectroscopy data supports the hypothesis that the extreme C-terminus of the HlyA molecule influences the structure/folding properties of HlyA and nicely

complements our whole cell experiments which initially led us to the assumption of a dual role for the C-terminus of HlyA.

13

Discussion

Secretion of proteins carrying a C-terminal secretion signal via the Type I pathway, are in all probability translocated in an unfolded form across the cell envelope (see Discussion in (Pimenta *et al.*, 2005)). Consistent with this idea, different lines of evidence indicate that Type I polypeptides do actually undergo some folding on the cell surface. First, previous studies have implicated lipopolysaccharide (LPS) as a requirement for formation of haemolytically active HlyA (Bauer & Welch, 1997). Second, mutations in either TolC (Vakharia *et al.*, 2001) or HlyD (Pimenta *et al.*, 2005) also result in secreted HlyA with reduced haemolytic activity. This seems likely to result from perturbed translocation through the translocator, conceivably leading to uncoordinated misfolding as the protein emerges on the surface, since *in vitro* denaturation and renaturation of HlyA secreted from these mutants largely restored haemolytic activity and therefore normal folding. Strikingly, such a restoration or rescue of the normal folding pathway was not obtained with the HlyA mutants studied here. Finally, an important contributor to folding of HlyA on the surface is most likely the binding of calcium ions to the RTX repeats, as first suggested by (Baumann *et al.*, 1993) based on the crystal structure of the Type I protein alkaline protease from *P. aeruginosa*. In reality, the extremely low levels of free Ca^{2+} present in the *E. coli* cytoplasm (less than one μM), which is equivalent to around 100 ions (Jones *et al.*, 2002), most probably precludes or severely limits any folding in the cytoplasm based on this mechanism.

Residues close to the C-terminus of HlyA were previously shown to be important for secretion of the toxin to the medium, since progressive deletion of from 7 up to 27 residues from the C-terminus, resulted in secretion of HlyA to the medium at levels of 30% to less than 0.5% respectively, compared to the wild type toxin (Holland *et al.*, 2003). The *hlyA99* mutation involves *4* substitutions in the last 6 C-terminal residues including the terminal Ala to Val (see Figure 1), with the most significant changes probably being substitutions of small hydroxylated Thr residues (position -4 and -6) for larger Ile residues. In unpublished studies we showed that the terminal Ala could be replaced by Pro or Gln without any detectable effect on secretion. However, compatible with some specific function, the immediate upstream region is relatively well conserved (L-Hx-Hx-Hx-A, where Hx is hydroxylated or Ala) in HlyA-like RTX toxins. Importantly, previous studies showed that Type I signal sequence mutations, mostly reducing secretion levels to well below 50%, mapping to positions -15 to -46, with respect to the C-terminus, were recessive, i.e. they alleviated

competitive inhibition of secretion of wild type HlyA by the co-expressed CIZ-HlyA fusion. Thus, such mutations apparently affected an early step in secretion of HlyA, probably recognition of the translocator (Holland *et al.*, 2003). In contrast, the *hlyA99* mutation when present in CIZ-HlyA was shown to be dominant in competition experiments, indicating that the mutation primarily affects a later step - *after* initiation of translocation of HlyA (Figure 2).

The amount of HlyA99 protein detected as secreted to the medium was reduced, compared to the wild type with final levels varying from 30-50% in different experiments. We note, however, as we show in this study (see also (Pimenta *et al.*, 2005)) that secretion efficiency can be routinely underestimated since significant amounts of wild type HlyA are translocated to the outer cell surface but not released. This is in line with recent findings that in addition to direct extrusion to the medium HlyA can subsequently be released from the surface in the form of outer membrane vesicles (Balsalobre *et al.*, 2006). Interestingly, even larger amounts were apparently found on the surface with the HlyA99 mutant compared to the wild type (Figure 5A), consistent with the altered folding of the mutant protein.

Further evidence that translocation is little affected by the HlyA99 mutation was shown by pulse chase experiments which showed that the time course for translocation of the mutant is similar to that of wild type HlyA. Importantly, the HlyA Del6 deletion mutation, which like *hlyA99* has a major effect on the activity of HlyA, showed only a minimal secretion defect with close to 70% of wild type levels in the medium. We conclude therefore that the effect of these C-terminal mutations is primarily to reduce the activity of secreted molecules rather than their translocation efficiency.

Three possible explanations for the reduced haemolytic activity of the HlyA mutants can be envisaged: (i) if the extreme C-terminus of HlyA is specifically required for modification by HlyC; (ii) if the extreme C-terminus is directly implicated in lysis of erythrocytes; (iii) if the C-terminus has a specific role in re-folding of secreted molecules. Previous studies (Stanley *et al.*, 1994) have shown that the two specific sites for HlyC dependent acylation are located 288 and 414 residues, respectively, upstream of the C-terminal secretion signal. An involvement of the C-terminal in the acylation reaction seems extremely unlikely since HlyA lacking the N-terminal part containing the proposed amphipathic helices or deletion of the C-terminal part, which contains the secretion signal, were still acylated normally *in vitro* (Stanley *et al.*, 1994). Despite many detailed genetic and

biochemical studies of the properties of HlyA and its interaction with membranes, no evidence has been presented in the literature to indicate that the C-terminal of HlyA is directly involved in haemolytic activity. In contrast, we suggest that several findings in this study point to a role for the extreme C-terminal in protein folding. Thus, the cis-dominant effect of the *hlyA99* mutation on the *activity* of β-lactamase fused to the C-terminal of HlyA is most easily explained in this way. Moreover, the HlyA mutant proteins analysed in this study were essentially refractory to reactivation following denaturation in urea, consistent with inherently defective molecules, which cannot refold correctly *in vitro*. This is in complete contrast to the successful restoration of activity to inactive HlyA secreted from HlyD or TolC mutants (Pimenta *et al.*, 2005; Vakharia *et al.*, 2001). This result, combined with the relatively normal kinetics of translocation of HlyA99, appears to rule out effects on folding of these HlyA mutants incurred through perturbed movement through the translocator.

Importantly, tryptophan fluorescence spectroscopy studies to monitor protein folding in the presence of urea clearly revealed significant differences between wild type pro-HlyA and the pro-HlyA Del6 mutants at low concentrations of urea (Figure 6). The wild type molecule in fact appeared more susceptible to structural changes under these conditions suggesting that the mutant may have a relatively more stable or compact conformation – perhaps less compatible with insertion of the HlyA molecule into membranes. The reduced activity of the deletion mutant may be particularly instructive since this implies a positive, active role in the normal re-folding for the C-terminal rather than a disruptive effect on folding created by the multiple mutations in HlyA99. The results of this experiment nevertheless point towards a crucial involvement of the extreme C-terminus of HlyA in the folding of the toxin, acting in concert with other folding mechanisms, as the polypeptide emerges on the cell surface from the translocator.

Interestingly, Chenal *et al*. (Chenal *et al.*, 2009; Sotomayor Perez *et al.*) recently showed that mM concentrations of Ca^{2+} ions *in vitro* promote the compaction of the normally disordered RTX region of a Type I protein, together with increased formation of stable secondary and tertiary structures. This is consistent with the findings of Pimenta *et al*. (Pimenta *et al.*, 2005) who showed that the amount of HlyA secreted and the activity of HlyA increased in line with the extracellular Ca^{2+} concentration over a mM range. Chenal *et al*. (2009) indeed proposed that Ca^{2+} dependent folding of the RTX region of emerging HlyA molecules could contribute a nucleus for folding of the more proximal regions of the protein.

Intriguingly, the geometry of the HlyA molecule, with conceivably at least two distinct types of folding pathway triggers, positioned towards the C-terminal of the protein, the RTX Ca^{2+} repeats and the C- terminal end itself, suggests that the C-terminus may lead the way out of the translocator. Finally, we conclude that the role of the 50 – 60 amino acid HlyA secretion signal region may not be limited to targetting HlyA to the translocator but may also be involved in promoting the correct folding of the toxin.

17

Methods

Bacterial strains and growth conditions

The *E. coli* strain NM522 (Δ(*lac-proAB*), *thi-1*, *supE*, *hsdR17* (r_k^-,m_k^-), [F', *proAB, lacIq,* ZΔM15]) was used for expression and secretion of HlyA and βlac-23kDaHlyA. Cells were grown in Luria broth (LB) at 37°C or at 30°C for competition experiments, in order to limit expression from the thermo-inducible λ promoter (see below). 10 mM $CaCl_2$ was added to LB when cultures were to be assayed for HlyA toxin activity. For translocation kinetics, SE 5000 expressing *hlyCA* (pLG813) and *hlyBD* (pLG814) was grown in M63 minimal medium plus 1mM $CaCl_2$ at 37°C. *E. coli* BL21(DE3) (*ompT gal dcm lon hsd*SB(rB- mB-) λ(DE3 [*lacI lac*UV5-T7 gene 1 *ind1 sam7 nin5*])) was used for production of wild type pro-HlyA (pSU2726) and pro-HlyA Del6 (pSU2726 del6) as inclusion bodies. Cultures were grown at 37°C in 2xYT broth and cells were harvested 3 h after induction. Strain CJ236 (*dut, ung, thi-l*, *relA*:pCJ105(Cm^r)) was used in order to produce uracil-rich single strand phage DNA for oligonucleotide mutagenesis. This strain was grown as indicated by the manufacturer (Biorad). When required, antibiotics were supplied at a final concentration of: 25 µg/ml kanamycin, 25 µg/ml chloramphenicol, 100 µg/ml ampicillin, 10 µg/ml tetracycline. 0.5 mM IPTG was added to the culture to induce expression of hybrid proteins under the control of *lac* promoters.

Deletion of the terminal 18 nucleotides of *hlyA* to generate *hlyAdel6*

The *hlyAdel6* mutation was constructed using PCR with pLG813 as template DNA and the following oligonucleotides: H3, 5'-GAGCTCAAATGCCAACAATAACC-3', hybridizing to the 5' end of *hlyA*; and KR1, 5'-AAATTAATAAA**TTA**TATTGAGTTCCG-3', hybridizing to *hlyA* codons 1015 to 1018 (underlined) and to 3' non-coding sequence (stop codon is depicted in bold) thereby deleting amino acid codons 1019 to 1024 (inclusive) but leaving the termination codon intact. Note that the four 5' nucleotides of KR1 correspond to half of a blunt *SwaI* restriction site. The 3.1 kb PCR product was digested with *HindIII* and the 2.4 kb fragment cloned into *HindIII/SwaI* digested pLG813. The *hlyAdel6* mutation was confirmed by sequencing. HlyA Del6 was constructed using ligase chain reaction and the following oligonucleotides: HlyAdelstop_for 5'-TATGGACGGAACTCAATA**TAA**TTGACAG-3', and HlyAdelstop_rev 5'-TGCTGATGCTGTCAA**TTA**TATTGAGTTC-3', which introduce a stop codon (bold) in pSU2726. Introduction of the stop codon was confirmed by sequencing.

Transfer of signal mutations into genes encoding βlac-23kDaHlyA and CIZ-HlyA

The point mutations F989P and (Δ55) in the HlyA secretion signal were transferred from plasmid pLG816 containing these mutations into pLG811, carrying the CIZ-HlyA fusion (LacZ fused N-terminal to the 81kDa C-terminal domain of HlyA), by *in vitro* recombination using the *Bgl*II and *Nco*I unique restriction sites present in both plasmids and localized at -86 and -850 bp from the 3' end of *hlyA*, respectively. In the case of the *hlyA99* mutation, the *Sal*I and *Nco*I sites were used to transfer the DNA fragment from pLG813-*hlyA99* into pLG811. Transfer of *hlyA99* into the gene encoding βlac-23kDaHlyA was achieved by ligation of the 0.25 kb *Bgl*II/*Sma*I fragment of pLG813 carrying the mutation into pPSG51 cut by *Bgl*II and *Hpa*I. The authenticity of the *in vitro* recombinant was confirmed by DNA sequencing.

Denaturation-renaturation of HlyA activity

These were carried out as described previously (Pimenta *et al.*, 2005).

Standard haemolytic assay and activity of HlyA determined by the titration method

These were carried out as described previously (Pimenta *et al.*, 2005). In the titration method, one haemolytic unit (HU_{50}) is defined as the amount of HlyA necessary to produce 50% lysis of the erythrocytes. All results are expressed as averages of duplicate samples and are given per ml of culture supernatant.

Measurement of β-lactamase activity in culture supernatants

This was performed as described by (Chervaux *et al.*, 1995). Units of β-lactamase activity were proportional to the amount of fusion protein over at least a 20-fold range (0.05 – 1 μg).

Preparation of protein samples from cells and supernatants

Cells were recovered from cultures by centrifugation at 12000 x g for 10 min and resuspended in SDS sample buffer. Protein containing supernatants were obtained by two further successive centrifugations at 27000 x g each for 15 min and protein was precipitated by addition of TCA (final concentration 10% (w/v). After 1 h on ice, proteins were pelleted by 30 min centrifugation at 16000 x g and resuspended in SDS sample buffer. Each sample was boiled for 10 min before loading on the gel.

Purification of wild type and HlyAdel6

Pro-HlyA (lacking the internal acylation sites) and wild type HlyA were purified from inclusion bodies (IBs). IBs were washed three times with buffer A (50 mM Tris-Cl, 1 mM DTT, 1 mM EDTA, 0.1 % NaN_3, 0.5 % Triton X-100, pH 7.0) and once with buffer B (50 mM Tris-Cl, 1 mM DTT, 0.1 % NaN_3, pH 7.0). After every washing step the sample was centrifuged at 30000 x g, 30 min, 4°C. IBs were finally dissolved in 50 mM Tris-Cl, 8 M urea, pH 7.0. Purification was achieved by anion exchange chromatography (DEAE fast flow sepharose, GE Healthcare) with 50 mM Tris-Cl, 8 M urea, 0/300 mM NaCl, pH 7.0 and size exclusion chromatography (50 mM Tris-Cl, 8 M urea, pH 7.0. Subsequent cation exchange chromatography (SP sepharose, GE HEalthcare) and another SEC step resulted in pro-HlyA purified to homogeneity, which was suitable for fluorescence spectroscopy studies (suppl. Fig. 3). During an early attempt to purify wild type, acylated HlyA, we encountered problems with the hydrophobic molecule sticking to the anion exchange column resin. Furthermore, the purified protein showed a strong tendency to form high molecular weight aggregates. We considered that this problem might be due to the acylation of pro-HlyA. Therefore, we decided to purify proteins (wild type HlyA and HlyA Del6) for tryptophan fluorescence measurements, following expression in a strain lacking *hlyC* (see Methods) that normally activates HlyA via acylation of the two lysine residues. This procedure enabled us to purify successfully the two proteins without visible contamination, which is important for the fluorescence spectroscopy (Figure S3).

Trypsin treatment

E. coli NM522 carrying pPSG51 (wild type or *hlyA*99 signal sequence) and pLG814 or pLG339 (as a vector control minus *hlyBD*) were grown at 37°C in LB plus antibiotics as described above. βlac-23KHlyA synthesis was induced by 0.5 m IPTG at A_{600} = 0.5 and growth was followed to A_{600} = 4. Supernatants were separated from cells by centrifugation at 4°C (20 min at 3000 x g in a Sorvall SA600 rotor). 1 ml aliquot of each supernatant was kept as a trypsin minus control and trypsin (Bovine Pancreas 100 μg/ml in 100 mM Tris pH 8) was added to the remaining supernatant, final concentration 10 μg/ml. A 1 ml aliquot was immediately taken and mixed with 30 μg/ml of trypsin inhibitor (Sigma). Samples were taken at intervals and proteins precipitated by 10% TCA; 0.2 A_{600} units were loaded for SDS PAGE (12% acrylamide), before transfer to nitrocellulose filters. Proteins were then revealed using anti-β-lactamase or anti-haemolysin antibodies.

For treatment of whole cells, bacteria (3 OD units, A_{600}) were suspended in $MgCl_2$ (10 mM) Tris-HCl (10 mM pH 7.2) plus 50 μg/ml trypsin and incubated at 4°C for 30 min; digestion

was stopped by PMSF (5 mM) and excess trypsin inhibitor. Under these conditions, trypsin does not penetrate to the periplasm (Halegoua & Inouye, 1979).

Kinetic analysis of HlyA translocation

E. coli SE5000 (pLG814; pLG813 encoding either *hlyA* or *hlyA99*) was grown in M63 medium (1 mM $CaCl_2$) to an A_{600} = 0.5; 7 ml samples were labelled with [^{35}S-] methionine (20 μCi/ml) for 30s and incorporation stopped by addition of cold methionine (0.4 mg/ml); 1 ml samples were taken at different chase times and mixed with 0.9 ml ice cold phosphate buffer (10 mM, pH 7.5 plus 50 μg/ml BSA as carrier, 3 mM sodium-azide and 50 μM CCCP). Samples were centrifuged x 2 to give cell free supernatants; protein was precipitated with 10% TCA (w/v) and precipitates were suspended in 20 μl sample buffer and analyzed by SDS-PAGE (12% acrylamide) and by fluorography.

Tryptophan fluorescence spectroscopy

Protein samples (wild type pro-HlyA and pro-HlyA Del6) were prepared by dilution from 50 mM Tris-Cl, 8 M urea, pH 7.0 into assay buffer containing 50 mM Tris-Cl, 20 mM Ca^{2+}, 0.5-8 M urea, pH 7.0. Protein samples were incubated between 24 and 120 h at 4°C in assay buffer to reach equilibrium. Protein fluorescence was measured with a Fluorolog 3 instrument (HoribaJobinYvon) at 25°C. Exitation wavelength was 295 nm and slits were set to 2 nm. Emission was recorded between 310-500 nm and slits were set to 5 nm. For subsequent analysis the change in normalized fluorescence intensity at 329 nm was followed.

Acknowledgements

We would like to thank CNRS, Université de Paris XI, Association pour la Recherche sur le Cancer, La Ligue, AFLM and Ministère de la Recherche et de l'Espace and Rhone-Merieux (Contract 92T0345), for supporting this work. C. Chervaux is also pleased to acknowledge support of the Ministère de la Recherche et de l'Espace and La Ligue and Fondation Singer-Polignac, K. Racher is pleased to acknowledge CIES for a Chateaubriand Fellowship. Anti-βla antibodies were kindly provided by Gérard Leblon (Orsay). We are also indebted to F. M. Goñi and H. Ostolaza for providing us with the pSU2726 and pSU2781 plasmids and Mrs. M. Blum for technical assistance.

Table Legends

Table 1: Comparison of wild type HlyA with variants carrying the *hlyA99* or *hlyAdel6* mutation: effects on secretion and activity levels (A) Comparison of secretion levels and haemolytic activity from culture supernatants of HlyA variants relative to wild type toxin. Values given are averages of three independent experiments. (B) Haemolytic activity (per unit HlyA) before and after denaturation/renaturation of HlyA variants. Values given are averages of two independent experiments.

Table 2: A βlac-HlyA fusion carrying the HlyA secretion signal mutation *hlyA99* has reduced specific activity. β-lactamase activity was calculated for culture supernatants containing the β-lactamase 23kDaHlyA fusion protein (βlac-23kDaHlyA) carrying the wild type secretion signal or the *hlyA99* mutant secretion signal, expressed from pLG813 and pPSG51 respectively. In order to compare apparent specific activities, the amount of secreted protein was determined by densitometry following SDS-PAGE analysis (see Figure 5).

Figure Legends

Figure 1: (A): C-terminal sequence of the mutant HlyA99 compared with the wild type sequence. Double arrows indicate amino acid changes. (B): Haemolytic assay for the *hlyA99* mutant. *E. coli* NM522 containing the low copy number plasmids pLG814(*hlyBD*) and pLG813(*hlyCA*) carrying wild type or mutant signal sequences. Panels (C) and (D) show respectively Western blot analysis and Coomassie-Blue staining of supernatant proteins from cultures (pLG814, *hlyBD*) also expressing *hlyC* and *hlyA* wild type (lanes 1 and 4) or the *hlyA99* mutant (lanes 2 and 6) from pLG813; supernatants from cells lacking *hlyBD* are shown in lanes 3 and 5. Molecular weight markers are indicated on the left and the position of HlyA is indicated on the right.

Figure 2: Competition for secretion between wild type HlyA toxin (pLG813) and CIZ-HlyA (pLG811) containing either a wild type or a mutant secretion signal. All strains also express *hlyBD* from pLG814. Panel (A) shows the growth of SE5000 *E. coli* in LB at 30°C co-expressing wild type HlyA and the 200kDa fusion protein CIZ-HlyA, containing wild type (□) or mutant signals: F989-P (◊), *hlyA99* (o), and Δ55 (Δ). Dotted lines indicate the haemolytic activity (corresponding to the amount of HlyA secreted in culture supernatant as described in Methods). Panel (B) lanes 1 to 5 show Western blot analysis of culture supernatants precipitated with TCA after harvesting at a time around the maximum for secretion in this medium ($A_{600} \approx 4$). Each lane was loaded with 1 A_{600} equivalent. Lane 1, samples from the culture co-expressing wild type HlyA and CIZ-HlyA; lane 2, CIZ-HlyA (F989-P); lane 3, CIZ-HlyA99; lane 4, CIZ-HlyAΔ55. Lane 5 corresponds to a sample from strain SE5000, which expresses wild type toxin but not the CIZ-HlyA fusion.

Figure 3: Substantial amounts of wild type HlyA and HlyA99 produced in the presence of *hlyBD* are secreted to the surface and are accessible to exogenous trypsin. Strain SE5000 expressing *hlyBD* (pLG814) and *hlyA* or *hlyA99* (from pLG813) was grown in LB medium at 37°C. Total cells were harvested at $A_{600} = 6$ and the supernatant, containing Hly secreted to the medium, was removed by centrifugation and washing. The cells, resuspended in 10 mM Tris-HCL + 10 mM MgCl2 (see Methods), were either left untreated or treated with trypsin (50 μg/ml) as described in Methods. Total cell protein of cells of each strain (OD equivalents) was then analyzed by SDS-PAGE, followed by western blotting against anti-HlyA antibody.

Figure 4: Kinetics of translocation of wild type HlyA and HlyA99. Strain SE5000 (pLG813, pLG814) was grown at 37°C in M63 (+ 1 mM $CaCl_2$) to A_{600} = 0.5 and pulse labelled with [^{35}S-] methionine for 30s, chased in cold medium and samples were analyzed by SDS-PAGE and fluorography; X-ray films were scanned to quantify gel bands in arbitrary units (A.U.). SE5000 (pLG813) expressed either wild-type *hlyA* or *hlyA99*.

Figure 5: Analysis of the secretion efficiency of the βlac-23kDaHlyA fusion protein (encoded by (pPSG51) carrying the *hlyA99* mutation. Panel (A) Coomassie-Blue stained gel. Lanes 1 to 4 correspond to different A_{600} equivalents of samples containing the secreted βlac-23kDaHlyA with a wild type secretion signal. Lane 5 corresponds to 1 A_{600} equivalent of supernatant from a culture expressing βlac-23kDaHlyA99; lane 6, 1 A_{600} supernatant equivalent from a culture expressing wild type βlac-23kDaHlyA in a strain lacking *hlyBD.* Panel (B): anti-HlyA antibody for western blot analysis of the same supernatant samples as in Panel A, lanes 1-4 with the A_{600} loading equivalent indicated. Panel (C): Measurement of supernatant levels of secretion of βlac-23kDaHlyA, wild type secretion signal or *hlyA99*. As in panel (A) and (B), supernatants from NM522 cultures expressing HlyBD and βlac-23kDaHlyA wild type secretion signal or *hlyA99* were analysed by SDS-PAGE and Coomassie-Blue staining. In order to compare amounts of secreted proteins in each culture supernatant, serial dilutions were loaded on the same gel. Lane 1, 2 and 3 are respectively 3, 2 and 1 A_{600} equivalents of wild type culture supernatant and lanes 4 and 5 represent respectively 4 and 2 A_{600} equivalents of the culture expressing the βlac-23kDaHlyA99 fusion. The position of the βlac-23kDaHlyA protein is indicated on the right.

Figure 6: Protein fluorescence spectroscopy of wild type pro-HlyA (o) and pro-HlyA Del6 (•). Protein samples were purified to homogeneity and prepared and analyzed as described in Methods. A characteristic change in fluorescence emission was observed at 329 nm and normalized fluorescence was plotted against urea concentration. For low urea concentrations (0.5–1 M) a significant difference in protein fluorescence is detected which can be assigned to a difference in protein structure. Values given are averages of three independent experiments and different equilibration times (24–120 h).

Table 1

(**A**)

Protein sample	Amount of protein secreted to the medium (% of wild type HlyA)	Activity of culture supernatants (% of wild type HlyA)	Calculated relative specific activity (%)
HlyA	100	100	100
HlyA99	30	12	40
HlyA Del6	67	25	37

(**B**)

Protein sample	Haemolytic activity of culture supernatant per unit HlyA protein (% of wild type HlyA)	Haemolytic activity after renaturation from 6 M GnCl per unit HlyA protein (% of wild type HlyA)
HlyA (wild type)	40.4 (100)	49.1 (100)
HlyA99	15.7 (39)	19.8 (40)
HlyA Del6	15.1 (37)	21.0 (43)

Table 2

Protein sample	β-lactamase activity per A_{600} unit of culture supernatant (μmol/min/A_{600})	β-lactamase specific activity in culture supernatant (% of wild type βlac-23kDaHlyA)
wild type βlac-23kDaHlyA	0.227	100
hlyA99 mutant βlac-23kDaHlyA	0.028	40

References

Andersen, C., Koronakis, E., Bokma, E., Eswaran, J., Humphreys, D., Hughes, C. & Koronakis, V. (2002). Transition to the open state of the TolC periplasmic tunnel entrance. *Proc Natl Acad Sci U S A* **99**, 11103-11108.

Balakrishnan, L., Hughes, C. & Koronakis, V. (2001). Substrate-triggered recruitment of the TolC channel-tunnel during type I export of hemolysin by Escherichia coli. *J Mol Biol* **313**, 501-510.

Balsalobre, C., Silvan, J. M., Berglund, S., Mizunoe, Y., Uhlin, B. E. & Wai, S. N. (2006). Release of the type I secreted alpha-haemolysin via outer membrane vesicles from Escherichia coli. *Mol Microbiol* **59**, 99-112.

Bauer, M. E. & Welch, R. A. (1997). Pleiotropic effects of a mutation in rfaC on Escherichia coli hemolysin. *Infect Immun* **65**, 2218-2224.

Baumann, U., Wu, S., Flaherty, K. M. & McKay, D. B. (1993). Three-dimensional structure of the alkaline protease of Pseudomonas aeruginosa: a two-domain protein with a calcium binding parallel beta roll motif. *Embo J* **12**, 3357-3364.

Benabdelhak, H., Kiontke, S., Horn, C., Ernst, R., Blight, M. A., Holland, I. B. & Schmitt, L. (2003). A specific interaction between the NBD of the ABC-transporter HlyB and a C-terminal fragment of its transport substrate haemolysin A. *J Mol Biol* **327**, 1169-1179.

Chenal, A., Guijarro, J. I., Raynal, B., Delepierre, M. & Ladant, D. (2009). RTX calcium binding motifs are intrinsically disordered in the absence of calcium: implication for protein secretion. *J Biol Chem* **284**, 1781-1789.

Chervaux, C., Sauvonnet, N., Le Clainche, A., Kenny, B., Hung, A. L., Broome-Smith, J. K. & Holland, I. B. (1995). Secretion of active beta-lactamase to the medium mediated by the Escherichia coli haemolysin transport pathway. *Mol Gen Genet* **249**, 237-245.

Chervaux, C. & Holland, I. B. (1996). Random and directed mutagenesis to elucidate the functional importance of helix II and F-989 in the C-terminal secretion signal of Escherichia coli hemolysin. *J Bacteriol* **178**, 1232-1236.

Delepelaire, P. (2004). Type I secretion in gram-negative bacteria. *Biochim Biophys Acta* **1694**, 149-161.

Goni, F. M. & Ostolaza, H. (1998). E. coli alpha-hemolysin: a membrane-active protein toxin. *Braz J Med Biol Res* **31**, 1019-1034.

Halegoua, S. & Inouye, M. (1979). Translocation and assembly of outer membrance proteins of Escherichia coli. Selective accumulation of precursors and novel assembly intermediates caused by phenethyl alcohol. *J Mol Biol* **130**, 39-61.

Herlax, V. & Bakas, L. (2007). Fatty acids covalently bound to alpha-hemolysin of Escherichia coli are involved in the molten globule conformation: implication of disordered regions in binding promiscuity. *Biochemistry* **46**, 5177-5184.

Holland, I. B., Benabdelhak, H., Young, J., De Lima Pimenta, A., Schmitt, L. & Blight, M. A. (2003). Bacterial ABC transporters involved in protein translocation. In *ABC proteins: From bacteria to man*, pp. 209-241. Edited by I. B. Holland, S. P. Cole, K. Kuchler & C. Higgins. London: Academic Press.

Holland, I. B., Schmitt, L. & Young, J. (2005). Type 1 protein secretion in bacteria, the ABC-transporter dependent pathway (review). *Mol Membr Biol* **22**, 29-39.

Hyland, C., Vuillard, L., Hughes, C. & Koronakis, V. (2001). Membrane interaction of Escherichia coli hemolysin: flotation and insertion-dependent labeling by phospholipid vesicles. *J Bacteriol* **183**, 5364-5370.

Jones, H. E., Holland, I. B. & Campbell, A. K. (2002). Direct measurement of free Ca(2+) shows different regulation of Ca(2+) between the periplasm and the cytosol of Escherichia coli. *Cell Calcium* **32**, 183-192.

Kenny, B., Chervaux, C. & Holland, I. B. (1994). Evidence that residues -15 to -46 of the haemolysin secretion signal are involved in early steps in secretion, leading to recognition of the translocator. *Mol Microbiol* **11**, 99-109.

Koronakis, V., Koronakis, E. & Hughes, C. (1989). Isolation and analysis of the C-terminal signal directing export of *Escherichia coli* hemolysin protein across both bacterial membranes. *EMBO J* **8**, 595-605.

Koronakis, V., Sharff, A., Koronakis, E., Luisi, B. & Hughes, C. (2000). Crystal structure of the bacterial membrane protein TolC central to multidrug efflux and protein export. *Nature* **405**, 914-919.

Pimenta, A. L., Racher, K., Jamieson, L., Blight, M. A. & Holland, I. B. (2005). Mutations in HlyD, part of the type 1 translocator for hemolysin secretion, affect the folding of the secreted toxin. *J Bacteriol* **187**, 7471-7480.

Sanchez-Magraner, L., Viguera, A. R., Garcia-Pacios, M., Garcillan, M. P., Arrondo, J. L., de la Cruz, F., Goni, F. M. & Ostolaza, H. (2007). The calcium-binding C-terminal domain of Escherichia coli alpha-hemolysin is a major determinant in the surface-active properties of the protein. *J Biol Chem* **282**, 11827-11835.

Sotomayor Perez, A. C., Karst, J. C., Davi, M., Guijarro, J. I., Ladant, D. & Chenal, A. Characterization of the regions involved in the calcium-induced folding of the intrinsically disordered RTX motifs from the bordetella pertussis adenylate cyclase toxin. *J Mol Biol* **397**, 534-549.

Stanley, P., Packman, L. C., Koronakis, V. & Hughes, C. (1994). Fatty acylation of two internal lysine residues required for the toxic activity of Escherichia coli hemolysin. *Science* **266**, 1992-1996.

Vakharia, H., German, G. J. & Misra, R. (2001). Isolation and characterization of Escherichia coli tolC mutants defective in secreting enzymatically active alpha-hemolysin. *J Bacteriol* **183**, 6908-6916.

Fig. 1 Jumpertz *et al*. (2010)

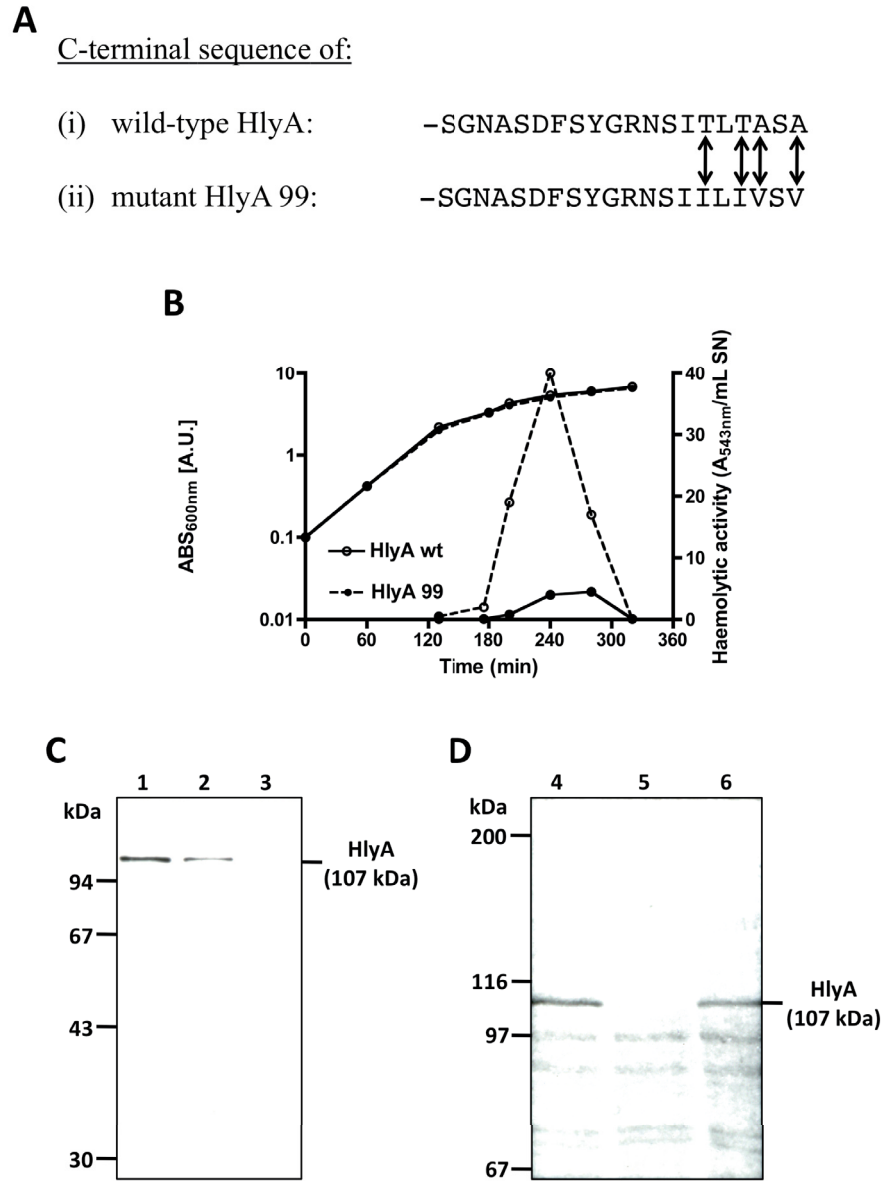

Fig. 2 Jumpertz *et al*. (2010)

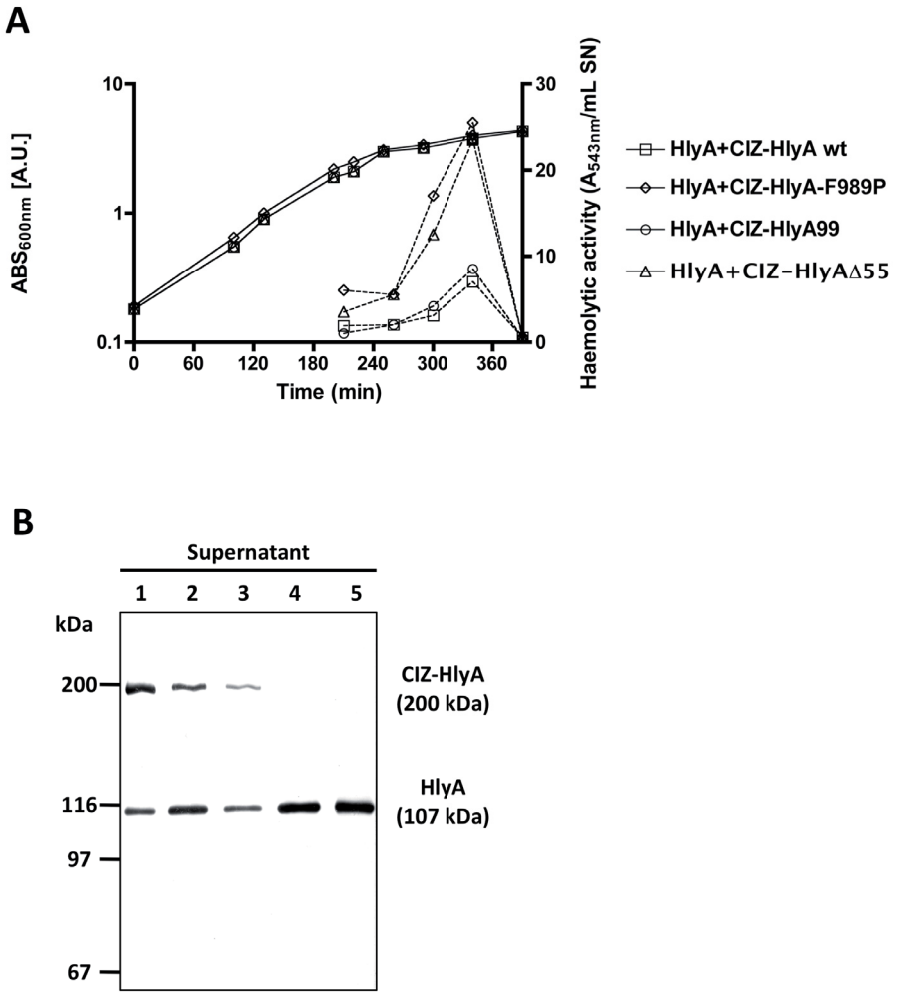

Fig. 3 Jumpertz *et al*. (2010)

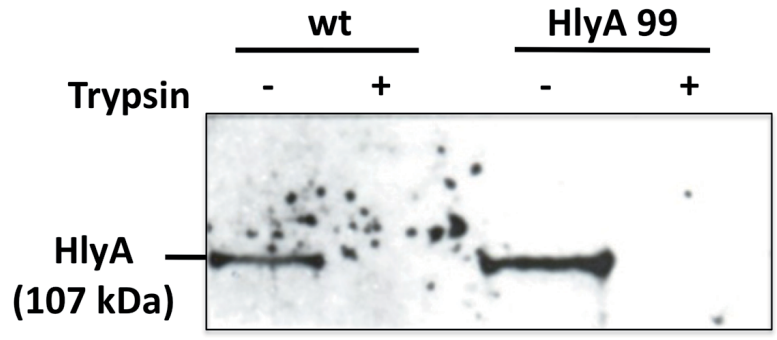

Fig. 4 Jumpertz *et al*. (2010)

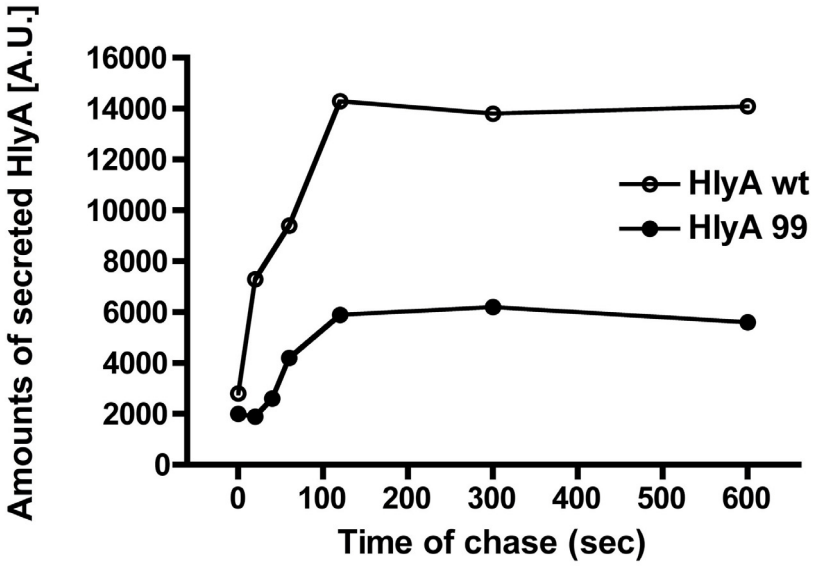

Fig. 5 Jumpertz *et al*. (2010)

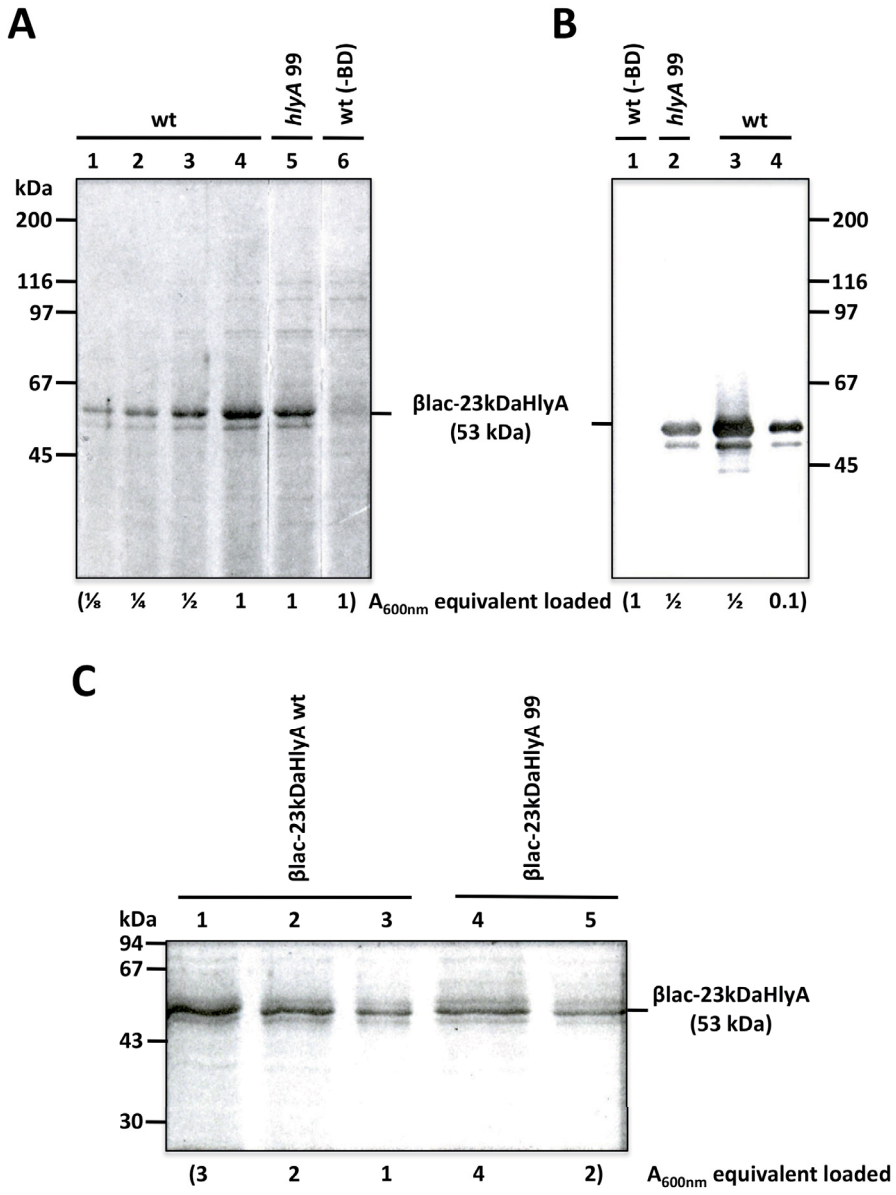

Fig. 6 Jumpertz *et al*. (2010)

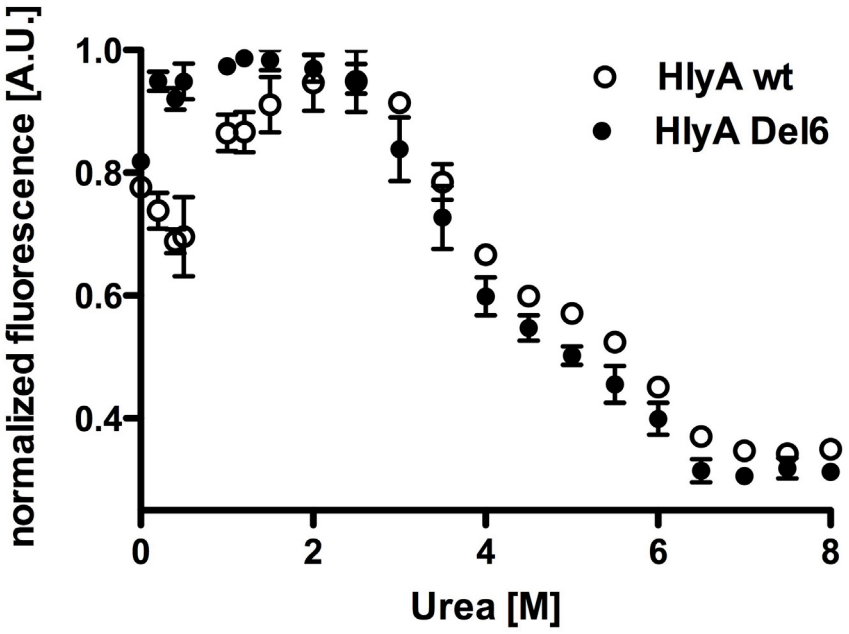

36

Supplementary Material

Supplementary Figure 1: Schematic drawing of the functional domains of the haemolytic cytotoxin HlyA. Reproduced with modifications from (Ludwig & Goebel, 2000).

Supplementary Figure 2: Mutagenic analysis of the HlyA C-terminal secretion peptide has identified two possible functional roles.

Supplementary Figure S3: Cell associated HlyA is digested by exogenous trypsin while intracellular HlyA is inaccessible to trypsin.
(A) Strain SE5000 (carrying plasmids pLG813 (*hlyCA*) and pLG814 (*hlyBD*) were grown in LB medium at 37° C, harvested at an OD = 4, resuspended in buffer (10 mM Tris-HCL + 10 mM $MgCl_2$) and treated with trypsin (10 mM Tris-HCL + 10 mM $MgCl_2$) Samples of total cell protein were separated by SDS-PAGE and western blotted against HlyA antibody. The Figure also shows that in the absence of *hlyBD*, relatively little HlyA accumulates inside cells.
(B) Strain SE5000 with pLG813 expressing *hlyCA* (WT secretion signal or *hlyA99*), and pLG814 (*hlyBD*) was grown in LB medium at 37° C, harvested at an OD=4, suspended in buffer and treated with different amounts of trypsin (50 µg/ml) or left untreated (see Methods). Samples of total cell protein were separated by SDS-PAGE and stained with Coomassie blue. The results show that under these conditions cells are impermeable to trypsin and treatment affects surface exposed proteins but not cytoplasmic protein.

Supplementary Figure 4: Silver stained SDS-PAGE of wild-type proHlyA and proHlyA Del6. Protein samples were loaded onto the gel after purification by anion exchange chromatography, SEC, cation exchange chromatography, and a final SEC step. Protein samples are highly pure (> 99%) and therefore ideally suited for protein fluorescence studies that will obviously be disturbed by impurities of the sample.

Fig. S1 Jumpertz *et al.* (2010)

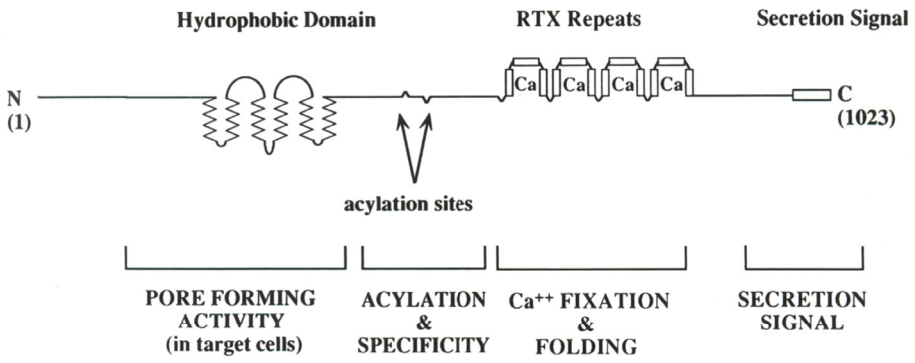

Fig. S2 Jumpertz *et al.* (2010)

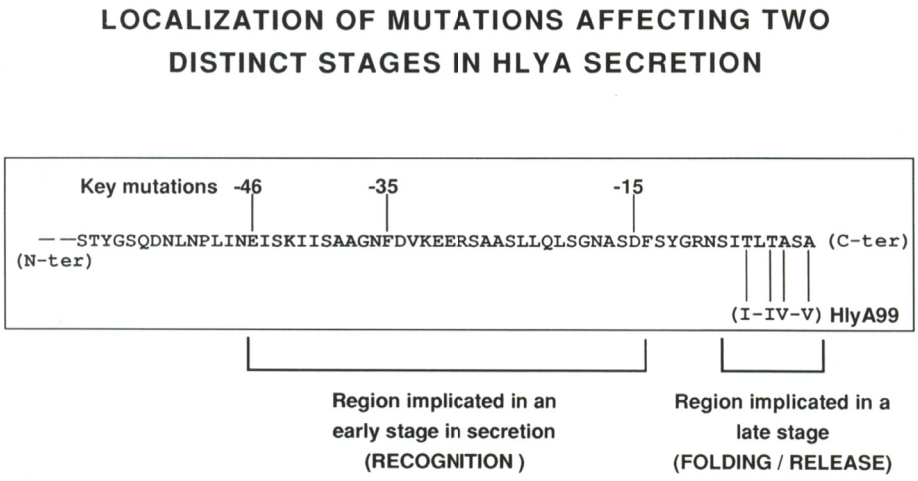

Fig. S3 Jumpertz *et al.* (2010)

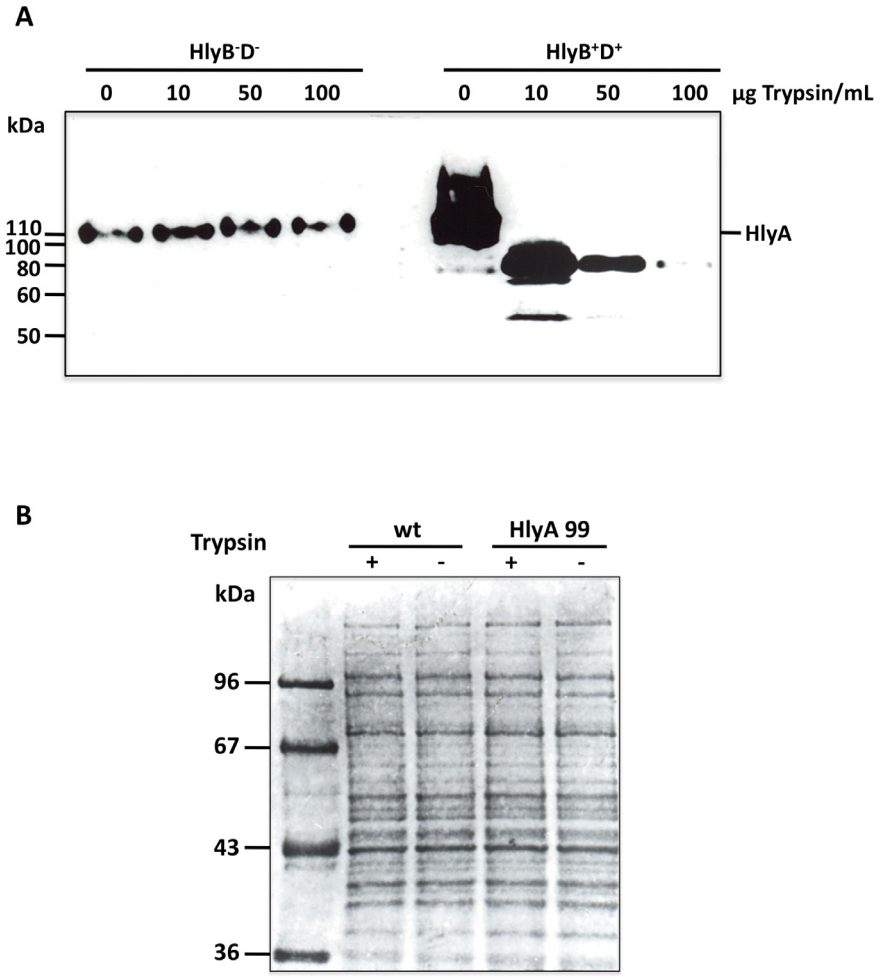

Fig. S4 Jumpertz *et al.* (2010)

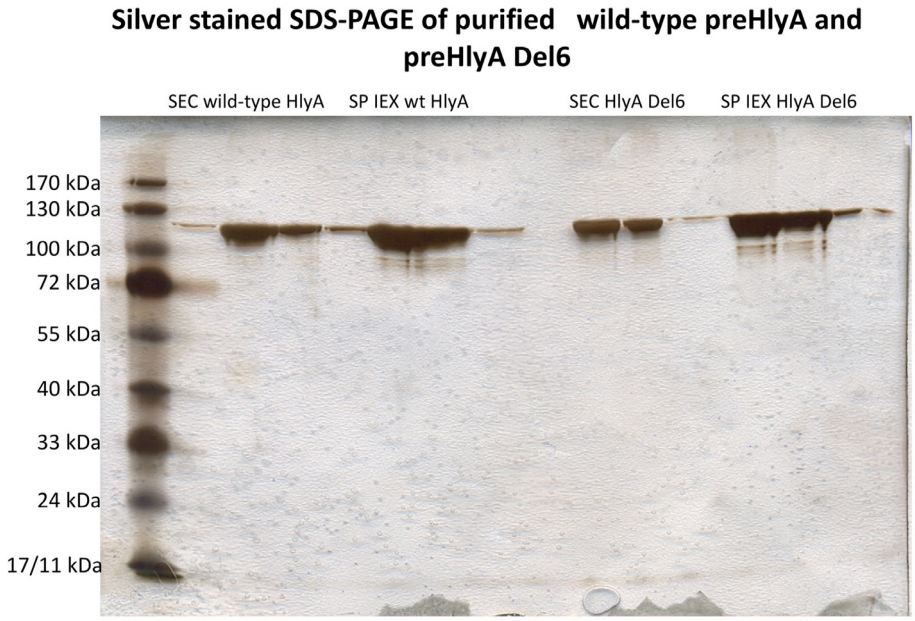

5

Proportionate work on this publication: 50 %

Published in: Microbiology (formerly Journal of General Microbiology), *in press*

Impact factor: 3.110

Paper V

Elsevier Editorial System(tm) for Analytical Biochemistry
Manuscript Draft

Manuscript Number:

Title: High throughput evaluation of detergent concentration and their CMC values

Article Type: Full Length Article

Section/Category: Physical Techniques

Keywords: Detergent; cmc determination; fluorescence; mixed micelles

Corresponding Author: Prof. Dr. Lutz Schmitt,

Corresponding Author's Institution: Heinrich Heine University

First Author: Lutz Schmitt

Order of Authors: Lutz Schmitt; Thorsten Jumpertz; Britta Tschapek; Nacera Infed; Sander H Smits; Robert Ernst, Dr.; Thorsten Jumpertz; Britta Tschapek; Nacera Infed; Sander H Smits; Robert Ernst

Abstract: Determination of the CMC value of detergents routinely used in biological applications is still a technically challenging task but necessary to follow possible changes of the CMC due to different buffer compositions, temperature, pH or in solutions that are used for protein activity assays or crystallization. Here, we report a method to determine the CMC values of detergents through a fast and robust assay that relies on the fluorescence of Hoechst 33342 using a 96-well plate reader. Furthermore, this assay provides the possibility and sensitivity to measure changes in the CMC of detergent mixtures. The examples described here emphasize the potential and the applicability of this assay and demonstrate that analysis of the physico-chemical parameters of detergents can now be investigated in virtually every laboratory.

Suggested Reviewers: Gerrit van Meer Prof. Dr.
Chairman Membrane Enzymology, Institute of Biomembranes, University of Utrecht
g.vanmeer@uu.nl
Dr. van Meer is an internationally recognized expert in the field of lipids and detergents

Thomas Pomorski Prof. Dr.
Associate Professor, Department of Plant Biology, University of Copenhagen
tgp@life.ku.dk
Dr. Pomorski is an expert in the field of the interaction of membrane proteins with lipid/detergents. He will truly be able to judge the potential of our findings

Arun Radakrishnan Prof. Dr.
Assitant Professor, Institute of Biochemistry, Weill Cornell Medical College
arunr@med.cornell.edu

Cover Letter

Institut für Biochemie
Prof. Dr. Lutz Schmitt

HEINRICH HEINE UNIVERSITÄT DÜSSELDORF

40225 Düsseldorf
Universitätsstraße 1
Gebäude 26.32.03/26.42.03
Tel 0211-81-10773
Fax 0211-81-15310
Lutz.Schmitt@uni-duesseldorf.de

Düsseldorf, 25.05.2010

ANALYTICAL BIOCHEMISTRY
– Editorial office –

Dear Sirs and Madams,

Enclosed please find the manuscript entitled " High throughput evaluation of detergent concentration and their CMC values" by Thorsten Jumpertz, Britta Tschapek, Nacera Infed, Sander H. J. Smits and Lutz Schmitt, which we like to submit to Analytical Biochemistry.

Here we describe an assay that allows in a high-throughput manner (96 well format) to determine the concentration as well as the critical micellar concentration of detergents under a broad range of experimental conditions. Furthermore, this assay provides the sensitivity and potential to investigate mixtures of detergents as well. In light of the importance of detergent in many research areas such as membrane proteins or surface characterizations, we think that this assay will provide a novel tool to study detergents, their mixtures and their physical-chemical properties in a robust, sensitive and easy-to-handle manner.

In light of these considerations, we think that Analytical Biochemistry is the perfect journal to publish our data.

Sincerely Yours

(Lutz Schmitt)

High throughput evaluation of detergent concentration and their CMC values

Thorsten Jumpertz[1,2], Britta Tschapek[1], Nacera Infed[1], Sander H. J. Smits[1], Robert Ernst[1,3], and Lutz Schmitt[1]*

[1]Institute of Biochemistry, Membrane Transport Group, Heinrich Heine University Duesseldorf, Universitaetsstrasse 1, 40225 Duesseldorf, Germany

[2]Present address: Institute of Neuropathology, Molecular Neuropathology Group, Medical School Duesseldorf, Moorenstrasse 5, 40225 Duesseldorf, Germany

[3]Present address: Max Planck Institute for Molecular Cell Biology and Genetics, Pfotenhauerstrasse 108, 01307 Dresden, Germany

*Corresponding author. Phone: +49 211 8110773, Fax: +49 211 8115310, E-mail address: Lutz.Schmitt@uni-duesseldorf.de

Subject category: Physical Techniques/Special Topics

Abstract

Determination of the CMC value of detergents routinely used in biological applications is still a technically challenging task but necessary to follow possible changes of the CMC due to different buffer compositions, temperature, pH or in solutions that are used for protein activity assays or crystallization. Here, we report a method to determine the CMC values of detergents through a fast and robust assay that relies on the fluorescence of Hoechst 33342 using a 96-well plate reader. Furthermore, this assay provides the possibility and sensitivity to measure changes in the CMC of detergent mixtures. The examples described here emphasize the potential and the applicability of this assay and demonstrate that analysis of the physico-chemical parameters of detergents can now be investigated in virtually every laboratory.

Keywords

Detergent; cmc determination; fluorescence; mixed micelles

Abbreviations

$C_{12}E_8$: Polyoxyethylene(8)dodecyl ether; CMC: critical micellar concentration; CyMal7: 7-Cyclohexyl-1-heptyl-β-D-maltoside; dd: double distilled; DDM: Dodecyl-maltoside; DM: decyl-maltoside; FC-14: 1-myristoyl-2-hydroxy-sn-glycero-3-phospho-(1'-rac-glycerol); FC-16: 1-palmitol-2-hydroxy-sn-glycero-3-phospho-(1'-rac-glycerol); NP-40: nonyl phenoxylpolyethoxylethanol; β-OG: beta-octylglucoside; PFO: perfluorooctanoic acid; SAXS/NS: small angle X-ray/neutron scattering.

Facing the fact that the „–omics“ era has reached almost every branch of natural, life, and medical sciences, new techniques often have to prove their potential of handling an enormous number of samples or experimental conditions that have to be screened during the quest to find the right conditions for e.g. one-pot-synthesis, stabilizing drugs, or crystallizing proteins.

Genome projects estimate that roughly 30-40 percent of all proteins encoded in the human genome are membrane embedded or membrane associated proteins (MPs) [1; 2]. Additionally, MPs account for about 70 percent of all drug targets [3]. It is therefore of great importance to functionally and structurally describe MPs. A major obstacle is to solubilize MPs from their native environment, the lipid bilayer, in a functional and active form. To overcome this intrinsic problem a huge variety of biologically important detergents have emerged and new ones are being constantly synthesized to match the ambitious needs of biochemists and medicinal pharmacologists [4]. But not only the solubilisation of MPs is a critical procedure; subsequent steps such as purification, dialysis, concentration, biochemical assays, and crystallization are performed in the continuous presence of detergents and numerous additives specific for the desired experiment [5; 6; 7]. These additional substances (salt, glycerol, buffer, metal-ions, sugars, etc.) as well as physical parameters (e.g. pH, temperature) influence the critical micellar concentration (CMC) of detergents. Since detergents prevent MPs from aggregation, a precise knowledge of the detergent concentration and its CMC at a given experimental condition may become crucially important.

Different methods already exist to determine the CMC of detergents, e.g. fluorescence techniques [8], infrared spectroscopy [9], thin layer chromatography [10], colorimetric assays [11], or refractive index measurements [12]. All these experiments are not accessible for laboratories working on a regular basis with MPs/detergents. They are also not suited for mid- to high-throughput screening.

We therefore developed an easy-to-use, robust, and fast assay for the determination of the CMC value of detergents routinely used in biological applications which makes it possible to follow changes of the CMC due to different buffer compositions or in solutions that are used for protein crystallization. The assay is based on the dye Hoechst 33342 that displays literally no fluorescence in hydrophilic environments, but emits efficiently in hydrophobic environments. Thus, in ddH_2O, aqueous buffers, and buffers containing detergents below the CMC no or only marginal Hoechst 33342 fluorescence can be detected (supplementary Figure S1). Upon constant increase of the concentration of detergent, the CMC value will be reached and micelles start to form. As soon as this point is passed, micelles begin to incorporate Hoechst 33342 which can be

visualized by an increase of the fluorescence signal. This point represents the CMC of the detergent (Figure 1). The assay described here is optimized for 96-well fluorescence plates and data can be evaluated with a plate reader („ELISA reader“) available in almost every laboratory working with membrane proteins.

Formation of micelles was followed upon fluorescence increase at maximum emission of Hoechst 33342 in the respective buffer/detergent mixture (457±10 or 487±10 nm, 460±40 nm for the Fluorolog 3 and plate reader set-up, respectively; for further details see Supplementary Material). We obtained the CMC values for detergents shown in Table 1 in 50 mM HEPES pH 7.2, 50 mM NaCl, 5% (w/v) glycerol except for PFO, which precipitated in HEPES buffer and was therefore dissolved in NaPi or ddH_2O. We determined the dn/dc value (data not shown) and micelle size for the detergents shown in Figure 1 for cross-validation of our results. From light scattering experiments the molecular mass of detergent micelles was calculated to be 88 kDa for Triton X-100, 76 kDa for DDM, 80 kDa for FosCholine16, and 47,4 kDa for $C_{12}E_8$ (Supplementary Figure S2). These values are in good agreement with literature values (Table 1).

For DDM, a detergent routinely used for membrane protein purification and crystallization, we also showed that micelle formation and size depend on salt concentration. Additionally, a great impact on the CMC value in the presence of buffer/salt is shown for PFO (0.8% in ddH_2O versus 0.2% in buffer). Increasing the NaCl concentration from 0 to 1 M decreases the CMC of DDM nearly 4-fold (Supplementary Figure S3). The largest change (2-fold) was observed for no salt and 200 mM NaCl, while a nearly linear decrease of the CMC value was detected in the case of further increases up to 1 M NaCl. For PFO we compared the change of the CMC between ddH_2O and a buffer (50 mM NaP_i, 50 mM NaCl, 5% (w/v) glycerol) (Supplementary Figure 4). Again, a nearly 4-fold reduction of the CMC was observed and highlights the capability of our assay to easily analyze the influence of certain parameters on the physico-chemical behavior of the detergent. Equally, the influence of buffer compounds, ionic strength, nature of the salt, temperature, and other parameters can be addressed.

From the fluorescence intensity it is also possible to determine the detergent concentration in a certain sample as long as the buffer composition does not differ from the control measurement (same experiments as in Figure 1). We used this approach to determine the detergent concentration of membrane protein preparations after e.g. concentration and regularly observed an increase in detergent concentration although the molecular weight cut-off of the concentrator should prevent concentration of empty micelles (data not shown).

An interesting observation is that crystal quality of membrane proteins can dramatically improve when a second detergent is added. A recent paper nicely describes the purification and crystallization strategies of the Na^+-H^+-antiporter NhaA from *E. coli* and the authors assume that the mixture of detergents used improved crystal contacts thereby allowing a subsequent structure determination [13]. Employing our assay, we were able to detect changes in the CMC of one detergent in the presence of a second detergent (Supplementary Figure S4). When titrating e.g. FC-14 to a solution containing DDM at half critical micellar concentration we obtained a shift in the CMC of pure FC-14 and an increase of fluorescence in the presence of two detergents. The latter might indicate that (i) more Hoechst 33342 molecules can bind on average to such a mixed micelle or that (ii) due to the additional presence of other detergent molecules a higher number of (mixed) micelles can form (for the formation of mixed micelles see [14; 15; 16]). A similar behavior could be observed for a mixture of detergents with a rather large CMC value like DM and β-OG or a mixture of large and small CMC (DDM and DM; data not shown). These results emphasize the sensitivity and potential of the assay not only for pure systems but also and even more important for mixtures of detergents. In this context, we would also like to mention that the difference in fluorescence for the detergents examined here (see Figure 1) results most likely from local environmental effects on Hoechst 33342 fluorescence - this difference might be used to further analyze mixtures of detergents.

Highly sophisticated and reliable approaches such as NMR, SAXS/NS or contact angle measurements will result in similar values than the method described here. Most of the time, relative changes of the CMC due to changes in temperature, buffer composition or additives are in the focus. Our method thus provides a fast and robust way to analyze such changes. We also performed the experiments for FC-16 using ANS (8-Anilinonaphthalene-1-sulfonate; ANS has also been extensively used to examine the CMC, see for example [8]) as the reporter dye (data not shown) and obtained similar results. This demonstrates that the assay is not restricted to Hoechst 33342 and other dyes specifically adapted to certain problems (for example pH or redox sensitive) might be employed.

In summary, the described method has proven as a valuable and robust tool for addressing questions arising in all areas of research dealing with detergents or protein-detergent complexes. Transfer into 96-well plate format and the striking simplicity make this method suitable to follow (bio)physical questions that were not too easy to address before. We are convinced that upon basis of this assay further developments will be achieved to investigate

different detergent/detergent-protein-complex parameters and eventually leads to an auxiliary biochemical “tool-box” for membrane protein research.

6

Acknowledgements

We are indebted to Silke Zobel for initial fluorescence measurements. This work was supported by the DFG (grant Schm1279/5-3), VW foundation (grant I/82 604) and from the European Community's Seventh Framework Programme FP7/2007-2013 under grant agreement n° HEALTH-F4-2007-201924, EDICT Consortium to L.S.

Literature

[1]E. Wallin, and G. von Heijne, Genome-wide analysis of integral membrane proteins from eubacterial, archaean, and eukaryotic organisms. Protein Sci 7 (1998) 1029-38.
[2]A. Krogh, B. Larsson, G. von Heijne, and E.L. Sonnhammer, Predicting transmembrane protein topology with a hidden Markov model: application to complete genomes. J Mol Biol 305 (2001) 567-80.
[3]J. Drews, Drug discovery: a historical perspective. Science 287 (2000) 1960-4.
[4]R.M. Garavito, and S. Ferguson-Miller, Detergents as tools in membrane biochemistry. J Biol Chem 276 (2001) 32403-6.
[5]M.C. Wiener, A pedestrian guide to membrane protein crystallization. Methods 34 (2004) 364-72.
[6]L.E. Fisher, D.M. Engelman, and J.N. Sturgis, Detergents modulate dimerization, but not helicity, of the glycophorin A transmembrane domain. J Mol Biol 293 (1999) 639-51.
[7]L.E. Fisher, D.M. Engelman, and J.N. Sturgis, Effect of detergents on the association of the glycophorin a transmembrane helix. Biophys J 85 (2003) 3097-105.
[8]E.B. Abuin, E.A. Lissi, A. Aspee, F.D. Gonzalez, and J.M. Varas, Fluorescence of 8-Anilinonaphthalene-1-sulfonate and Properties of Sodium Dodecyl Sulfate Micelles in Water-Urea Mixtures. J Colloid Interface Sci 186 (1997) 332-8.
[9]C.J. daCosta, and J.E. Baenziger, A rapid method for assessing lipid:protein and detergent:protein ratios in membrane-protein crystallization. Acta Crystallogr D Biol Crystallogr 59 (2003) 77-83.
[10]L.R. Eriks, J.A. Mayor, and R.S. Kaplan, A strategy for identification and quantification of detergents frequently used in the purification of membrane proteins. Anal Biochem 323 (2003) 234-41.
[11]A. Urbani, and T. Warne, A colorimetric determination for glycosidic and bile salt-based detergents: applications in membrane protein research. Anal Biochem 336 (2005) 117-24.
[12]P. Strop, and A.T. Brunger, Refractive index-based determination of detergent concentration and its application to the study of membrane proteins. Protein Sci 14 (2005) 2207-11.
[13]E. Screpanti, E. Padan, A. Rimon, H. Michel, and C. Hunte, Crucial steps in the structure determination of the Na+/H+ antiporter NhaA in its native conformation. J Mol Biol 362 (2006) 192-202.
[14]P. Sehgal, J.E. Mogensen, and D.E. Otzen, Using micellar mole fractions to assess membrane protein stability in mixed micelles. Biochim Biophys Acta 1716 (2005) 59-68.
[15]R. Nagarajan, Molecular Theory for Mixed Micelles. Langmuir (1985) 331-341.
[16]E.A.G. Aniansson, and S.N. Wall, On the Kinetics of Step-Wise Micelle Association. The Journal of Physical Chemistry 78 (1974) 1024-1030.

Table legends

Table 1. Comparison of CMC values of different detergents obtained by the Hoechst 33342 assay and literature values (taken from www.affimetrix.com/estore). n. d.: not determined. Errors reported are standard deviation determined by equation (1). [a]: measured in ddH_2O.

Figure legends

Figure 1. Comparison of the CMC determination of DDM, Triton X-100 and FC-16 via a Fluorolog 3 (A) or 96-well plate reader set-up (B). Data were analyzed according to equation (1) (see supplementary material). The determined CMC values for these and further detergents are listed in Table 1. Differences in maximum fluorescence between Fluorolog 3 and plate reader measurements are due to different receiver gains of the plate reader instrument. The difference in maximum fluorescence between e.g. DDM and FC-16 is likely due to local environment effects on Hoechst 33342 fluorescence like local pH, water penetration, and hydrophobicity of the detergent.

Table

Tables

Table 1

Detergent	CMC value [%, (w/v)] (Plate reader)	CMC value [%, (w/v)] (Fluorolog)	CMC value [%, (w/v)] (Literature)	Aggregation number (Literature)	Aggregation number (MALS)
$C_{12}E_8$	n. d.	0.0039 ± 0.0001	0.0048	123	87
CyMal7	n. d.	0.011 ± 0.002	0.0099	150	n. d.
DM	0.093 ± 0.002	0.092 ± 0.001	0.087	69	n. d.
DDM	0.0081 ± 0.0002	0.0083 ± 0.0002	0.0087	78- 149	148
FC-14	0.0055 ± 0.0001	0.0067 ± 0.0002	0.0046	108	n. d.
FC-16	0.00054 ± 0.00005	0.00055 ± 0.00003	0.00053	178	196
NP-40	n. d.	0.0044 ± 0.0002	0.003-0.018	100- 155	n. d.
PFO	0.80 ± 0.02 0.20 ± 0.01[a]	0.81 ± 0.02	1.18	106- 179	n. d.
Triton X-100	0.018 ± 0.001	0.015 ± 0.0001	0.010-0.016	75- 165	136

Figure
Click here to download high resolution image

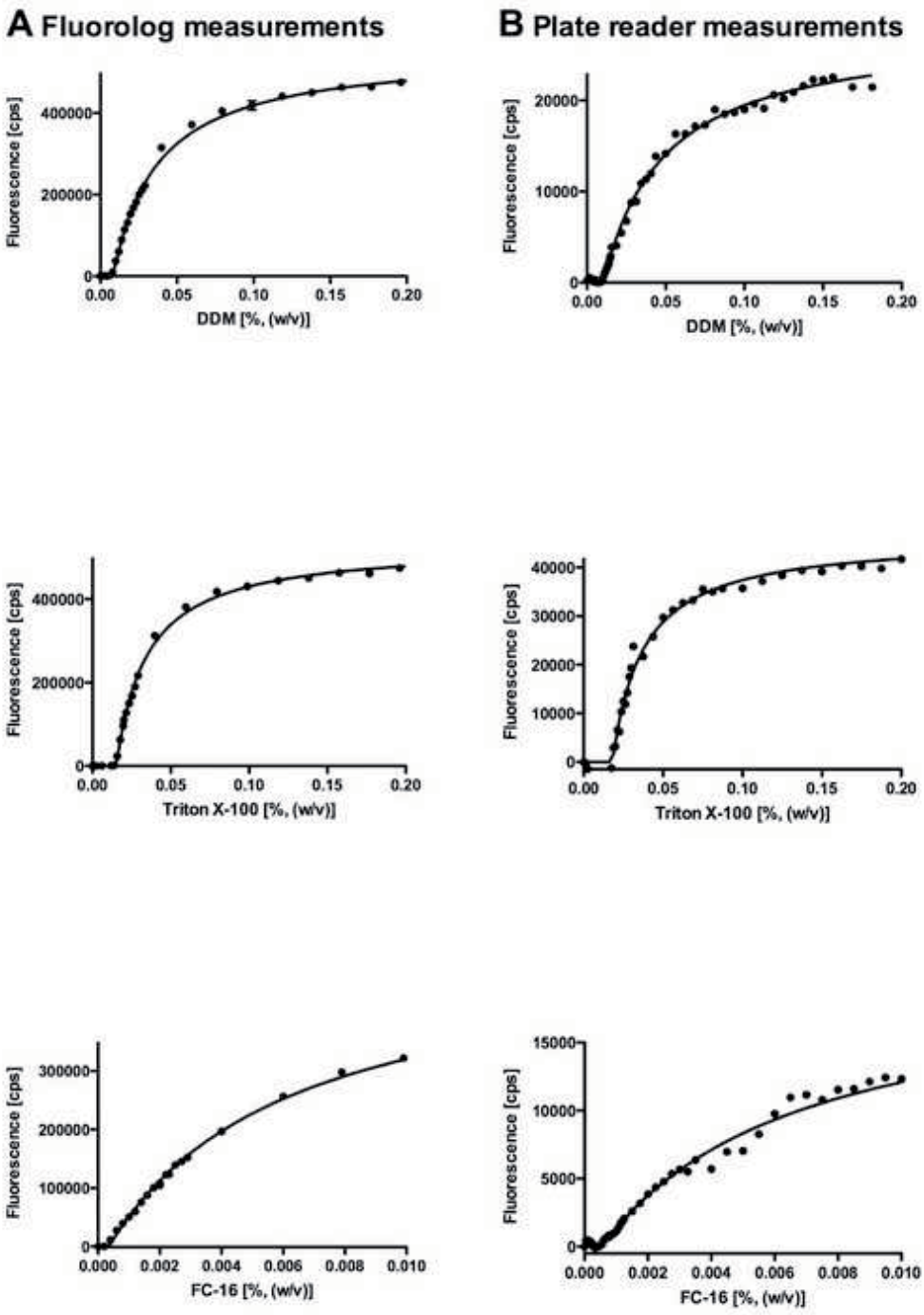

Supplementary Material (for Online Publication)
Click here to download Supplementary Material (for Online Publication): Jumpertz_et_al_SupplMat.doc

Supplementary Material

Materials and Methods

Fluorescence Spectroscopy To determine the CMC various detergents were titrated into a fluorescence cuvette from a stock solution. The cuvette contained either ddH_2O (MilliQ grade, 0.45 µm filter sterilized) or buffer (50 mM Na-phosphate, 50 mM NaCl, 5% (w/v) glycerol) supplemented with 7 µM Hoechst 33342. The detergent stock solution also contained 7 µM Hoechst 33342 to circumvent dilution of the fluorescent dye. The resulting fluorescence was measured on a Horiba-Jobin-Yvon Fluorolog 3 spectrophotometer with λ_{EX}=355nm, λ_{EM}=457nm (λ_{EM}=487nm for perfluorooctanoic acid) and the slit width was 2 and 0.5 nm, respectively. Data points were recorded until a mean standard deviation below 0.5% was reached. To transfer the method of CMC determination via Hoechst 33342 into a less laborious and time-consuming set-up, we used 96-well plates suitable for fluorescence spectroscopy (Greiner bio-one, FIA plate, black, flat bottom, medium binding), pipetted up to 80 different concentrations for each detergent (this step can also be automated by a pipetting robot) into 96-well plates and recorded emission spectra (filters used: λ_{EX}=355±10nm, λ_{EM}=460±80nm, BMG Labtech, Halle, Germany). Data recorded from Fluorolog 3 and plate reader gave virtually identical results (Table 1). Fluorescence data were background corrected and analyzed according to equation (1) using Prism (Version 5, GraphPad Inc.):

$$F = \frac{F_{\max}([Det] - cmc)}{(K_{0.5} - cmc) + ([Det] - cmc)} \qquad \text{equation (1)}$$

Here, F is the measured fluorescence, F_{max} the maximal fluorescence, [Det] the absolute detergent concentration, $K_{0.5}$ the midpoint of the fit function and cmc the critical micellar detergent concentration, which is determined by the fit.

dn/dc Measurements We determined the dn/dc values for certain detergents (Triton X-100, DDM, PFO) and compared these values with data found in the literature (see for example www.affimetrix.com/estore). In brief, 1 mL of a 0.25 g/mL Triton X-100, 1 g/mL DDM, 0.25 g/mL PFO stock solution was injected in appropriate dilutions via the direct injection mode. Refractive index measurements were used to calculate dn/dc values from peak area versus sample concentration at fixed sample volume (optiLAB rex, Wyatt Technologies, Santa

Barbara, CA, USA). The dn/dc values were used to calculate micelle size/mass from subsequent light scattering experiments.

Multiple Angle Light Scattering (MALS) To measure micelle size, we used a MALS set-up miniDAWN Treos/optiLAB rex (Wyatt Technologies, Santa Barbara, CA, USA) connected to an Äkta Purifier (GE Healthcare, Freiburg; Germany) and used either a Superose 6 or a Superdex 200 10/300 analytical size exclusion column. 200 µL of a detergent solution (5% w/v DDM, 2% w/v FC-16, 5% w/v Triton X-100, 30% w/v PFO) were applied onto the column. Flow rate was 0.2 mL/min. UV detection was at 280 nm, light scattering was detected at angles of 0°, 90°, and 107° and the obtained values were averaged. MALS data was evaluated using the program ASTRA (Wyatt Technologies, Santa Barbara, CA, USA). For PFO the micelle size could not be determined reliably. Due to its surface properties inherent to per-fluorinated substances, PFO interacted intensively with the column material. Using an asymmetric-flow field-flow-fractionation set-up (Eclipse AF4, Wyatt Technologies, Santa Barbara, CA, USA) connected to a MALS detector no conclusive results could be produced since the detergent seemed to interact with the membrane and the teflon fittings.

Measurements of detergent mixtures To measure the CMC values of detergent mixtures, we applied the same methodology used for the determination of CMC values of single detergents. In the examples presented here, the wells were preloaded with FC-16, DM, and β-OG at half the CMC and then titrated with either DDM, DM, or β-OG and the fluorescence of Hoechst 33342 was measured as described above.

Supplementary Figure S1

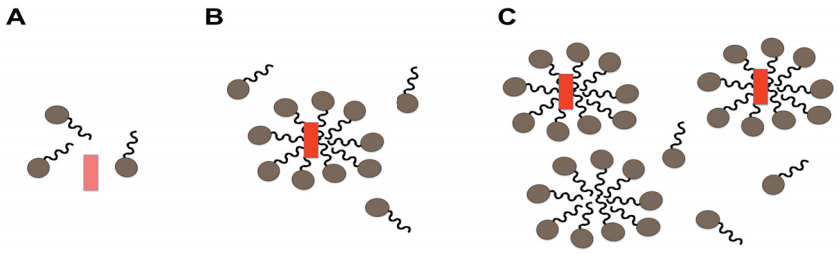

Supplementary Figure S1. Model of micelle formation and the Hoechst 33342 dependent assay. Below the critical micellar concentration (CMC) only detergent monomers are present in solution and no fluorescence of Hoechst 33342 (pale red square) is measured (**A**). When the detergent concentration increased to the CMC, micelles form and provide a hydrophobic environment for Hoechst 33342 resulting in its fluorescence (deep red square) – this point can easily be determined using the assay presented in this study (**B**). Increasing the detergent concentration will increase the concentration of micelles while the concentration of detergent monomers remain constant. Under saturating conditions, newly formed micelles are not saturated with Hoechst 33342 anymore and no further increase in fluorescence can be detected (**C**).

Supplementary Figure S2

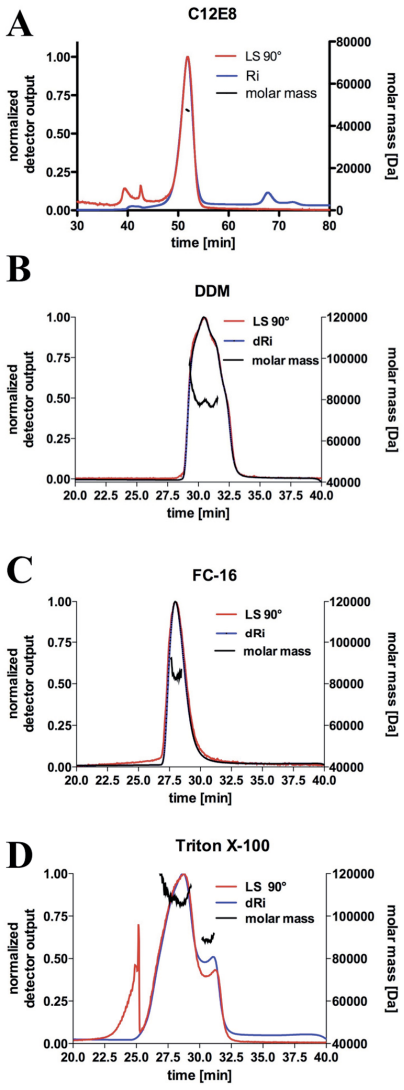

Supplementary Figure S2. MALS (multiple angle light scattering) combined with size-exclusion chromatography for $C_{12}E_8$ (**A**), DDM (**B**), FC-16 (**C**), and Triton X-100 (**D**) solutions. To determine the molecular masses of the corresponding detergent micelles, dn/dc values were determined by refractive index measurements (see Materials and Methods for further details).

Supplementary Figure S3

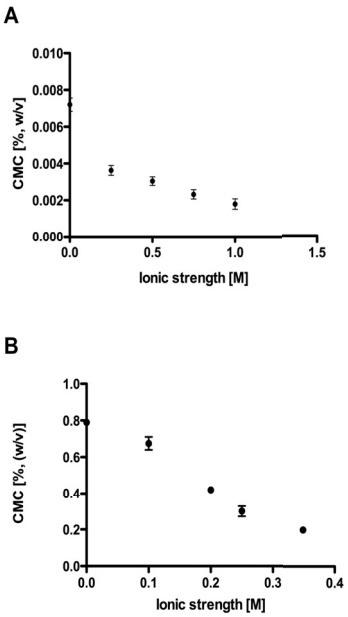

Supplementary Figure S3. Salt dependency of the CMC of DDM (**A**) and PFO (**B**). Decreasing concentrations of DDM or PFO are required for the formation of micelles if the ionic strength of the solution is increased.

Supplementary Figure S4

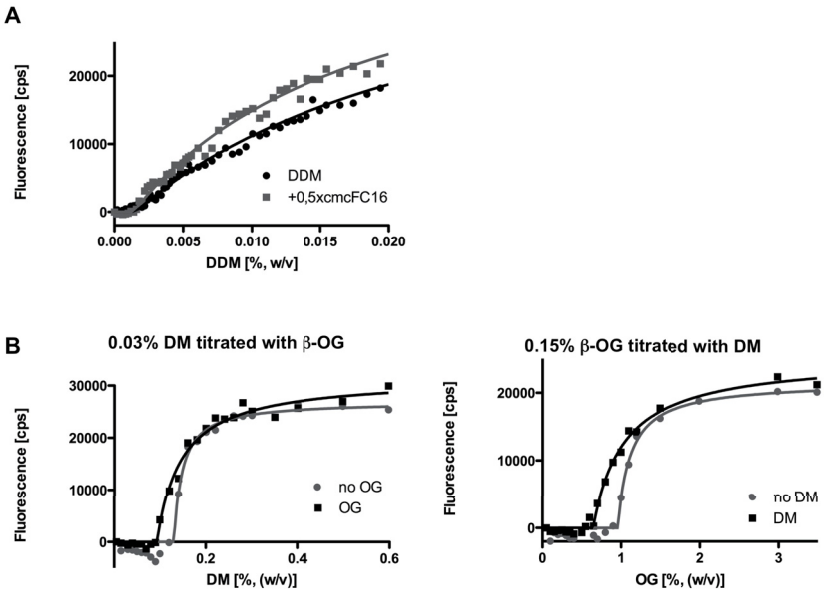

Supplementary Figure S4. Analysis of detergent mixtures. We tried to detect mixed micelles with detergents routinely used in membrane protein research. (**A**). FC-16 was supplied at a concentration of 0.5xCMC and DDM was added step-wise (grey squares). The resulting fluorescence curve and the CMC determined from the titration experiments showed small but significant changes compared with the one of pure DDM (black squares). This indicated formation of mixed micelles. (**B**) When using detergents with a higher CMC (DM and β-OG) mixed micelles were also observed. The CMC value of pure DM (0.087%) is shifted towards larger values in the presence of β-OG (left panel). The same behavior was observed for the inverse experiment (right panel).

Proportionate work on this publication: 40 %

Submitted to: Analytical Biochemistry

Impact factor: 3.088

5. Summary

The present work examines the Type I secretion system of *E. coli*. In enterohaemorrhagic *E. coli* strains a toxin, Haemolysin A (HlyA) is secreted by the Type I machinery. This toxin has the ability to bind to the host cell membrane and leads to subsequent lysis of the attacked cells. HlyA interacts with the host cell in such way that it distrubs the membrane integrity by insertion. The size of HlyA is about 107 kDa with an extensive hydrophobic stretch at the N-terminus which makes it ideally suited to form a pore in the host cell membrane. But this is only one hypothesis how HlyA acts on cells. There are experiments describing specific receptor binding regions within the toxin and data from that it is concluded that HlyA interacts with cellular signalling pathways. The mechanism of action of HlyA is by far not understood. In this work the focus is laid on the folding of the toxin into its native form. One of the results suggests that the secretion signal has a dual function and is also responsible for proper folding of the toxin.

The Type I secretion system consists of several protein that assemble into a ternary complex. Haemolysin B (HlyB, ABC transporter) and Haemolysin D (HlyD, membrane fusion protein) are located in the inner membrane. Together with the porin-like protein TolC they form a continous channel/tunnel across the periplasm to secrete the subtrate HlyA. The ABC transporter HlyB consists of a transmembrane part and a soluble nucleotide binding domain that provides the energy neccessary for transport by ATP hydrolysis. Another focus of this work is the functional characterization of the nucleotide binding domain (NBD) which explains its catalytic cycle on a molecular basis and offers a model how allostery in this protein is established. Together with the structural data derived from the crystal structure of the HlyB-NBD the biochemical data offers the possibility to test for ABC transporter inhibitors/modulators in the future since ABC transporters play a crucial role in multidrug resistance of cancer cells or different diseases like cystic fibrosis.

The third part of the thesis deals with a biophysical method to measure the CMC (critical micelle concentration) value of detergents on a mid- to high-throughput scale. This is extremely useful since the CMC changes upon temperature, salt concentration and other parameters. For the purification, characterization, and crystallization of membrane proteins a screening procedure for buffers containing detergent is quite important.

6. Zusammenfassung

Die vorliegende Arbeit beschäftigt sich mit der Analyse der Type I Sekretionssystems aus *E. coli*. In enterohaemorrhagischen *E. coli* Stämmen wird ein Toxin (Haemolysin A, HlyA) mit Hilfe des Type I Sekretionsapparates sekretiert. Das Toxin besitzt die Fähigkeit an die Membran der Zielzellen zu binden und die Zellen zu lysieren. HlyA interagiert dabei mit der Zielzelle, indem es die Membranintegrität durch Einlagerung zerstört. Das 107 kDa große HlyA besitzt an seinem N-Terminus einen ausgeprägten Bereich amphiphiler Helices, der es geradezu prädestiniert mit den Membranen der Zielzellen zu interagieren und in diesen eine Pore zu bilden. Dies ist allerdings nur ein Mechanismus, wie HlyA auf Zielzellen wirkt. Andere Experimente beschreiben spezifische Rezeptorbindungsstellen in HlyA über die es mit Zellen wechselwirkt und die zelluläre Signaltransduktion beeinflusst. Der endgültige Mechanismus der Funktionsweise von HlyA ist allerdings noch längst nicht verstanden. Ein Schwerpunkt dieser Arbeit liegt auf der Faltung des Toxins in seine native/aktive Form. Dabei haben die Ergebnisse gezeigt, dass das Sekretionssignal am C-Ternimus von HlyA eine doppelte Funktion hat und Einfluss auf die korrekte Faltung des Toxins nimmt.

Das Type I Sekretionssystem besteht aus verschiedenen Proteinen die sich ternären Komplex bilden. Der ABC-Transporter Haemolysin B (HlyB) und das Membranfusionsprotein Haemolysin D (HlyD) befinden sich in der inneren Membran. Zusammen mit den Porin-ähnlichen Protein TolC, das sich in der äußeren Membran befindet, bilden diese Komponenten einen durchgängigen Kanal beziehungsweise Tunnel, der das Periplasma durchzieht und die Sekretion des Toxins HlyA in einem Schritt über beide Membranen ermöglicht. Der ABC-Transporter HlyB besteht aus einem Transmembranteil und einer löslichen Domäne, der Nukleotidbindungsdomäne (NBD), die durch Hydrolyse von ATP für den Transport benötigte Energie zur Verfügung stellt. Ein weiterer Fokus dieser Arbeit beschäftigt sich mit de funktionallen Charakterisierung der NBD, erklärt die molekularen Grundlagen des katalytischen Zyklus dieses Enzyms und bietet einen Erklärungsansatz, für die beobachtete Kooperativität in diesem Protein. Zusammen mit strukturellen Daten aus den Kristtallstrukturen der NBD bietet sich die Möglichkeit dieses intensiv charakterisierte Protein als Modellystem zu verwenden, um in Zukunft Inhibitoren/Modulatoren für ABC-Transporter zu testen, da diese Proteinfamilie eine gewichtige Rolle bei der Entstehung von multidrogenresistenten Krebszellen und verschiedenen Krankheiten wie Mukoviszidose spielt.

Ein dritter Aspekt dieser Arbeit beschreibt die Etablierung einer Methode zur Bestimmung der kritischen micellaren Konzentration (CMC) von Detergenzien auf Basis einen Mittel- bis Hochdurchsatztestverfahrens. Da sich die CMC bei Änderung der Pufferbedingungen, Salzkonzentration, Temperatur und weiterer Parameter ändert, ist ein einfacher und schneller „*Screen*“ von Vorteil. Dies trifft insbesondere zu, wenn es um die Aufreinigung, Charakterisierung und Kristallisation von Membranproteinen geht, die sich während der gennanten Arbeitsschritte in solubilisiertem Zustand in ständigem Kontakt mit Detergenz befinden, das die Lipidumgebung der natürlichen Zellmembran nachahmen soll.

7. Literature

Aller, S. G., J. Yu, A. Ward, Y. Weng, S. Chittaboina, R. Zhuo, P. M. Harrell, Y. T. Trinh, Q. Zhang, I. L. Urbatsch & G. Chang, (2009) Structure of P-glycoprotein reveals a molecular basis for poly-specific drug binding. *Science* **323**: 1718-1722.

Andersen, C., E. Koronakis, E. Bokma, J. Eswaran, D. Humphreys, C. Hughes & V. Koronakis, (2002) Transition to the open state of the TolC periplasmic tunnel entrance. *Proc Natl Acad Sci U S A* **99**: 11103-11108.

Aniansson, E. A. G. & S. N. Wall, (1974) On the Kinetics of Step-Wise Micelle Association. *J Chem Phys* **78**: 1024-1030.

Bakas, L., H. Ostolaza, W. L. Vaz & F. M. Goni, (1996) Reversible adsorption and nonreversible insertion of Escherichia coli alpha-hemolysin into lipid bilayers. *Biophys J* **71**: 1869-1876.

Cortajarena, A. L., F. M. Goni & H. Ostolaza, (2001) Glycophorin as a receptor for Escherichia coli alpha-hemolysin in erythrocytes. *J Biol Chem* **276**: 12513-12519.

Cortajarena, A. L., F. M. Goni & H. Ostolaza, (2003) A receptor-binding region in Escherichia coli alpha-haemolysin. *J Biol Chem* **278**: 19159-19163.

Dean, M., (2009) ABC transporters, drug resistance, and cancer stem cells. *J Mammary Gland Biol Neoplasia* **14**: 3-9.

Fernandez, L. A. & V. de Lorenzo, (2001) Formation of disulphide bonds during secretion of proteins through the periplasmic-independent type I pathway. *Mol Microbiol* **40**: 332-346.

Fernandez, L. A., I. Sola, L. Enjuanes & V. de Lorenzo, (2000) Specific secretion of active single-chain Fv antibodies into the supernatants of Escherichia coli cultures by use of the hemolysin system. *Appl Environ Microbiol* **66**: 5024-5029.

Fraile, S., A. Munoz, V. de Lorenzo & L. A. Fernandez, (2004) Secretion of proteins with dimerization capacity by the haemolysin type I transport system of Escherichia coli. *Mol Microbiol* **53**: 1109-1121.

Hanekop, N., M. Hoing, L. Sohn-Bosser, M. Jebbar, L. Schmitt & E. Bremer, (2007) Crystal structure of the ligand-binding protein EhuB from Sinorhizobium meliloti reveals substrate recognition of the compatible solutes ectoine and hydroxyectoine. *J Mol Biol* **374**: 1237-1250.

Hanekop, N., J. Zaitseva, S. Jenewein, I. B. Holland & L. Schmitt, (2006) Molecular insights into the mechanism of ATP-hydrolysis by the NBD of the ABC-transporter HlyB. *FEBS Lett* **580**: 1036-1041.

Havarstein, L. S., D. B. Diep & I. F. Nes, (1995) A family of bacteriocin ABC transporters carry out proteolytic processing of their substrates concomitant with export. *Mol Microbiol* **16**: 229-240.

Holland, I. B., L. Schmitt & J. Young, (2005) Type 1 protein secretion in bacteria, the ABC-transporter dependent pathway (review). *Mol Membr Biol* **22**: 29-39.

Horn, C., L. Sohn-Bosser, J. Breed, W. Welte, L. Schmitt & E. Bremer, (2006) Molecular determinants for substrate specificity of the ligand-binding protein OpuAC from Bacillus subtilis for the compatible solutes glycine betaine and proline betaine. *J Mol Biol* **357**: 592-606.

Juliano, R. L. & V. Ling, (1976) A surface glycoprotein modulating drug permeability in Chinese hamster ovary cell mutants. *Biochim Biophys Acta* **455**: 152-162.

Jumpertz, T. & e. al., (2009) ABC Transporters: A Smart Example of Molecular Machineries. In: ABC Transporters in Microorganisms. A. Ponte-Sucre (ed). Norwich: Caister Academic Press, pp. 1-34.

Koronakis, V., C. Hughes & E. Koronakis, (1991) Energetically distinct early and late stages of HlyB/HlyD-dependent secretion across both Escherichia coli membranes. *EMBO J.* **10**: 3263-3272.

Koronakis, V., A. Sharff, E. Koronakis, B. Luisi & C. Hughes, (2000) Crystal structure of the bacterial membrane protein TolC central to multidrug efflux and protein export. *Nature* **405**: 914-919.

Kos, V. & R. C. Ford, (2009) The ATP-binding cassette family: a structural perspective. *Cell Mol Life Sci* **66**: 3111-3126.

Kotake, Y., S. Ishii, T. Yano, Y. Katsuoka & H. Hayashi, (2008) Substrate recognition mechanism of the peptidase domain of the quorum-sensing-signal-producing ABC transporter ComA from Streptococcus. *Biochemistry* **47**: 2531-2538.

Langston, K. G., L. M. Worsham, L. Earls & M. L. Ernst-Fonberg, (2004) Activation of hemolysin toxin: relationship between two internal protein sites of acylation. *Biochemistry* **43**: 4338-4346.

Li, Y., C. Hess, B. von Specht & H. P. Hahn, (2000) Molecular analysis of hemolysin-mediated secretion of a human interleukin-6 fusion protein in Salmonella typhimurium. *FEMS Immunol Med Microbiol* **27**: 333-340.

Lim, K. B., C. R. Walker, L. Guo, S. Pellett, J. Shabanowitz, D. F. Hunt, E. L. Hewlett, A. Ludwig, W. Goebel, R. A. Welch & M. Hackett, (2000) Escherichia coli alpha-hemolysin (HlyA) is heterogeneously acylated in vivo with 14-, 15-, and 17-carbon fatty acids. *J Biol Chem* **275**: 36698-36702.

Ludwig, A. & W. Goebel, (2000) Dangerous signals from E. coli toxin. *Nat Med* **6**: 741-742.

Nikaido, H. & Y. Takatsuka, (2009) Mechanisms of RND multidrug efflux pumps. *Biochim Biophys Acta* **1794**: 769-781.

Ostolaza, H., L. Bakas & F. M. Goni, (1997) Balance of electrostatic and hydrophobic interactions in the lysis of model membranes by E. coli alpha-haemolysin. *J Membr Biol* **158**: 137-145.

Oswald, C., S. H. Smits, M. Hoing, L. Sohn-Bosser, L. Dupont, D. Le Rudulier, L. Schmitt & E. Bremer, (2008) Crystal structures of the choline/acetylcholine substrate-binding protein ChoX from Sinorhizobium meliloti in the liganded and unliganded-closed states. *J Biol Chem* **283**: 32848-32859.

Pimenta, A. L., K. Racher, L. Jamieson, M. A. Blight & I. B. Holland, (2005) Mutations in HlyD, part of the type 1 translocator for hemolysin secretion, affect the folding of the secreted toxin. *J Bacteriol* **187**: 7471-7480.

Riordan, J. R. & V. Ling, (1979) Purification of P-glycoprotein from plasma membrane vesicles of Chinese hamster ovary cell mutants with reduced colchicine permeability. *J Biol Chem* **254**: 12701-12705.

Sanchez-Magraner, L., A. R. Viguera, M. Garcia-Pacios, M. P. Garcillan, J. L. Arrondo, F. de la Cruz, F. M. Goni & H. Ostolaza, (2007) The calcium-binding C-terminal domain of Escherichia coli alpha-hemolysin is a major determinant in the surface-active properties of the protein. *J Biol Chem* **282**: 11827-11835.

Schmidt, H., E. Maier, H. Karch & R. Benz, (1996) Pore-forming properties of the plasmid-encoded hemolysin of enterohemorrhagic Escherichia coli O157:H7. *Eur J Biochem* **241**: 594-601.

Schmitt, L., H. Benabdelhak, M. A. Blight, I. B. Holland & M. T. Stubbs, (2003) Crystal structure of the nucleotide binding domain of the ABC-transporter haemolysin B:

Identification of a variable region within ABC helical domains. *J Mol Biol* **330**: 333-342.

Sehgal, P., J. E. Mogensen & D. E. Otzen, (2005) Using micellar mole fractions to assess membrane protein stability in mixed micelles. *Biochim Biophys Acta* **1716**: 59-68.

Shapiro, A. B., A. B. Corder & V. Ling, (1997) P-glycoprotein-mediated Hoechst 33342 transport out of the lipid bilayer. *Eur J Biochem* **250**: 115-121.

Shepherd, F. H. & A. Holzenburg, (1995) The potential of fluorinated surfactants in membrane biochemistry. *Anal Biochem* **224**: 21-27.

Soloaga, A., M. P. Veiga, L. M. Garcia-Segura, H. Ostolaza, R. Brasseur & F. M. Goni, (1999) Insertion of Escherichia coli alpha-haemolysin in lipid bilayers as a non-transmembrane integral protein: prediction and experiment. *Mol Microbiol* **31**: 1013-1024.

Stanley, P., L. C. Packman, V. Koronakis & C. Hughes, (1994) Fatty acylation of two internal lysine residues required for the toxic activity of Escherichia coli hemolysin. *Science* **266**: 1992-1996.

Sugamata, Y. & T. Shiba, (2005) Improved secretory production of recombinant proteins by random mutagenesis of hlyB, an alpha-hemolysin transporter from Escherichia coli. *Appl Environ Microbiol* **71**: 656-662.

Symmons, M. F., E. Bokma, E. Koronakis, C. Hughes & V. Koronakis, (2009) The assembled structure of a complete tripartite bacterial multidrug efflux pump. *Proc Natl Acad Sci U S A* **106**: 7173-7178.

Uhlen, P., A. Laestadius, T. Jahnukainen, T. Soderblom, F. Backhed, G. Celsi, H. Brismar, S. Normark, A. Aperia & A. Richter-Dahlfors, (2000) Alpha-haemolysin of uropathogenic E. coli induces Ca2+ oscillations in renal epithelial cells. *Nature* **405**: 694-697.

Valeva, A., I. Siegel, M. Wylenzek, T. M. Wassenaar, S. Weis, N. Heinz, R. Schmitt, C. Fischer, R. Reinartz, S. Bhakdi & I. Walev, (2008) Putative identification of an amphipathic alpha-helical sequence in hemolysin of Escherichia coli (HlyA) involved in transmembrane pore formation. *Biol Chem* **389**: 1201-1207.

Valeva, A., I. Walev, H. Kemmer, S. Weis, I. Siegel, F. Boukhallouk, T. M. Wassenaar, T. Chavakis & S. Bhakdi, (2005) Binding of Escherichia coli hemolysin and activation of the target cells is not receptor-dependent. *J Biol Chem* **280**: 36657-36663.

Worsham, L. M., M. S. Trent, L. Earls, C. Jolly & M. L. Ernst-Fonberg, (2001) Insights into the catalytic mechanism of HlyC, the internal protein acyltransferase that activates Escherichia coli hemolysin toxin. *Biochemistry* **40**: 13607-13616.

Wu, K. H. & P. C. Tai, (2004) Cys32 and His105 are the critical residues for the calcium-dependent cysteine proteolytic activity of CvaB, an ATP-binding cassette transporter. *J Biol Chem* **279**: 901-909.

Zaitseva, J., S. Jenewein, T. Jumpertz, I. B. Holland & L. Schmitt, (2005a) H662 is the linchpin of ATP hydrolysis in the nucleotide-binding domain of the ABC transporter HlyB. *Embo J*.

Zaitseva, J., S. Jenewein, C. Oswald, T. Jumpertz, I. B. Holland & L. Schmitt, (2005b) A molecular understanding of the catalytic cycle of the nucleotide-binding domain of the ABC transporter HlyB. *Biochem Soc Trans* **33**: 990-995.

Zaitseva, J., S. Jenewein, A. Wiedenmann, H. Benabdelhak, I. B. Holland & L. Schmitt, (2005c) Functional characterization and ATP-induced dimerization of the isolated ABC-domain of the haemolysin B transporter. *Biochemistry* **44**: 9680-9690.

Die hier vorgelegte Dissertation habe ich eigenständig und ohne unerlaubte Hilfe angefertigt. Die Dissertation wurde in der vorgelegten oder in ähnlicher Form noch bei keiner anderen Institution eingereicht. Ich habe bisher keine erfolglosen Promotionsversuche unternommen.

Düsseldorf, den 01. Juni 2010

(Thorsten Jumpertz)

Danksagung

Lutz: für die interessanten Themen und großzügigen Möglichkeiten bei meiner Arbeit immer freie Hand zu haben, für Dein Interesse an den Ergebnissen und den Einsatz, dass wissenschaftliche Neugier immer einen Platz in Deinem Institut hat.

Britta: wo soll ich anfangen? Danke, dass Du inzwischen drahtlose Kopfhörer für die diversen DreamDance Sampler hast. Aber vor allem dafür, dass Du immer versucht hast pragmatische Lösungen zu finden und Dich so sehr für alles im als auch außerhalb des Labors eingesetzt hast.

André, Nino & Sander: ein ähnlich ungleiches Team gibt es wohl nur bei Ice Age. Aber auch bei der Nisin-Gang scheint es ja offensichtlich gut zu funktionieren. André, ich lege die lustigen Figuren unserer Homepage jetzt in Deine Verantwortung – und pass gut auf Petri auf! Nino, bitte vergiss niemals die entsprechende Playlist vor den Fortuna-Spielen abzuarbeiten – Dein Büro würde es vermissen. Sander, vielen Dank für Dein Bemühen, dass sich alle wohlfühlen und vorwärts kommen. Und für den Apfelkuchen!

Christian, Miro & Patrick: ...ach, euch werde ich ja sowieso nicht los, sobald ihr meine neue Telefonnummer rausbekommen habt. Trotzdem wünsche ich euch viel Spaß und vor allem Erfolg mit den Haemolysin Projekten. Ich denke ihr werdet noch viele neue Fragen aufwerfen und dafür sorgen, dass es nicht so schnell langweilig wird.

Frau Blum & Frau Rasid: vielen Dank dafür, dass sie sich um alles gekümmerst haben, mit dem ich am liebsten nichts zu tun haben möchte. Zwar auf ganz unterschiedliche Art und Weise, aber es hat die Arbeit sehr viel entspannter gemacht.

Jan: es wird Zeit ;)

Martina: es tut mir aufrichtig leid, dass ich ständig Deinen Bürostuhl verstellt habe – aber wenn Du ehrlich bist, wirst Du es eines morgens vermissen...

Nacera: wenn Du weiterhin alle Dinge so akribisch auseinander nimmst und zu erklären versuchst, werden wir es schwer haben...

Nils: Dich kann ich mit Fug und Recht als konstante Größe in meiner Zeit bei Lutz bezeichnen. Und ich bin immer wieder beeindruckt, woher Du auf so viele Dinge quasi aus dem Nichts eine Antwort zauberst. Ich bin mir ziemlich sicher, dass ich diesen Service schon sehr bald vermissen werde.

Petra: dafür, dass die dunkle Seite manchmal bis zum Morgengrauen wach ist. Die Zeitleiste ist inzwischen bestimmt schon völlig zerfleddert, also bitte... Ich wünche Dir alles erdenklich Gute für die Zukunft – Du hast es verdient.

Philipp, bei Dir fallen mir immer nur drei Worte ein: Burger, Ouzo und Fahrrad. Bilde daraus einen sinnvollen Satz!

Rakesh: all the best for you!

Silke: zusammengerechnet waren das in den ganzen Jahren vermutlich sehr viele Stunden Kaffepause – wer weiss, wie ich ohne die echt nette und lustige Abwechslung geendet hätte. Aber viel wichtiger: was machst Du jetzt in den nächsten 33,5 Jahren?

Tatu: ...jetzt fällt mir gerade nur Dein Chef ein, weil ich schon wieder Hunger habe. Nein, Spaß beiseite – ich weiss ja, wo ich Dich finden kann, Nachbar!

Uli: dafür, dass hinter der nüchternen Fassade ein unentdecktes Talent an der Karaokemaschine steckt

Vero: vermutlich werde ich das Bild der Atmungskette aus Deinem Pilz nie wieder los, weil Du es tief in meine Netzhaut gebrannt hast. Besonders beeindruckend fand ich Deinen aufopferungsvollen Umgang mit unseren bzw. Deinen Praktikanten – wäre jeder so, hätten wir vermutlich das beste Bildungssystem der Welt.

Allen meinen ehemaligen Kollegen für ihre teils enorme Arbeit, ohne die ich nicht so weit gekommen wäre.

...und dann gibt es noch eine ganze Menge weiterer Leute mit denen ich gearbeitet habe – jeder einzelne von ihnen war eine positive und bereichernde Erfahrung. Die Idee von Wissenschaftlern, die sich gegenseitig unkompliziert helfen und offen für Neues sind, um vielleicht irgendetwas Besonderes zu entdecken, hat in meinem Fall funktioniert. Einen besseren Start hätte man sich nicht wünschen können.

Meiner Familie & meinen Freunden dafür, dass sie so gar kein Interesse an Biochemie haben und mich somit davor bewahrt haben, alles zu ernst zu nehmen.